

AD-A247 088

## ENTATION PAGE

Form Approved  
OMB No. 0704-0188

1a. R UI		1b. RESTRICTIVE MARKINGS NONE	
2a. S...		3. DISTRIBUTION/AVAILABILITY OF REPORT UNLIMITED	
2b. DECLASSIFICATION/DOWNGRADING SCHEDULE N/A		5. MONITORING ORGANIZATION REPORT NUMBER(S) N/A	
4. PERFORMING ORGANIZATION REPORT NUMBER(S) N/A		7a. NAME OF MONITORING ORGANIZATION Office of Naval Research, Code 1132P	
6a. NAME OF PERFORMING ORGANIZATION Georgia Institute of Technology		7b. ADDRESS (City, State, and ZIP Code)	
6b. ADDRESS (City, State, and ZIP Code) School of Aerospace Engineering, 0150 Atlanta, Georgia 30332		9. PROCUREMENT INSTRUMENT IDENTIFICATION NUMBER N00014-85-K-0803	
8a. NAME OF FUNDING/SPONSORING ORGANIZATION Office of Naval Research		10. SOURCE OF FUNDING NUMBERS	
8b. ADDRESS (City, State, and ZIP Code) Dept. of the Navy, Code 1132P 800 N. Quincy Street Arlington, VA 22217-5000		PROGRAM ELEMENT NO.	PROJECT NO
		TASK NO	WORK UNIT ACCESSION NO
11. TITLE (Include Security Classification) COMBUSTION MECHANISMS OF SOLIDS			
12. PERSONAL AUTHOR(S) E. W. Price, R. K. Sigman, C. P. Markou			
13a. TYPE OF REPORT FINAL	13b. TIME COVERED FROM 10/85 TO 8/88	14. DATE OF REPORT (Year, Month, Day) 1992, February 24	15. PAGE COUNT 141
16. SUPPLEMENTARY NOTATION			
17. COSATI CODES		18. SUBJECT TERMS (Continue on reverse if necessary and identify by block number)	
FIELD	GROUP	SUB-GROUP	
		COMBUSTION, SOLID PROPELLANT	
19. ABSTRACT (Continue on reverse if necessary and identify by block number)			
<p>This report summarizes the studies of ingredient decomposition and sandwich burning during the period October 1985 to September 1988. A CO<sub>2</sub> laser pyrolysis facility was built and preliminary tests on propellant ingredients were conducted. Results showed presence of a liquid state or reacting froth on the surface of all ingredients tested (AP, AN, PBAN, NMMO and BAMO-THF).</p> <p>Ingredient combustion behavior was studied by the edge burning sandwich method using sandwiches of AP with PBAN, NMMO and BAMO-THF. The effects of Fe<sub>2</sub>O<sub>3</sub>, Fe<sub>3</sub>O<sub>4</sub> and catocene (10% level in the binder lamina) were evaluated. Burning with BAMO-THF was qualitatively similar to that with PBAN, with the</p> <p style="text-align: right;">CONTINUED</p>			
20. DISTRIBUTION/AVAILABILITY OF ABSTRACT <input checked="" type="checkbox"/> UNCLASSIFIED/UNLIMITED <input type="checkbox"/> SAME AS RPT. <input type="checkbox"/> DTIC USERS		21. ABSTRACT SECURITY CLASSIFICATION UNCLASSIFIED	
22a. NAME OF RESPONSIBLE INDIVIDUAL E. W. Price		22b. TELEPHONE (Include Area Code) 404-894-3063	22c. OFFICE SYMBOL

## 19. ABSTRACT (cont.)

leading edge of the oxidizer-binder diffusion flame playing an important role in the burning behavior. The catalysts all produced similar enhancement of burning rate. All showed formation of a concentrated layer of iron oxide on the binder surface, which apparently catalyzes decomposition of heavy fuel molecules and corresponding formation of the leading edge of the O/F flame closer to the surface. Tests of sandwiches with pure NMMO binder did not show any effect of the O/F flame on burning rate, suggesting low reaction rate between the primary decomposition products of AP and NMMO. Presence of  $\text{Fe}_2\text{O}_3$  catalyst in the NMMO

led to burning rates similar to those with the other catalyzed binders, indicating catalytic breakdown of fuel fragments, high reaction rate, and correspondingly high burning rate. These interpretations are supported by a variety of other observations (in addition to burning rate) that are summarized in the report.

COMBUSTION MECHANISMS OF SOLIDS

Final Technical Report on Contract N00014-85-K-0803

by

E. W. Price, R.K. Sigman and C. Markou  
School of Aerospace Engineering  
Georgia Institute of Technology  
Atlanta, GA 30332

for

OFFICE OF NAVAL RESEARCH  
Arlington, VA 22217-5000

February 1992



Accession For	
DTIC GRA&I	<input checked="" type="checkbox"/>
DTIC TAB	<input type="checkbox"/>
Unannounced	<input type="checkbox"/>
Justification	
By	
Distribution/	
Availability Codes	
Dist	Avail and/or Special
A-1	

92-05528



92 3 03 003

## INTRODUCTION

The objectives of the present research were to clarify the mechanism of decomposition of ingredients of solid propellants at combustion zone temperatures, and relate the decomposition behavior to the controlling processes in propellant combustion. The high temperature decomposition studies consisted primarily of design and assembly of a 1200 watt  $\text{CO}_2$  laser pyrolysis facility, using equipment provided under a DOD Equipment Grant (Ref. 1). The role of ingredient decomposition on the overall propellant combustion process was studied using primarily the "sandwich burning" method (Ref. 2, 3). The present report summarizes progress in these two areas.

A large part of the high temperature decomposition work was reported previously in Ref. 1, and will be reviewed here only in summary form. The laser facility became operational only late in the contract period, so that the actual pyrolysis testing was primarily a demonstration-of-potential for the method.

The sandwich burning studies involve extension of earlier studies to determine a) the mechanisms by which ballistic modifiers change the burning rate of AP composite propellants, and b) the behavior of new binder materials (BAMO-THF and NMMO) in burning of AP-binder-AP sandwiches. These studies will be presented in summary form, with a more detailed description in the form of a Ph.D. thesis in Appendix A.

## LASER PYROLYSIS

The goal of the laser pyrolysis facility was to permit a variety of controlled experiments in which test samples were heated by infrared radiant flux at levels from 100 to 1000 watts per  $\text{cm}^2$  (24 to 240  $\text{cal}/\text{cm}^2 \text{ sec}$ ). This would permit decomposition at the temperatures and rates typical of propellant combustion, with a variety of experimental advantages over combustion:

- a) Ingredients can be studied individually.
- b) Heating rate can be varied independently of other variables.

- c) High heating rate can be achieved with either ingredients or propellants at low pressures where the gas phase reaction zone is spread out enough for spatial resolution by various measurement methods.
- d) Decomposition can be started, stopped, or oscillated by controls on the laser. "Quenched" samples are available for microscopic evaluation.

The principal features desired of the laser facility were

- a) A 1200 - 1500 watt continuous output infrared beam, reasonably homogeneous.
- b) A beam conditioner-delivery system that permitted uniform illumination of a 1 cm<sup>2</sup> sample surface.
- c) An optical bench for mounting 2 - 3 experiments (test chambers, instrumentation) in the beam delivery location. A suitable enclosure to prevent inadvertent exposure to laser illumination.
- d) An exhaust system and flushing flows for test chambers.
- e) A control system that operates the laser, test instrumentation, recorders, etc., according to prescribed controls, pre-programmed for each test and/or controlled in real time by measured variables.

All of these features were accomplished during the present contract except for completion of the control system.

The central features of the facility are summarized in Fig. 1 and 2, which describe the general layout and the optical paths. The optical bench and enclosure are shown in Fig. 3. The laser is a Penn Research Corp. 1200 watt continuous fast axial flow CO<sub>2</sub> laser (Fig. 4). This laser can be operated at levels of 100 - 1200 watts; the beam output can be turned on and off and oscillated at frequencies up to 3500 Hz by input electronic controls. The beam has a Gaussian intensity distribution. Various means were used to obtain a

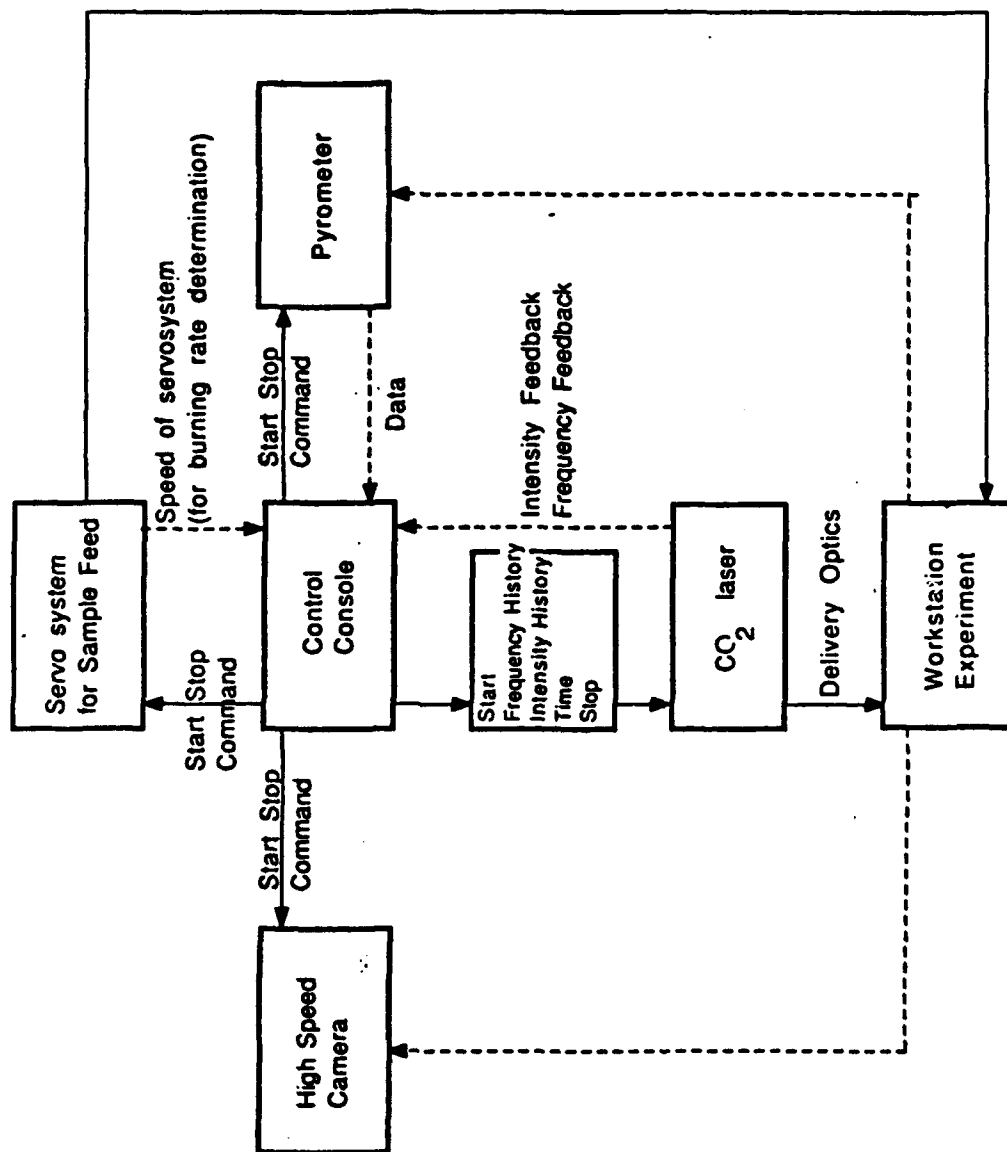


Fig. 1 Diagram showing components and network for the CO<sub>2</sub> laser pyrolysis facility.

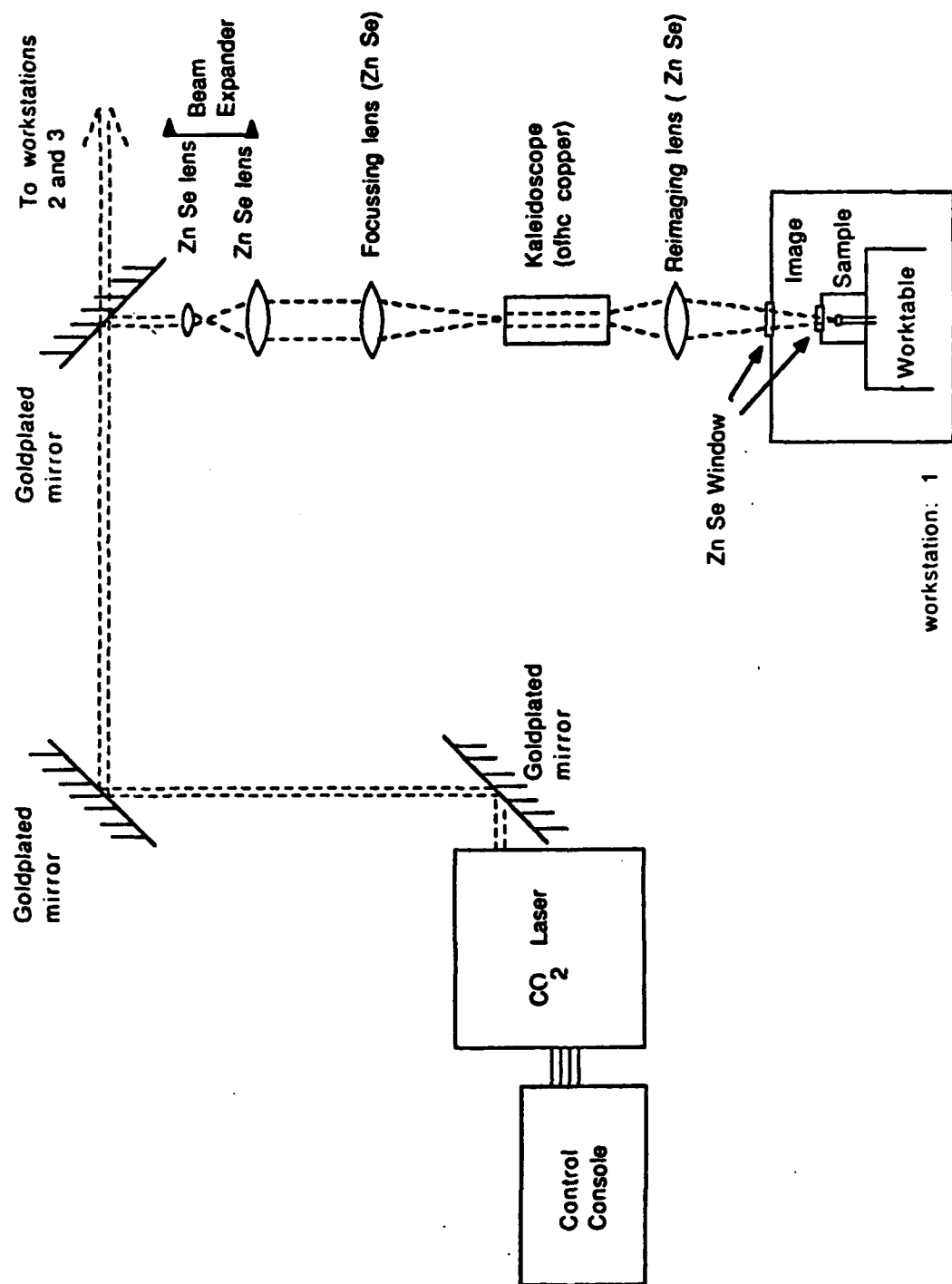


Fig. 2 Sketch of the optical path for the CO<sub>2</sub> laser beam.

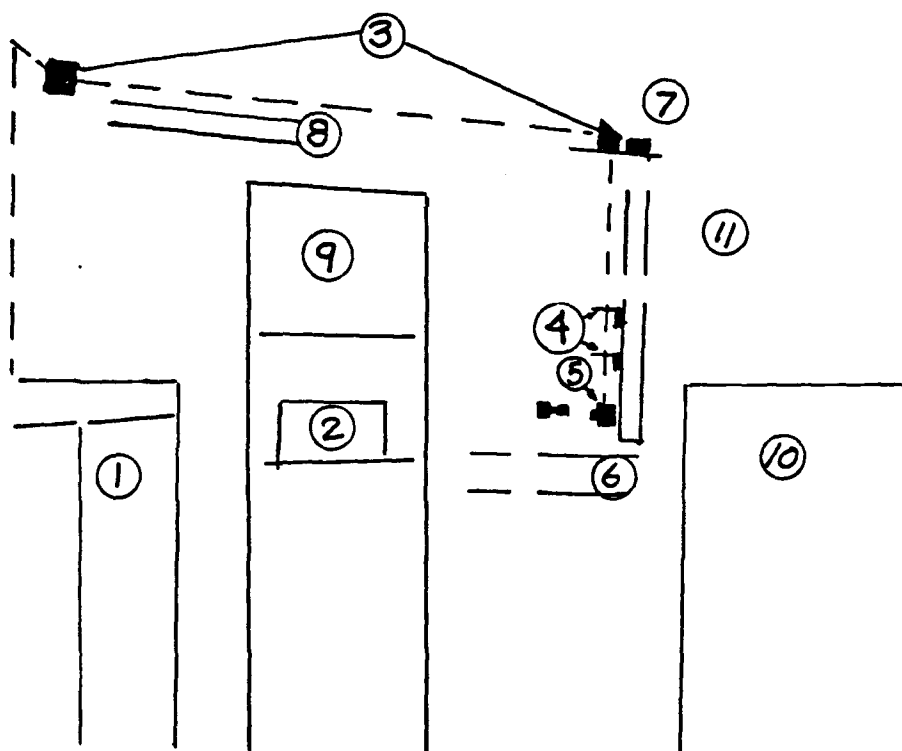


Fig. 3 Layout of laser facility showing (1) laser and (2) laser controls. The laser beam (---) leaves the front of the laser and reflects from 4 gold coated copper mirrors [2 are visible (3)] before passing through the final 2 beam conditioning lenses (4) and striking the sample in the chamber (5). The beam can be positioned at any point on the optical bench (6) using the motorized (7) traversing system (8) with remote controls (9). The video recording system (10) is outside the polycarbonate safety enclosure (11).

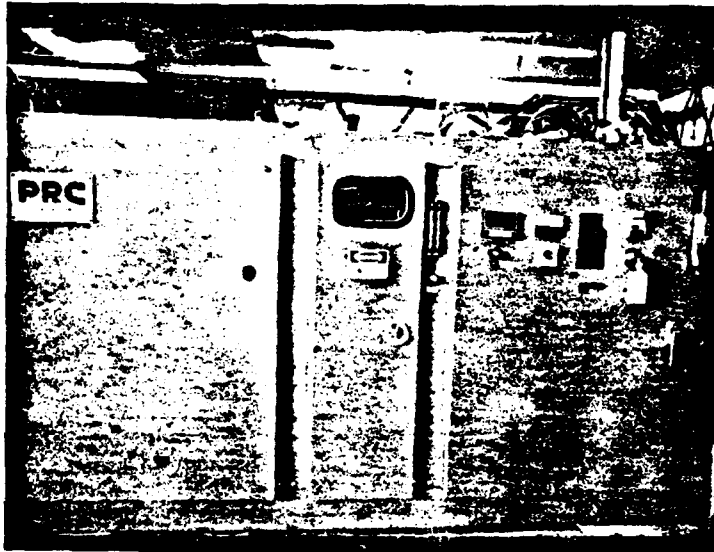


Fig. 4 Photograph of the 1200 watt CO<sub>2</sub> laser.

"flat" intensity distribution, with only moderate success. Tests to date have simply used the relatively flat part of the distribution.

A test chamber was constructed (Fig. 5) for atmospheric pressure testing, providing for flushing with desired atmospheric gas, an infrared window at the top for the laser beam, and additional windows for sample illumination, combustion photography, and other optical measurements.

The control system indicated in Fig. 1 was not yet operational at the closing date of the contract. Components were on hand and most were in use for related ongoing research.

Exploratory tests were run on samples of polymers, single crystal and dry-pressed ammonium perchlorate, and dry-pressed ammonium nitrate. Fig. 6 shows typical surface features of these materials as revealed by scanning electron microscope images of the surfaces of samples after beam cut-off-quench (tests conducted at 1 atmosphere of nitrogen). Tests were also run with sustained steady state pyrolysis on polymer samples, monitored by video camera to provide surface regression rate. These were exploratory tests in preparation for correlation of pyrolysis rate and surface temperature vs heat flux. Work was suspended before the system for surface temperature measurement was implemented.

In general, the facility met all expectations except for a) lack of complete beam uniformity (rejection of about 30% of beam energy in order to achieve acceptable beam uniformity), and b) lack of fully automated control of experiments. It is anticipated that these shortfalls will be remedied in future projects.

### **SANDWICH BURNING STUDIES**

The "sandwich burning" method for study of combustion of heterogeneous propellants has been highly developed in earlier studies, and now combines

- a) A simple (two-dimensional) geometry (Fig. 7)
- b) An extensive background of theory and experimental results pertaining to combustion of such systems

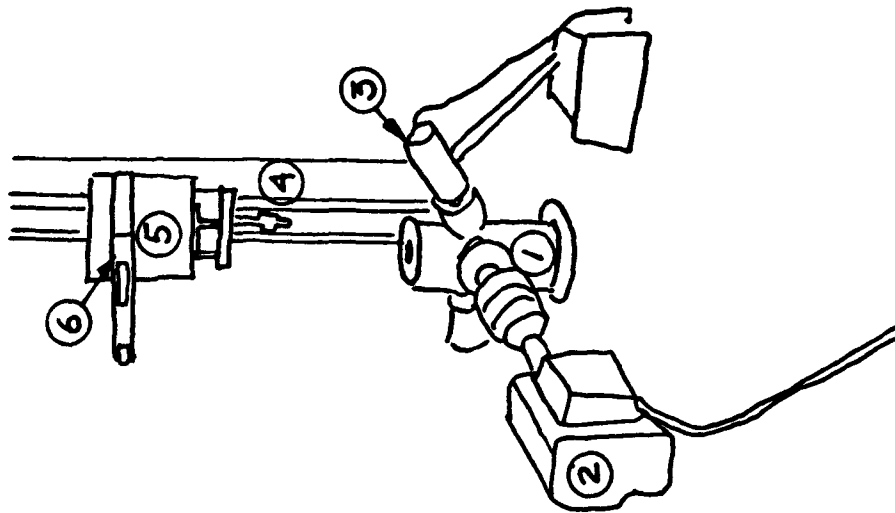
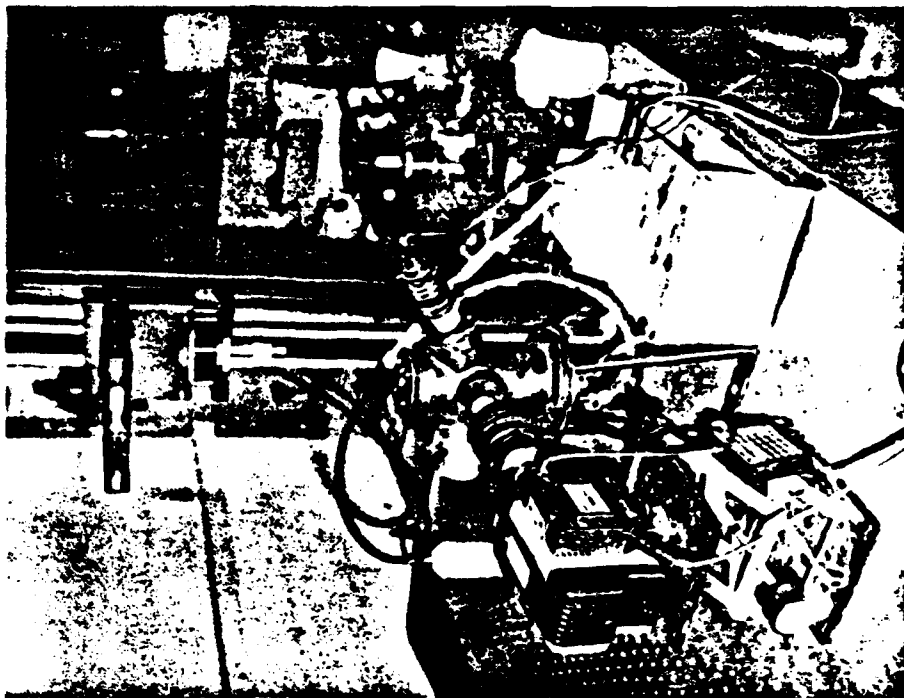


Fig. 5 Test set-up with flushed chamber. a) Layout of video and sample chamber showing 1) sample chamber, (2) video camera, (3) lamp, (4) optical rail for vertical positioning of beam adjusting lenses, (5) lens holder and adjustment, and (6) zinc selenide lens (not visible).

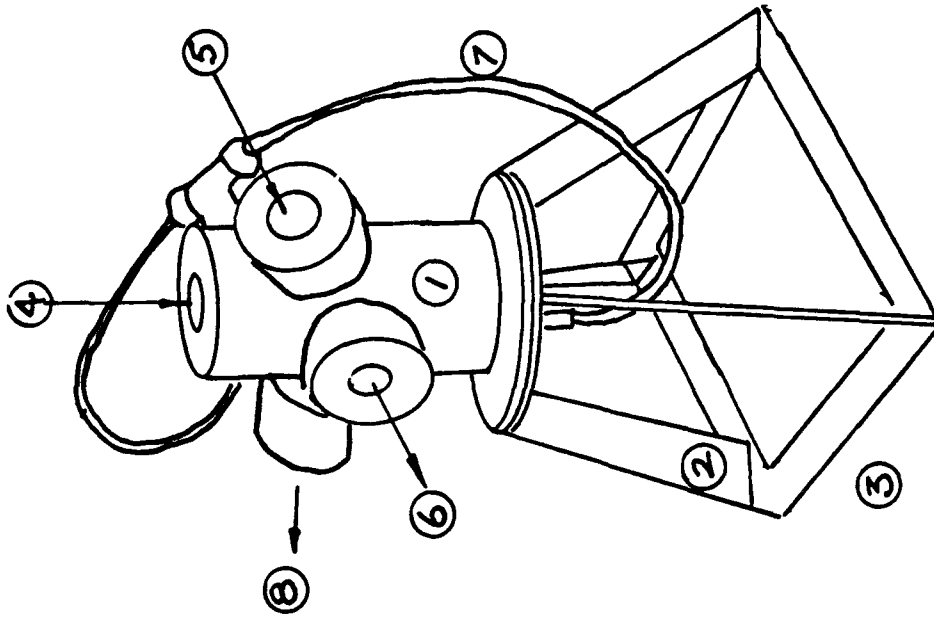
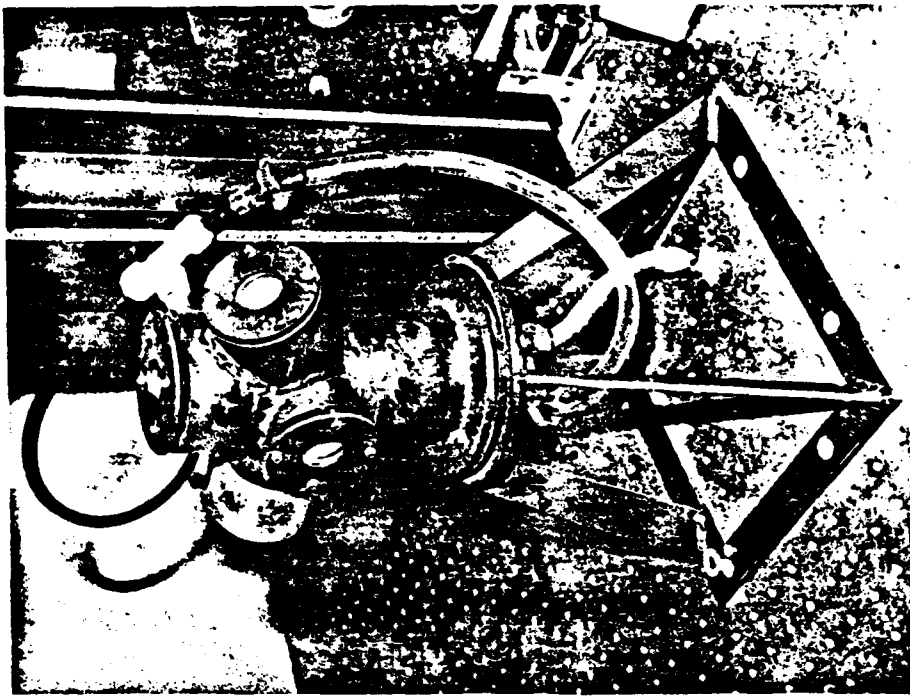
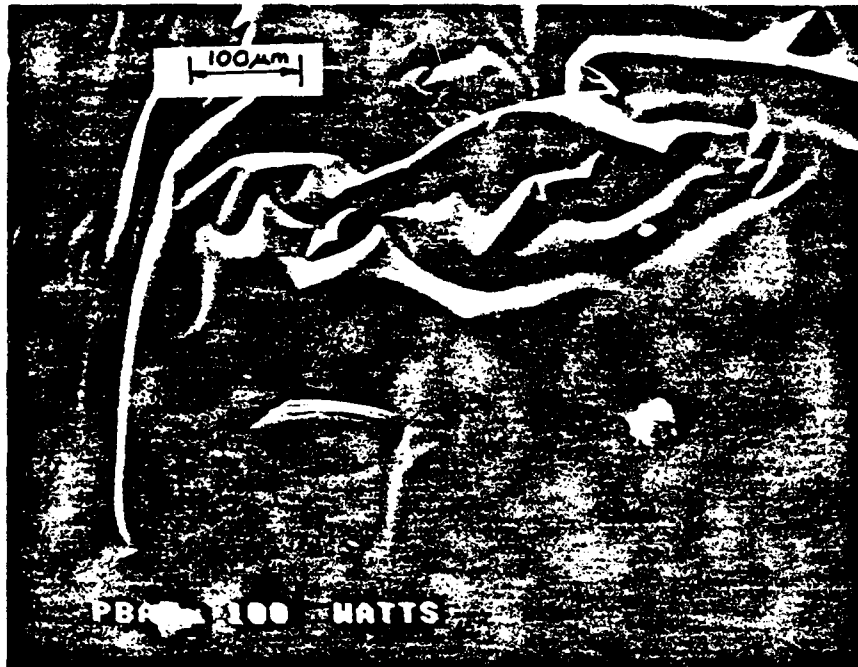


Fig. 5 Test set-up with flushed chamber. b) Laser pyrolysis chamber: (1) chamber, (2) stand, (3) optical bench, (4) zinc selenide window, (5) external illumination window, (6) camera window, (7) nitrogen purge and window flushing line, and (8) exhaust. (Exhaust tube, primary and secondary pumps are not shown.)

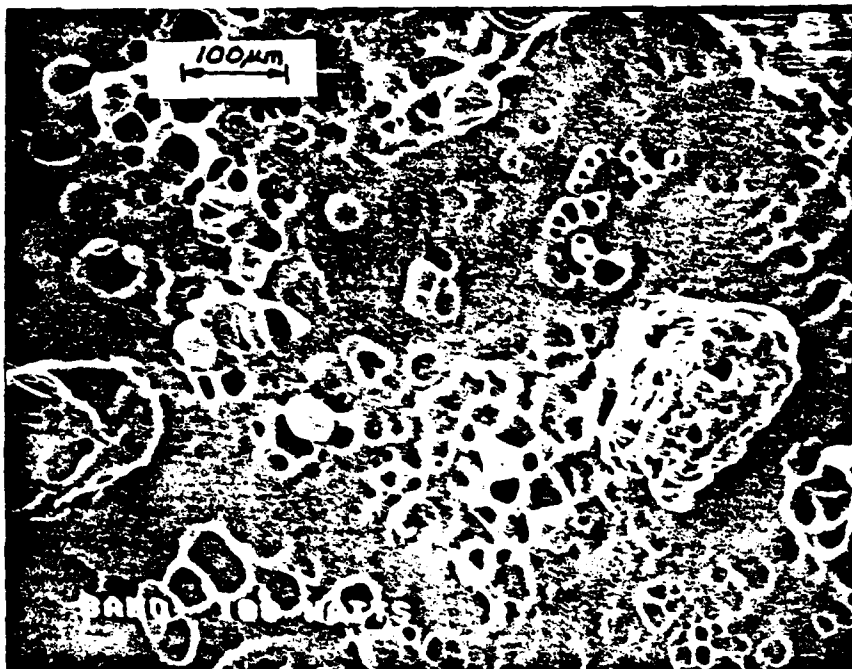


- a) PBAN binder (center of heated area is to the lower right). Indicates a non-bubbling, residue-free surface.

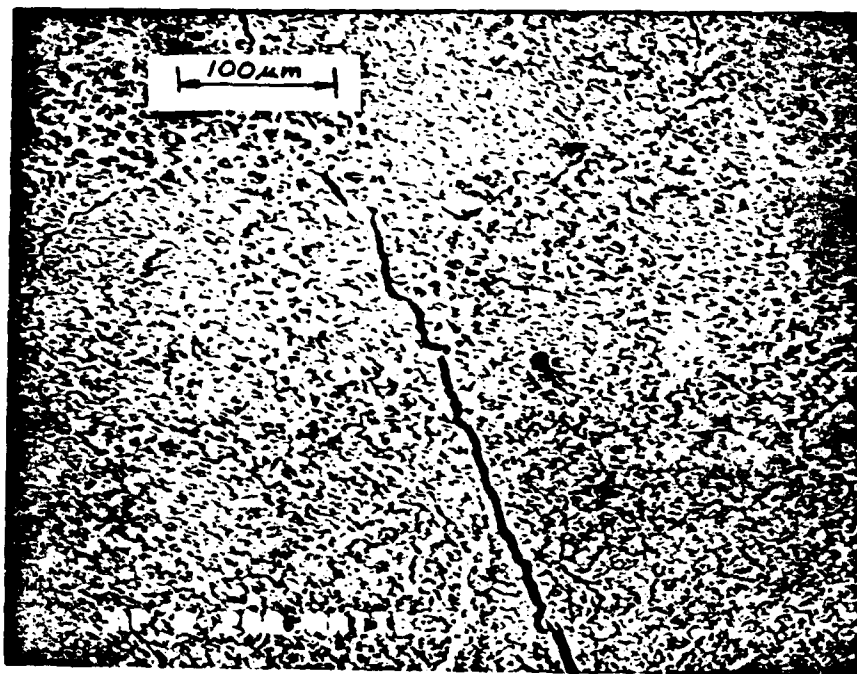


- b) PBAN binder with 10% 5  $\mu\text{m}$   $\text{Fe}_2\text{O}_3$  (center of heated area to the lower right).  $\text{Fe}_2\text{O}_3$  concentrated in clumps 250  $\mu\text{m}$  across.

Fig. 6 Typical surfaces of quenched samples.

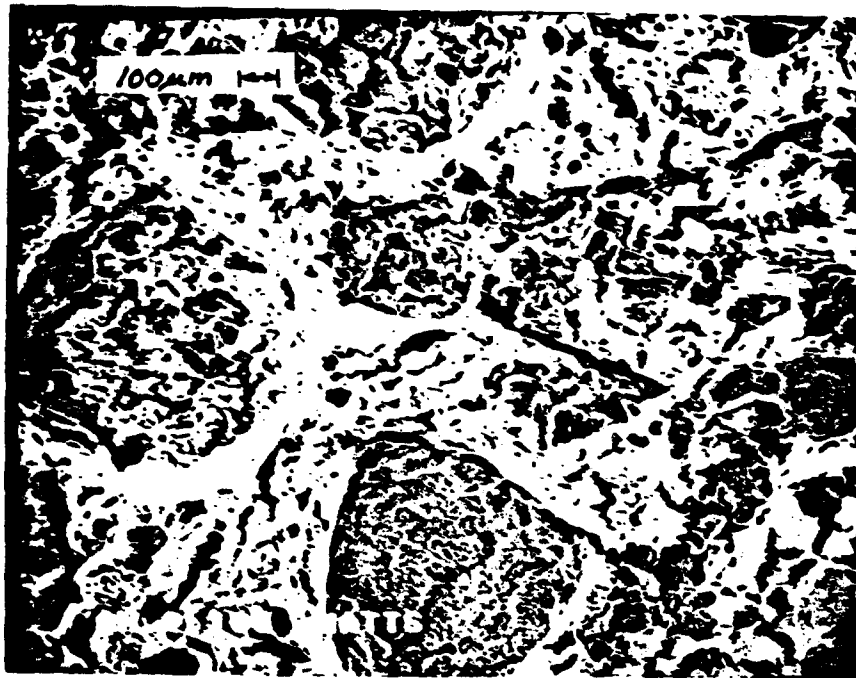


c) BAMO-THF binder. Indicates molten surface with subsurface bubbling.



d) Ammonium perchlorate single crystal. Indicates surface froth.

Fig. 6 Typical surfaces of quenched samples.



- e) Dry pressed ammonium nitrate. Suggests extensive melt layer with large bubbles and in-depth decomposition.

Fig. 6 Typical surfaces of quenched samples.

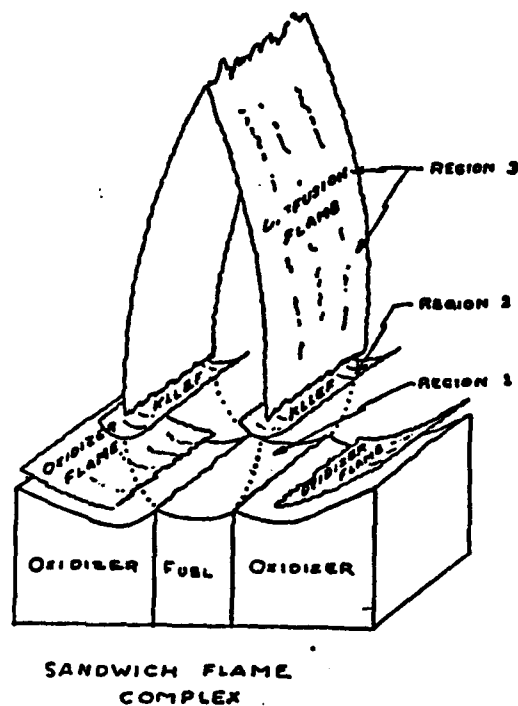


Fig. 7 Flame complex for an edge burning AP/binder/AP sandwich. The lower portion is a picture of a quenched surface, the upper part a sketch of the flame (based on theory and results of past studies).

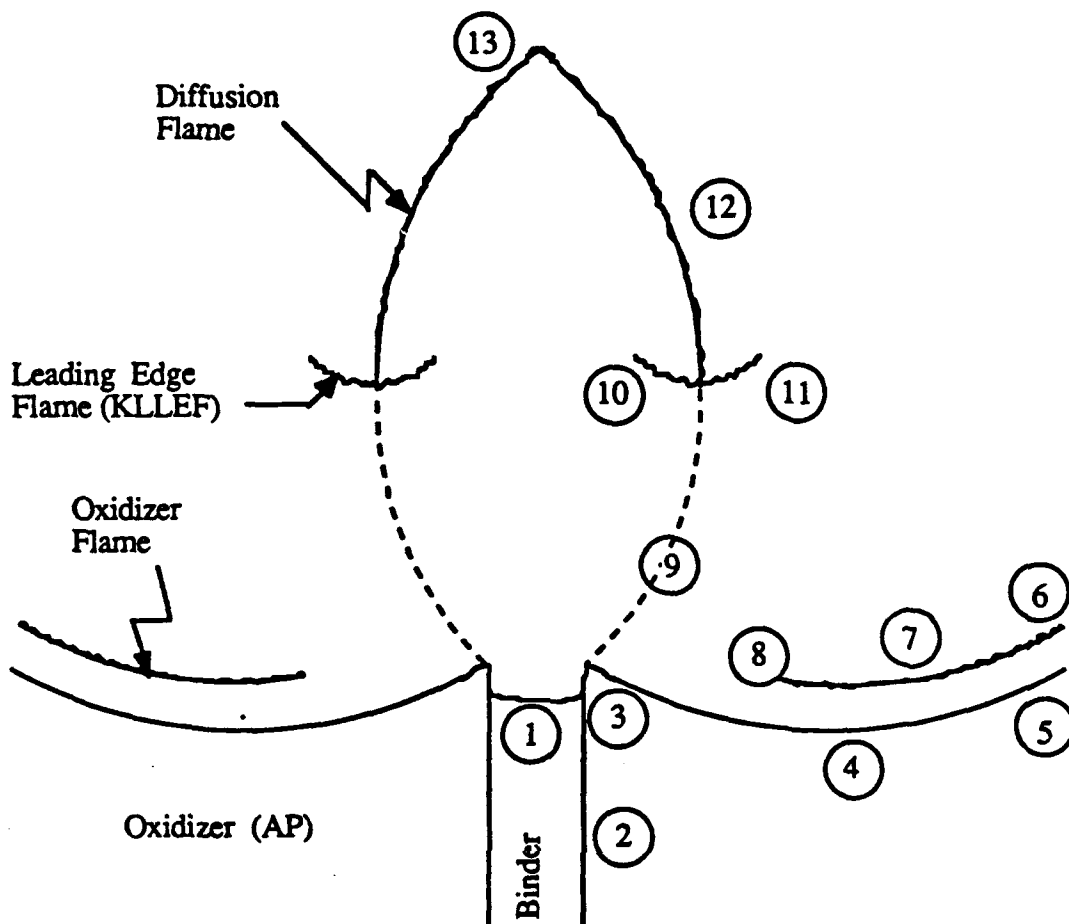
- c) Small, easily fabricated test samples particularly suited to study of new propellant ingredients that may be available in only small quantities

Experimental results include sample burning rate, burning surface profiles, and detailed features of the burning surface. When combined with combustion zone theory, it is often possible to determine the effect of ingredient variables on the structure of a flame zone, which is usually too microscopic for direct observation. In effect, the tests allow determination of the rate-controlling steps in the combustion by reconciling the measurable features noted above with flame theory that is made relatively tractable by use of the simple sandwich geometry. The reader is referred to details and procedure in Ref. 2 and in Appendix A. In this summary, the principal conclusions of Appendix A are summarized. This consists of conclusions regarding mechanism of burning rate catalysts, and unique features of combustion with BAMO-THF and NMMO binders. The binder studies were somewhat limited because the materials became available only late in the program.

Figure 8 summarizes the key features of the combustion zone of sandwiches with laminae of AP and organic binder, and will be used extensively in the following in explanation of the effect of catalysts and changes in fuel material. Figure 9 shows the burning rate of uncatalyzed PBAN sandwiches, to which the effects of catalysts and other binders are compared here.

#### Iron-containing Catalysts (PBAN Binder)

Several iron compounds have been used effectively to catalyze the burning rate of AP-HC binder propellants, and some preliminary studies (e.g., Ref. 4) have shown a similar catalysis of sandwich burning rate. In the present study the effect of  $\text{Fe}_2\text{O}_3$ ,  $\text{Fe}_3\text{O}_4$ , and catocene was studied with (usually) 10% catalyst added to the binder lamina (analogous to 1% in a propellant). Tests (combustion photography and interrupted burning) were run at 300, 500 and 1000 psi (room temperature). A range of binder lamina thickness from 25 - 150  $\mu\text{m}$  were used. The observable features (burning rate, surface profile and microscopic features) were documented and interpreted. The results with PBAN binder without, and with catalyst, included the following (described relative to the features in Fig. 8).



Principal features of the combustion zone microstructure and processes as suggested by accumulated results: 1) binder lamina; 2) interface plane between binder and oxidizer; 3) oxidizer surface adjoining binder-smooth band; 4) leading edge of the oxidizing burning front; 5) oxidizer region that regresses at the normal AP self-deflagration rate; 6) AP flame; 7) leading edge region of AP flame; 8) oxidizer flame, modified by the anomalous decomposition in the smooth band; 9) oxidizer-fuel diffusion region, with stoichiometric surface indicated by broken line; 10-11) kinetically limited leading edge flame (KLLEF) (fuel-rich and oxidizer-rich sides); 12) diffusion flame; 13) tip of diffusion flame

Fig. 8 Details of the flame complex (from Ref. 2).

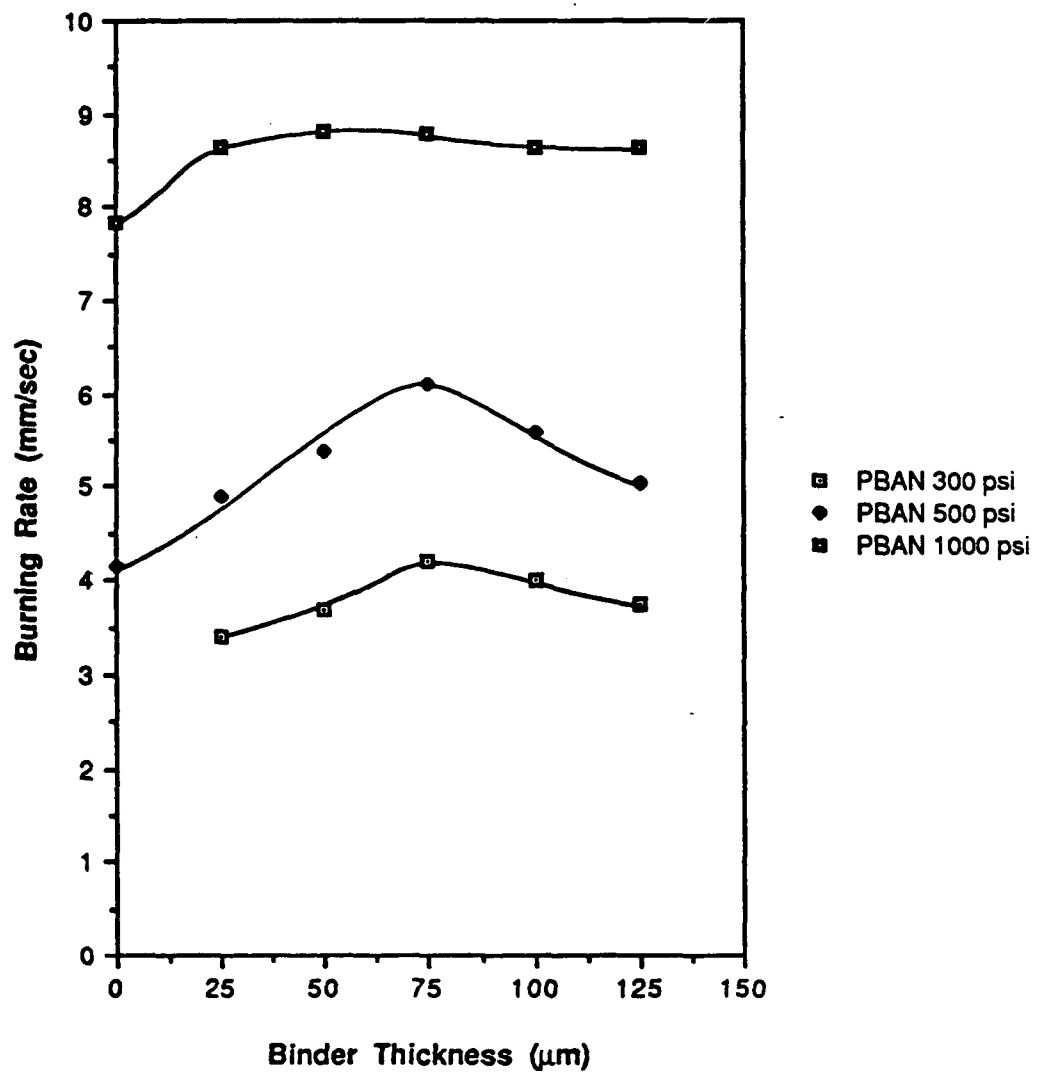


Fig. 9 Burning rate of AP/PBAN/AP sandwiches.

1. Surfaces of the AP laminae more than about 100  $\mu\text{m}$  from the binder burned in a manner similar to pure AP self deflagration ((5) in Fig. 8: i.e., the oxidizer-binder interaction is localized to a region close to the binder).
2. The sandwich burning rate was higher than the AP self deflagration rate, and always increased with the iron catalyst present. ( $300 \leq p \leq 1000$  psi)
3. The quenched samples were roughly "V" shaped on the macroscopic scale, with the angle of the "V" conforming to the relation

$$r_{\text{AP}}/r_{\text{sandw}} = \cos \theta$$

between the sandwich burning rate and the independently determined AP rate ( $\theta$  is the angle of inclination of the AP surface). However, the microscopic features of the surface close to the oxidizer-binder contact planes showed complicated variations indicative of the processes in the region of oxidizer-binder interaction, (1) to (4) in Fig. 8.

4. The burning rate with catalyst in the binder lamina was almost always higher than with no catalyst. The rate always showed a maximum at a particular intermediate binder lamina thickness (Fig. 9 shows results for no catalyst, and Fig. 10 shows typical results for a catalyzed binder.)
5. Catalyzed samples generally showed concentration of iron oxide on the binder surfaces (even with catocene). Under certain special conditions where concentration did not occur, burning rate was not enhanced. The oxide concentrate was determined to be primarily  $\text{Fe}_3\text{O}_4$  (post-test).
6. In no case was there evidence of burning down the oxidizer-binder contact surfaces ahead of adjoining binder (some results with propellants suggest that interface burning might become important at pressures below 50 psi or so (Ref. 5)).
7. In all cases there was a leading edge of the burning profile in the AP laminae ((4) in Fig. 8) with protrusion of the AP immediately adjacent to the contact planes ((3) in Fig. 8), accompanied by a region of relatively

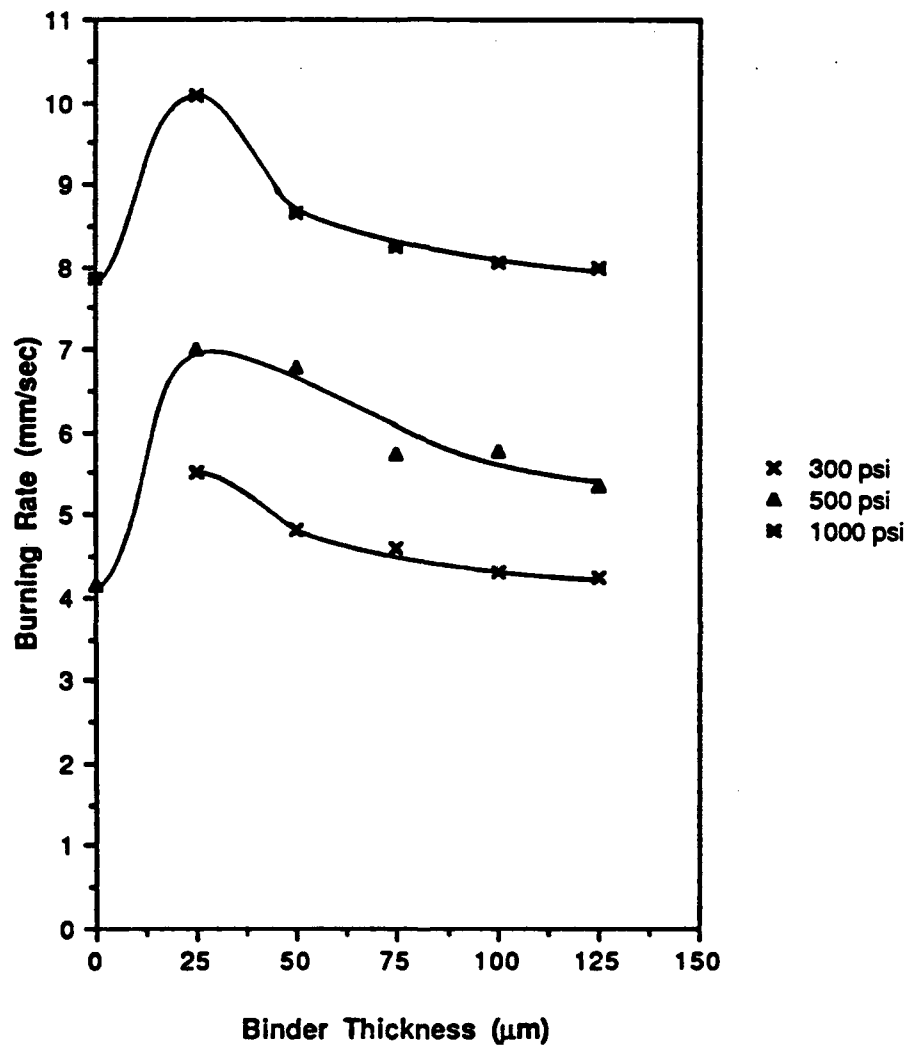


Fig. 10 Example of effect of catalyst on burning rate (10%  $\text{Fe}_3\text{O}_4$  in the binder lamina; compare with Fig. 9).

smooth AP surface between the contact plane and the leading edge. However, this "smooth band" region became narrower, with less protrusion of the AP under conditions that yielded high burning rate, degenerating down to a mere ledge of AP (concave upward) adjoining the contact plane in the fastest burning samples.

8. At 1000 psi the AP rate is comparable to the uncatalyzed sandwich rate (Fig. 10) and the macroscopic profile is relatively flat. With catalyst present, a "V" shaped profile was present, consistent with #3 above.
9. Rate enhancement by the catalysts was always less with thick binder laminae (Fig. 11 and App. A), a condition where the fuel supply for the KLEFs is high but advance of the flame closer to the surface to increase rate is impeded by high heat loss to the protruding binder lamina.

Interpretation of catalyst effects will be made below as a conclusion, based on the foregoing general observations of results and more detailed results (and arguments) in Appendix A. But before presenting the conclusion, it is helpful to note some features of the catalyst "situation" that have often been neglected in previous publications on the subject. Most studies have been made using particulate catalysts, which are ordinarily protected from contact with the oxidizer in the solid phase by encapsulating binder (i.e., catalytic interaction with AP is impeded). In addition, the low mobility in the condensed phase limits catalytic action on the binder as well (except with the liquid catalyst). Thus, the extent of condensed phase catalysis of binder decomposition is limited except in locations where concentration of the catalyst occurs (as it did with all catalysts at the binder surface, even with catocene). The effectiveness of catocene was not dramatically different from that of  $\text{Fe}_2\text{O}_3$  and  $\text{Fe}_3\text{O}_4$ , indicating that homogeneous distribution in the binder did not make possible condensed phase reactions of importance that might be impeded by heterogeneity with particulate catalysts. It should be noted that the opportunity for particulate catalysts to act in the gas phase is also limited, by the low collision probability of gas phase molecules in the short time between release of a catalyst particle from the surface and the time the particle has passed the burning rate-controlling parts of the gas phase flame.

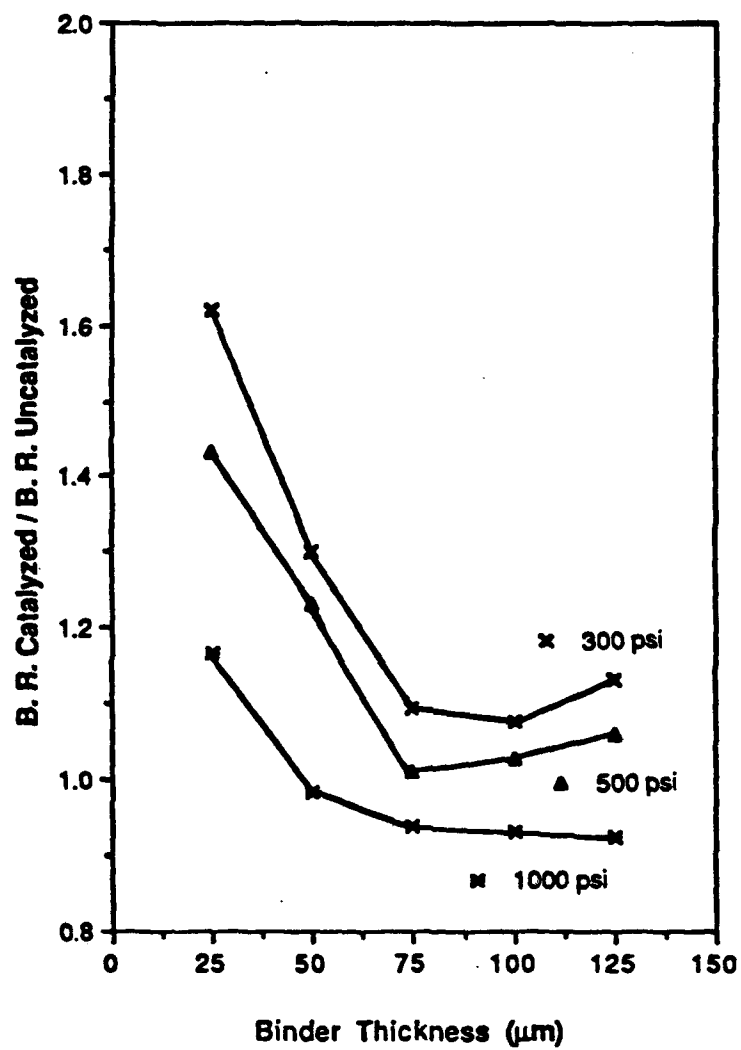


Fig. 11 Ratio of catalyzed and uncatalyzed burning rates for AP/PBAN/-AP sandwiches ( $\text{Fe}_3\text{O}_4$  catalyst).

It is argued here that under the conditions of this study, the primary action of the catalyst is in "cracking" large fuel molecules released in the binder decomposition. This is aided by the formation of a catalyst layer on the binder surface, through which fuel molecules must pass, thus optimizing the opportunity for catalysis. This breakdown of the heavy fuel molecules is necessary to establish an oxidizer-fuel flame, and the catalytic breakdown enables that high temperature flame to be established closer to the surface with a corresponding increase in burning rate. This scenario is supported by so many detailed results (App. A, Ref. 6, 7) that it may be considered to be "proven" as conclusively as anything ever is in this microscopic propellant flame "world" where proof by direct measurements of details can't be made. The mechanisms involved are equally applicable for AP-HC binder propellants (in the same pressure range), so that the same catalytic effects are observed in propellants as in sandwiches. Rather different scenarios may be applicable under conditions where the O/F flame is less important to control of burning rate (e.g., at very low pressure where flameless burning occurs without catalysts, or at high pressures where the AP self deflagration dominates burning).

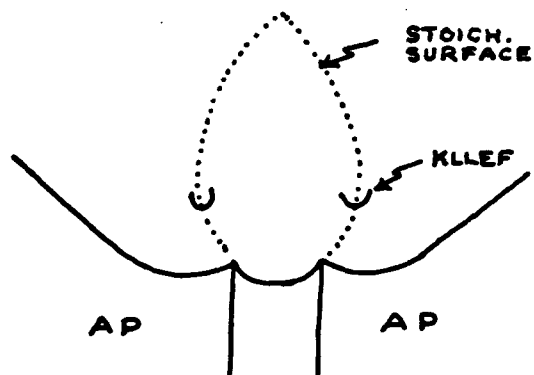
#### Sandwiches with Other Binders (Non-catalyzed)

During this study two new binder materials became available that had not yet been evaluated in propellants, but looked promising in some Navy applications. While AP was not the optimum oxidizer for use with these binders, use of more promising oxidizers was compromised by safety considerations, and the extensive background with AP sandwiches offered a good framework in which to judge the combustion behavior of the new binders, and at the same time to extend the sandwich burning theory to new-fuel situations. Accordingly, a limited set of tests analogous to the AP/PBAN ones were run with BAMO-THF binder and NMMO binder in place of PBAN. The detailed results are contained in Appendix A.

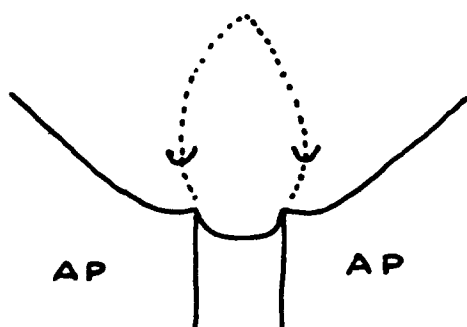
Before discussing the test results for the new binders, some comments about binders are in order. Both BAMO-THF and NMMO decomposed at lower temperature than PBAN. While PBAN decomposition is endothermic, BAMO-THF is slightly exothermic and NMMO more so. Compared to PBAN, both are dilute fuels, NMMO being the most dilute. All three have about the same stoichiometric flame temperature with AP

/NMMO a little "cooler." Upon heating, BAMO-THF loses nitrogen at a temperature where it is in a melt state, resulting in a bubbling surface. From these characteristics, one would expect certain changes in details of sandwich burning with AP. A more dilute fuel causes the stoichiometric surface of the O-F mixing fan (Fig. 12a) to be shifted toward the fuel flow (Fig. 12b), causing the KLLEF to be shifted similarly. Thus the KLLEFs supply more of their heat to the fuel surface, lessening the lateral heat flow from the oxidizer lamina to the binder lamina, and hence reducing the usual protrusion of AP near the contact plane. This effect is further enhanced by low heat requirement for decomposition (due to binder exothermicity and low decomposition temperature). The binder is expected to be more recessed, a condition that further decreases lateral heat flow from the hotter AP surface layer to the binder, further decreasing the protrusion of AP at the contact plane. If the binder is strongly exothermic, it will heat the AP instead, leading to an entirely different surface profile (Fig. 12c), in which heat flow from the binder to the AP retards a rate that is dominated by the binder; the binder regression will be retarded near the contact plane and have a concave surface. If the (now fast burning) binder lamina is thick enough, it will not be retarded at its center by lateral heat loss to the AP and will burn at its own rate. Under these conditions the KLLEFs cease to be important factors in the burning rate, but will still affect the details of the surface profile near the contact plane. However, the KLLEF is relatively less important because it involves less heat release and is poorly located when more of the heat release has occurred in the binder decomposition. As will be seen, none of the binders used was sufficiently exothermic to have the rate dominated by binder heat release.

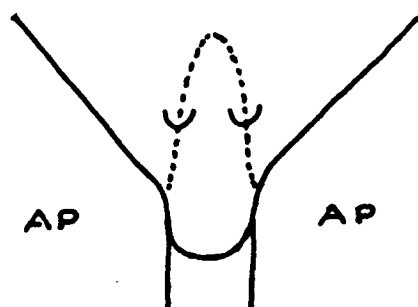
The foregoing scenario is based on physical reasoning, but was constructed under the stimulus of emerging experimental results with the new binders and comparison with earlier results with PBAN binder. This is illustrated by Fig. 13 and 14, which show the burning rate for the three binders (NMMO was tested at only 2 pressures). Referring to Fig. 13, the opposing effects of mild exothermicity of BAMO-THF and its lower fuel content result in only small change in burning rate relative to PBAN under most conditions. With thick binder laminae, the rate with BAMO-THF was higher because the effect of the low fuel



12a  
Endothermic binder,  
high fuel value



12b  
Easily pyrolyzed,  
slightly exothermic  
binder, intermediate  
fuel value



12c  
Easily pyrolyzed,  
exothermic binder,  
relatively low  
fuel value

Fig. 12 Sketch indicating the expected effect of fuel value of the binder material on the flame complex (e.g., PBAN is a concentrated fuel, BAMO-THF a relatively dilute fuel).

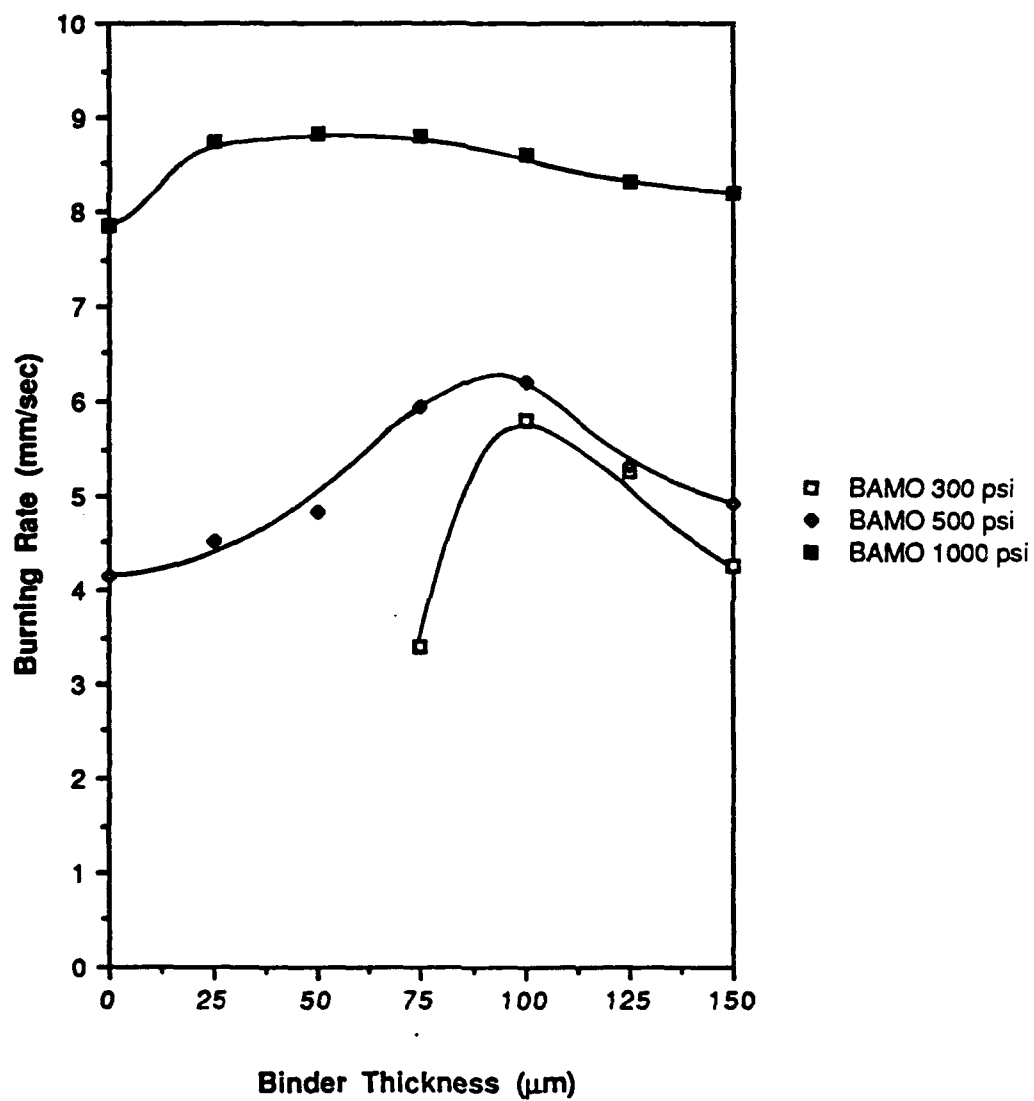


Fig. 13 Burning rate of AP/BAMO-THF/AP sandwiches.

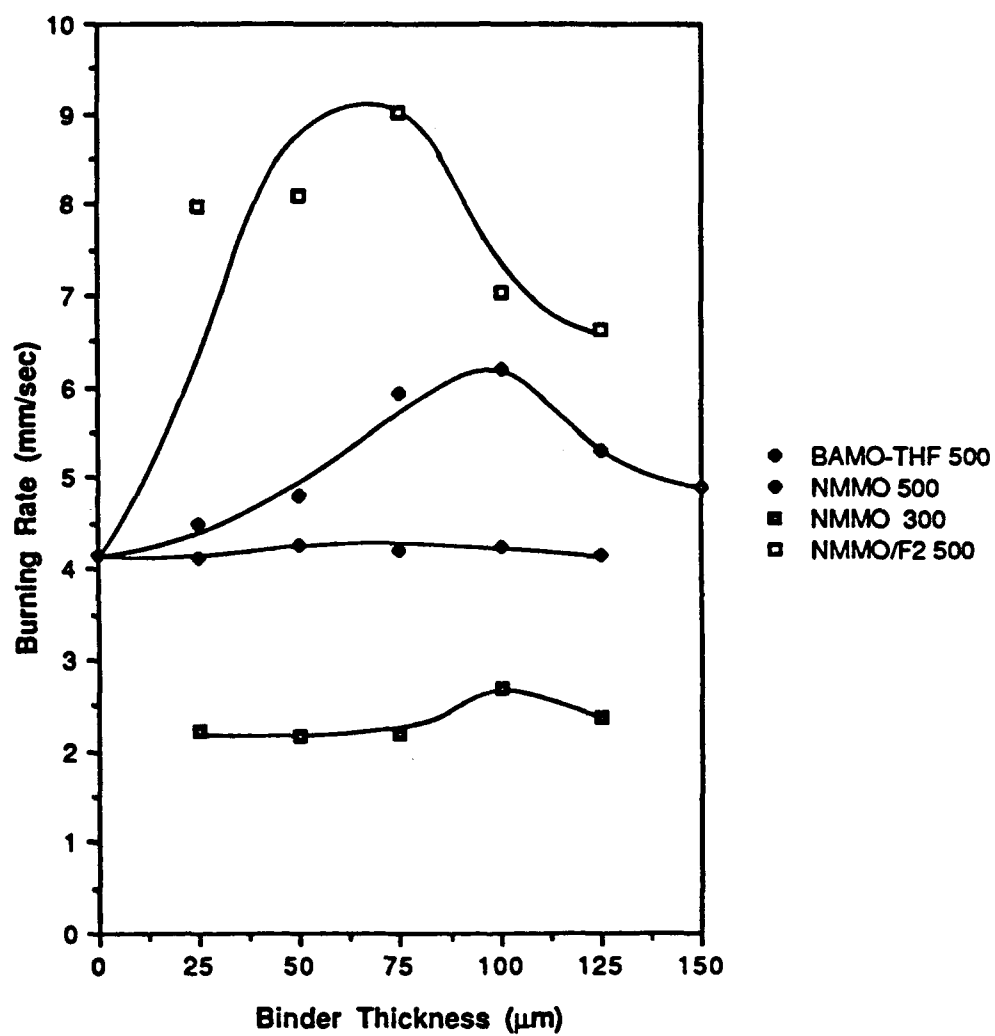


Fig. 14 Burning rate of AP/NMMO/AP sandwiches.

value is compensated for by an excess of fuel present.\* At lower pressures, where rate is particularly dependent on the O-F flame, the dilute fuel effect of BAMO/THF led to lower rate under fuel-deficient thin binder conditions (thin binder samples would not burn at all at 300 psi). The observations of quenched samples and flame photography support the above interpretations. In general, the burning rate is strongly affected by the leading edge of the O-F flame with BAMO-THF as in the case of PBAN binder, with the fuel exothermicity playing an important role only under conditions of low pressure and thick binder where the AP deflagration is marginal, the fuel supply for the KLLEF is plentiful, and the mild binder exothermicity is relatively more important. The burning rate was conspicuously higher than with PBAN under these low pressure conditions, to a degree that remains unexplained. The shift in the maximum of the rate curve to greater lamina thickness with BAMO-THF probably reflects the lower fuel value compared to PBAN (the maximum results from an optimum in a trade-off between heat loss to the binder lamina (low with thin laminae) and fuel deficiency (severe with thin laminae)).

From the comparison of burning rates with PBAN and NMMO binder in Fig. 14, the rate with NMMO is conspicuously lower. Further, the sandwich rates with NMMO are nearly independent of lamina thickness and equal to the rate of the AP lamina, a result that suggests that the rate is not appreciably affected by either the KLLEFs or the exothermicity of the NMMO decomposition. The apparently negligible contribution of the KLLEFs implies large standoff distance, which in turn implies low reaction rates between the initial oxidizer and binder decomposition products. The exothermicity of the binder decomposition was not enough to affect the sandwich rate, although it might be important in a conventional propellant where rate is determined in part by the time required to burn through binder membranes between AP particles. The results would suggest that such a propellant might not burn below the AP self deflagration limit (just below 300 psi) because of the limited contribution of the KLLEFs to the surface heat balance.

---

\* This effect was particularly conspicuous at low pressure, suggesting that fuel exothermicity was an important factor under these marginal burning conditions.

### Iron-containing Catalysts (BAMO-THF and NMMO binders)

In general, the effect of the catalysts on burning rate was the same with BAMO-THF as with PBAN, with a large rate enhancement at low binder thicknesses (notably in the domain where the KLLEFs are coupled, fuel supply is less than optimum and heat loss to the binder lamina is recovered in the coupled KLLEFs (Fig. 15). Under these conditions, catalytic breakdown of the fuel can be accompanied by positioning of the KLLEFs closer to the surface, and correspondingly increasing burning rate. As noted above, this is impeded at high binder thicknesses by the presence of a protruding binder lamina and separation of the KLLEFs, with heat losses to the excess binder that does not support the KLLEFs (Fig. 16).

Figure 17 shows the burning rates of uncatalyzed and  $\text{Fe}_3\text{O}_4$  catalyzed BAMO-THF sandwiches, and Fig. 18 shows the results as ratio of catalyzed rate to uncatalyzed rate. A similar graph for PBAN sandwiches is shown in Fig. 11 for comparison. Note that the catalyst enhances the rate of the BAMO-THF sandwiches more than the PBAN sandwiches. This was true under most conditions tested for all three of the catalysts, a point of some practical importance. The reason for greater catalyst effect with BAMO-THF is not unambiguously established. However, it is notable that the catalyzed PBAN rate curves in  $\text{Fe}_2\text{O}_3$  and  $\text{Fe}_3\text{O}_4$  (e.g., Fig. 19a) peak at a much lower binder lamina thickness than the catalyzed BAMO-THF rate curves (Fig. 19b) (roughly 25  $\mu\text{m}$  vs 70  $\mu\text{m}$ ). The drop-off in rate at higher lamina thickness has to this point been attributed to the increasing heat "loss" from the KLLEF to the thick (and protruding) binder lamina. In the case of BAMO-THF, this effect is less significant because the binder is more easily pyrolyzed and doesn't protrude under most conditions. Thus the decline in rate due to heat loss is reached at a greater lamina thickness. This contrast between PBAN and BAMO-THF sandwich rate was less conspicuous for uncatalyzed sandwiches (Fig. 20).

The greater rate enhancement by catalysts with BAMO-THF binder is presumably at least in part due to reduced heat requirement to pyrolyze the binder, which causes it to be more recessed than with PBAN, with correspondingly less lateral heat drain from the rate controlling region in the AP into the binder. However, there are other relevant factors whose importance is still unknown. There is not

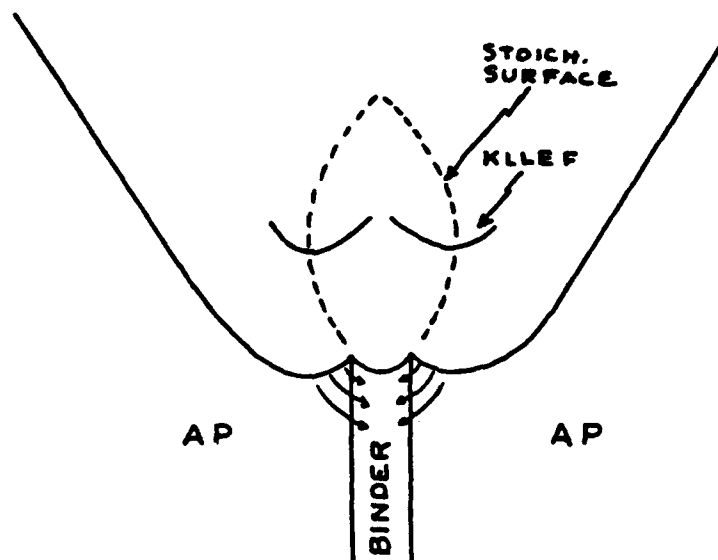


Fig. 15 Flame complex for thin-binder sandwich: lateral heat flow from AP to binder is limited by low binder mass; fuel vapor flow just sufficient to support KLLEFs.

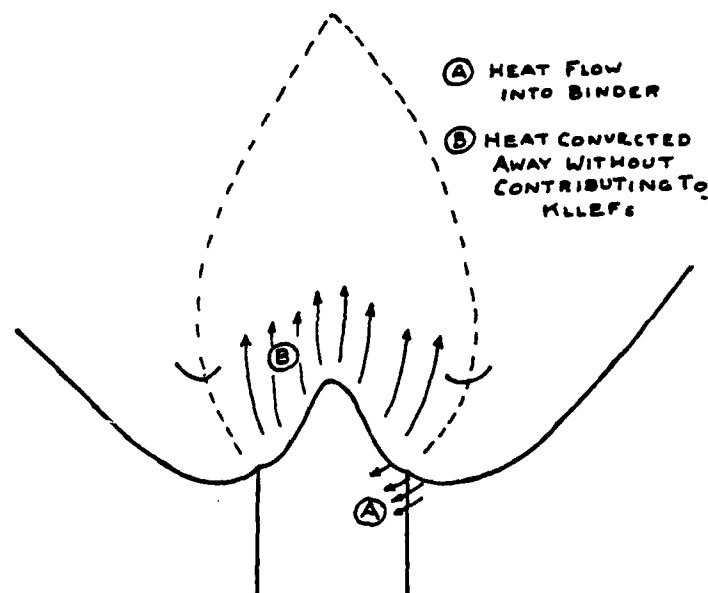


Fig. 16 Flame complex for thick-binder sandwich: relatively large lateral heat flow from AP to binder; not all needed for fuel supply to the KLLEFs, and convected out of the burning-rate controlling region before producing any heat release.

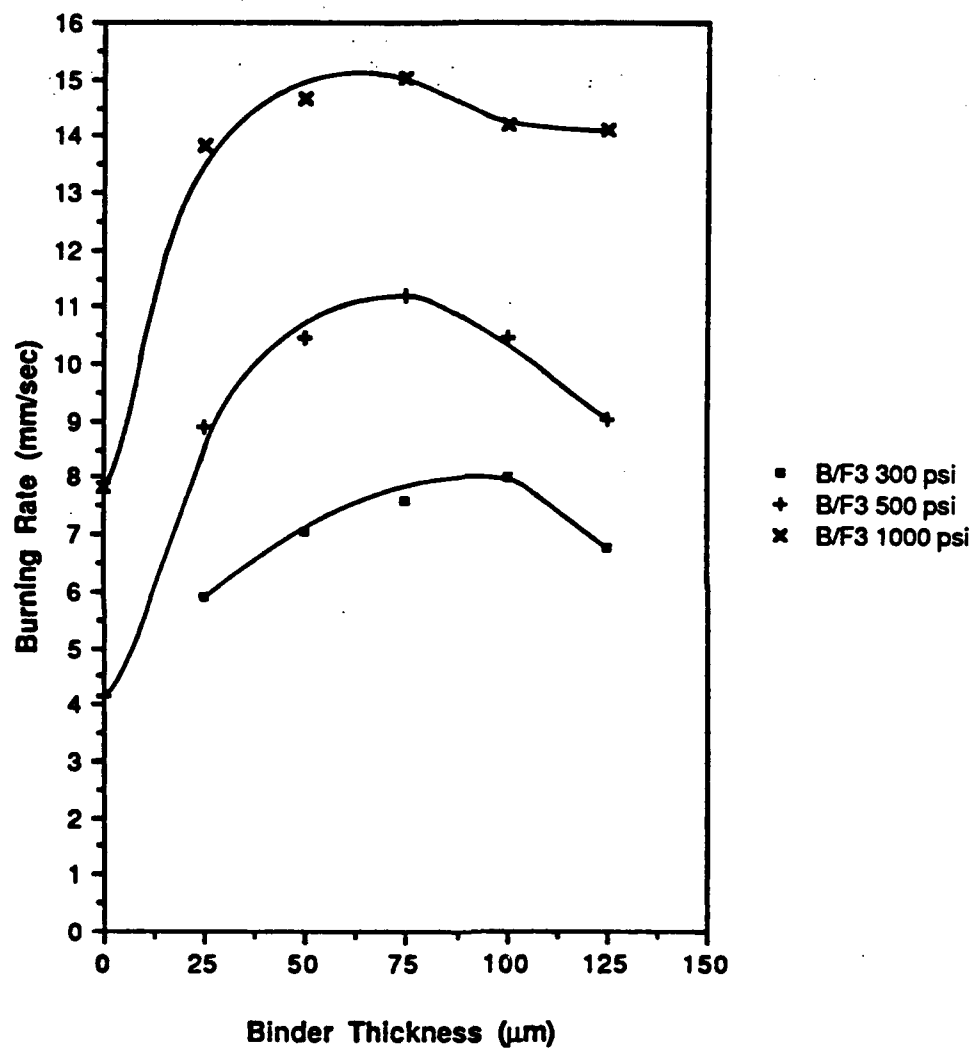


Fig. 17 Burning rate of AP/BAMO-THF/AP sandwiches with 10%  $\text{Fe}_3\text{O}_4$  in the BAMO-THF.

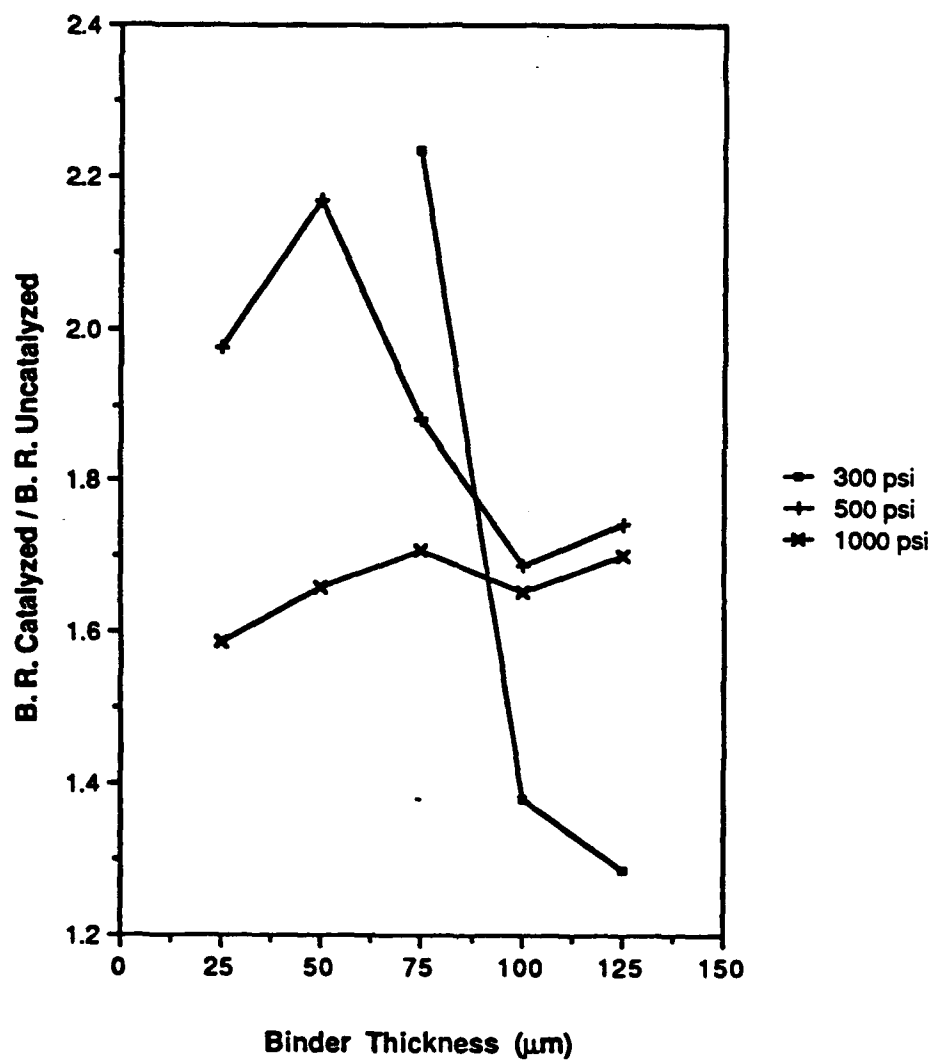


Fig. 18 Ratio of burning rates for BAMO-THF with and without catalyst ( $\text{Fe}_3\text{O}_4$ ) (compare with Fig. 11 for PBAN).

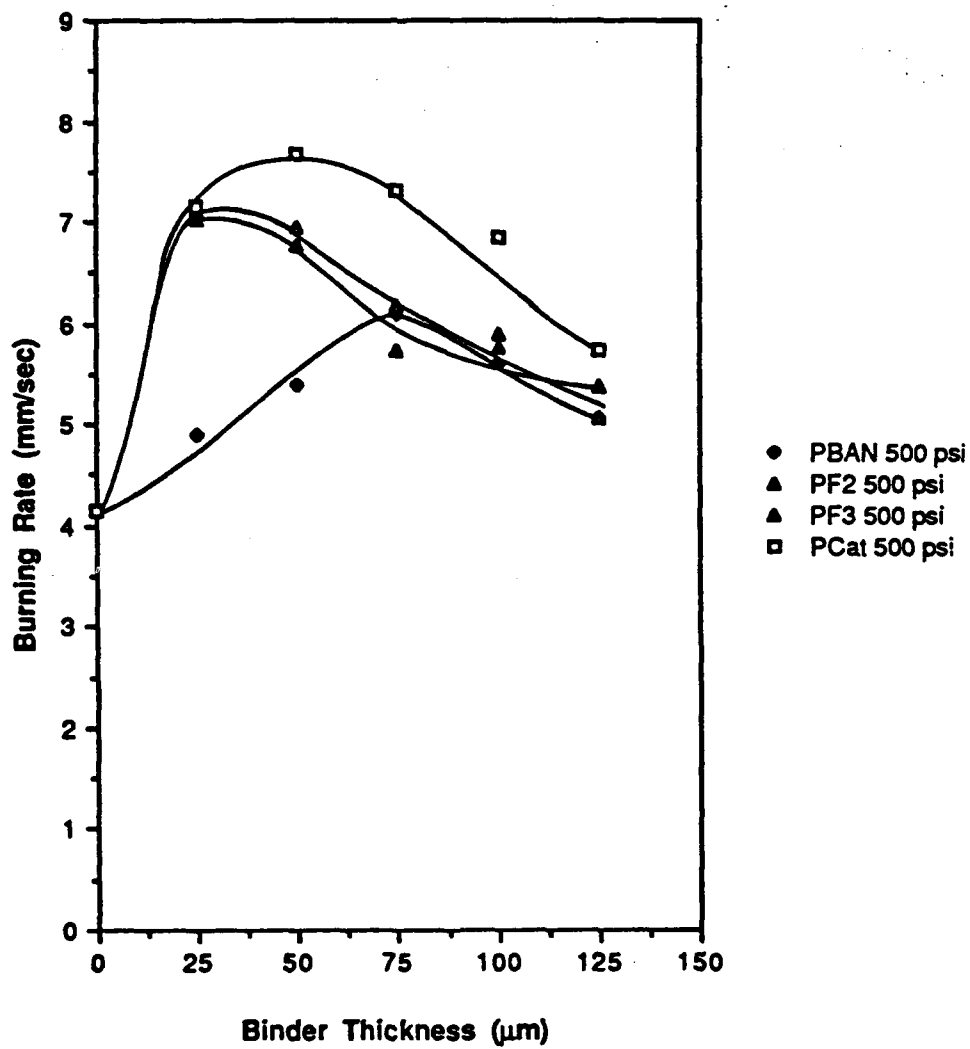


Fig. 19 Comparison of effect of catalysts on burning rate for PBAN and BAMO-THF sandwiches at 500 psi.

a) PBAN with three different catalysts.

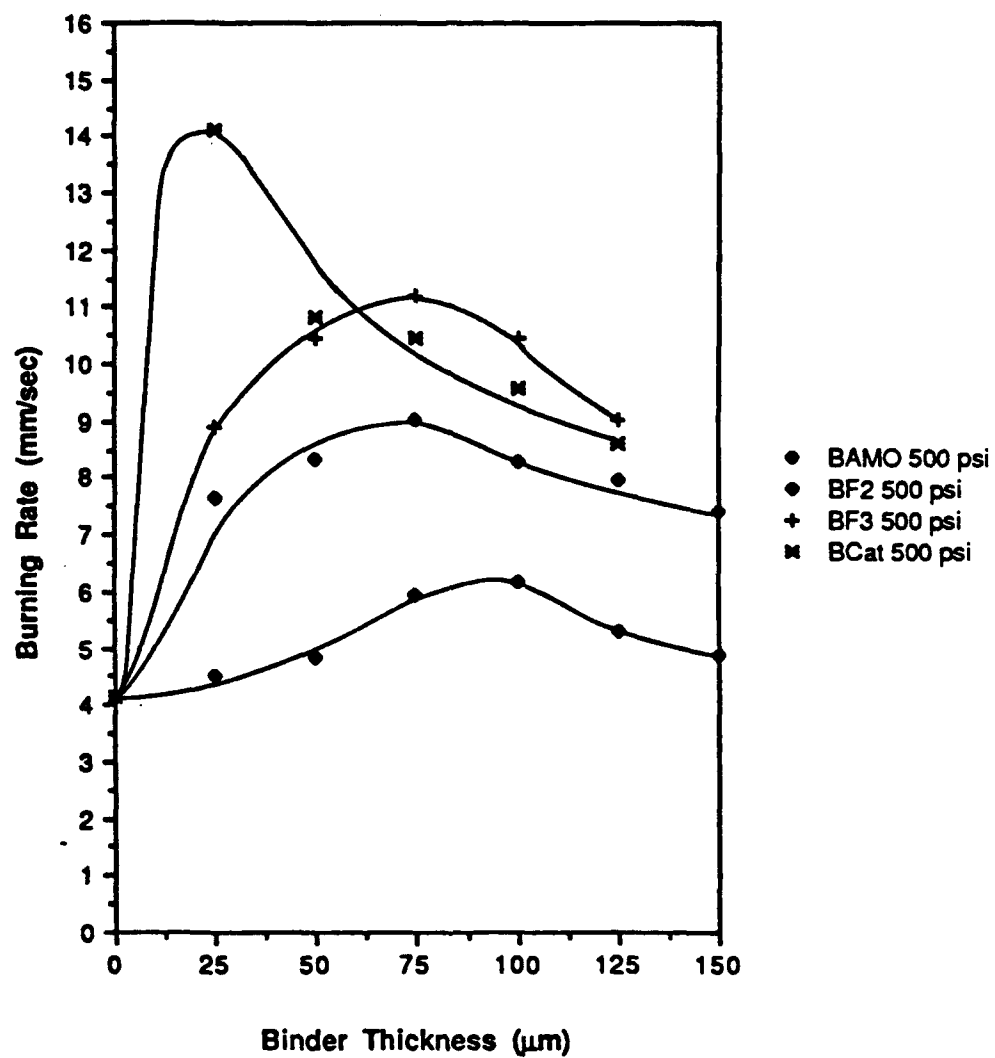


Fig. 19 Comparison of effect of catalysts on burning rate for PBAN and BAMO-THF sandwiches at 500 psi.

b) BAMO-THF with three different catalysts.

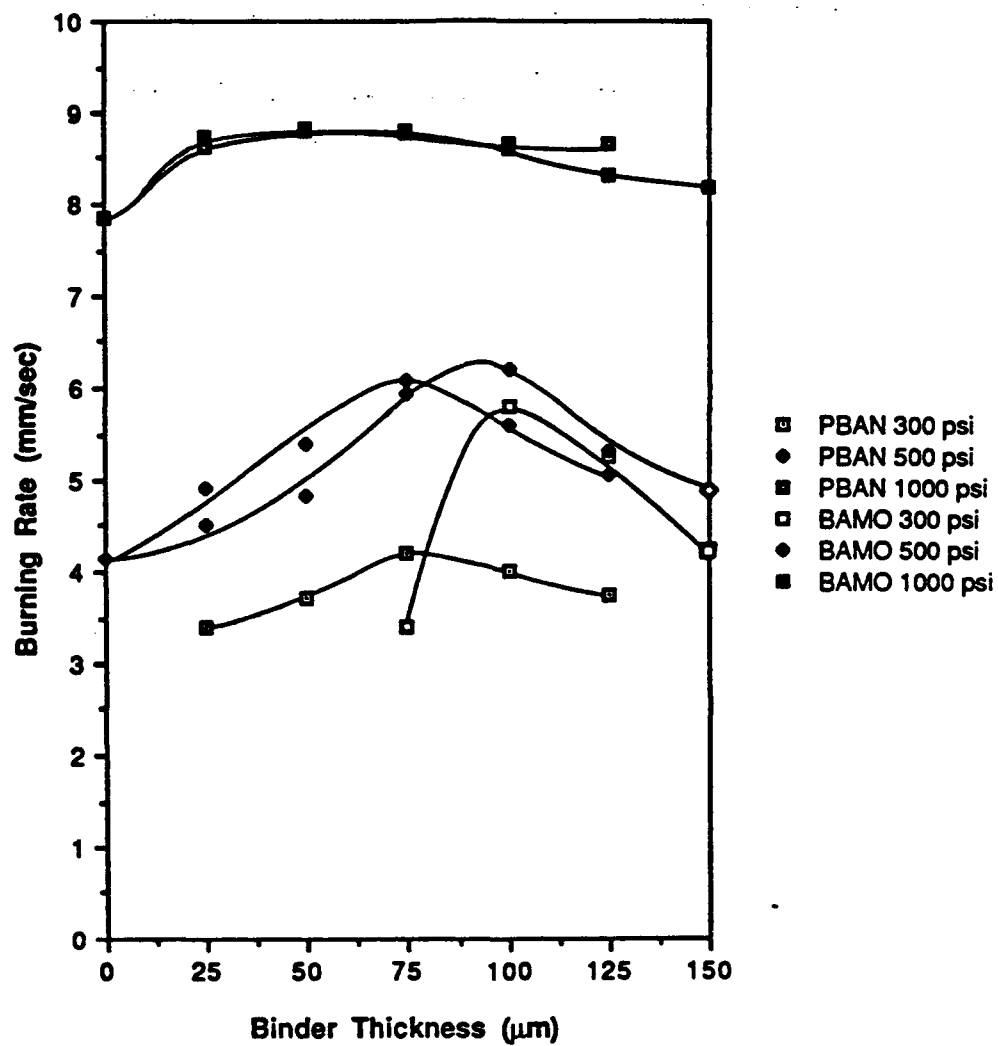


Fig. 20 Comparison of burning rates of uncatalyzed sandwiches.

sufficient data on the extent of the catalyst concentration on the surface, and little information about the nature of the fuel vapors or the catalyst interaction with them. These aspects of the process may differ with kind of binder, kind of catalyst, pressure, and binder lamina thickness. However, all of the catalysts formed surface concentrations of iron oxide on the binder and enhanced burning rate, under all conditions, except under isolated conditions when no surface concentration was evident.

The tests with NMMO + catalyst were limited by available time to one pressure and one catalyst. The burning rate data are included in Fig. 14. Noting there the result described earlier for uncatalyzed NMMO, the effect of the catalyst was dramatic. This result is consistent with the earlier speculation that with pure NMMO binder, the KLLEFs are remote from the surface due to "slow kinetics" of the reactions in the mixing fan, but that the binder vapor decomposition is catalyzed by the concentrated catalyst layer on the surface, enabling the KLLEFs to be established close to the surface. The effect is more dramatic in the case of NMMO because the rate was so low without catalyst. In terms of an NMMO/AP propellant, a catalyst may be very important to achievement of favorable ballistics.

#### REFERENCES

1. Price, E.W., Sigman, R.K., and deGroot, W.A., "Instrumentation for a High Temperature Decomposition Facility," Final Report on Contract N00014-87-G-0035 to Office of Naval Research, School of Aerospace Engineering, Georgia Institute of Technology, Atlanta, GA, May 1988.
2. Price, E.W., Sambamurthi, J.K., Sigman, R.K., and Panyam, R.R., "Combustion of Ammonium Perchlorate-Polymer Sandwiches," Combustion and Flame, Vol. 63, pp. 381-413, 1986.
3. Price, E.W., Handley, J.C., Panyam, R.R., Sigman, R.K., and Ghosh, A., "Combustion of Ammonium Perchlorate-Polymer Sandwiches," AIAA Journal, Vol. 19, pp. 380-386, 1981.
4. Handley, J.C., and Strahle, W.C., "Behavior of Several Catalysts in the Combustion of Solid Propellant Sandwiches," AIAA Journal, Vol. 13, pp. 5-6, 1975.
5. Krishnan, S., and Periasamy, C., "Low-Pressure Burning of Catalyzed Composite Propellants," AIAA Journal, Vol. 24, pp. 1670-1675, 1986.
6. Price, E.W., and Sambamurthi, J.K., "Mechanism of Burning Rate Enhancement by Ferric Oxide," CPIA Publication No. 412, Vol. I, 1984.
7. Price, E.W., Sambamurthi, J.K., and Sigman, R.K., "Further Results on the Combustion Behavior of AP/Polymer Sandwiches with Additives," CPIA Publication No. 432, Vol. I, 1985.

APPENDIX A

EFFECT OF DIFFERENT BINDERS AND ADDITIVES  
ON SANDWICH BURNING

by Christos P. Markou

Ph.D. Thesis, November 1988  
Georgia Institute of Technology

-

**EFFECT OF DIFFERENT BINDERS AND ADDITIVES  
ON  
SANDWICH BURNING**

**A THESIS  
Presented to  
The Faculty of the Division of Graduate Studies**

**By  
Christee P. Markou**

**In Partial Fulfillment  
of the Requirements for the Degree  
Doctor of Philosophy in Aerospace Engineering**

**Georgia Institute of Technology  
November, 1988**

**EFFECT OF DIFFERENT BINDERS AND ADDITIVES  
ON  
SANDWICH BURNING**

**Approved**

**Edward W. Price, Chairman**

**Warren C. Strahle**

**Robert E. Sigman**

**Date Approved by Chairman**

## TABLE OF CONTENTS

Acknowledgements.....	page ii
List of Tables.....	vi
List of Illustrations.....	vii
List of Abbreviations.....	xiii
Summary.....	xiv
<b>I. INTRODUCTION.....</b>	<b>1</b>
1.1 Literature Survey.....	1
1.1.1 Background.....	1
1.1.2 Literature Review on Theoretical Models.....	4
1.1.3 The Oxidizer - Binder Sandwich Approach.....	10
1.1.4 Literature Review on Sandwich Burning.....	14
1.1.5 Literature Review on the Effect of Additives.....	27
1.2 Objectives of the Research.....	40
<b>II. EXPERIMENTAL PROCEDURE.....</b>	<b>43</b>
2.1 Overview.....	43
2.2 Experimental Techniques.....	44
2.2.1 Combustion Photography.....	44
2.2.2 Quench Burning Method.....	46

2.2.3 Sandwich Preparation.....	46
2.2.4 Optical Microscope Studies.....	47
2.2.5 Scanning Electron Microscope Studies.....	48
2.2.6 Laser Pyrolysis.....	49
<b>III. EXPERIMENTAL STRATEGY.....</b>	<b>50</b>
<b>IV. EXPERIMENTAL RESULTS.....</b>	<b>55</b>
4.1 Burning Rate and Movie Studies.....	55
4.1.1 Pure Binder Sandwiches.....	56
4.1.1.1 Motion Picture Study: BAMO-THF.....	56
4.1.1.2 Burning Rate Study: BAMO-THF.....	57
4.1.1.3 Exploratory Study of NMMO.....	59
4.1.2 Catalyzed Binder Sandwiches: Fe <sub>2</sub> O <sub>3</sub> .....	60
4.1.2.1 Effect on PBAN Sandwiches.....	60
4.1.2.2 Effect on BAMO-THF Sandwiches.....	61
4.1.2.3 Comparison of effects on PBAN and BAMO-THF Binders.....	62
4.1.2.4 Effect on NMMO Sandwiches.....	62
4.1.3 Catalyzed Binder Sandwiches: Fe <sub>3</sub> O <sub>4</sub> .....	63
4.1.3.1 Effect on PBAN Sandwiches.....	63
4.1.3.2 Effect on BAMO-THF Sandwiches.....	64
4.1.3.3 Comparison of effects on PBAN and BAMO-THF Binders.....	65
4.1.4 Catalyzed Binder Sandwiches: Catocene.....	65
4.1.4.1 Effect on PBAN Sandwiches.....	65
4.1.4.2 Effect on BAMO-THF Sandwiches.....	66
4.1.4.3 Comparison of effects on PBAN and BAMO-THF Binders.....	67

4.1.5 Comparison of effects of all catalysts on PBAN.....	68
4.1.6 Comparison of effects of all catalysts on BAMO-THF.....	68
4.1.7 Conclusion of effect of additives on the burning rate of sandwiches and the visible combustion zone.....	69
4.1.8 Pressure dependency of the burning rate of sandwiches.....	70
4.2 Studies of Quenched Sandwiches.....	72
4.2.1 Pure Binder Sandwiches.....	73
4.2.1.1 BAMO-THF.....	73
4.2.1.2 NMMO.....	75
4.2.2 Catalyzed Binder Sandwiches: Fe <sub>2</sub> O <sub>3</sub> .....	76
4.2.2.1 Effect on PBAN Sandwiches.....	76
4.2.2.2 Effect on BAMO-THF Sandwiches.....	77
4.2.3 Catalyzed Binder Sandwiches: Fe <sub>3</sub> O <sub>4</sub> .....	78
4.2.3.1 Effect on PBAN Sandwiches.....	78
4.2.3.2 Effect on BAMO-THF Sandwiches.....	79
4.2.4 Catalyzed Binder Sandwiches: Catocene.....	80
4.2.4.1 Effect on PBAN Sandwiches.....	80
4.2.4.2 Effect on BAMO-THF Sandwiches.....	83
4.2.5 Further Observations on the Quenched Sandwich Surface.....	84
4.3 Study of Tapered Sandwiches.....	87
4.3.1 Pure Binder Tapered Sandwiches.....	87
4.3.2 Catalyzed Binder Tapered Sandwiches.....	88
4.4 Laser Studies.....	88
<b>V. DISCUSSION</b> .....	90
5.1 Theory of the Flame Complex.....	91

5.2 Binder Description.....	93
5.3 Possible Effects of Binder and Catalyst Variables on Sandwich Combustion based on Qualitatively Theory.....	94
5.3.1 Expected Effects of Binder Properties on Combustion.....	94
5.3.2 Expected Effects of Catalysts.....	98
5.4 Interpretation of Results.....	99
5.4.1 Comparison of BAMO-THF Binder Sandwich Results with PBAN.....	99
5.4.2 Comparison of NMMO Binder Sandwich Results with PBAN.....	101
5.4.3 Results of Catalyzed Sandwiches.....	102
5.5 Secondary Results.....	105
<b>VI. CONCLUSIONS AND RECOMMENDATIONS</b> .....	107
<b>APPENDIX</b>	
A. Preparation of Binders.....	193
B. Experimental Data.....	195
<b>BIBLIOGRAPHY</b> .....	203
<b>VITA</b>	

## LIST OF TABLES

Table	Page
5-1 Qualitative Comparison of Binder Decomposition Properties.....	94
1 Burning Rate Data.....	195
2 Burning Rate Ratio Data.....	200

## LIST OF ILLUSTRATIONS

Figure	Page
1-1 Oxidizer-Binder Sandwich.....	112
1-2 Multilayer Oxidizer-Binder Sandwich.....	113
1-3 Phalanx Flame at Steady State.....	114
1-4 Sketch of Individual Flame.....	115
1-5 Sketch of the "Cavity".....	115
1-6 Mechanisms Influencing Sandwich Regression.....	116
1-7 Analytical Sandwich Combustion Model.....	117
1-8 Flame Structure.....	118
1-9 Tapered Oxidizer-Binder Sandwich.....	119
1-10 Sketch of Diffusion Flamelets from an AP-Binder Tapered Sandwich.....	119
1-11 Structure of the Sandwich Combustion Zone.....	120
1-12 Model of Burning down the Interface between an Oxidizer and a Fuel Slab... 121	
1-13 Principal Features of the Combustion Zone Microstructure.....	122
2-1 Experimental Procedure.....	123
4-1 Burning Rate of PBAN Sandwiches.....	124
4-2 Burning Rate of BAMO-THF Sandwiches.....	125
4-3 PBAN & BAMO-THF: Burning Rate Comparison.....	126
4-4 Some Details observed during Sandwich Burning.....	127
4-5 Burning Rate of NMMO Sandwiches.....	128

4-6 Burning Rate of PBAN + 10% Fe <sub>2</sub> O <sub>3</sub> Sandwiches.....	129
4-7 PBAN: Burning Rate Ratios (Fe <sub>2</sub> O <sub>3</sub> case).....	130
4-8 Burning Rate of Catalyzed and Uncatalyzed PBAN at 300 psi.....	131
4-9 Burning Rate of Catalyzed and Uncatalyzed PBAN at 500 psi.....	132
4-10 Burning Rate of Catalyzed and Uncatalyzed PBAN at 1000 psi.....	133
4-11 Burning Rate of BAMO-THF + 10% Fe <sub>2</sub> O <sub>3</sub> Sandwiches.....	134
4-12 BAMO-THF: Burning Rate Ratios (Fe <sub>2</sub> O <sub>3</sub> case).....	135
4-13 Burning Rate of Catalyzed and Uncatalyzed BAMO-THF at 300 psi.....	136
4-14 Burning Rate of Catalyzed and Uncatalyzed BAMO-THF at 500 psi.....	137
4-15 Burning Rate of Catalyzed and Uncatalyzed BAMO-THF at 1000 psi.....	138
4-16 Effect of Fe <sub>2</sub> O <sub>3</sub> on both binders at 300 psi.....	139
4-17 Effect of Fe <sub>2</sub> O <sub>3</sub> on both binders at 500 psi.....	140
4-18 Effect of Fe <sub>2</sub> O <sub>3</sub> on both binders at 1000 psi.....	141
4-19 Burning Rate of PBAN + 10% Fe <sub>3</sub> O <sub>4</sub> Sandwiches.....	142
4-20 PBAN: Burning Rate Ratios (Fe <sub>3</sub> O <sub>4</sub> case).....	143
4-21 Burning Rate of BAMO-THF + 10% Fe <sub>3</sub> O <sub>4</sub> Sandwiches.....	144
4-22 BAMO-THF: Burning Rate Ratios (Fe <sub>3</sub> O <sub>4</sub> case).....	145
4-23 Effect of Fe <sub>3</sub> O <sub>4</sub> on both binders at 300 psi.....	146
4-24 Effect of Fe <sub>3</sub> O <sub>4</sub> on both binders at 500 psi.....	147
4-25 Effect of Fe <sub>3</sub> O <sub>4</sub> on both binders at 1000 psi.....	148
4-26 Burning Rate of PBAN + 20% Catocene Sandwiches.....	149
4-27 PBAN: Burning Rate Ratios (Catocene case).....	150
4-28 Burning Rate of BAMO-THF + 20% Catocene Sandwiches.....	151
4-29 BAMO-THF: Burning Rate Ratios (Catocene case).....	152
4-30 Effect of Catocene on both binders at 300 psi.....	153

4-31 Effect of Catocene on both binders at 500 psi.....	154
4-32 Effect of Catocene on both binders at 1000 psi.....	155
4-33 PBAN: Effects of Catalysts at 300 psi.....	156
4-34 PBAN: Effects of Catalysts at 500 psi.....	157
4-35 PBAN: Effects of Catalysts at 1000 psi.....	158
4-36 BAMO-THF: Effects of Catalysts at 300 psi.....	159
4-37 BAMO-THF: Effects of Catalysts at 500 psi.....	160
4-38 BAMO-THF: Effects of Catalysts at 1000 psi.....	161
4-39 Burning Rate vs. Pressure.....	162
4-40 Maximum Burning Rate vs. Pressure: PBAN Sandwiches.....	163
4-41 Maximum Burning Rate vs. Pressure: BAMO-THF Sandwiches.....	164
4-42 Burning Rate vs. Pressure: Thick PBAN case.....	165
4-43 Burning Rate vs. Pressure: Thick BAMO-THF case.....	166
4-44 Quenched Surface Details of: a) A Composite Solid Propellant b) An AP/Binder+AP filled Sandwich.....	167
4-45 Dependence of the Surface Profile of PBAN Binder Sandwich on Pressure for various Binder Lamina Thickness.....	168
4-46 Quenched Surface of a PBAN Binder Sandwich.....	169
4-47 Dependence of the Surface Profile of BAMO-THF Binder Sandwich on Pressure for various Binder Lamina Thickness.....	170
4-48 Quenched Surface of a BAMO-THF Binder Sandwich.....	171
4-49 Quenched Surface of a NMMO Binder Sandwich.....	172
4-50 Dependence of the Surface Profile of PBAN + 10% Fe <sub>2</sub> O <sub>3</sub> Binder Sandwich on Pressure for various Binder Lamina Thickness.....	173
4-51 Quenched Surface of a PBAN + 10% Fe <sub>2</sub> O <sub>3</sub> Binder Sandwich.....	174

4-52 Dependence of the Surface Profile of BAMO-THF + 10% Fe <sub>2</sub> O <sub>3</sub> Binder	
Sandwich on Pressure for various Binder Lamina Thickness.....	175
4-53 Quenched Surface of a BAMO-THF + 10% Fe <sub>2</sub> O <sub>3</sub> Binder Sandwich.....	176
4-54 Dependence of the Surface Profile of PBAN + 10% Fe <sub>3</sub> O <sub>4</sub> Binder	
Sandwich on Pressure for various Binder Lamina Thickness.....	177
4-55 Quenched Surface of a PBAN + 10% Fe <sub>3</sub> O <sub>4</sub> Binder Sandwich.....	178
4-56 Dependence of the Surface Profile of BAMO-THF + 10% Fe <sub>3</sub> O <sub>4</sub> Binder	
Sandwich on Pressure for various Binder Lamina Thickness.....	179
4-57 Quenched Surface of a BAMO-THF + 10% Fe <sub>3</sub> O <sub>4</sub> Binder Sandwich.....	180
4-58 Dependence of the Surface Profile of PBAN + 20% Carocene Binder	
Sandwich on Pressure for various Binder Lamina Thickness.....	181
4-59 Quenched Surface of a PBAN + 20% Carocene Binder Sandwich.....	182
4-60 Dependence of the Surface Profile of BAMO-THF + 20% Carocene Binder	
Sandwich on Pressure for various Binder Lamina Thickness.....	183
4-61 Quenched Surface of a BAMO-THF + 20% Carocene Binder Sandwich.....	184
4-62 Spontaneous Quench Limits for Tapered Sandwiches Burning at	
Constant Pressure.....	185
5-1 Details of the Surface Profile and the Flame Structure at Different Pressures	
(Binder Lamina Thickness is assumed Moderate; 50 - 75 $\mu$ m).....	186
5-2 Flame Structure at Different Binder Lamina Thickness.....	187
5-3 Adiabatic Flame Temperature of an AP/PBAN Mixture.....	188
5-4 Adiabatic Flame Temperature of an AP/BAMO-THF Mixture.....	189
5-5 Adiabatic Flame Temperature of an AP/NMIMO Mixture.....	190
5-6 Comparison of Mixing Fields for a Concentrated and a Dilute Fuel.....	191
5-7 Fuel Deficient Condition with Dilute Fuel.....	192

## LIST OF ABBREVIATIONS

AP : Ammonium Perchlorate
BAMO-THF : 3,3(bis-azido-methyl)oxetane) - Tetrahydrofuran
BBCI : n-butyl(bis)cyclopentadienyl
B MCP : Bismethylchromium
CC : Copper Chromite
CTPB : Carboxy-terminated-polybutadiene
F : Ferrocene (Biscyclopentadienyl Iron)
FR : Ferricinium Reineckate
HTPB : Hydroxy-terminated-polybutadiene
IB : Iron Blue (Ammonium Iron-hexacyanoferrate)
IO : Iron Oxide
NMIMO : 3-Nitratomethyl-3-Methyloxetane
PBAA : Polybutadiene Acrylic Acid
PBAN : Polybutadiene Acrylic Acid Acrylonitrile
PC : Polycarbonate
PETP : Polyethyleneterephthalate
PMMA : Polymethylmethacrylate
PS : Polystyrene
PSU : Polysulfide
PTFE : Polytetrafluoroethylene
PU : Polyurethane

In the present study the qualitative theory of flame complex described earlier for the PBAN binder was applied and extended for the case of new energetic binders and postulates were developed and proposed for the action of the iron based catalysts introduced in the binder lamina.

This new expanded flame theory was able to qualitatively predict burning rate trends, surface profiles and flame structure based on ingredient properties related to combustion, thermochemistry of the Oxidizer/Binder system, pressure changes and binder lamina thickness variations.

## SUMMARY

An experimental investigation into the effects of the energetic binders BAMO-THF and NMMO on sandwich burning has been conducted. Two-dimensional sandwich models of a composite propellant consisting of a layer of binder "sandwiched" between two slabs of ammonium perchlorate were employed. Comparable tests using BAMO-THF and NMMO (energetic binders) and PBAN (standard inert binder) were carried out and the effects of three catalysts ( $\text{Fe}_2\text{O}_3$ ,  $\text{Fe}_3\text{O}_4$  and catocene) added to the binder were studied. The amount of modifier added was sustained in percentages encountered in real propellant mixtures. Prior work on the burning of uncatalyzed and catalyzed binder sandwiches was reviewed.

Combustion photography was used for the measurement of the sample's burning rate and to extract information on the combustion zone regarding color, particle concentration, smoke, binder melt. Optical and scanning electron microscopy were employed to provide information on the surface details, color, residual accumulation, binder and/or oxidizer protrusion of the quenched sandwich's surface. Both combustion photography and microscopy were helpful in sketching the surface profiles of the samples at different pressures for several binder thicknesses.

The burning rates for uncatalyzed and catalyzed binder sandwiches were plotted as a function of binder lamina thickness and of test pressure. The effectiveness of each catalyst was measured at each test condition.

## CHAPTER I

### INTRODUCTION

The ultimate goal in *the* solid rocket composite propellant research is the construction of an analytical model which will be able to calculate the burning characteristics of a propellant from its formulation.

In order to be able to develop such a model it is necessary to identify and understand the controlling mechanisms that govern the combustion process. The burning of a solid propellant is characterized by complicated geometry (three-dimensionality, heterogeneity), complex chemistry (multiple sequential reactions) and very small dimensions (1 - 400  $\mu\text{m}$ ).

The oxidizer / binder sandwich system was proposed and applied to alleviate some of the complexities encountered in composite propellants. It is a geometrically simple system with an ordered structure which allows easier examination and understanding of the combustion zone.

The oxidizer / binder laminate system will be employed throughout this study to provide further information on the mechanisms of burning and to investigate the behavior of energetic binders and the effect and action of burning rate catalysts.

#### 1.1 Literature Survey

##### 1.1.1 Background

Combustion of solid rocket propellants is an applied science that has its origins in the science of the internal ballistics of guns. Solid propellants have a variety of applications: they are used in satellite boosters, ballistic missiles, rocket boosters for aircraft take-off, air launched missiles, tactical weapons, sounding rockets, gas generators for life vests and air bags in cars.

The term solid propellant has several connotations, including (a) the rubbery or plastic-like mixture of oxidizer, fuel, and other ingredients that have been processed and constitute the finished product, (b) the processed but uncured product, and (c) a single ingredient, such as the fuel or the oxidizer. Acronyms and chemical symbols are used indiscriminately as abbreviations for propellant and ingredient names.

Processed or cured modern propellants fall into three general types: double-base, composite, and composite double-base.

Double-base propellants form a homogeneous propellant grain, usually a nitrocellulose type of gunpowder dissolved in nitroglycerin plus minor percentages of additives. Both the major ingredients are explosives and function as a combined fuel, oxidizer, and binder. When combined, however, nitrocellulose and nitroglycerin form a compound which is less explosive than each individual component.

Composite propellants form a heterogeneous propellant grain with the oxidizer crystals and a powdered fuel (aluminum) held together in a matrix of polymeric binder (synthetic rubber, plastic, epoxy, etc.) Many composite propellants are less hazardous to manufacture and handle than double-base propellants.

Composite modified double-base propellants, are in one sense a combination of the double-base and composite propellants, usually a crystalline oxidizer and powdered metal fuel held together in a matrix of nitrocellulose-nitroglycerin. The hazards of processing and handling this type of propellant are similar to those of double-base propellants.

Propellant ingredients are generally classified according to their function, for example, fuel, oxidizer, binder, curing agent, or burn-rate catalyst. Ingredients used in small amounts are often called additives and usually fulfill functions other than those of fuel, oxidizer, or binder. Often an ingredient serves more than one function; for example, in composite double-base propellants the binder is the blended nitrocellulose-nitroglycerin complex, with each of these two ingredients having its own fuel and oxidizer chemical elements. Usually the binder also acts as a fuel, and in some propellant formulations, such as polymer-based nonmetallized composite propellants, the binder is the only fuel. When an ingredient has both oxidizing and fuel components it has the potential of being an explosive. Additives are used for many purposes, including accelerating or lengthening the curing time, improving the physical properties, (including the rheological properties), adding opaqueness to a transparent propellant to prevent radiation heating at places other than the burning surface, increasing or reducing the burning rate, improving bonding, limiting migration of chemical species from the oxidizer to the binder or vice versa, and improving the aging characteristics or the moisture resistance.

In the 1940's the first papers on solid fueled rockets appeared in the literature but even in the 1950's the science of propellant combustion was largely dependent on empirical methods.

The increasing limitations of motor testing associated with the cost and dangers of firing large motors forced an aggressive research effort to understand and correct problems in the existing programs. The decade of 1960 was extremely productive from the standpoint of increased understanding of propellant combustion.

In the 1970's (starting from 1966) attempts at the development of combustion models - theoretical and/or experimental - began in earnest. It was a first attempt to predict

and understand the combustion behavior by way of physical insight/and ingredient chemistry rather than empirical methods.

Recent trends in propellants and applications continue to produce new needs for understanding. Interest has grown in propellants that produce no optically visible exhaust trail from the missile and at the same time do not pollute the environment. There is a desire to increase the energy contents of the propellant without being a hazard if the combustion does not proceed as planned.

Today's problems are characterized by increased complexity and increased cost of problem "solving" by empirical means. But before solving practical problems there is need to study all the underlying principles and mechanisms, and to advance the understanding and methods.

### 1.1.2. Literature Review on Theoretical Models

Research has revealed a qualitative understanding of propellant combustion. It is clear that the exothermic reactions which sustain the combustion may occur in varying degrees in the gas phase, on the burning surface or in the condensed phase. The relative importance of the different reaction steps differs according to the composition of the propellant, details of the propellant microstructure and the environmental conditions. In most practical combustion situations, the relative importance of these steps in the combustion process is unknown and prediction is largely based on experience rather than theory. The failure of analytical models is not entirely due to the complexity of the combustion process, but is enhanced by the continuing ignorance of many of the basic aspects of combustion, such as fundamental kinetics data for binder and oxidizer decomposition, gas phase reactions, and interface reactions.

Advances in the understanding of the combustion of heterogeneous, composite solid propellants depend on identifying the key steps of the overall reaction and on more detailed

knowledge of the three-dimensional aspects of the phenomenon, which are caused by the heterogeneity of the propellant structure.

The first work in solid rockets is accumulated by Wimpres [1] in his book and by a collection of papers in the Journal of Physical and Colloid Chemistry [2].

Early surveys of solid propellant combustion have been presented by Geckler [3] in 1954. He stated that, "A great deal of study of solid propellant combustion appears to have been expended unnecessarily because of inadequate experimental facts". He also mentioned that no theoretical studies of composite propellant combustion had been published at that time. Gutman [4] in 1960 understood that the lack of knowledge of the fundamental combustion mechanisms was the basic reason for not being able to theoretically describe the composite propellant burning process.

The essential distinction between the combustion processes involved in the burning of homogeneous double-base propellants and composite propellants was stressed by Rice [5]. He proposed a columnar diffusion flame model, which was the first of the diffusion controlled models of composite propellant burning. The model gives the correct qualitative dependence of burning rate on oxidizer particle size but causes the burning rate to be insensitive to pressure, in contradiction to experimental observations.

Wilfong, Penner and Daniels [6] introduced the idea that the rate controlling reaction in the thermal decomposition of a double-base propellant occurs in the monomolecular surface layer exposed to the flame zone. Schultz and Decker [7] applied this concept to the combustion of solid composite propellants in the form of a two-temperature postulate which suggested that the gasification of binder and oxidizer at the propellant surface proceeds independently, and that these reactions are rate controlling. Chaiken [8] used this postulate of the independence of the regression rates of the oxidizer and the binder in developing the thermal layer theory for the combustion of ammonium nitrate (AN)

composite propellants. Using the gas phase reactions associated with the oxidizer alone, a thermal reaction layer was assumed to exist around a spherical oxidizer particle embedded in the binder; reactions involving the binder were regarded as having no significant influence on the processes occurring at the oxidizer surface. Anderson et al. [9] proposed a model for the combustion of ammonium nitrate composite propellants. It was postulated that the oxidizer gasifies first and its gaseous products undergo an exothermic reaction near the surface to establish an adiabatic flame which governs the pyrolysis of the propellant binder. The binder pyrolysis products then react with the gaseous products of the oxidizer to form a diffusion flame at a relatively large distance from the surface. Their statements that changes in the chemical structure of the binder have only a minor influence on the burning characteristics, along with the large distance of the final diffusion flame from the surface, lead to their conclusion that the binder-oxidizer diffusion flame has insignificant influence on the processes occurring at the oxidizer surface. In a later investigation, Chaiken and Anderson [10] considered the role of the binder in composite propellant combustion and extended the thermal layer theory to ammonium perchlorate (AP) based propellants. Several cases were presented for the interaction mechanisms of the binder gases with the oxidizer, but no theoretical developments nor supporting data were given.

Sutherland [11] examined an analytical diffusion flame model for the combustion of AP type propellants. He proposed that flamelets formed by the diffusive transport of oxidizer and fuel decomposition products provide the heat release necessary to support the combustion process. The model contains no explicit dependence of burning rate and flame structure on pressure. However the surface temperature appears as the important parameter in the development. The model must be considered incomplete as it does not provide any procedure to determine the surface temperature.

In 1960 Summerfield et al. [12] expanded the earlier work of Sutherland to include the effects of pressure, oxidizer particle size, and fuel-oxidizer ratio. They proposed a physicochemical representation of the combustion zone including surface reaction and a gas flame zone which incorporates chemical reaction and diffusive mixing. Their model, the Granular Diffusion Flame (GDF) model, was one of the early models for heterogeneous propellant combustion. The GDF model is a one-dimensional model in which it is assumed that the gasification process at the solid regressing surface is driven by conductive heat feedback from a two-stage flame occurring in the gas phase. This two-stage flame is composed of the gaseous constituents released by either surface pyrolysis or sublimation (both endothermic) from a dry surface. It is assumed that the flow is laminar. A premixed flame (exothermic) is postulated to exist above the AP surface with ammonia and perchloric acid as the premixed reactants. The products of this premixed reaction which are rich in oxygen and oxygen-containing compounds, then serve as a reactant along with the gaseous fuel constituents to form a diffusion flame at a much greater distance from the surface than the first stage ammonia and perchloric acid flame. The fuel gases are presumed to enter the oxidizer-fuel (diffusion) flame zone in the form of tiny gas pockets whose mass is independent of pressure. Both the rates of diffusional mixing and chemical reaction determine the overall reaction rate of the diffusion flame. An expression for burning rate is obtained in which the chemical reaction is rate controlling at low pressures while diffusion is rate controlling at high pressures. This theoretical burning rate law contains two parameters which may not be calculated directly due to insufficient basic information on parameters involved in their calculation. One parameter is called the "Gas-Phase Reaction Time Parameter" and it varies inversely as the chemical reaction rate in the gas phase. This parameter is related to the binder-oxidizer ratio of the propellant. The other parameter is called the "Diffusion Time Parameter" and again varies inversely as the

chemical reaction rate in the gas phase. This parameter is related to the average oxidizer particle size. In order to test the GDF model, a series of experiments have been conducted by various investigators. The results obtained by Blair et al. [13] and Stiezin et al. [14] gave good correlation between theory and tests over a broad range of conditions for the propellants reported. Later investigations [15, 16, 17, 18] show evidence that both binder and oxidizer exhibit a molten or liquid layer on the burning surface which could possibly lead to a premixed combustion flame. These results are in conflict with the hypothesis of the GDF theory and bear further investigation.

In 1966, Hermance [19] proposed a model of composite propellant combustion which incorporated the surface processes of endothermic fuel pyrolysis, exothermic binder decomposition, exothermic heterogeneous chemical reaction between fuel binder and oxidizer decomposition products, and gas phase combustion of the final fuel and oxidizer decomposition products. It was the first model to attempt to predict burn rate effects due to ingredient particle size. The prediction of the burning rate dependence upon pressure and oxidizer particle size agrees quite well with experimental results, although the predicted effect of oxidizer loading is in error. The model neglects gas phase diffusion and assumes a dominating interfacial reaction around the oxidizer particle producing a fissure which, in fact, has been observed only in isolated cases.

A qualitative description for combustion of composite propellants based on flame structure was postulated by Fenn [20]. He envisions the burning process to be driven by a gas phase fuel-oxidizer diffusion flame situated over the interfacial area between the solid fuel surface and the solid oxidizer surface. A small premixed flame is assumed to exist at the leading edge of the overall flame and this premixed flame is said to lead the attack on the interfacial area. The effects of pressure, binder-oxidizer ratio and oxidizer particle size are qualitatively predicted by this model.

Culick and Deborah [21] presented a simple, one-dimensional, diagnostic aid to understand the burning of composite propellants. They used an inverse approach to the problem; they assumed that the burning rate-pressure relation was known and based on that they explored the roles played by various physical and chemical propellant properties on the rate of heat release, flame thickness and stand off distance. The combustion model assumed a uniform gas phase combustion zone with heat transfer matching conditions at a reacting solid phase interface. This approach, although very simple, is quite useful for qualitatively examining the influence of propellant properties on the combustion process.

In 1970 Beckstead, Derr and Price [22] developed a more realistic model for AP type propellants. This model (known as the BDP model) allowed for an exothermic reaction taking place at the propellant surface as could occur due to the AP partially decomposing exothermically in the thin surface melt of the AP (which had been reported by Boggs [17] and by Hightower and Price [34]). Three separate flame zones are considered: (1) a primary diffusion flame between the decomposition products of the binder and the oxidizer, (2) a premixed oxidizer flame, and (3) a final diffusion flame between the products of the other two flames. The oxidizer regression is taken as being the over-all rate controlling process. The results obtained by this model show that the calculated surface temperature and the effect of oxidizer concentration predicted by the model are in agreement with observed experimental trends. The predicted effect of particle size is somewhat greater than the observed experimentally while the effect due to initially heating or cooling the solid propellant is in excellent agreement with the test data.

In 1973, Culick [23] proposed the Petite Ensemble Model (PEM), to take into account polydisperse oxidizer particle size distribution, which treats the composite propellant using statistical means. In 1982 Renie [24] extended the PEM to consider aluminum combustion.

Other models proposed recently consist of: (1) the Deur-Glick model [25] developed in 1984, which is an over simplified model employed mainly to show the importance of considering condensed phase heterogeneity effects and interaction between oxidizer and fuel pairs, and (2) Miller's "Fastest Path" model [26], which is not fully developed yet. It is worthy to note that Miller's concept for a "Fastest Path" Model (named as "Least Time Path" Model) was conceived earlier by Price, Strahle, Handley, and Sheshadri, [27], in 1976, and extended by Strahle, [28], in 1978. It is mainly a proposed mechanism which states that combustion will follow the path which allows it to proceed at the fastest rate through the propellant.

### 1.1.3 The Oxidizer - Binder Sandwich Approach

All the analytical models, described above, were proposed after a great deal of observation, ordering of observations and recognition of critical features of behavior. Construction of adequate hypotheses was involved in order for those models to explain and exhibit the observed features of behavior. Experiments and analysis that followed helped in improving the models and expanding their areas of application.

The final and absolute purpose of the analytical model is to be able to predict the burning characteristics given the propellant formulation. But the very first step to success in constructing an analytical model depends on how well the combustion processes can be recognized, understood, and explained. In propellant combustion, reaction zones and thermal layers that control the macroscopic burning are of the same dimensional order as the granularity of the propellant ingredients. Unfortunately, observational methods generally do not have adequate spatial resolution at those dimensions. The situation is further complicated by the uncertain relevance of flame theory when applied to such small, geometrically and chemically complicated flame systems. In spite of these difficulties, it is

necessary to obtain knowledge regarding the combustion zone structure in order to recognize critical features of behavior and construct relevant models.

A strategy to alleviate some of the experimental difficulties of observation is to study combustion of geometrically simple systems such as the oxidizer-binder sandwich. By edge burning these laminate structures, the combustion zone often conforms to a two-dimensional steady state configuration, hopefully amenable to more meaningful observation and theoretical interpretation. Unfortunately, the microcombustion zone is still substantially inaccessible to observation, because requisite spatial resolution is not attainable. One exception to the limitation of spatial resolution in measurements is the quench-burning experiment, which permits detailed study of the surface of a quenched sample under high magnification. Interruption of burning is achieved by rapid depressurization of the combustor. The details of the burning surface microstructure are largely preserved and can be used in explaining the combustion zone structure (along with other information).

The oxidizer-binder sandwich was introduced "as a compromise between the complexity of the three-dimensional combustion zone and the naivety of the one-dimensional approximation" ([29]). By the use of a suitable technique the dimensional relations of a conventional propellant microstructure could be approximated while preserving the relative simplicity of a two-dimensional configuration.

The oxidizer-binder sandwich has the advantages of:

(1) Low cost and simultaneous control over microstructure and placement of ingredients. To make up composite propellant samples with systematic changes in relevant variables, is not only very costly, but the resulting samples are of chaotic character on a microscopic (<1 mm) scale.

(2) Relative ease of observation during burning.

(3) Ordered structure that qualitatively establishes the structure of the combustion zone.

(4) Relative amenability of processes to analytical modeling (two-dimensional steady state behavior). The oxidizer-binder laminate, (see figure 1-1), allows examination of the multi-dimensional heat transfer, mixing and combustion aspects of the propellant combustion problem but in two rather than three dimensions and without the statistical complexity of the overall propellant surface.

As with any simplified model of a complex system, the sandwich model fails to simulate some important aspects of propellant combustion, and may also produce some effects that are of only secondary importance with propellants. The main shortcomings of the method are:

(1) The dimensions of the ingredient layers are not the same as encountered in actual propellants. Oxidizer particles in propellant ordinarily have an effective radius in the range of 2 - 200  $\mu\text{m}$ , so that distances from oxidizer binder interfaces are in that range, and the flame environment occurring in that range is the one relevant to propellant surfaces. A relevant theory or experiment is one that correctly describes conditions or processes in the 200  $\mu\text{m}$  range from the interface. This implies that relevant experimental observations of sandwich burning must pertain to the 200  $\mu\text{m}$  range relative to the interface, and the experiment must simulate propellant behavior in that region. Although the oxidizer-binder sandwich is an order of magnitude larger than 200  $\mu\text{m}$ , it has been clearly observed that the surface pattern, around the oxidizer-fuel interface, has the same features as the real propellant surface. Therefore no significant attention should be paid to AP in areas further than 500  $\mu\text{m}$  from the interface.

(2) The relatively steady state nature of burning. Being made primarily of particulate ingredients, the combustion of heterogeneous propellants is locally intermittent. Thus any condition on the burning surface of a sandwich that requires a generation time longer than

the propellant particle burning time will not be fully developed on the propellant surface because of the interruption of particle burnout. As an example at pressures above 1000 psi the AP laminae of a sandwich is regressing so rapidly compared to the binder that the situation is not typical of propellant combustion; the height of the binder protrusion above the AP is times greater than the heterogeneity of typical propellants. This does not mean that the phenomena observed during nearly steady burning are not relevant, but rather that those resulting from slow processes will not become fully developed in particle burning.

(3) The reaction zone does not encounter heterogeneity in the direction of burning. This is the result of the ordered structure implied by having the laminae of oxidizer and binder. The steady state burning and the ordered structure, though absent in a propellant, are very important in the sandwich system. They are the means by which observation during burning becomes easier and the structure of the combustion zone is constrained to relatively predictable configuration.

(4) The "edgewise burning" of the interface. In the sandwich, the geometry constrains the burning front to proceed in the direction of the interface. Because of the granular nature of ingredients in propellants, the interfaces are not only discontinuous, but inclined in varying degrees to the mean burning surface of regression. There may be a significant portion of the particle burning in which edge burning is approximated, but it is not presently established what contribution each part of the particle burning history makes to the overall burning rate, or to the structure of the burning surface and gas phase combustion zone. The "edgewise burning" is used in sandwich burning to reduce the complexity of the whole combustion process.

(5) The sandwich approach fails to simulate the variability of the binder thickness.

Despite all the above the simplicity of the sandwich model, it is uniquely useful in studying and understanding the fundamental laws of solid propellant combustion.

A step further in the oxidizer-binder sandwich combustion is the construction and production of multilayer sandwiches; oxidizer-binder sandwiches that are made of a number of alternate oxidizer and binder layers (see figure 1-2). The development of these sandwiches is in a primitive stage [30] but there is rapid progress. The goal is to achieve multilayer sandwiches of about 10 oxidizer and 9 binder layers with thicknesses 200  $\mu\text{m}$  and 25  $\mu\text{m}$  respectively. The multilayer sandwiches can be thought as an "ordered composite propellant". The most important advantage which they have is that the thickness of the layers is very close to the dimensions encountered in actual propellants.

The 2-D sandwich model has been criticized for reasons mentioned above. To a large extent these criticisms developed from an expected direct comparability of the sandwich results to composite propellant burning. Direct comparability is not the intent of the method which was developed to study the controlling mechanisms under non-ambiguous conditions. The identification and understanding of these mechanisms can be applied to construct a proper composite propellant theoretical model. It can also be applied in investigating the combustion behavior of new ingredients employed in propellant compositions. The sandwich technique is useful for studying the important events occurring at or near the oxidizer-binder interface and the flames occurring above the interface. The sandwich approach is advantageous in that the separation of ingredients into precisely definable regions provides greater resolution of observation, while providing an opportunity to observe interactions arising from the combination of oxidizer and fuel. It greatly simplifies description of combustion zone processes, and hence aids in understanding observed combustion behavior.

#### 1.1.4 Literature Review on Sandwich Burning

Nachbar in 1957, [31] and 1960, [32], was the first to talk about the sandwich model approach to simulate propellant combustion. He proposed the use of a model consisting of a two-dimensional array of thin slabs of fuel and oxidizer. He obtained, theoretically, an expression for the burning rate of such an array. He accounted for slab dimensions, flame temperature, initial temperature and latent heats of sublimation of fuel and oxidizer. His major assumption was that the decomposition of the solid directly into gaseous reactants occurred at the solid-gas interface for both fuel and oxidizer (these surfaces were considered dry, and no solid-phase reactions were assumed). Nachbar also did not account for the influence of pressure on the burning rate and he mentioned that there were no experiments on sandwich burning ever reported.

The first experiments on sandwich burning were reported by Bakhman and Polikarpov [33]; but in 1966, Hightower and Price [34] presented the first systematic experimental results on sandwich burning. Their study consisted of microscopic examination of burned and quenched ammonium perchlorate/binder sandwiches. AP single crystals of excellent quality were used as oxidizer laminae and PBAA as binder. The tests were run in a nitrogen pressurized combustion bomb over the pressure range 100 to 1200 psig. The major observation was the pressure dependent surface pattern. They also mentioned that the ballistic modifiers affect the general characteristics of the surface pattern. Evidence that some liquid might be present on the burning surface of the oxidizer was observed and it was noted that there was no indication of significant oxidizer-binder interface reactions.

Powling, [35], in 1967 studied single AP/binder systems over the pressure range 100 to 1800 psig in an inert atmosphere and stated that the burning rates at low pressures were little affected by properties of the fuel-binder other than heat of combustion. At higher pressures the burning rate could be enhanced by the diffusion flame of oxidizer products and fuel pyrolysis products. He mentioned that relatively stable liquid products from the

pyrolysis of certain binders appeared to be able to inhibit flame penetration, presumably by effectively melting and flowing over AP surfaces and filling potential crevices.

Austin, [36], the same year, in his attempt to describe the flame temperature profile of AP/fuel-binder sandwich measured that the diffusion flame had a much higher temperature than the AP monopropellant flame. In his tests he employed pressures of 300 and 500 psi. His statement that "At low pressures, the diffusion flame is closer to the interface of the sandwich than at higher pressure, so the diffusion flame has a greater influence on the burning rate at lower pressure" contradicted Powling [35] and showed that there was still a long way to understand sandwich combustion and more generally propellant burning (Austin's results did not seem to be consistent with the higher burning rates obtained at higher pressures).

Hightower and Price [29], presented in 1968, their experimental study based on single crystal AP/hydrocarbon binder propellant sandwiches which had been burned and quenched in nitrogen atmosphere over a range of pressures (100 to 1200 psia) applicable to rocket motor combustion conditions. The sandwiches were examined using optical and scanning electron microscopes. The studies conducted on the quenched samples (their surfaces and profiles) had yielded useful information on the nature of significant heat release mechanisms occurring at or near the burning surface. There was evidence to indicate the existence of a thin decomposing melt on the surface of AP under normal self-deflagration conditions. They gave an explanation for the existence of the frothy liquid on the AP burning surface. The material at high heating rates had less time for decomposition before reaching any given temperature. So a melting point might be encountered, which would not be observed at lower heating rates, where the sample would decompose before the melting point was reached. The burned sandwich profiles showed that the point of maximum regression occurred in the AP crystal and not at the oxidizer/binder interface - as

it was believed earlier, [35] - but at a short distance from it. That point of maximum regression was to be determined by heat flow from the leading edge of the diffusion flame. Hightower and Price indicated that the diffusion flame played an important role especially below the AP low pressure deflagration limit, since without its influence self-sustained deflagration is impossible. Finally, they observed a continuous surface across the interface between the binder and AP crystal (no recess at the interface). This indicated that interfacial reactions were not significant in determining regression of the surface, at least for AP/hydrocarbon binder systems.

Fenn [20], as was mentioned earlier, expanded Nachbar's model - single AP/single binder slabs - to alternate layers of AP and binder. He clearly distinguished the different processes that were involved at high and low pressures. He proposed that at the surface each species was gasified independently (i.e. different surface temperature) to form adjacent streams of gaseous fuel and oxidant which then mix by diffusion and react exothermically to form combustion products. At low pressures the mixing process was fast and the time required to reach the final state was determined by chemical kinetics (chemical reaction rates). At high pressures the mixing process was slow, compared to reaction rates, and the time required to reach the final state was determined by diffusion rates. Fenn, attempted to explain the dependence of propellant burning rate on oxidizer size. He based his physical arguments on the multiple layer sandwich configuration where the layers of fuel and oxidizer were thin. For thin layers the total heat flux to the surface near the interface, including the contributions from the gas phase and by conduction through the solid would be larger than for thick laminar. Consequently, the regression rate of the interfacial surface would be greater in the thin layers. Finally, he tried to argue the pressure dependence of the burning rate based on his phalanx flame model (the phalanx

flame is the exposed premixed reaction zone kernel which spreads the attack of the hot reaction gases of the unburned solid, as shown in figure 1-3).

Nadaud [37], in 1968, presented some data on AP, solid fuel rods joined side by side in an inert atmosphere and a pressure domain 5-80 atm. He tried different binders and he mostly agreed with Fenn's theory.

In 1969, Ermolaev, Korotkov, and Frolov, [38] made qualitative conclusions necessary to characterize the combustion processes of sandwich burning:

- a) The burning rate depended strongly on pressure and the nature of the components
- b) The rate of flame propagation through a layered charge was dominated by kinetic processes, including specifically decomposition of the ingredients and the kinetics of the near surface oxidizer-fuel flame
- c) Layered charges burned more rapidly than mixtures of the same components with an oxidizer particle size equal to the thickness of the oxidizer layer.

The same investigators in 1970 [39], proposed a theoretical analysis similar to Fenn's theory. They showed that taking into account the conditions of combustion of the gas mixture at the "roots" (see figure 1-4, very similar to Fenn's phalanx) of the flame led to the emergence of a dependence of the sandwich burning rate on kinetic factors. By filming their tests (multilayer AP/binder sandwich systems) they observed that the flame front was broken down into a number of tongues, which penetrate into the condensed phase along the contact surfaces. For very thin layers the individual tongues interacted with one another affecting the overall burning rate.

(With the exception of Hightower and Price's paper [29] all the rest of the literature in the 1960's was concentrated on the progress of flame propagation along the contact surface between oxidizer and fuel slabs).

Bakham and Librovich [40], in 1970, investigated the flame propagation along the interface between fuel slab and oxidizer slab (the slabs were thicker than 200  $\mu\text{m}$ ). They experimented with burning of an oxidizer slab pressed between two fuel slabs (or vice versa) at a pressure range 0-30 atm. They did not consider AP, because it could burn at  $p > 20$ -40 atm without any fuel.  $\text{KClO}_4$ ,  $\text{KClO}_3$ ,  $\text{BaO}_2$  and  $\text{KMnO}_4$  were employed as oxidizers and PMMA, PE and PVC were taken as fuel. The main interest in their research was concentrated on the shape of the burning surface and the dependence of flame velocity on pressure and layer thickness.

They proposed a "cavity" shape (see figure 1-5) appearance between the binder and oxidizer slabs during combustion and they observed:

a) An increase of the flame velocity along the fuel/oxidizer interface resulted from

- (1) Increase of pressure
  - (2) Decrease of density of the oxidizer slab
  - (3) Decrease of thickness of the oxidizer slab placed between two thick slabs of fuel
- b) The chemical reaction in the front region of the cavity played a determining role in the burning velocity. A change in chemical kinetics near the tip of the cavity influenced the velocity

c) Since the burning rate was governed by the kinetic processes taking place at the tip of the cavity, the change in the slab thickness could influence the rate only if the slabs were thinner than the heated regions

d) Asymmetries of the cavity were attributed to different heat of gasification of the oxidizer and of the fuel

e) Far from the tip pure diffusional burning occurred.

Based on the existence of the "cavity" shape they proposed a theoretical model, which could be applied along the burning down of the interface between the solid oxidizer and the fuel.

Varney [18], in his Ph.D. dissertation did a very thorough analysis on the quench combustion of two-dimensional propellant sandwiches. Using the optical microscope he investigated the effects of binder type, binder lamina thickness and combustion pressure level on the surfaces and the surface profiles of the quenched samples. He worked with four binders (PS, PBAA, CTPB and PU) and he verified:

- a) The presence of a binder melt on the oxidizer surface at pressure levels from 300 psig to 2400 psig of nitrogen (he concluded that the presence of fuel, augmented the characteristic AP deflagration rate)
- b) The continuous interfacial contours observed at the binder-oxidizer interface, at every combustion pressure level, indicated that significant interfacial reactions between the binder and oxidizer did not occur.

He proposed that the mechanisms influencing the sandwich regression (see figure 1-6) could be dominated by one, or a combination of:

1. Oxidizer monopropellant combustion characteristics
2. A gas phase flame zone resulting from binder and oxidizer products
3. Binder decomposition characteristics and condensed phase reactions
4. Heterogeneous binder-oxidizer interfacial reactions.

Finally, Varney did an experimental investigation using the method of differential scanning calorimetry; he determined the thermal decomposition characteristics of the four conventional solid propellant binders mentioned above. His results provided a qualitative understanding of binder thermal decomposition behavior but caution must be exercised in

using them for actual combustion situations where pressure and heating rates are several orders of magnitude higher (especially the heating rates).

Jones [41], in his Ph.D. thesis in 1971, approached the sandwich combustion from a different point of view. He burned two-dimensional sandwiches in a window combustion bomb pressurized with nitrogen at pressures up to 3200 psig. Using a high speed motion picture camera he photographed the combustion process and verified the existence of a flowable binder melt and no evidence of heterogeneous interfacial reactions. He proposed the structure of a flame for the AP/binder sandwich as consisting of an AP flame, a base flame and a diffusion flame between the AP combustion products and the binder decomposition products. The base flame, (see figure 1-7) which included reactions between the AP decomposition and deflagration products and the binder pyrolysis products, constituted the ignition region for the diffusion flame which consumed the binder. (The base flame was very close to what Varney described earlier as a premixed flame).

Varney and Strable [42], in 1972, extended their work and conclusions and indicated that there was considerable interplay between oxidizer and binder species on the oxidizer portion of the sandwich. This was attributed primarily to binder melt formation prior to gasification. They observed that binder characteristics had a pronounced effect on the sandwich profile and they demonstrated that regression characteristics of sandwiches prepared by pressing polycrystalline AP yielded results in accord with those obtained using single crystal AP.

Boggs and Zum [43] in their investigation in 1972, combined the results they obtained from cinephotomicrography of the actual combustion process and from the scanning electron microscopy of the surface of rapidly quenched samples (pressurization by nitrogen in the range 100-1000 psi was employed). They studied the effects of different binders

(CTPB, HTPB, PU) in sandwiches and their conclusions were in full agreement with the results of Hightower and Price [29], Varney [18] and Jones [41]:

- a) No evidence for interfacial reactions between AP and binder was observed
- b) The leading point of the regression was always in the AP
- c) All of the binders tested displayed a liquid.

They postulated a "candle" diffusion flame for  $p < 300$  psig and a turbulent diffusion flame for higher pressures (see figure 1-8). They also addressed a whole series of questions that must be answered and the work needed to be done in the field of the composite solid propellant combustion.

Brown, Kennedy and Netzer [44], in 1972, carried out an experimental investigation of AP/binder (PBAA) sandwich combustion in standard and high acceleration environments (100-800 psi of nitrogen were employed). Their observations and conclusions consisted of:

- a) For binder thickness greater than 100  $\mu\text{m}$  there was little effect of acceleration on the burning rate.
- b) For pressures below the deflagration limit of AP the average burning rate remained constant under acceleration or decreased below the nominal rate and may extinguish completely
- c) A small amount of binder flow onto the AP enhanced the burning rate but excess binder build up, could quench the reaction.
- d) Below the AP low pressure deflagration limit the sandwich burner flames were laminar and above it they appeared to be turbulent.
- e) Two distinct flame regions were observed, one above the binder and one near the binder/AP interface.

They introduced the concept of the tapered sandwich (a sandwich whose binder thickness graduated from 100  $\mu\text{m}$  to 5  $\mu\text{m}$ ; the tapered binder layer thickness allowed the amount of binder available to the deflagrating AP to vary from a fuel-rich to fuel-lean situation; see figure 1-9) to observe the flame structure. Using high speed motion pictures they found that the diffusion flamelets were taller, further apart, and appeared to survive longer where the binder was thick (see figure 1-10). It was seen that the flamelets disappeared and new ones appeared in successive pictures at 2500 pictures per second, while a double row of flamelets was observable at the thick binder locations. The newly developed tapered two-dimensional AP/binder sandwich approach was applied in a series of experiments conducted by Handley, Price and Ghosh [48]. Both quenched combustion techniques and cinephotomicrography of the burning samples were used to observe the deflagration process and the interaction of the diffusion flamelets with it. Four binders (PS, PBAN, CTPB, HTPB), were tested over the 1.38 MPa (200 psi) to 13.8 MPa (2000 psi) pressure range. The use of the scanning electron microscope helped in study of the quenched sandwich surface in more detail. The binder layer that remained between the two AP layers consisted of binder material that had not pyrolysed, binder material that had melted and resolidified, intermediate decomposition material and char layers. There was difference noted between the four binders examined mainly on the surface profiles and on the apparent viscosity of the binder when exposed to the combustion process and then quenched by rapid depressurization. Characteristic AP surface deflagration patterns were obtained on the AP surface far away from the binder and its melt flow for all pressures except 1.38 MPa. It was also mentioned that :

- a) The AP surface near the binder/oxidizer interface was always smoother than the characteristic AP surface far from the binder, and

Murphy and Netzer [45], in 1974, conducted a series of color schlieren studies on combustion tests of AP/binder sandwiches in nitrogen atmosphere and over the pressure domain 100-1000 psi. They verified earlier results (on binder flow, binder thickness) and they gave a more detailed information of the flame shape: At pressures below the low pressure deflagration limit of AP, the visible flame had a single closed structure. As the pressure increased the AP began to deflagrate faster, leaving a protruding binder. Once this stage was reached, the single closed flame was divided into a two flame structure, one on each side of the protruding binder. Those visible flames were canted outward over the deflagrating AP and became unsteady or "turbulent" as a result between the AP deflagration products with the AP/binder diffusion flame.

Abraham and Netzer [46], in 1975, studied the AP/binder sandwich combustion in standard and high acceleration environments (pressurized nitrogen up to 1250 psi was used). They observed burning rate augmentation at high accelerations which they attributed to AP/binder interactions close to their initial interface.

In 1979, Price, Sigman and Handley [47], presented a series of results obtained from observations on quenched samples of composite solid propellants. There was extreme similarity between the surfaces of the quenched propellant samples and the quenched sandwiches:

- a) AP particle surfaces were convex and protrude at low pressure, flat and even with the mean surface at the pressure deflagration limit of AP, and were concave below the mean surface at higher pressure.
- b) There was characteristic raised porous region in the middle of the AP above 3.47 MPa.
- c) The binder became increasingly evident as pressure was increased, with the appearance of a melt state.

b) The deflagration of the AP adjoining the binder/oxidizer interface was retarded. High speed motion pictures were taken to determine burn rates, profile regression and to observe the diffusion flameless. The results supported previous investigations and showed that the flameless were locally always perpendicular to the regressing surface.

In 1980, Price, Panyam and Sigman [49], and in 1981, Price, Handley, Panyam, Sigman and Ghosh [50], perceived that the thick binder layers, used in the sandwich approach so far, were not simulating effectively propellant combustion, where very thin binder elements were normally present. Tests run on sandwiches with tapered binder laminas (burned on the tapered edge) showed conspicuous difference in features of quenched surfaces along the tapered binder lamina. The protrusion of the AP along the AP-Binder interface was present under all conditions, but the protrusion of the binder laminas was present only along the thick-binder part of the quenched surface. The surface of the protruding AP, which often appeared to have some binder melt overlay with thick binder, still exhibited a smooth surface with thin binder, but the binder was recessed and the AP no longer appeared to have experienced binder melt flow. They proposed that the protrusion of the AP near the AP-Binder interface was due to local lateral heat drain from the AP thermal wave into the cooler endothermic binder lamina, and suggested that this might lead to local quenching of the AP self-deflagration and decomposition of the AP by dissociative sublimation (explaining also the difference in surface quality of this part of the AP surface). The lateral heat flow argument was tested by using a gold lamina (nonreactive heat sink) and mica (non-reactive insulator) in place of the binder lamina and the results confirmed the argument. A more complex flame structure was proposed for the sandwich combustion. It consisted of a leading edge that was a kinetically limited (premixed) flame, with a transition to a trailing diffusion-controlled flame further from the interface (see figure 1-11). The experimental observations and mechanistic arguments that applied on sandwich

combustion were interpreted and applied on composite solid propellant combustion theory. They suggested that the diffusion flame would be appropriate to the outer flame since it occurred between two initially unmixed gases, and that a kinetically limited flame stood in the near surface mixing fan from each AP/binder interface. They argued that chemical kinetics permitting, the mixing and reaction for the primary oxidizer-fuel flame were completed within 100-200  $\mu\text{m}$  of the surface.

In 1982, Price, Panyam, Sambamurthi and Sigman [51] reported further experimental results on the combustion of sandwiches. By using finer AP powder, in the dry pressed AP laminas, they observed that the details of the polycrystalline microstructure of the AP laminas had little effect on sandwich burning. They proposed that the region of the flame near the burning surface involved a complex of interactive flames:

- a) An AP flame,
- b) Kinetically limited pre-mixed flames between binder and AP vapors in the mixing fans, and
- c) Trailing diffusion-limited flames.

From experimental observations and physical arguments, they concluded that there was a region, called "propagation (or flame) velocity controlling" region, very important for the combustion behavior. That region included the kinetically limited leading edge of the oxidizer/fuel flame (KLLEF) and supplied most of the heat to pyrolyze the binder (see figure 1-12).

In 1983, Price and Sambamurthi [52], presented further results on the dependence of the burning rate of AP/binder sandwiches on the thickness of the binder lamina. They obtained burning rate curves for AP-PBAN sandwiches at different pressures, for different binder thicknesses. All curves showed a point of maximum regression rate for binder

thickness between 50 and 100  $\mu\text{m}$ , and showed that at high pressures the sandwich burning rate was dominated by the self deflagration rate of the AP.

In 1984 and in 1986, Price, Sambamurthi, Sigman and Panyam [53], [54], reported a series of experimental studies on combustion of sandwiches, and the results were used to develop a relatively detailed qualitative model for the combustion zone microstructure (see figure 1-13). They presented (based on new and previously obtained results), the principal features of the sandwich combustion zone microstructure and processes, and the dependence of the flame complex on pressure for various binder thicknesses. They argued the effect of pressure on the principal features of the combustion zone and developed physical and mechanistic arguments for the interpretation of results from:

- a) Deflagration limit tests,
- b) Sandwich burning rate tests,
- c) Bimodal propellant burning rate tests,
- d) Surface details and surface profiles of quenched sandwiches, and
- e) Sandwich burning tests, where the binder lamina was filled with AP powder or had been substituted by a good conductor or a nonconductive material.

#### 1.1.5 Literature Review on the Effects of Additives

While scientists were trying to further develop the two-dimensional sandwich model, understand its combustion and relate it to composite solid propellants, other research continued on the physical and chemical properties of oxidizers, binders, metals and other ingredients involved in composite solid rocket propellants.

Most of the research efforts were concentrated on some particular ingredients that were broadly used in the manufacturing of common propellants. Ammonium perchlorate (its properties, decomposition and deflagration) was extensively studied (references [55]

through [64]) as the most common oxidizer. Aluminum was used as a metal fuel and many investigators studied the properties, the role it played in combustion, and its effect on combustion instabilities ([65], [67]). Many binders were investigated and their decomposition and role in propellant combustion was examined ([68], [69], [70]).

At the same time, it was known that certain ingredients could be used (and were used) in low concentrations as burning rate catalysts or suppressants. There was much research effort involved as those compounds were added to the oxidizer or the binder and experiments were run to find out how those additives reacted with the propellant ingredients.

The introduction of additives to an oxidizer/binder sandwich system was first reported by Hightower and Price [34], in 1966. In their AP/PBAA sandwiches, they used carbon, copper chromite and lithium fluoride as ballistic modifiers in the binder lamina. They noticed that the additives used affected the general characteristics of the surface pattern, and suggested that further investigation had to be employed.

Powling [35] obtained the rates of flame penetration down a binder (PIB)/oxidizer (AP) interface. The burning rate of the system with 1% copper chromate (CC) in the AP was higher than the burning rate of the uncatalyzed system. The effect was stronger when 10% CC was added into the binder.

Nadaud's experiments [37], using AP rods joined side by side to solid fuel (PIB) rods in an inert atmosphere (pressure range 5-80 atm), agreed qualitatively with Powling's. The addition of CC in polybutadiene rods gave also burning rate curves higher than the

Ermolaev, Korotkov and Frolov [38], used lithium fluoride (LiF) and iron oxide ( $\text{Fe}_2\text{O}_3$ ) as additives in their layered systems. Their tests were run in nitrogen and pressure domain 5-100 atm. They introduced 1 and 3% by weight of the sample into either the oxidizer (Ammonium Perchlorate) or the binder (Polyformaldehyde). They observed

that LiF and  $\text{Fe}_2\text{O}_3$  introduced into the binder layers increased the burning rate. The effect of the additives into the AP was quite different since  $\text{Fe}_2\text{O}_3$  increased the burning rate but LiF decreased it by 50% or more. From this they concluded that  $\text{Fe}_2\text{O}_3$  acted as a burning rate catalyst (3%  $\text{Fe}_2\text{O}_3$  had stronger effect than 1%) and LiF acted as a burning rate suppressant (especially for 3% LiF) for the mixture. Discussing their results, they suggested that the change in the burning rate of sandwiches, when additives were introduced, was probably caused by the action of the additive on either the kinetics of the gas reactions taking place near the flame "roots" (see figure 1-4) or on the rate of decomposition of the components. When the additive was introduced into the binder they proposed that the additive particles entered the gas phase in condensed form and probably played the part of catalysts of the heterogeneous reactions in the combustion zone. When LiF was added to the oxidizer, the decomposition rate of the AP decreased (there was probably a melt on the surface, since AP and LiF form an eutectic - also suggested by Hightower and Price [29]), which led to retardation of the combustion. On the contrary,  $\text{Fe}_2\text{O}_3$  accelerated both the thermal decomposition and the burning rate of AP.

Pittman [71], in 1969, examined the catalytic effects of iron-containing burning-rate catalysts ( $\text{BBCl}$ , IO) by burning propellant strands (with AP as oxidizer and CTPB as binder). He stated that the site of catalytic action in burning propellants was difficult to locate, because the combustion zone that could contribute to rate control was very thin, involved a heterogeneous solid phase, a heterogeneous gas phase, and above all, a very steep thermal gradient was superimposed across this zone. He noted that the catalyst might contribute to the rate control in one or more of the following regions:

- a) Fuel/oxidizer diffusion flame
- b) Monopropellant decomposition flame
- c) Surface AP exothermic decomposition

- d) Subsurface AP exothermic decomposition
- e) AP/binder heterogeneous subsurface decomposition
- f) Gaseous AP/condensed binder surface reaction
- g) Endothermic (or exothermic) binder pyrolysis
- h) Endothermic AP dissociation and gasification.

Pittman concluded that:

1. The catalytic effectiveness increased at higher pressures (shown by measuring the strand burning rates of a variety of propellants).
2. Mixing the catalyst into the binder increased the catalytic effectiveness much more than coating the AP with catalyst or using an AP-catalyst coprecipitated oxidizer.
3. Catalysts did not act beneath the burning surface to enhance AP decomposition or to catalyze oxidizer/binder heterogeneous reactions.
4. Catalysts, probably, acted in the gas phase to increase the reaction rate of perchloric acid and its initial decomposition products.
5. Particles of  $\text{Fe}_2\text{O}_3$  could act as catalysts while still attached to the condensed phase by protruding into both monopropellant and diffusion flame zones.

Jones [41], in 1971, and Jones and Strahle [72], a year later, presented their results using CC and  $\text{Fe}_2\text{O}_3$  (IO=Iron Oxide) as catalysts into oxidizer (AP)/binder(CTPB) sandwich systems. They concluded that CC was a more effective catalyst than IO (for the systems they studied) and that the addition of CC and IO in the AP was the most effective method of increasing the burning rate (the augmentation increased with pressure increase). Introduction of the additives into the binder or at the AP/binder interface were less effective. Based on high speed combustion photography they observed that:

- a) At all pressures CC appeared to primarily catalyze the AP deflagration process with a minor effect upon the oxidizer/binder gas phase reactions.

b) At pressures below 100 psia the IO had a primary catalytic effect upon the binder/oxidizer gas phase reactions while inhibiting AP deflagration, but at pressures above 1000 psia the IO catalyzes primarily the AP deflagration process and not the oxidizer/binder gas phase reactions.

c) Neither CC or IO promoted heterogeneous reactions of gases with the solid fuel binder and neither modified the pyrolysis mechanism of the solid fuel binder.

Inami, Rajapakse, Shaw and Wise [73], in 1971, presented their study which was based on AP+CC/Gas Fuel system. Their results indicated that copper chromate played the dual role of accelerating the decomposition of AP and of promoting the oxidation of the impinging fuel by heterogeneous reactions at the surface of the solid AP+CC. These surface catalyzed reactions yielded a net exothermic heat release.

In 1973, Lobanov, Churnev and Bakhtanov [74], experimented with Fe<sub>2</sub>O<sub>3</sub> in charges (mixtures of AP with PMMA or AP and PS). They proposed that to understand the mechanism of the action of catalysts on the burning rate of combustion of condensed systems, it was important to know the actual concentration of catalyst particles in the zone which determined the combustion rate. They observed that iron oxide concentrated on the charge surface. Their experiments showed that:

- a) The concentration of catalyst on the surface layer of extinguished charges could be considerably greater than the concentration of catalyst in the starting charge.
- b) The degree of build-up of catalyst was minimal for a composition with a maximal combustion rate.
- c) When the pressure increased, the degree of catalyst build-up rose.
- d) The fine iron oxide particles agglomerated and formed a porous layer on the surface, and jets of gas broke through this layer. In some cases there was a cyclic increase of the

layer to a determined thickness, breakaway and entrainment by the gas,  $t^{1/2}$  growth of a new layer, etc.

Strahle, Handley and Milkie [75], studying AP/HTPB sandwich systems with catalysts, qualitatively confirmed Jones' earlier results (on AP/CTPB sandwiches). From combustion photography studies they showed that the leading edge of regression for a catalyzed solid propellant sandwich was always away from the binder (as Hightower and Price [34], Varney [18], and Boggs and Zurn [43] had showed for uncatalyzed AP). Handley and Strahle [76], [77] verified the results of the previous study by employing the use of scanning electron microscope on quenched sandwiches.

Strahle, Handley and Kumar [78], extended their work to include more quenched sandwich combustion studies; so they could view the surface structures and melt behavior in the presence of catalysts and compare them with known results. They used AP as oxidizer, HTPB as binder and four catalysts: CC, IO, IB, F, which were added in the oxidizer, in the binder or at the interface. Their new conclusions consisted of:

- a) The copper compounds in CuO<sub>2</sub>O<sub>2</sub> had a greater catalytic effect upon the AP deflagration rate than the iron compounds. The iron compounds had a stronger catalytic effect upon the binder/oxidizer reactions.
- b) In all cases catalysts reduced the extent of binder melts, which could be a rate-augmenting process.
- c) The effect of catalysts on the burning rate was generally augmented as the pressure increased.
- d) The surface structure of AP during deflagration changed markedly when catalysts were present in the AP, probably suggesting that alteration of condensed phase reactions took place in the AP.

Handley in his thesis [79], reported most of his earlier published work and he added the following:

- a) All combinations, in pairs, of the four catalysts he used, (he added catalyst in the AP and in the binder at the same time) exhibited either a positive or a possible synergistic effect on both the sandwich burning rate or the oxidizer regression rate when tested at 600 psia
- b) A positive synergistic effect on sample burn rate was detected for cast composite propellant samples; this effect was as strong as for the two-dimensional sandwich samples
- c) The burning rate of the sandwiches when they were uniformly loaded (catalyst added in the oxidizer and the binder) was greater than the burn rate of the sandwiches when catalyst was added either in the oxidizer or in the binder or at the oxidizer/binder interface.

Martynyuk, Bakhman and Lobanov [80], in 1977, added catalyst to a layer of oxidizer, because they believed that the efficiency of a catalyst incorporated in the oxidizer was close to that in composite systems. They observed that:

- a) The effectiveness of catalytic action ( $\text{Fe}_2\text{O}_3$ ) in a laminate system (AP/PMMA) increased significantly with an increase in pressure.
- b) A maximum value was obtained for the burning rate when the  $\text{Fe}_2\text{O}_3$  content was optimum (2% in this specific case where  $p=40$  atm).

They studied the effect of inhibitors (PC, PTER, PETP films) along the contact of the boundary between fuel and oxidizer during the combustion of the PMMA/AP system. Their inhibiting properties were associated with their ability to form a residual coke layer on the surface (for the conditions under investigation). The coke layer impedes diffusion of the gasification products from the fuel and oxidizer to the combustion zone, leading to quenching of the sample.

Korobeinichev, Kovalenko and Lesnikovich [81], studied the effect of catalysts through thermal decomposition and combustion of mixtures of oxidizer and binder. From their data it was concluded that:

#### I. For the decomposition of the AP+PS system:

- a) Iron oxide was much more active than copper oxide ( $\text{CuO}$ ), under the same
- b) For the catalysts BMCP and FR, it was the decomposition fragments of BMCP and FR respectively that catalyzed the decomposition of the system (since the decomposition temperature of those catalysts was less than the temperature at which they had an appreciable catalytic effect on the decomposition of AP and the composite systems).

The compounds formed during their decomposition process, had a large specific surface.

#### II. For the decomposition of AP+PMMA mixtures under conditions of rapid heating (300 °C/sec):

- a) Performing the experiments under almost vacuum conditions, it was easier to find all the decomposition products and determine which reactions were affected by the catalyst.
- b)  $\text{CuO}$  was more active than  $\text{Fe}_2\text{O}_3$  in accelerating the decomposition of AP and the oxidation of the polymer, which led to a greater increase in the rate of heat release in the condensed phase. They argued that the change in the order of activity of the iron and copper oxides was associated with the difference in the temperature dependences of their

#### III. For the combustion of the composite system:

- a) The burning rate of the composite systems was increased. The order of decreasing effectiveness on the burning rate was  $\text{CuO}$ ,  $\text{CuCr}_2\text{O}_4$ ,  $\text{Fe}_2\text{O}_3$ . This series coincided with that for AP decomposition at 300 - 400 °C and with the system (AP+PMMA) decomposition under rapid heating conditions, but did not coincide with the activity order for the AP+PS system decomposition at 300 - 400 °C.

- b) The organometallic catalysts decreased their activity as the pressure increased.

This was attributed either to less concentration of the catalysts on the surface or to the fact that with increase in the heating rate in the combustion wave as the pressure rose, the time required for the organometallic compound to decompose with the formation of combustion catalyst was probably greater than the dwell time of the additive in the reaction zone of the

Finally, they reported that :

1. There was no correlation between the catalytic decomposition and combustion of the mixture was observed

2. Their data were in agreement with the views of previous investigators in the Soviet Union, who stated that the catalyst acted in the condensed phase.

Kishore and Sunitha [82], in 1978, tried to relate the acceleration of the AP decomposition and the enhancement of the burning rate of AP-based composite propellants. They argued that if the oxides operated in the same way in the decomposition and in the combustion, then the Redox potential of the oxides (measure of the extent of the electron transfer process) should be correlated with the burning rate, i.e., lower the Redox potential the higher should be the burning rate. They, also, proposed that the catalyst action mechanism could be explained on the basis of the formation of metal perchlorate intermediates, which being more thermally unstable, might bring down the decomposition Foster and Miller [83], in 1978, worked with composite AP/HTPB propellant strands with Iron Oxide as a catalyst. They reported that:

- a) A saturation level of catalyst existed at which no further increase in burning rate was obtained. The level of saturation increased with pressure,
- b) The high surface area catalyst showed a higher rate than the low surface area material,
- c) The strongest augmentation in burning rate was observed for lower pressures.

Kishore and Sunitha [84], in 1979, in their literature survey on the effect of Transition Metal Oxides on Decomposition and Deflagration of Composite Solid Propellant Systems briefly described tests and results on the effect of Transition Metal Oxides on:

1. Propellant Combustion.
2. Combustion of Condensed Mixtures.
3. Sandwich Propellant Combustion.
4. AP Deflagration.
5. Decomposition of AP.
6. Decomposition of KP.

They also defined the areas of interest that still needed to be investigated as:

1. The effect of Transition Metal Oxides (TMO) as a function of pressure.
2. The effect of particle size of TMO on combustion and decomposition.
3. The effect of mixture ratio on the effectiveness of catalyst.
4. The effect of initial temperature on the effectiveness of catalyst.
5. The concentration of catalyst and its effect on pressure deflagration limit and deflagration rate in AP deflagration.
6. The effect of catalyst in the presence of metals, i.e., aluminum.

Kishore, Pai Verneker and Sunitha [85], in 1980, working on AP+PS and on AP+CTPB propellant systems proposed that one of the ways by which Transition Metal Oxides (TMO) acted was the formation of reactive Transition Metal Perchlorate Amine (TMPA) intermediates. That was indicated by the correlation between thermal stability of TMPAs and burning rate of the propellants containing TMOs and TMPAs.

Foster [86], in 1981, performed screening experiments, while trying to develop composite propellants with very low burning rate pressure sensitivities and a broad range of burning rates. He concluded that:

- a) In the high rate regime chromium dioxide and iron oxide proved to be effective by providing strong rate augmentation, while maintaining relatively low pressure exponents
- b) In the medium burning rate regime copper phthalocyanine was an effective catalyst
- c) For obtaining low rates, calcium oxide was used as a rate suppressant.

Price and Sambamurthi [87], in 1984, examined the mechanism of burning rate enhancement of propellants by catalysts. They introduced the catalyst ( $\text{Fe}_2\text{O}_3$ ) in the binder lamina (25-125  $\mu\text{m}$ ) of AP/HC binder propellants. Tests were run in a combustion bomb pressurized by nitrogen from 1.38 to 5.52 MPa. Combustion Photography was employed to observe burning and to measure burning rates. The Scanning Electron Microscope was used to microscopically study the burned surfaces of the interrupted samples. Their results indicated that enhancement of the burning rate depended on the concentration of the catalyst on the binder surface. The concentrated layer of catalyst permitted adequate contact of the fuel vapors with the surface of the catalyst. They argued that the heavy fuel molecules were pyrolyzed passing through the sintered catalytic bed on the binder surface (It is worth noting at this point that many of the catalysts added in composite solid propellants are used in the gun propellant industry and petroleum refinery industry as fuel cracking compounds). It is argued that the smaller fuel fragments were more easily oxidized and were responsible for the establishment of the kinetically limited leading edge (KLEP) of the oxidizer/fuel flame closer to the surface. The dragging of the KLEP closer to the surface augmented the burning rate as was earlier explained [53].

Extending their sandwich work they introduced  $\text{Fe}_2\text{O}_3$  in a family of propellants and they concluded that  $\text{Fe}_2\text{O}_3$  catalyzed the breakdown of the binder molecules to smaller fragments, which were easily oxidized and brought the oxidizer/binder flame closer to the surface, enhancing finally the burning rate.

In 1985, Price, Sambamurthi and Sigman [88], employed thin binder sandwiches in their study. They added catalyst in the binder and noted that interpretation of the oxidizer-catalyst experiments never included reference to the fact that the catalyst in a real propellant situation was immersed in binder, and that combustion zone conditions were thus not usually conducive to interaction of oxidizer and catalyst. In their APPBAN sandwiches experimental work they added 10% additive in the 50  $\mu\text{m}$  thick binder and they chose  $\text{Fe}_2\text{O}_3$  for a more detailed study using a range of binder thicknesses, additive loading and test pressure.

Using high speed combustion photography techniques and scanning electron microscopy they observed and speculated that:

1. Al,  $\text{Al}_2\text{O}_3$ , ZnC and  $\text{B}_4\text{C}$  had only moderate effect on burning rate, and showed relatively little concentration on the burning surface.
2. Iron blue,  $\text{Fe}_2\text{O}_3$  and copper chromite exhibited significant concentration on the binder surface, and burning rate enhancement.
3. The concentrating additives showed bright flame in the region above the additive, and occasional streaks that were fragments of concentrates leaving the surface. The concentrated additive acted as a catalyst bed through which the large fuel molecules had to flow. The catalytic or partial oxidative breakdown of the large fuel molecules yielded fuel species that were more readily oxidized by the AP vapors, resulting in close proximity of the oxidizer/fuel flame to the surface.
4. Increasing concentration of additives was accompanied by decreasing presence of the smooth AP surface close to the oxidizer/binder interface plane (the smooth AP surface became irregular). The above AP surface details appeared to be related to approach of the oxidizer/fuel flame to the surface, which suppressed endothermic AP sublimation and favored exothermic AP deflagration.

5. CuO, ferrocene and  $\text{Cr}_2\text{O}_3$  enhanced the burning rate with minimal (or less) surface concentration. It was believed that catalysis of the fuel pyrolysis occurred.

6. Aluminum hydroxide and antimony oxide were strong burning rate suppressants. The first probably reduced the temperature of binder vapors, since it had a high heat of vaporization and the second was reported to be a free radical scavenger that would inhibit the oxidizer/fuel flame.

7. LiF and  $\text{BiF}_3$  reduced the burning rate, but not as much as it was expected on the basis of earlier results in propellants.

8. Introduction of 1%  $\text{Fe}_2\text{O}_3$  into the oxidizer increased the burning rate moderately over the whole binder thickness range.

9. With catalysts in the binder, condensed phase or surface reactions of the AP were not catalyzed and condensed phase AP/binder interaction was not increasing sample burning rate.

Their results, contradicted earlier studies ([76], [79]) since from those previous experiments it was concluded that introduction of additives into the binder had little effect on the burning rate. It is worthy, though, to note that the earlier tests involved thick binder sandwiches (150 - 200  $\mu\text{m}$ ), different binder (HTPB) and low concentrations of  $\text{Fe}_2\text{O}_3$  in the binder (2.5%).

Krishnan and Periasamy, [89], in 1986, performed a series of studies on catalyzed and uncatalyzed AP/CTPB propellants. They examined the burning characteristics of the propellants under subatmospheric pressures, because they claimed that at subatmospheric pressures, the combustion zone thickness was large and the oxidizer and fuel had enough time to mix to form a premixed flame. They employed scanning electron microscope and visual observation of burning strands and they concluded that:

1. At subatmospheric pressures there was possible presence of interfacial heterogeneous reactions on composite solid propellant burning surfaces. It is suggested in these references that use of thick binder laminar can lead to effects not normally present in propellants, but for the thickness in question the burning rate was not catalyzed.
2. At subatmospheric pressures as the catalyst's concentration increased, the low pressure deflagration limit also increased. This was attributed to the increases in interfacial reactions that might have resulted in faster undercutting of the AP particles and prematurely releasing the AP particles from the surface.

3. The catalytic effect of Copper catalysts was generally less than that of Iron catalysts at subatmospheric pressures and greater at high pressures.

Fong and Hamshere [90], [91], in 1986, presented in their studies - working on AP/HTPB composites propellants - evidence that condensed phase chemical reactions could be rate limiting at lower pressures during combustion. They worked on AP/HTPB propellants and employed Copper Chromite,  $\text{Cr}(\text{Salen-N-decyl})_3$ , and metal phthalocyanine complexes. They stated that the Transition Metal Oxides had an unknown chemical composition and morphology, since partially hydrated states and varied oxometal bridging could result in mixed and varying metal oxidation states. An evidence supporting their statement was that the effectiveness of various metal oxide catalysts varied from batch to batch, even when they were produced from a single manufacturer. To the contrary, Transition Metal Organometallic compounds, were effective catalysts, and well defined entities. Studying DTA thermograms and burning rate curves they concluded that:

1. The additives they used catalyzed the binder thermal decomposition, so consequently condensed phase chemical reactions could be rate limiting at low pressures during combustion (The additives catalyzed the depolymerization of the binder to form lower molecular weight melts on the surface. Enhanced reactions that occurred in the

binder melt provided gaseous decomposition products. These gaseous species could also mix with AP and binder melt on the burning surface to induce exothermic reactions. These chemical reactions could be promoted by the embedded catalyst particles).

2. Iron compounds followed by Chromium and Copper compounds were the more effective burning rate enhancers at the pressures studied (2-14 MPa).

### 1.2 Objectives of the Research

The ultimate objectives of every dedicated researcher in the combustion field are to understand combustion and to be able to control it.

Until now science is in its first steps towards these two major objectives. Although much research has been done and many results have been obtained there is a lot remaining to be explored and understood.

From the preceding literature review it is quite evident that there is a wide variety of views regarding the mechanism of composite solid propellant combustion.

Many theories are very specific; apply only to particular cases. Other theories are highly speculative often conflicting with experimental results. In general, no theory is able to solve a particular combustion problem and predict realistically the results. This is because of the very large number of parameters entering each case. The most important parameters are a wide range of pressure, the various properties of the different oxidizers, the different fuels, binders and additives used, different particle sizes, preheating of the sample, inert or reactive atmosphere. Finally the whole problem is strongly three-dimensional and deals with three phases of the matter. Now it is clear why a general mathematical combustion model is extremely difficult.

In order for a combustion model to be accepted, it must give the same results (show the same trends) as those obtained by experiments. The two-dimensional sandwich approach is employed in this study in order to verify simple combustion models which are

developed. This is a compromise between the complexity of the real three-dimensional combustion and the oversimplification of a one-dimensional combustion model. The two-dimensional sandwich permits viewing the flame structure and the surface profile in great detail.

The general purpose of this study is to further understand the combustion mechanism of composite solid rocket propellant combustion through experiments and investigation of their results. The role of energetic binders on sandwich burning will be examined, and the effect of different additives will be discussed.

The main object is to observe how the energetic binder BAMO-THF and NIMO behave in a sandwich system and compare their behavior with previous results. Tained for PBAN binder sandwiches. Movie tests were run in order to plot the burning rate curves versus binder lamina thickness or test pressure. The motion pictures provide some information on the shape of the profile, the flame color and/or brightness, and the existence of smoke and/or particle trails. For the same test conditions, quench experiments were run to obtain detailed surface information of the sample; particularly close to the interface. They assisted in providing further information needed to sketch the surface profiles at different pressures and binder lamina thicknesses. Low pressure tests were run employing tapered sandwiches; useful information on the low pressure deflagration limit was extracted from the results.

Further investigation employed the introduction of several catalysts in the binder lamina in order to obtain information on their effect on the burning rate and on how the surface of the sandwich changed when compared with the respective (same binder lamina thickness and test pressure) uncatalyzed binder case. An exploratory investigation on the effect of catalysts on the low pressure deflagration limit was also conducted.

The experimental results presented in this dissertation are going to be carefully analyzed and studied. The flame complex theory presented in reference [54] will be expanded to predict the detailed effects of binder properties and catalysts on burning rate trends, surface profiles, and flame structure. The experimental results will be used to validate the qualitative theory.

## CHAPTER II

### EXPERIMENTAL PROCEDURE

#### 2.1 Overview

This experimental investigation was conducted in the Propulsion Laboratory of the School of Aerospace Engineering of the Georgia Institute of Technology.

The basic components of the laboratory's facilities are:

1. A high pressure combustion chamber used for combustion photography.
2. A high pressure combustion chamber used for quenched burning.
3. A high intensity light source.
4. A high speed movie camera.
5. A movie projector/motion analyzer.
6. A video camera-monitor-recorder component system.
7. An optical microscope.
8. A scanning electron microscope.
9. A 1200 Watt infrared laser.

In Figure 2-1 the flowchart of the different experiments employed is presented. Using the procedures described in this chapter, the oxidizer discs and binder are prepared and the sandwiches are constructed. A portion of the sandwiches is used in a window pressurized vessel and their burning is filmed. Analyzing these movies yields information on the sample's surface profile and its flame structure, and on any particles or smoke being emitted. The regression rate is measured and the sandwich burning rates are plotted as a

function of binder lamina thickness and test pressure. The effectiveness of catalysis is also calculated for each test condition. Other sandwiches are used for "instantaneously" interrupted combustion experiments in a pressurized chamber. Their quenched surface is examined under the optical and scanning electron microscopes to collect information on surface profiles, the oxidizer / binder interface region, particle concentration and color differences.

The experiments mentioned above are the main sources of obtaining information on sandwich burning. Two more techniques of secondary importance were employed, which assisted in verifying some of the results gathered through combustion photography and microscopy of the quenched samples' surface. These consist of: a) Tapered sandwiches, ignited at pressures lower than the AP self-deflagration limit, and allowed to self-extinguish are examined in the microscopes to provide the minimum binder lamina thickness required for combustion. b) Pure or catalyzed binder samples pyrolyzed under a high power infrared laser beam and inspected to collect information on their surface characteristics and any residual concentration.

A full description of the experimental techniques that were employed is explained in the next paragraphs.

## 2.2 Experimental Techniques

### 2.2.1 Combustion Photography

Combustion photography was employed for direct observation of the combustion behavior and for measuring the burning rate. A high pressure combustion apparatus with a variable flow, variable pressure nitrogen purge system was used for this technique. This apparatus was designed by the Naval Weapons Center [65] and the nitrogen flow system is

shown in reference [79]. The samples were externally illuminated with a 2500 watt Xenon light source whenever necessary. A Leica 16 mm movie camera was initially employed to obtain high speed motion pictures using speeds of 200-500 frames/sec. A Vivitar preset 85 mm focal length lens was attached to the camera. A combination of extension tubes and a lens adapter was used in order to obtain appropriate magnification of the sample on the film. The motion pictures were analyzed using an Advantix <sup>LW International Model 2</sup> ~~MT-8 by EIKI-Industriat Co.~~ <sup>movie projector with</sup> ~~movie projector with variable speed and frame counter~~.

A video component system was introduced later. This system consisted of a Panasonic WV-3260/8AF color video camera with the lens and extension tubes described above, a Panasonic AG-1950 video cassette recorder, a Panasonic WV-3203A power supply, and a Sony KV-25XBR Trinitron high resolution TV/monitor.

Although the movie camera yields greater resolution, much time is spent between filming and viewing a combustion movie while the film is processed commercially. Any mistakes in an initial test will be repeated in future experiments until the first test movie is developed and viewed.

This can be eliminated by using the video component system. The sample can be viewed in real time as it burns and the whole combustion process can be reviewed immediately after burning using the video tape replay. Any mistakes (smoke, light, etc.) can be recognized and corrections will be made in order for the next test to be a success.

The video component system has the shortcoming of limited framing rate and resolution. The video camera can be operated only at a frame rate of 30 frames/sec. This is good enough for obtaining the burning rate but becomes useless when studying processes that take place in less than 1/30th of a second. The strobe effect shutter has a speed of 1/1000th of a second for exposure at 1/60th of a second intervals. This high shutter speed enables the video camera to freeze the motion and to provide a sharp image.

### 2.2.2 Quench Burning Method

The quench burning method was employed in order to interrupt the combustion process and view the burning surface of the sample. The high pressure combustion system used is illustrated in reference [18]. The sample was burned in a high pressure vessel which interrupts burning by rapid decompression. The abrupt pressure release was accomplished by a burst diaphragm disc consisting of several layers of mylar as originated by Varney [18]. The number of mylar disks required to hold the combustion vessel test pressure was predetermined experimentally. After a preset time following ignition, an abrupt electric current heated a nichrome wire - located between the mylar disks - causing a sufficient number of mylar disks to melt and the remaining disks to rupture. This sudden pressure drop interrupted the combustion of the burning sample. The sample was carefully removed and was preserved for further analysis by the scanning electron microscope.

The quench burning method was initially questioned because there was no certainty that the surface obtained from quenching was the real surface, occurred during the combustion. Currently there is strong evidence that supports the technique. Surface details obtained from tapered sandwiches and from samples quenched due to heat loss to metal slabs attached at the sides of the sample supported the quench burning technique since all the interrupted burning surfaces were very similar [66]. Furthermore, high magnification movies show many of the microscopic features.

### 2.2.3 Sandwich Preparation

A sandwich configuration is a layer of binder of definite thickness sandwiched between two pressed oxidizer laminae. A typical sandwich is shown in Figure 1-1. The

sandwiches were burned edgewise and examined under the microscope or studied through combustion photography.

The oxidizer laminae were prepared from compacted, polycrystalline disks of oxidizer. The oxidizer was propellant grade 99.7% purity, low alkali Kerr-McGee AP with particle size in the 90-130  $\mu\text{m}$  range (it was ground in a Heiko grinder). The compacted oxidizer disks were made by pressing 1.7 grams of ammonium perchlorate into a 2.54 cm diameter disk in a Carver hydraulic press at 220 MPa for 2 hours. The disks were very carefully cut into quarters and, bonded together in layers using binder. The binder thickness was controlled by shims of known thickness placed at the edges between the cut AP quarters. The samples were secured with cellophane tape on a teflon sheet and placed in an oven to cure. The cured samples were carefully cut and sanded down to the desired dimensions. Their thickness and uniformity of the binder layer were examined by an optical microscope and then they were stored in desiccators (dry environment) until they were tested.

The study of the role of burning rate catalysts was examined by introducing these additives into the binder during its preparation (the preparation of binders is fully described in appendix A). In earlier studies ([72], [75] - [80], [87], [88]) additives were introduced into the AP, into the binder or at the oxidizer/binder interface. For quite some time it was believed that the catalytic action of the additives affects mainly the oxidizer. This view was misleading because in the very thick binder sandwiches previously used, the overall burning rate was controlled by the oxidizer. It is worthy also to note that in preparing a composite solid propellant the catalyst is introduced into the binder and mixed with it prior to the propellant manufacturing. Additive particles are always contained in the binder and the chances that they are in contact with an oxidizer particle are extremely slim.

Preparation of tapered sandwiches is very similar to the preparation of regular sandwiches. The difference is that a 125  $\mu\text{m}$  shim is placed between the cut AP quarters at

one end only. At the other end, the two AP quarters are in contact. The thickness of the binder in a tapered sandwich (Figure 1-9) starts from nearly zero and increases to about 125  $\mu\text{m}$ . Tapered sandwiches were ignited on the thick binder end at low pressures (below the AP self deflagration limit) and self extinguished when the oxidizer-binder flame could not sustain combustion. These tests were used in order to obtain the spontaneous quench limit at constant pressure.

#### 2.2.4 Optical Microscope Studies

A Leitz optical microscope was employed in this study. The sandwiches were examined before doing the experiments to verify that the binder layer was continuous. The binder thickness was also measured.

The optical microscope also provided a fast way to study the surface and the surface profile of the quenched samples. It is important to note that the optical microscope preserves the samples color contrast, and the identification of surface compounds is easier than using the scanning electron microscope.

#### 2.2.5 Scanning Electron Microscope (SEM) Studies

The SEM is very important in high resolution studies of interrupted burning tests on propellant sandwiches. It has been extensively used in solid propellant research studies [66],[67]. The scanning electron microscope used in this investigation is an International Scientific Instruments Model 60.

The key advantages of the SEM over the optical microscope are a broad range of magnifications with a high depth of field. Resolution to the submicron range is attainable even under adverse conditions.

The sample to be studied was mounted on an aluminum stub and was coated with a thin layer of gold in an International Scientific Instruments PS-2 coating unit for deposition of a conductive film on the surface to be examined. The sample was then placed in the SEM's specimen chamber. The surface profile was viewed and the quenched surface was analyzed carefully at different orientations of the stage. Polaroid pictures were taken wherever required.

A sample SEM Polaroid photograph is illustrated in Figure 4-44. The bars in the upper left corner of the micrographs represent the length scale; in this figure the fourth dimensional bar in the upper left represents a length of 100  $\mu\text{m}$ .

#### 2.2.6 Laser Pyrolysis

The laser pyrolysis facility of the Combustion/Propulsion Laboratory of the School of Aerospace Engineering was involved in providing helpful information about the binder surface and particularly on any particle concentrations formed when a catalyzed binder was employed.

A P.R.C. model FHI-140, 1300 Watt CO<sub>2</sub> laser, produces an infrared beam which gives a strong heat flux to the binder surface. This beam is directed to the surface through a system of gold coated copper mirrors, lenses and a copper kaleidoscope for beam homogenation.

### CHAPTER III

#### EXPERIMENTAL STRATEGY

This dissertation presents an experimental investigation of different binders and various additives used in the combustion of composite solid propellants. Their effect on the combustion of the oxidizer / binder system is explored.

In this study two binders were examined: PBAN - which has been studied by previous investigators [49] - [54] and it is used here as a basis for comparison - and BAMO-THF which is a new binder and belongs in the newly developed family of high density energetic binders. Later in the investigation another, somewhat higher energy binder designated as NMMO became available, and screening tests on NMMO-AP sandwiches were run and are reported. The oxidizer used in this study was ammonium perchlorate (AP). The oxidizer laminae of all types of sandwiches tested were made of AP because: a) it is the most commonly used oxidizer, b) its properties are known and it has been studied thoroughly and c) all earlier studies used as a reference or for comparison in this dissertation had been using AP.

The effectiveness of several catalysts as well as their mechanisms of action were studied. Based on various experimental methods and physical analysis, arguments were developed to explain the way the different catalysts act.

The catalysts involved in this investigation were iron based compounds:

$\text{Fe}_2\text{O}_3$ : Ferric oxide, which is a red powder,

$\text{Fe}_3\text{O}_4$ : Ferrous or Ferrosiferic oxide, which is a black powder,

Carocene: a new organic compound used as a catalyst in the composite solid propellant industry. Carocene is in liquid form.

In the present study the catalysts were restricted to the binder. The site of most important catalytic action is believed to be in the binder for the reason that in a real propellant the particles of the catalyst are embedded in the binder and the probability of an oxidizer and a catalyst particle being in contact is extremely low (when a composite propellant is manufactured, the catalyst is added in the binder prior to mixing all the ingredients together).

Some investigators [78], [79] employed catalysts in the oxidizer or at the binder / oxidizer interface. Their results were not totally relevant to composite solid propellants since in a real propellant the particles of catalyst were always surrounded by polymeric binder.

In the case of the powdered catalysts ( $\text{Fe}_2\text{O}_3$  and  $\text{Fe}_3\text{O}_4$ ), 10% by weight was added in the binder while liquid Carocene was 20% of the binder. This loading is in agreement with real propellant compositions, in which the catalyst is 2.5% of the composite solid propellant (the binder is about 17% of the weight).

Previous studies [87], [88] also concluded that 10%  $\text{Fe}_2\text{O}_3$  in the binder is very close to the optimum percentage of catalyst in the binder lamina of a PBAN sandwich. A screening test of 5% and 10% of  $\text{Fe}_3\text{O}_4$  introduced in BAMO-THF binder showed that an addition of 10% of  $\text{Fe}_3\text{O}_4$  enhances the burning rate of the sandwiches more than the addition of 5%.

The series of experiments performed consisted of the employment of the following types of sandwiches:

In some earlier reports ([75] - [79]) binder thicknesses of 200  $\mu\text{m}$  and more were examined. These results although not of much significance and importance to composite solid propellant combustion nicely complement the present study.

Finally, the Movie tests provided visual information on the burning surface, the shape of the burning surface profiles and on the visible flame structure.

B. "Quenched" tests and Microscopy studies: Quench tests are the experiments from which the sample suddenly interrupts its burning because of rapid depressurization of the combustion vessel.

These interrupted burning tests were performed on the same sample types that are mentioned before and for the same pressures and binder thicknesses. The Movie tests were carried out prior to the Quenched tests because they provided information on the burning rate. From the burning rate the exact time to interrupt combustion after ignition can be estimated in order for the sandwich combustion to reach a steady state before quenching.

The quenched surface of the sandwiches was studied under the optical and the scanning electron microscopes and photographs were taken. Details related to color differences, surface characteristics of the oxidizer and the binder, and features of the catalyst (particle size, color, concentration, structure etc.) were noted. Information was extracted on the oxidizer / binder interface region.

The microscopy studies and the movies taken during sandwich burning provided the information needed to draw the surface profiles as a function of pressure and binder thickness.

C. Tapered sandwiches: As noted earlier (pg. 24), these provide information on the spontaneous quench limit at constant pressure (this pressure is below the low pressure deflagration limit of ammonium perchlorate). Systematic tests on PBAN tapered sandwiches reported in previous studies [49] - [54] were compared with tapered

1. AP / PBAN / AP, to verify earlier results.
2. AP / PBAN + 10%  $\text{Fe}_2\text{O}_3$  / AP, to support previous investigations.
3. AP / PBAN + 10%  $\text{Fe}_3\text{O}_4$  / AP.
4. AP / PBAN + 20 % Caocene / AP.
5. AP / BAMO-THF / AP.
6. AP / BAMO-THF + 10%  $\text{Fe}_2\text{O}_3$  / AP.
7. AP / BAMO-THF + 10%  $\text{Fe}_3\text{O}_4$  / AP.
8. AP / BAMO-THF + 20 % Caocene / AP.
9. AP / NIMMO / AP (screening tests).
10. AP / NIMMO + 10%  $\text{Fe}_2\text{O}_3$  / AP (screening tests).

The following experimental techniques were involved in the investigation:

A. "Movie" or "video" tests: Tests of all the types of sandwiches mentioned above, were performed at various pressures and using different binder thicknesses. Burning rates were measured from these experiments and curves were plotted of the burning rate versus binder thickness for each pressure condition. Curves were also sketched of the ratio of catalyzed over uncatalyzed burning rates of sandwiches.

The tests were performed at three different pressures: 300, 500 and 1000 psi. These pressures were chosen because they are encountered in solid rocket motors and they are consistent with pressures used in earlier studies ([53], [54]).

Binder thicknesses of 25, 50, 75, 100 and 125  $\mu\text{m}$  were chosen so easy comparison can be made with previously obtained results. The thicknesses mentioned above are realistic since scanning electron micrographs showed that the AP particles are embedded in the binder and the distance between two neighboring AP particles was always in the range of less than 125  $\mu\text{m}$ .

sandwiches of PBAN + 10%  $\text{Fe}_2\text{O}_3$ , PBAN + 20 % Catocene, BAMO-THF, and BAMO-THF + 10%  $\text{Fe}_2\text{O}_3$ . For a complete series of tapered sandwich tests, graphs were plotted of the test pressure versus the binder thickness at which the combustion spontaneously quenched.

## CHAPTER IV

### EXPERIMENTAL RESULTS

#### 4.1 Burning Rate and Movie Studies

An investigation of the combustion of oxidizer / binder sandwiches was conducted using cinephotomacrography and video techniques.

The sandwiches tested involved ammonium perchlorate as the oxidizer and PBAN or BAMO-THF as the polymeric binder. Three additives were employed in the binder lamina to study the effect of catalysts on the combustion of sandwiches.

The movies and the videos were primarily used to obtain values of the sample burning rates. The burning rate data were taken after a steady profile had been developed. For the steady profile the burning rate was measured at the point of maximum regression of the sandwich. The burning rate curves were plotted as a function of binder thickness and for different pressures.

As previously noted the binder thickness was varied between 25 - 125  $\mu\text{m}$  and the tests were run at pressures of 300, 500 and 1000 psi (2.1, 3.45 and 6.9 MPa respectively).

In some cases the burning rate was measured for binder lamina thicknesses different than the above mentioned ones. [All experimental data are shown in Appendix B].

The plan was to have at least two experiments, so two measurements can be obtained under each test condition. Then the average burning rate of these two (or more) tests was calculated to obtain a data point corresponding to a particular binder thickness at a specific pressure. In some cases though, the data points on the burning rate curves were generated

from one experiment. This happened whenever a sample burned nicely and uniformly and its burning rate was found to be consistent with the burning rates of samples tested under adjacent binder lamina thicknesses at the same pressure. Under some other test conditions some experimental data were discarded since the experiments from which they were obtained resulted in failures (a: uneven burning = sandwich burned faster on one side than on the other, or burned on the rear side which did not permit visual observation of the flame front; b: smoke and bad position of the ignition wire made measuring of the burning rate impossible since they obstruct sample visualization).

The effect of catalyst was presented as burning rate ratio curves in which the burning rate data have been normalized by dividing the burning rate of catalyzed binder sandwiches over the corresponding uncatalyzed binder sandwich burning rate (corresponding means the employment of the same binder, same binder thickness and pressure).

#### 4.1.1 Pure Binder Sandwiches

PBAN is the most commonly used binder (considering quantity used) and its effects on sandwich burning have been studied in detail earlier [51] - [54]. PBAN motion pictures and burning rate data obtained previously and during the course of this study (see figure 4-1) were used as the basis for comparison with the motion pictures of BAMO-THF and NMMO binders and their burning rate (see figures 4-2, 4-3 and 4-5).

4.1.1.1 Motion Picture Study: BAMO-THE. By studying PBAN and BAMO-THF motion pictures the following were observed:

- a) PBAN sandwiches had a yellow / orange visible flame, which was always much brighter and more yellowish than the BAMO-THF sandwich orange flame for the same conditions.

- b) BAMO-THF sandwiches did not burn when the thickness of the binder lamina was less than  $75 \mu\text{m}$  at 300 psi. Samples with binder lamina of about  $75 \mu\text{m}$  at this pressure were difficult to ignite and sustain combustion. PBAN sandwiches always burned under all the conditions examined (including very thin binders at low pressures).

- c) At thick binder laminas at 1000 psi pressures it was clearly observed that PBAN binder protrudes. A separate flame was also visible above each region of the binder / oxidizer interface. With BAMO-THF binder less protrusion of the binder was noted from the motion pictures. The binder lamina was recessed for all thin binders tested.

- d) PBAN samples were also noted to produce much more dark smoke than BAMO-THF sandwiches under the same test conditions (something that was expected since PBAN includes more carbon; responsible also for the much brighter yellow / orange visible flame).

- e) As the flame propagated downwards on the binder / oxidizer interface region a melt was observed on the non-burning end of the sample ahead of the burning front when PBAN binder was employed. This was more noticeable at thick binder laminas ( $\geq 100 \mu\text{m}$ ) - in these cases a dark colored globe was formed on the binder just in front of the leading edge of the flame (see figure 4-4a). In the case of BAMO-THF this type of melt was not encountered. Instead some binder pieces became curly and they were observed to leave away from the leading part of the propagating flame (see figure 4-4b).

- f) A dark strip was observed during burning all along the binder surface of the BAMO-THF (see figure 4-4c); something that was not observed when PBAN was used (inspection of the quenched sample surfaces under the optical microscope verified the existence of dark pieces on the top of the binder).

4.1.1.2 Burning Rate Study: BAMO-THE. The burning rate of BAMO-THF sandwiches was very similar to the burning rate of PBAN sandwiches. A series of tests

was run to reproduce the PBAN binder sandwich burning rate data, reported previously [54]. The burning rate curves were reproduced for the 300 and 500 psi pressures but there was a deviation in the data for the 1000 psi case. At this particular pressure all the burning rate data were slightly lower than the ones measured earlier. Since the prepolymer and the other ingredients mixed were from the same containers used to obtain the previously obtained curves, it is suspected that some aging of the ingredients (especially of the prepolymer) took place. Evidence to support this argument was provided by the changing in color of the PBAN (during the period since the tests in reference [54]) from light yellow / brown to dark brown - which is an indication of polymeric degradation of the binder.

From the burning rate curves (see figures 4-1, 4-2 and 4-3) the following were observed:

a) The burning rate curves for both binders go through a maximum. For BAMO-THF the maximum occurred always at thicker binders than for PBAN, especially at low pressures. This was expected since BAMO-THF/more binder (fuel) is needed in order to support combustion (concluded from the fact that BAMO-THF binder sandwiches at 300 psi ignited and burned only when the binder lamina was thick and from results on tapered sandwiches - they are discussed later; BAMO-THF is not a good fuel). At 1000 psi the self-deflagration of AP dominated the burning of the sandwich and any major effects of binder thickness cannot be observed clearly.

b) The burning rate curve peak shifted to thinner binder lamina as the test pressure increased. This was observed for both binders examined (a detailed explanation can be found in reference [54]).

c) At 300 psi thick (100 - 150  $\mu\text{m}$ ) BAMO-THF binder sandwiches burned faster than PBAN sandwiches having the same thickness. Given the fact that BAMO-THF at 300 psi did not burn below 75  $\mu\text{m}$  lamina thickness it is concluded that the kinetics and energetics

of the two binders are different and important in explaining the behavior of each binder. At 1000 psi the burning rate curves were almost identical.

4.1.1.3 *Exploratory Study of NMMO*. A series of screening tests involving the behavior of a new energetic binder (NMMO) in a sandwich system was examined. NMMO decomposes exothermically with a Differential Thermal Analysis (DTA) curve similar to BAMO-THF. At the same time it has smaller fuel value than BAMO-THF.

Sandwiches with NMMO as the binder (AP was used as the oxidizer) were ignited and burned at 300 and at 500 psi. The burning rates measured are presented at the end of Table 1 (Appendix B).

At 300 psi in nitrogen the burning rate was almost the same over the range of binder thicknesses used (25 - 125  $\mu\text{m}$ ). A pale short flame was observed when the binder lamina was thick (125  $\mu\text{m}$ ). Dark pieces were observed on the binder surface for thick binders. No visible flame was observed for thin binders. All sandwiches had a U-shaped surface profile. It is important to note that NMMO binder sandwiches burned to completion for thin binders at 300 psi; a major difference between NMMO and BAMO-THF binders.

At 500 psi in nitrogen short yellow flames were visible when the binder thickness employed was more than 100  $\mu\text{m}$ . No visible flame was observed when the sample was thin. The exposed binder surface was black in color (it seemed like dark pieces on the binder). No smoke was observed - nothing like the black smoke of PBAN sandwiches was encountered. Binder flow melt was observed under the leading edge of the flame on the front of the sample. A flat surface profile was observed in the region near the binder lamina for all cases. The burning rate was almost identical to the burning rate of pure AP (see figure 4-5).

#### 4.1.2.2 Effect on BAMO-THF Sandwiches. (see figures 4-11, 4-12, 4-13, 4-14 and 4-15)

a)  $\text{Fe}_2\text{O}_3$  was a burning rate catalyst for BAMO-THF at all cases of binder lamina thickness and pressure studied. The effect was stronger at low pressures and thin binders (as with PBAN) - for this case an increase of more than 40% was measured (generally more than that measured with PBAN binder). At 300 psi and for 75  $\mu\text{m}$  binder lamina thickness the burning rate was doubled - recall that the pure uncatalyzed BAMO-THF sandwiches burned slowly under these conditions and in some tests they did not even ignite. At 1000 psi the effect of  $\text{Fe}_2\text{O}_3$  was around 40% for the entire range of binder lamina thickness.

b) Thin BAMO-THF sandwiches that would not burn at 300 psi ignited and burned for all binder lamina thicknesses when 10%  $\text{Fe}_2\text{O}_3$  was used in the binder (introduction of in the BAMO-THF binder was responsible for getting over the binder thickness limit. This  $\text{Fe}_2\text{O}_3$  is consistent with results from tests employing tapered sandwiches. The catalyzed tapered sandwiches burned to a thinner binder limit than pure BAMO-THF sandwiches, under the same pressure conditions).

c) The highest burning rate with  $\text{Fe}_2\text{O}_3$  catalyzed BAMO-THF sandwiches was always measured for 75  $\mu\text{m}$  binder lamina thickness at all pressures examined.

d) Under the same pressure the addition of  $\text{Fe}_2\text{O}_3$  in the BAMO-THF binder lamina shifted the peak of the burning rate curve to lower binder thicknesses. At 1000 psi the above observation cannot be stated because all uncatalyzed sandwiches with 25 - 100  $\mu\text{m}$  thick laminas had almost the same burning rate.

e) BAMO-THF sandwiches catalyzed with  $\text{Fe}_2\text{O}_3$  produced a much brighter flame than the pure BAMO-THF sandwiches. Strips were observed to come off and trails from hot particles also appeared to leave the burning surface close to the interface.

#### 4.1.2 Catalyzed Binder Sandwiches: $\text{Fe}_2\text{O}_3$

##### 4.1.2.1 Effect on PBAN Sandwiches. (see figures 4-6, 4-7, 4-8, 4-9 and 4-10)

a)  $\text{Fe}_2\text{O}_3$  enhances the burning rate of PBAN sandwiches at all pressures for all binder lamina thicknesses tested. The effect was stronger as the pressure increased and the binder lamina became thinner. At low pressure (300 psi) and thin binders an 80% increase in burning rate was measured. 20 - 50% enhancement occurred with thin binders at 500 and 1000 psi while for thick binders the increase in burning rate was observed to be 10 - 20% at all pressures.

b) As the pressure increased the introduction of  $\text{Fe}_2\text{O}_3$  in PBAN made the curve peaks shift towards lower binder lamina thickness.

c) At the same pressure the employment of  $\text{Fe}_2\text{O}_3$  in the binder lamina shifted the peak of the burning rate curve to thinner binders.

d) Some parts (or the whole) of the burning binder surface became bright when the catalyst was added in the binder lamina. It appeared that the thinner the binder the more continuous the brightness along the binder. This brightness was correlated with the formation of a catalytic bed on the binder.

e) Hot particle trails and strips were observed leaving the burning surface from the area around and above the binder / oxidizer interface. This was considered as evidence of breaking of the catalytic bed - its pieces were carried away by the produced gases.

f) No indication of binder melt ahead of the flame front at the end surface of the sample was observed.

#### 4.1.2.3 Comparison of effects of $\text{Fe}_2\text{O}_3$ on PBAN and BAMO-THF binders. (see figures 4-16, 4-17 and 4-18)

- a) Although  $\text{Fe}_2\text{O}_3$  catalyzed both binders its effect on BAMO-THF was stronger than on PBAN.
- b) A bright layer (or bright pieces) were observed on the binder surface for both catalyzed binder cases. The flame or hot catalyzed bed was brighter than the flame of the uncatalyzed binder sandwiches tested under the same conditions - especially for BAMO-THF binder.
- c) Strips (probably pieces of concentration of catalyst) were observed coming off the surface. Hot particles (not very many) were also coming off the combustion zone - their trails were observed on the pictures.
- d) As the pressure decreased the effect of catalyst became stronger for both binders tested, permitting BAMO-THF sandwiches to burn under conditions for which uncatalyzed sandwiches would not burn.
- e) Pronusion of the binder at high pressures and thick binders was stronger in the PBAN + 10%  $\text{Fe}_2\text{O}_3$  case than the corresponding BAMO-THF case.

4.1.2.4 Effect on NMMO Sandwiches. At 500 psi and in inert atmosphere ( $\text{N}_2$ ) the burning rate increased 100% at some cases (see figure 4-5; the experimental data at the end of Table 1). All samples had a sharp V-shaped surface profile. An orange flame was developed for thick binders (100 - 125  $\mu\text{m}$ ) which was not bright; for thinner binders almost no visible flame was encountered. A dark surface was observed underneath the visible flame (thick binder case). Particles were coming off the binder surface and their trails appeared on the screen.

#### 4.1.3 Catalyzed Binder Sandwiches: $\text{Fe}_3\text{O}_4$

##### 4.1.3.1 Effect on PBAN Sandwiches. (see figures 4-19, 4-20, 4-8, 4-9 and 4-10)

In general catalysis by  $\text{Fe}_3\text{O}_4$  was similar to catalysis by  $\text{Fe}_2\text{O}_3$ , but the effect was not as large.

- a) For thin binder laminae (25 - 50  $\mu\text{m}$ ) the burning rate of PBAN + 10%  $\text{Fe}_3\text{O}_4$  binder sandwiches was enhanced at the pressures of 300 and 500 psi.
- b) At the same pressure the introduction of  $\text{Fe}_3\text{O}_4$  in the binder lamina shifted the maximum of the uncatalyzed burning rate curve to thinner binders.
- c) The burning rate curve peak occurred at 25  $\mu\text{m}$  under all pressures tested.
- d) The orange / yellow flame that pure PBAN sandwiches produced was not as bright as in the case of PBAN sandwiches catalyzed with  $\text{Fe}_3\text{O}_4$  for thin binder laminae.
- e) Although some hot particle trails could be seen on the movies, brightness on the binder surface was not observed.
- f) No indication of binder melt was noted to lead the downward flame propagation which was observed with uncatalyzed PBAN sandwiches (see figure 4-4d).
- g) At 300 psi the burning rate was augmented more than 15% for all binder thicknesses. For binder lamina thicknesses of 50  $\mu\text{m}$  or lower an increase of 30 - 60% was calculated.
- h) At 500 psi for thin binders (25 - 50  $\mu\text{m}$ ) the burning rate was increased by 20 - 40% but was not affected when the lamina became thicker.
- j) At 1000 psi and for 25  $\mu\text{m}$  binder lamina an enhancement of 15% was measured for the burning rate. For thicker binders the burning rate was either unaffected or decreased by less than 10%, and strong binder protrusion was observed as with uncatalyzed samples.

#### 4.1.3.2 Effect on BAMO-THF Sandwiches. (see figures 4-21, 4-22, 4-13, 4-14 and 4-15)

- a) For all binder thicknesses and at all pressures the burning rate increased by  $\text{Fe}_3\text{O}_4$  by more than 30% and for some cases it was doubled.
- b) The lower the pressure the more effective the action of  $\text{Fe}_3\text{O}_4$  as a catalyst in the BAMO-THF binder - with the exception of thick binders (100 - 125  $\mu\text{m}$ ) at 300 psi where rates with uncatalyzed binder were high compared to the trend at high pressure.
- c) The highest burning rate was observed at 75  $\mu\text{m}$  for pressures of 500 and 1000 psi and at 100  $\mu\text{m}$  for 300 psi.
- d) At the same test pressure the addition of  $\text{Fe}_3\text{O}_4$  in the BAMO-THF binder lamina shifted the peak of the uncatalyzed burning rate curve to thinner binder laminas. As in the case of  $\text{Fe}_2\text{O}_3$  this is not a very accurate statement for the 1000 psi pressure; at this pressure the burning rate of the uncatalyzed BAMO-THF sandwiches was about the same for the 25 - 100  $\mu\text{m}$  binder lamina thickness range.
- e) At 300 psi the addition of  $\text{Fe}_3\text{O}_4$  made possible the burning of samples with thicknesses below 75  $\mu\text{m}$ . The effect on thick binder sandwiches at 300 and 500 psi was not as strong as for thin samples. At 1000 psi the burning rate of catalyzed sandwiches was 70 - 80% higher than the burning rate of uncatalyzed samples for the whole binder lamina thickness range.
- f) The introduction of  $\text{Fe}_3\text{O}_4$  in the BAMO-THF produced brighter flame than the pure binder case but not as bright as in the  $\text{Fe}_2\text{O}_3$  case (indication that a hot catalytic bed may not exist). Particle trails were observed but no brightness over the burning binder surface was confirmed.

#### 4.1.3.3 Comparison of effects on PBAN and BAMO-THF Binders. (see figures 4-23, 4-24 and 4-25)

- a)  $\text{Fe}_3\text{O}_4$  can be considered as a good burning rate catalyst for BAMO-THF binder. Its catalytic effects on PBAN are not very strong.
- b)  $\text{Fe}_3\text{O}_4$  catalyzed thin PBAN binders more than thick ones. At 1000 psi pressure for lamina thicknesses larger than 50  $\mu\text{m}$  a decrease in the burning rate was measured. Its catalytic effect on BAMO-THF was almost constant for the different binder lamina thicknesses under the same pressure.
- c) The  $\text{Fe}_3\text{O}_4$  - catalyzed BAMO-THF produced a much brighter visible flame than the one observed for uncatalyzed samples. In the case of PBAN the reverse was true; brighter flame was seen in the case of uncatalyzed sandwiches.
- d) Particle trails were observed for both catalyzed binder cases.
- e) The lower the pressure the stronger the catalytic action of  $\text{Fe}_3\text{O}_4$ .
- f) Protrusion of the catalyzed PBAN binder was very clear for thick binder laminas at 1000 psi. In the case of catalyzed BAMO-THF no clear visual evidence was provided from the movies.
- g) No indication of melt was observed ahead of the flame front for both binders (during edge observation).
- h) The burning rate curve peak was shifted to thinner binders for catalyzed PBAN as the pressure increased. For catalyzed BAMO-THF the maximum occurred around the same binder lamina thickness for all pressures tested.

#### 4.1.4 Catalyzed Binder Sandwiches: Catocene

##### 4.1.4.1 Effect on PBAN Sandwiches. (see figures 4-26, 4-27, 4-8, 4-9, 4-10)

- a) Catocene strongly enhances the burning rate of PBAN sandwiches at all pressures and all binder lamina thicknesses examined. An earlier study with catocene and other

ferrocene derivatives in propellants suggested that the increase of propellant burning rate was related to ease in decomposing the organic iron compounds, making molecular size iron oxide which was available very close to the surface and was necessary to enhance the burning rate. [97].

- b) The maximum of the burning rate occurred in the 25 - 50  $\mu\text{m}$  range of binder lamina thickness at all pressures tested.
- c) Under the same test pressure the addition of catocene in the binder lamina shifted the peak of the uncatalyzed burning rate curve to thinner binders.
- d) At all pressures tested the catalytic effect of catocene on PBAN increased as the binder lamina became thinner. The enhancement of burning rate for the 125  $\mu\text{m}$  thick binder case was about 10% but can go up to 80% for the 25  $\mu\text{m}$  thin binder case.

e) The visible flame was very bright (probably it is the hot catalytic bed) close to the burning binder surface (50  $\mu\text{m}$  thick binder sandwiches were very bright - indication of high temperature and probably the main reason why at 50  $\mu\text{m}$  the maximum burning rate was measured). Concentration of catalyst was observed to build up, break and go away from the combustion area although catocene was added as liquid in the binder (when the concentration broke away less brightness was observed). Hot particle trails were also observed.

f) No obvious evidence of binder melt ahead of the flame leading edge at the end of the surface of the sample was observed but clearly the formation of binder melt globes was not seen.

#### 4.1.4.2 Effect on BAMO-THF Sandwiches. (see figures 4-28, 4-29, 4-13, 4-14 and 4-15)

a) Catocene strongly enhances the burning rate of BAMO-THF binder sandwiches at all pressures and for all binder lamina thicknesses examined. The burning rate was

augmented by 50% at least - with the exception of thick (100 - 125  $\mu\text{m}$ ) binder laminae at low pressures (300 psi). The effect increased as the lamina became thinner at all pressures tested. At 1000 psi that trend was less developed and the burning rate enhancement was almost constant for all binder thicknesses (70 - 100% increase). At 300 psi the addition of 20% catocene in the binder made possible the combustion of BAMO-THF sandwiches with binder lamina thickness less than 75  $\mu\text{m}$  and even as low as 25  $\mu\text{m}$ .

- b) The highest burning rate was always measured at thin binder laminae (25  $\mu\text{m}$ ) for all the pressures employed. That also means that under the same test pressure the addition of catocene in the BAMO-THF binder lamina shifted the maximum of the uncatalyzed burning rate curve to thinner binders.
- c) The visible flame produced by catalyzed with catocene BAMO-THF sandwiches was much brighter than pure BAMO-THF samples. Few pieces were observed to fly away from the combustion zone and the existence of trails was not numerous.
- d) No indication of binder melt was observed ahead of the flame front.

#### 4.1.4.3 Comparison of effects of catocene on PBAN and BAMO-THF binders. (see figures 4-30, 4-31 and 4-32)

- a) Catocene is a very good catalyst for both binders studied. Its effect on BAMO-THF sandwiches was stronger than on PBAN.
- b) A bright layer or broken bright pieces were observed on the binder burning surface strip for both binder cases. This was clearly observed for thin binder laminae.
- c) The visible flame above the combustion region was brighter than the flame of the uncatalyzed binder sandwiches - especially when BAMO-THF binder was employed.
- d) The lower the pressure the stronger the effect of catocene in each binder, particularly when the binder lamina was thin.

- e) Strips were coming off the burning area and hot particle trails were observed - not as many with BAMO-THF as with PBAN binder.
- f) No indication of binder melt ahead of the flame front was encountered with both binders.

#### 4.1.5 Comparison of effects of all catalysts on PBAN (see figures 4-8, 4-9, 4-10, 4-33, 4-34 and 4-35)

1. Carocene was the best catalyst for PBAN with the exception of  $\text{Fe}_2\text{O}_3$  at 300 psi.  $\text{Fe}_2\text{O}_3$  was also effective in enhancing the burning rate of PBAN.  $\text{Fe}_3\text{O}_4$  was the least effective of the additives examined. Although it increased the burning rate at 300 and 500 psi it did not affect the burning rate at 1000 psi test pressure.
2. The effect of all catalysts was stronger as the pressure became lower and the binder lamina was thinner.
3. Brightness was observed on the burning binder surface strip for carocene and for  $\text{Fe}_2\text{O}_3$  catalysts but it was not encountered when  $\text{Fe}_3\text{O}_4$  was added in the binder.
4. An indication of binder melt accumulation was seen ahead of the flame front at the end of the surface of the sample but was not as strong as in the pure PBAN case. No melt was observed when  $\text{Fe}_3\text{O}_4$  was used. Protrusion of binder was very clear at 1000 psi with  $\text{Fe}_3\text{O}_4$  thick catalyzed binder (at this pressure  $\text{Fe}_3\text{O}_4$  slightly retarded the burning rate).
5. Particles were observed to leave the combustion zone and their trails were seen for the carocene and  $\text{Fe}_2\text{O}_3$  cases.

#### 4.1.6 Comparison of effects of all catalysts on BAMO-THF (see figures 4-8, 4-9, 4-10, 4-36, 4-37 and 4-38)

1. All three compounds used were very good burning rate catalysts for BAMO-THF.  $\text{Fe}_2\text{O}_3$  being slightly less effective than carocene and  $\text{Fe}_3\text{O}_4$ .

2. The effect of all three catalysts was almost constant for the different binder lamina thickness used at the same pressure. The large difference observed at 75  $\mu\text{m}$  and 300 psi was attributed to the fact that BAMO-THF burned with difficulty under these conditions and did not burn when the lamina was thinner.
3. All catalyzed BAMO-THF sandwiches - even thin ones - ignited at 300 psi burned without any difficulty. Uncatalyzed sandwiches of 75  $\mu\text{m}$  thickness burned one out of three times at 300 psi and did not burn at all when the binder lamina was thinner.
4. With the exception of thick binders at low pressures, the effect of the examined catalysts was always higher than 40% and in some cases higher than 100%.
5. Trails and strips coming off the combustion zone were observed at all catalyzed binder cases and the visible flame was much brighter than in the respective case of pure binder sandwiches.

#### 4.1.7 Conclusion on the effects of additives on the burning rate of sandwiches and the visible combustion zone

1. All additives examined enhanced the burning rate of both binders (with the exception of  $\text{Fe}_3\text{O}_4$  in PBAN at 1000 psi).
2. Carocene was the best burning rate catalyst for both binders. It was followed by  $\text{Fe}_2\text{O}_3$  in PBAN with  $\text{Fe}_3\text{O}_4$  trailing. Using BAMO-THF binder the effect of  $\text{Fe}_3\text{O}_4$  was stronger than the effect of  $\text{Fe}_2\text{O}_3$  under the same test conditions.
3. All catalysts acted more effectively when introduced to BAMO-THF binder than when added to PBAN.
4. The effectiveness of catalysts increased as the test pressure decreased. Stronger catalytic effects were also observed for thin binders.

5. Catalyzed BAMO-THF binder sandwiches were able to ignite and burn at low pressures even for thin binders.
6. Catalyzed BAMO-THF binder sandwiches produced a brighter visible flame than pure BAMO-THF samples.
7. A bright strip was observed on the burning binder surface. It was more evident at thin binders because the visible yellow flame was not very bright to disturb observation. In the case of  $\text{Fe}_3\text{O}_4$  in PBAN there was no indication of brightness on the binder. Strips and hot particle trails were observed in almost all experiments.

#### 4.1.8 Pressure dependency of the burning rate of sandwiches

The results of the sandwich burning rate tests were plotted in the figures presented throughout this chapter. In these figures the burning rate of sandwiches was plotted against the binder lamina thickness at the three different pressures tested. All these figures were characterized by:

1. At large binder laminae the burning rate appeared to approach a limit
2. As the binder lamina becomes thinner a maximum is obtained for the burning rate
3. As the binder thickness goes to zero the burning rate appears to approach the AP self-deflagration rate; for pressures above the AP self-deflagration rate. At lower pressures, a quench limit is encountered as the binder lamina thickness decreases.

In the figures 4-39 through 4-43 a partial cross plot of some of the previously presented curves is shown as burning rate versus pressure.

In figure 4-39 three curves are shown (figure 4-1 and reference [54] provided with the data):

- a. The AP self-deflagration rate
- b. The conditions for maximum sandwich burning rate and

- c. The burning rate for thick binder lamina sandwich ("thick slab limit")

Price et al. [54] concluded that extrapolating the maximum sandwich burning rate curve, the enhancement in burning rate over the AP self-deflagration rate was seen to go to zero; around 10 MPa pressure. The thick slab burning rate approached the AP rate at lower pressure; about 5 MPa. All the above results were obtained for the sandwich system with AP as the oxidizer and PBAN as the binder.

In figure 4-40 the maximum burning rate of PBAN sandwiches and PBAN sandwiches catalyzed with three additives are sketched. Data points are cross-plot points from curves plotted in figures 4-8, 4-9, and 4-10.

In figure 4-41 the maximum burning rate of pure BAMO-THF and catalyzed BAMO-THF sandwiches are plotted (the three compounds -  $\text{Fe}_2\text{O}_3$ ,  $\text{Fe}_3\text{O}_4$ , catocene - were used as catalysts). Data points are cross-plot points from curves plotted in figures 4-13, 4-14, and 4-15.

The AP self-deflagration rate is sketched on figures 4-40 and 4-41 for comparison purposes.

From these two figures it is clear that the maximum sandwich burning rate curves converge to the AP rate curve if the latter is extrapolated at higher pressures (this statement becomes questionable above 14 MPa; at this pressure a transition in the AP behavior occurs). The coalition of the maximum burning rate curves appears to occur above the 10 MPa pressure; limit that was postulated earlier, [54], for the pure PBAN sandwiches.

Figures 4-42 and 4-43 show the effect of catalyst on the thick binder limit (figure 4-42 summarizes the results with PBAN binder while figure 4-43 represents the effects of catalysts on BAMO-THF binder). The burning rate curve seems to approach the AP self-deflagration rate curve; this happens at a pressure higher than 5 MPa - pressure predicted for thick pure PBAN sandwiches.

#### 4.2 Studies of Quenched Sandwiches

A detailed study of the quenched surface of oxidizer/binder sandwiches was completed using optical and scanning electron microscopy. The effect of test variables (pressure, type of binder, binder lamina thickness, type of additive) on the burning surface profile and surface quality provide indirect evidence of what is happening to the flame structure. The similarities between the quenched surfaces of a sandwich and a composite solid propellant are identified and shown in figure 4-44.

Successful interrupted burning tests were run with sandwiches that involved AP as the oxidizer and PBAN or BAMO-THF as the polymeric binder (a screening series of tests with NMMO binder was also carried out). Three additives were employed in the binder lamina to investigate the effect of catalysts on the quenched sandwich surface.

The samples were partially burned at 300, 500 and 1000 psi in a dry nitrogen atmosphere. The binder lamina thickness of the samples was varied between 25 - 125  $\mu\text{m}$  in increments of 25  $\mu\text{m}$ . Slide pictures were taken for most of the cases on the optical microscope and micrographs were obtained from the scanning electron microscope.

The slide pictures were studied carefully with emphasis on the surface profile of the sample (AP slope, binder and/or oxidizer protrusion or recession etc.) and the features of the surface related to the catalyst (concentration, color, size and structure). The surface profiles for PBAN binder sandwiches are shown in figure 4-45 (see reference [54]).

Thorough investigation of the micrographs was carried out. The surface of the oxidizer was observed and any unusual surface details on it have been noted. The condition of the residual binder lamina was studied as well as any different feature on the AP/binder interface. The effect of the catalyst on the quenched sandwich surface and at the AP/binder interface was also investigated.

The scanning electron micrographs were taken at similar magnification for all samples. Low magnification pictures were typical of the sandwich surface; along the binder lamina, along the oxidizer/binder interface and on the oxidizer surface. The AP surface in locations far from the oxidizer/binder interface was observed to have the same characteristics for all samples burned at a particular pressure; similar surface features were observed earlier when pure deflagrating AP was quenched at pressures identical with the pressures used in this study. High magnification pictures show details of the binder surface and the interface as well as the features of the different catalytic particles and their formations. Figure 4-46 shows the details of the quenched surface of PBAN binder sandwiches.

#### 4.2.1 Pure Binder Sandwiches

##### 4.2.1.1 BAMO-THF

1. The burning surface profile was almost flat at pressures of 1000 psi - indicating that the AP self deflagration rate dominated the burning rate of the sandwich (see figure 4-47). As the pressure decreased the AP started to incline and a V-shape profile was obtained at 500 psi. The AP slope became steeper for thin binder laminas than for thick ones. At 300 psi the sandwich approached a U-shaped profile, and the AP on the upper arms of the "U" did not burn but broke away due to thermal stress (300 psi is very close to the self-deflagration pressure limit of AP).
2. The binder lamina of BAMO-THF had a bubbly and wavy surface under all the conditions examined (see figure 4-48). This was in contrast to features observed with PBAN binder whose surface was always very smooth without any wrinkles on it (see figure 4-46).

3. The energetic BAMO-THF binder lamina did not protrude strongly even when the pressure was high (1000 psi) and the binder lamina thick (125  $\mu\text{m}$ ). Protrusion of the

binder was developed as a ridge in the middle of thick the binder lamina (see figure 4-48b). In the case of the inert PBAN, under similar conditions the whole binder lamina protruded (see figure 4-46b). From DTA/DSC experiments it was shown that BAMO-THF has a much lower decomposition temperature than the PBAN polymer, and this can explain why the protrusion of the binder was less for BAMO-THF sandwiches than for PBAN samples. BAMO-THF binder lamina were observed to be recessed for thin binders (25µm). In all intermediate binder thickness conditions (50 - 100µm) the energetic binder had an almost flat surface (see figure 4-48a) while the inert PBAN binder was strongly protruding or strongly recessed depending upon binder lamina thickness and pressure applied (see figure 4-46a).

4. No signs of binder flow melt were encountered for BAMO-THF sandwiches (see figure 4-48); under certain conditions (high pressure, thick binder lamina) binder flow melt was observed for PBAN sandwiches (see figure 4-46).

5. The retarded AP burning adjacent to the interface, which was present with the inert PBAN binder, was absent with the energetic BAMO-THF binder (compare figures 4-46a and 4-48a).

6. The inert (PBAN) binder sandwiches had a definite smooth band (see figure 4-46a) while the energetic BAMO-THF binder sandwiches did not have a distinct smooth band on the AP close to the interface (see figure 4-48). From the SEM pictures it was concluded that the AP zone next to the binder/oxidizer interface had different surface characteristics than the rest of the AP which was self-deflagrating far from the leading edge of the diffusion flame, but the AP protrusion and smooth surface seen with PBAN binder sandwiches was absent.

#### 4.2.1.2 NMMO

1. The entire burning surface profile was flat at pressures of 500 and 1000 psi; the AP self-deflagration rate governs the sandwich burning rate.

2. The NMMO binder lamina surface was observed to be smooth at the pressures tested (see figure 4-49). Some wrinkles were observed (probably occurred during cooling of the binder melt). The surface looked like PBAN binder; no bubbles were encountered.

3. Some binder protrusion was observed for 75 µm thick sandwiches at 1000 psi. This protrusion was encountered at different locations along the binder lamina.

4. Signs of binder melt flow were observed, over the neighboring AP, on the quenched surface of the samples examined.

5. The AP surface adjacent to the interface had a more smooth, froth free appearance than the rest of the AP (which self-deflagrated).

#### 4.2.2 Catalyzed Binder Sandwiches: $\text{Fe}_2\text{O}_3$

4.2.2.1 Effect on PBAN Sandwiches. The effects of  $\text{Fe}_2\text{O}_3$  on PBAN sandwiches can be summarized as follows:

1. The slope of the burning surface profile for PBAN sandwiches catalyzed with  $\text{Fe}_2\text{O}_3$  was observed to be always steeper than the pure PBAN sandwiches (see figures 4-46 and 4-50). This was expected since the catalyzed binder sandwiches burned faster than the pure PBAN samples. Even at 1000 psi the flat surface profile of the uncatalyzed PBAN sandwiches became V-shaped when 10%  $\text{Fe}_2\text{O}_3$  was added to the binder.

2. Concentration of catalyst on the binder surface was observed under all conditions and in some cases a catalytic bed was formed (see figure 4-51). The formation of a continuous catalytic bed was encountered when the binder lamina had a thickness in the range of 50 - 100 µm under all pressures examined (see figure 4-51a). At lower pressures

(300 psi) a continuous catalytic bed was observed even when the binder was 125  $\mu\text{m}$  thick. Discontinuous catalytic bed formations or catalytic agglomerations were observed for thin binder laminae (25  $\mu\text{m}$ ) and when the binder protrusion was high (at high pressures and/or thick binders: the case of 125  $\mu\text{m}$  at 300 psi is excluded). In some cases aggregates were observed to emerge from the binder or to sit on the top of it (see figure 4-51b). The catalytic concentration had a dark silver/black color and was porous. The pores were smaller than 5  $\mu\text{m}$  in diameter. It was suspected at this point that the red iron oxide ( $\text{Fe}_2\text{O}_3$ ) became  $\text{Fe}_3\text{O}_4$  during combustion ( $\text{Fe}_3\text{O}_4$  is a black powder). An additional evidence of was obtained by demonstration of the magnetic properties of the catalyst's aggregation, which are exhibited only by  $\text{Fe}_3\text{O}_4$ . A literature survey, [92], suggested that evolution of oxygen occurs from ferric oxide in reducing environments above 600  $^\circ\text{C}$ . Therefore it is possible that ferric oxide acts also chemically as an oxidizer on the binder surface.

3. No wrinkles or bubbles were observed on the catalyzed binder surface which was immediately under the catalytic bed formation. Whenever a continuous catalytic structure was not observed, pieces of aggregated particles were sticking on the smooth binder surface.

4. Recessed binder was observed for 25  $\mu\text{m}$  binder lamina thickness at 500 psi and at 1000 psi. Protrusion of the catalyzed binder was observed for thicker binder laminae at all pressures, and its height was comparable with the pure PBAN sandwiches (see figure 4-51b).

5. For thick binder laminae and/or high pressures, the AP close to the oxidizer/binder interface was observed to burn in a different way than the rest of the AP - this can be an indication of a smooth band (the surface characteristics were different but a well defined smooth band was not seen).

4.2.2.2 Effect on BAMO-THF Sandwiches. They can be summarized as follows:

1. A sharp V-shaped surface profile was developed when the sandwich reached steady state burning at 500 psi; it was much steeper than the pure BAMO-THF binder case (see figures 4-47 and 4-52). At 1000 psi an open V-shape was observed in contrast with the flat profile of the pure binder at the same pressure. At 300 psi a U-shape profile was encountered and the AP was breaking into pieces as the combustion was propagating downwards the catalyzed binder lamina.

2. Catalytic bed formation was observed when the pressure was 300 psi or 500 psi (see figure 4-53a). At 1000 psi there was no catalytic bed formed but only pieces of concentrated particles on the binder surface (see figure 4-53b). The particle concentration of the catalytic bed was amorphous, while in the PBAN catalyzed with  $\text{Fe}_2\text{O}_3$  a more structured formation was observed (see figure 4-51a). At all pressures the residue concentration was black in color. Since  $\text{Fe}_2\text{O}_3$  is a red oxide; it was suspected, as in the PBAN case, that  $\text{Fe}_2\text{O}_3$  became  $\text{Fe}_3\text{O}_4$ . At 1000 psi and for thin binder laminae at 300 or 500 psi particles of concentrated oxide were observed to emerge from or sit on the binder surface without forming a continuous catalytic bed.

3. The binder surface was bubbly - characteristic of the BAMO-THF (see figure 4-53b). It was red in color whenever it was exposed under the dark catalytic bed.

4. No strong binder protrusion was observed even at thick binders (125  $\mu\text{m}$ ) at high pressures (1000 psi). This was not a surprise because pure BAMO-THF did not protrude much under conditions most conducive to protrusion.

5. The higher the pressure the cleaner the quenched surface of the AP far from the interface (less oxide was deposited on the oxidizer surface). The gases produced from the AP self deflagration carried away the oxide particles. As the pressure increased the AP

burned faster - more gases are produced which travelled faster. The fact of oxide particles being on the AP surface is believed to occur doing quench; there is no evidence that oxide particles were deposited on the self-deflagrating AP.

6. Smooth band was not observed as in the pure PBAN case but from the optical and the scanning electron microscope pictures it was evident that the AP region close to the oxidizer/binder interface was much cleaner than the rest of the AP surface (far from the interface).

#### 4.2.3 Catalyzed Binder Sandwiches: $\text{Fe}_3\text{O}_4$

##### 4.2.3.1 Effect on PBAN Sandwiches.

1. At 1000 psi the surface profiles of the sandwiches were flat (the AP self deflagration rate governed the burning rate of the sandwich - see figure 4-54). The only exception was with 25  $\mu\text{m}$  binder lamina when an open V-shape profile was developed. At 500 psi the V-shape was sharper and became U-shaped at 300 psi.

2. At 1000 psi particle accumulations were observed to be sitting on the binder surface or embedded in it (see figure 4-55b).

At 500 psi more residue concentration was observed on the binder and in some cases they were continuous sticking on the binder surface.

At 300 psi continuous catalytic bed formation was observed for binder thicknesses 50 - 75  $\mu\text{m}$ . For thicker binders the catalyst's particles aggregate and they either emerge from the binder or sit on top of it (see figure 4-55a).

3. The binder surface (when no particles were sitting on it) was always very clear and smooth (no bubbles or wrinkles were observed; see figure 4-55b).

4. The binder lamina was observed to protrude at all pressures; see figure 4-55b (except for 25 - 50  $\mu\text{m}$  binder thickness at 300 psi). Slight protrusion was also observed

for very thin binders (25  $\mu\text{m}$ ) at pressures of 500 and 1000 psi, something that was not observed with other additives in both binders at high pressures ( $\text{Fe}_3\text{O}_4$  was the only additive that was not a good catalyst for PBAN at high pressures). The protrusion was noticed to be higher as the pressure increased. In some cases (e.g. thick binders at 1000 psi) binder melt was observed and solidified binder melt bridges connecting the protruding binder lamina with the AP oxidizer were encountered (see figure 4-55b).

5. The maximum sandwich regression was always observed on the AP surface close to the binder/oxidizer interface at all pressures. A transition point was encountered for all the surface profiles obtained. A distinct smooth band was not observed but in some samples there was a difference in the burning characteristics of the AP surface very close to the binder/oxidizer interface and far from it.

6. Oxide particles were observed on the AP surface (they were probably deposited on the surface after quench). Their number increased as the pressure became lower and the binder lamina thicker. It is interesting to note here that the small black oxide particles that sit on the oxidizer became red (probably the black  $\text{Fe}_3\text{O}_4$  oxidizes to red  $\text{Fe}_2\text{O}_3$ ). Larger particles were red all around (because they were in contact with the AP oxidizer) but black at the center.

##### 4.2.3.2 Effect on BAMO-THF Sandwiches.

1. A V-shaped surface profile was observed at 500 psi and at 1000 psi for all binder thicknesses (see figure 4-56). It became U-shaped at 300 psi. At this pressure, cracks on the AP were encountered as the oxidizer could not self deflagrate and broke apart.

2. Catalytic bed or large particle concentrations were not observed on the binder surface; except the low pressure, thick binder cases. The oxide particles seemed to be embedded in the binder or formed small amorphous concentrates on its surface.

At 300 psi and for 25 - 50  $\mu\text{m}$  binder thicknesses no particle accumulation was observed on the binder surface; only some particles were observed to emerge from the binder surface. For 75  $\mu\text{m}$  binder lamina particles started concentrating on the surface and for 100 - 125  $\mu\text{m}$  a continuous<sup>5</sup> chartered structure was formed (see figure 4-57a). In this case some spherical aggregates were observed. Slight particle accumulation was encountered at pressures of 500 and 1000 psi for thin binders (25 - 50  $\mu\text{m}$ ). As the binder lamina thickness increased more residual concentration was noticed to emerge from the binder surface (see figure 4-57b).

3. The binder surface was not smooth and it was darker in color than the unburned binder surface (indication of carbon/char residues which were also observed with pure BAMO-THF sandwiches). Bubbles were noticed on the binder surface - characteristic of this binder. A strong binder lamina protrusion was not encountered even when appropriate conditions (high pressure, thick binder) supported it (see figure 4-57b).

4. A transition point on the surface profiles occurred closer to the binder/oxidizer interface as the pressure decreased and the binder lamina became thinner (see figure 4-57). The area between the point of inflexion and the interface was glazy (different burning characteristics) and the AP was very clear (no oxide particles were observed on its surface).

5. As the pressure increased the AP quenched surface became cleaner and less oxide particles deposited on it. The smaller particles on the AP surface were red in color ( $\text{Fe}_2\text{O}_3$ ) while the larger ones were black ( $\text{Fe}_3\text{O}_4$ ).

#### 4.2.4 Catalyzed Binder Sandwiches: Catocene

##### 4.2.4.1 Effect on PBAN Sandwiches

1. All samples at 500 psi and 1000 psi developed a V-shaped surface profile which approached the U-shape configuration at 300 psi pressure (see figure 4-58). Even at 1000

psi the V-shape was sharp; evidence of the high burning rate of the sandwich. At 300 psi the AP could not follow the combustion propagating downwards in the region around the binder and the AP slabs were breaking away into pieces due to thermal stress.

2. Although catocene was added to the binder in a liquid form, solid accumulation of residues was observed to concentrate on the binder surface (see figure 4-59). This residual accumulation in many cases formed a catalytic bed very similar to the one observed from quenched tests of PBAN sandwiches with 10%  $\text{Fe}_2\text{O}_3$  in the binder lamina. A catalytic bed structure was encountered at low pressure (300 psi). For thin binder laminas (25 - 50  $\mu\text{m}$ ) at higher pressure (500 psi) a stripe of accumulated particles along the binder surface was observed (see figure 4-59a). As the binder lamina became thicker the stripe itself became thicker and started to break down to shorter pieces. The particles that formed the catalytic bed structure were finer than the residues that built up the concentration on the PBAN + 10%  $\text{Fe}_2\text{O}_3$  binder lamina surface. The catalytic bed did not have the same structure as in the  $\text{Fe}_2\text{O}_3$  case. In that case a closed structure was covering the binder lamina. When catocene was employed it seemed that the closed structure opened up in the middle all along the binder and the two separate thin sheets of residue accumulation were observed to run along the oxidizer/binder interface.

At this point it is important to note that the particle concentrations on the binder surface were dark silver/black in color while catocene had a deep orange/red color. At the same time it was observed that the particle concentration had strong magnetic properties. It was suspected, as in the case of the addition of 10%  $\text{Fe}_2\text{O}_3$  in the binder, that the particles were  $\text{Fe}_3\text{O}_4$  accumulation; because  $\text{Fe}_3\text{O}_4$  is black in color and has magnetic properties. This observation motivated a further investigation which was the addition of  $\text{Fe}_3\text{O}_4$  in the binder to explore whether  $\text{Fe}_3\text{O}_4$  is the actual catalyst or it is just a product of the whole combustion process.

3. The binder surface was smooth but in numerous cases (300 psi pressure) particles were observed to be deposited on its surface (remains of a residual accumulation). When the binder was thick (above 75  $\mu\text{m}$ ) at pressures of 500 psi or 1000 psi the catalyzed PBAN binder surface was observed to have wrinkles and some agglomerated residues were emerging from it (see figure 4-59b). The binder underneath the catalytic bed was in most cases clear with a yellow/orange color. It seemed like the residues concentrated above it, unless the binder lamina was very thick the accumulated particles and the binder lamina were not in contact.

4. Strong binder protrusion was observed at all pressures (probably because the concentrated particles stayed on top of the binder surface and did not permit the observation of the real surface). At 1000 psi even the 50  $\mu\text{m}$  binder lamina protruded; suggesting catocene is not catalyzing binder decomposition. As the pressure decreased (500 psi) a protrusion was encountered for thicker than 75  $\mu\text{m}$  binders and for the lower pressure of 300 psi the binder lamina started protruding above 100  $\mu\text{m}$  thickness.

5. Binder melt flows were noticed for thick binders (above 100  $\mu\text{m}$ ) at 500 psi and 1000 psi. Under these conditions a number of bridges of solidified binder melt (see figure 4-59c) were also observed to connect the AP surface with the binder lamina.

6. The surface of the AP close to the interface was observed to have different characteristics than further away, and this probably is some indication of the existence of a smooth band. A transition point at the surface profile of the sample was also noted in some of the quenched sandwiches studied. It was measured to be 0 - 50  $\mu\text{m}$  far from the oxidizer/binder interface on the AP side. This distance decreased as the pressure decreased and as the binder lamina became thinner.

#### 4.2.4.2 Effect on BAMO-THF.

1. All sandwiches had a very sharp V-shaped surface profile at pressures above the AP self deflagration limit (500 psi and 1000 psi - see figure 4-60). At lower pressures (300 psi) a U-shaped profile was observed and the AP broke away from the burning region.

2. Under all conditions tested residual accumulation was observed on the binder surface (see figure 4-61).

At 1000 psi and for all binder lamina thicknesses particle aggregation was observed either on the binder surface or emerging from it. When the binder thickness was 25 - 50  $\mu\text{m}$  a continuous structure was formed over the binder (see figure 4-61b). More particles - quite a few of them concentrated in compact structures were closer to the interfaces while a porous formation was running over the middle and along the interfaces connecting them.

At 500 psi, continuous residual accumulation was encountered for all binder lamina thicknesses except 125  $\mu\text{m}$ ; in this case it appeared that particles were concentrated under the binder surface. For the 25  $\mu\text{m}$  binder lamina thickness a solid particle concentration was observed on the binder surface (see figure 4-61a). It was different from the corresponding tests with PBAN binder (and this statement applies to all cases comparing particle concentrated structure in PBAN and BAMO-THF with 20% catocene) because in that case thin porous sheets of concentrated particles were observed to run along the interfaces. In the BAMO-THF catalyzed with catocene, solid and compact aggregates were encountered. As the binder lamina thickness increased most of the residues concentrated very close to the interface and only a few of them remained on top of the binder along the center of its surface.

At 300 psi strong residual accumulation was observed for all binder lamina thicknesses which was always sitting on the binder surface. Continuous formations were noticed at all binder thicknesses.

For all cases the particles or concentrations observed on the surface of the binder lamina were dark grey/black in color as in the PBAN + 20% caoecene case.

3. Whenever the residual concentration was not present, the exposed binder surface was clear and bubbles were observed on its surface. Protrusion of the binder lamina was encountered at 1000 psi when the thickness was greater or equal than 75  $\mu\text{m}$  and at 500 psi when the lamina was thicker than 100  $\mu\text{m}$ . At 300 psi it was difficult to conclude anything on binder protrusion for thick laminas because the concentrated particles sit on top of the binder surface. The protrusion of the binder was less than for the respective PBAN + 20% caoecene cases but it was higher than what was observed for pure BAMO-THF sandwiches or BAMO-THF + 10%  $\text{Fe}_2\text{O}_3$  samples.

4. No transition point was observed on the AP surface but its characteristics very close to the interface were different than the rest of the AP surface.

5. While black particles were observed on the binder surface, some small red particles were sitting on the AP surface. This supported the argument that some reactions were happening between different iron oxides. In this case the dark particles ( $\text{Fe}_3\text{O}_4$ ) leave the combustion zone and some of them (the heaviest probably) land on the AP surface during quench. These particles on the AP surface are probably oxidized and become red ( $\text{Fe}_2\text{O}_3$ ).

#### 4.2.5 Further Observations on the Quenched Sandwich Surface

1. There was no visible binder melt flow over the oxidizer surface in the vicinity of the oxidizer/binder interface. Only in the case of thick PBAN binder with catalysts at 1000

psi pressure, solidified binder melt bridges were encountered to connect the protruding binder lamina and the AP oxidizer (eg., see figure 4-59b).

2. The surface of the sample was always continuous in the vicinity of the binder/oxidizer interface. This indicated that no condensed phase reactions were taking place between the oxidizer and the binder.

3. When catalyst was added in the binder the quenched oxidizer surface was noticed to have residue on it. These particles were more in number as the pressure decreased (the AP surface became "dirty").

4. Cracks were formed on the solidified AP surface. Two kinds of cracks were observed (see figure 4-49a):

a. Cracks a few microns wide; probably due to thermal contraction of the surface layer as it cools and solidifies

b. Larger cracks that develop parallel to the interface probably related to different thermal contraction and shrinking between AP and binder.

5. The AP surface was observed to be divided in three zones, which had different characteristics (see figure 4-46a). These surface features are believed to be related with different heat that is gained or lost on the surface (or heat released above the surface and heat drained to other parts of the sample).

Starting from the interface the AP surface was observed to be smoother than the rest of the AP. This region is mainly subject to heat losses to the binder and its dimensions depend on binder lamina thickness and test pressure. In many cases this band was not encountered.

The next region is wider; it is probably a transition area from the smooth band to the AP self-degradation. This part of the surface is heated higher than any other part of the

sample's surface. It is also characterized by the highest regression rate measured on the sandwich.

The last region is characterized by the AP self-deflagration. The surface is regressing and its characteristics are dependent on the test pressure (as it was proved from the SEM pictures).

6. Some questions were raised at this point about AP permeation mainly when catocene was used; questions related to the smooth band. When AP particles were placed in catocene it was observed that due to strong surface tension catocene immediately covered the AP particles and went to fill all pores of the particles. The thickness of the permeated AP in sandwiches with PBAN+20% catocene was measured and it was found to be more than 100  $\mu\text{m}$ . Additional information was obtained for catocene when a thin coat was painted on one AP lamina and a sandwich was made. The sandwich burned at 500 psi with a burning rate slightly faster than pure AP; liquid catocene did not stick to the AP laminae. Catocene was also coated on AP lamina and the system was ignited. The side of the coated AP burned on a table top test, while a plain AP lamina did not burn. Tests to explore catalytic effects of catocene on the AP were not attempted because of the unknown results of pressing an AP + catocene mixture.

7. The particle concentration was observed to be different for the two binders (the case of  $\text{Fe}_3\text{O}_4$  is not accounted for here since less particle accumulation was observed). In the case of catalyst added to PBAN a porous structure was formed. This formation was closed over the binder surface in the case of  $\text{Fe}_2\text{O}_3$ ; when catocene was added two distinct sheets of residual accumulation were observed to run along the binder/oxidizer interface. In the case of BAMO-THF with catalysts the particles formed a less porous structure. A continuous aggregation was encountered on the binder close to the interface and bridges of residual concentration connected the two stripes.

### 4.3 Study of Tapered Sandwiches

A screening study of the quenched surface of oxidizer/binder tapered sandwiches was conducted. Tapered sandwiches were ignited at different pressures in nitrogen atmosphere below the AP self-deflagration rate and they were let to self-extinction. The thickness of the binder lamina left was measured and it was plotted versus the test pressure.

#### 4.3.1 Pure Binder Tapered Sandwiches

The results from a complete series of tests on tapered sandwiches with BAMO-THF as the binder are presented in figure 4-62; in the same figure experimental data are presented on the spontaneous quench limits for tapered sandwiches with PBAN (on the same figure the results from catalyzed binder sandwiches are presented - they are discussed in the next section).

From the graph it is noted that the quench limit for BAMO-THF tapered sandwiches was measured for thicker binder laminae than for PBAN samples. Tests below 0.3 MPa were questionable because the ignition paste ignited but combustion of the sandwich probably never occurred.

The thicker binder limits were verified by the movie tests run at 300 psi pressure. At this pressure (which is close to the AP self-deflagration limit) samples of 25 - 50  $\mu\text{m}$  did not burn and the 75  $\mu\text{m}$  sandwich burned slowly.

The general features of the self-quenched sandwich surface were similar to those regular sandwiches quenched by rapid depressurization from comparable pressures. This indicated that the approach of the tapered sandwich to self-extinction did not involve development of any singular features of surface configuration.

#### 4.3.3 Catalyzed Binder Tapered Sandwiches

A complete series of experiments was conducted for PBAN and BAMO-THF binders with 10%  $\text{Fe}_2\text{O}_3$ . A limited number of tests was carried out to study the effect of catocene in PBAN.

From the curves (see figure 4-62) it is shown that the effect of  $\text{Fe}_2\text{O}_3$  on both binders produced the same effect on binder lamina thickness where self-quench was established. The curve was lower than the pure BAMO-THF curve (something already expected since catalyzed BAMO-THF burned very well at 300 psi while pure binder did not burn if the binder lamina thickness was less than 75  $\mu\text{m}$ ). The curve for the catalyzed PBAN tapered sandwiches was higher than the pure PBAN tapered sandwich curve.

The PBAN + 20% catocene graph is misleading. Self-extinction is believed to occur due to extreme conditions of heat loss to the metallic sample holder. It is expected that the catalyzed with catocene binder will burn to completion (this prediction is supported by the fact that thin PBAN sandwiches catalyzed with catocene burned to completion at atmospheric pressure; AP discs, also, painted with a thin layer of catocene burned on a table top test).

#### 4.4 Laser Studies

An exploratory study of the catalyzed binder surface was conducted employing the laser pyrolysis facility. The tests that were carried out included:

1. Pure PBAN
2. Pure BAMO-THF
3. PBAN + 10%  $\text{Fe}_2\text{O}_3$
4. PBAN + 10%  $\text{Fe}_3\text{O}_4$
5. PBAN + 20 % Catocene

The tests were conducted under the same environmental conditions using the same energy from the laser.

The conclusions obtained after investigating the sample's surface in the scanning electron microscope were:

1. The binder surface had the same characteristics as the ones observed with sandwiches,
2. The catalyst build up had the same structural formation observed from sandwich quenches, and
3. The catalyst's concentration had the same properties which were verified from the sandwich work (color, magnetic properties).

## CHAPTER V

### DISCUSSION

The experimental results of the present study were presented in detail in the previous chapter. An attempt will now be tried to address the trends of the experimental results and to propose physical mechanisms needed to explain any similarities or differences existing between them.

The proposed theory is based on qualitative arguments, and some of the experiments were designed to support or test the theory.

#### 5.1 Theory of the Flame Complex

The basis of the qualitative theory has been presented extensively by earlier investigations [53,54] and it will be summarized here.

Figure 1-13 is a sketch of the combustion zone of a burning sandwich, based on results obtained from experiments with PBAN binder. This picture represents a portion of the combustion zone within about 150  $\mu\text{m}$  of the plane of symmetry of the sandwich. This particular figure is characteristic for thin binder sandwiches (in which the non-energetic PBAN was used as the binder) burning at intermediate pressures (3 - 6 MPa). The changing in the shape of the combustion zone, as pressure and binder lamina thickness vary, was discussed in detail in reference [54]. Figure 5-1 shows the variation of the

combustion zone as the pressure changes. Figure 5-2 presents the trends in the combustion zone shape at different binder lamina thicknesses.

The numbered regions in the figure 1-13 designate areas of the combustion zone with unique features. By addressing and discussing these features a complete description of the combustion zone can be obtained. This can be used in understanding the experimental observations and explaining global combustion phenomena, such as burning rate and/or dynamic response of combustion to oscillations in the flow environment.

Region (1). The Binder Lamina. The binder lamina is recessed in quenched thin binder lamina sandwiches. As the thickness of the binder lamina progressively increases the binder starts to protrude. The binder lamina is decidedly protruding for thicknesses over 110  $\mu\text{m}$ . The surface quality of the binder and the height of the protrusion or recession strongly depend on the type of binder employed. The surface profiles sketched in fig. 4-45 show the tendency of the binder lamina to protrude at thick binder laminae/high pressures or to recess at thin binder laminae/low pressures.

Region (2). The Interface Plane. Binder-oxidizer interfacial reactions are ruled out as significant contributors to burning rate at the pressures tested; the oxidizer-binder interface was never the leading edge of the combustion front.

Region (3). Protruding AP - Smooth Band. The AP deflagration in the region near the interface plane appears to be retarded relative to region (4), and the AP surface there has a smooth quality. As the AP decomposes and burns lateral heat flows into the endothermic binder, resulting in a lower AP surface temperature and a less exothermic or an endothermic surface decomposition (dissociative sublimation). The extent of this region depends on the exothermicity of the binder used and/or the catalyst employed. The protruding AP adjoining the binder can be observed on the sandwich surface profiles sketched in figure 4-45 and in figure 5-1.

Region (4). The Leading Edge in the AP. The leading edge of the combustion front is located 25 - 50  $\mu\text{m}$  from the interface planes (see fig. 4-45); a transition of the surface quality of the AP is observed here on quenched samples. The front leads here because combined heat from the AP deflagration, and the near by O-F flame contribute and heat flows to the binder below.

Region (5). AP Self-Deflagration. Far from the interface the surface quality characteristics of the quenched AP are essentially the same as for AP self-deflagration (see fig. 5-1b). Surface regression rates are approximately the same as for self-deflagration.

Region (6). The AP Flame. Is presumed to occur under conditions possible for AP self-deflagration.

Region (7). Leading Edge AP Flame. A continuation of the AP flame into a region that must receive some heat from the oxidizer / fuel flame, leading to the higher regression rate of the surface at (4).

Region (8). Smooth Band Flame. The vapors from the underlying surface [region (3)] are postulated to be different from those for the rest of the AP flame.

Region (9). Oxidizer - Fuel Diffusion Area. It represents the region where mixing of the oxidizer and the fuel vapors occur. In this region (diffusion fan) reaction rates are low because unfavorable balance of heat flow and insufficient mixing and chemical preparation of the reactants prevent rapid temperature rise.

Region (10 - 11). Kinetically Limited Leading Edge Flame (KLLEF). At some point in the mixing fan of region (9) the temperature becomes sufficient to support a flame. The position and the extent of the KLLEF are unknown but they strongly depend on composition profiles in the mixing region and on flammability limits. The majority of the O/F reaction occurs in the KLLEF and therefore the KLLEF is the only truly high temperature flame near the burning surface and, as such, is generally important to the

burning rate. The position of the KLLEFs in the combustion zone is presented in figures 5-1 and 5-2 at different pressures and for different binder lamina thicknesses.

Region (12). Diffusion Flame. Downstream from the KLLEF continued reaction occurs as further interdiffusion of fuel and oxidizer vapors occurs. The temperatures are high because of the heat release upstream and the reaction rate is consequently controlled by the rate of mixing, rather than by reaction kinetics.

Region (13). The Stoichiometric Tip. Because of the oxidizer-rich overall stoichiometry of the sandwich the diffusion flame sheets close over the fuel, yielding a flame tip.

## 5.2 Binder Description

In the following the interpretation of the experimental results of sandwich burning rate measurements and quench tests will be made. But before interpreting these results, a few comments on the nature of the binders and their properties related to combustion are needed.

These binders are not as fully characterized as one would like, but can be qualitatively ranked relative to principal properties governing combustion:

1. Decomposition characteristics, including
  - a) Decomposition temperature, thought of here vs surface temperature for a given linear pyrolysis rate (but usually estimated by thermal decomposition experiments such as DTA or DSC, which have a heating rate much lower than the heating rates encountered in a real propellant, [95], [96])
  - b) Heat of "phase change" during transformation to vapors
2. Flame Temperature with AP
3. Stoichiometric mixture ratio with AP

Qualitative theory of sandwich burning as described in a previous section provides a basis for prediction of the detailed effect of binder properties. This, in combination with the present experimental results, provides an opportunity to validate the theory. In the following, the theory is used to predict the detailed effects of binder properties on burning rate trends, surface profiles, and flame structure. This will be followed by a comparison with observed rate trends and surface profiles, and implications relative to the (non-observable) flame structure.

The effect of ingredient decomposition temperature was examined in references [98] and [99]. The results show that, for typical binders and AP oxidizer, the binder decomposes more easily than the AP, and the pyrolyzing surface consequently assumes a location that is recessed relative to the adjoining AP surface, and at lower surface temperature. The quantitative details depend on the heat of decomposition at the surface and on details of the heat source (primarily the KLEFs), lateral heat flow between laminae, and heat of phase change (decomposition) at the surface. However a binder lamina that pyrolyzes easily (i.e., at relatively low temperatures) tends to be more recessed than a lamina of high decomposition temperature. When the binder lamina is thick, it protrudes, but the one that has a low decomposition temperature protrudes less. When a binder lamina decomposes at low temperature, the lateral heat flow from the hotter oxidizer is less, an effect that will tend to minimize the usual inhibiting effect on regression of the AP surface in the oxidizer - binder interface region. As a result the usual protrusion of the AP in this region of the surface profile will be less, and the identity of a leading edge in the AP (region 4 in fig. 1-13) will be less well defined.

Relative to heat of phase change, binders range from endothermic to strongly exothermic. The effect of heat of phase change was also examined in reference 98. Qualitatively, an endothermic decomposition demands more heat flow, both from the flame

The properties in 1a and 1b can be precisely defined only under specified conditions, in terms of reaction kinetics that are not now available. However the three binders can be qualitatively ranked relative to 1a and 1b as in table 5-1.

Binder	Decomposition Temperature *	Heat of Phase change
PBAN	High (~710 K; [95])	Endothermic
BAMO-THF	Intermediate ** (~464 K; [100])	Slightly exothermic
NMMO	Low (~460 K; [101])	Exothermic

Table 5.1 Qualitative Comparison of Binder Decomposition Properties.

(\* data obtained from low heating rate experiments)

\*\* BAMO-THF releases exothermally azido groups at this temperature and continues to decompose at higher temperature)

Relative to combustion properties with AP, Figures 5-3, 5-4, and 5-5 show the flame temperature of an AP/Binder mixture vs the mixture ratio based on adiabatic combustion to thermochemical equilibrium at 1000 psi (data supplied by R. Reed, U.S. Naval Weapons Center). The flame temperatures of BAMO-THF and PBAN are comparable when based on equivalence ratio, but BAMO-THF is a much more dilute fuel than PBAN, with a fuel to oxidizer mass ratio at stoichiometric being about twice as high for BAMO-THF. NMMO is also a dilute fuel, and also yields a somewhat cooler flame than the other two binders.

### 5.3 Possible Effects of Binder and Catalyst Variables on Sandwich

#### Combustion based on Qualitative Theory

#### 5.3.1 Expected effects of Binder Properties on Combustion

amount of combustible mixture (i.e., the flow rate through the KLLEF between fuel-rich and fuel-lean flammability limits (see fig. 5-6)). Qualitatively, the dilute fuel will reach a flame-viable concentration profile in a location more distant from the surface, an effect that would seem to assure lower burning rate for binders that are more dilute fuels. This effect would be particularly pronounced in thin binder situations where there is a deficiency of fuel already (see fig 5-7). Thus one may anticipate that the maximum in the curve of burning rate vs. binder thickness will be shifted to greater binder thickness when the binder is a dilute fuel.

The flame temperature in the KLLEF is a maximum at the stoichiometric mixture point, and drops off as the equivalence ratio changes from 1.0 along the KLLEF. The actual temperature at each point is governed by the heat flow situation, mixture ratio and by the particular fuel-oxidizer system (kinetics and thermochemistry). A system with high adiabatic stoichiometric flame temperature will normally lead to a KLLEF that stands close to the surface and yields high burning rates. A system with fast gas phase kinetics will do the same. In the binder system under consideration here, the thermochemistry is well known, but little is known about the vapor species or reaction rates. In the interpretation of results, this means that burning rate trends may be attributed to known flame temperature effects or used to infer kinetic effects, or both (a situation that assures agreement between experiment and theory, but calls for some independent validation of the reasoning!).

The effect of pressure on burning rate has been addressed previously in reference [54], but merits revisiting in the context of possible binder and catalyst effects. At high pressure, the oxidizer self-deflagration dominates the sandwich burning rate, while at low pressure the oxidizer will not burn without the oxidizer-fuel flame and the binder characteristics become particularly important. Thus at high pressure the burning rate is insensitive to binder thickness, but the pressure at which this happens will be higher if the O-F flame is

and via lateral conduction from the hotter AP. This in turn implies a less recessed binder lamina and more protrusion of the AP surface near the binder. A strongly exothermic binder may burn ahead of the oxidizer due to a higher self-deflagration rate (no steady state profile). If the binder is only moderately exothermic (or the lamina so thin that the reaction energy is primarily transferred to the adjoining AP), the lamina will seek a stable recessed location that is more recessed than an endothermic binder, with correspondingly less or no lateral heat flow from the oxidizer and less, or no protrusion of the AP adjoining the binder. Thick exothermic binder laminae do not require as much lateral heat flow from the AP and flame as required by endothermic binders, and hence protrude less than thick endothermic laminae, or not at all.

The energetics and kinetics of binder decomposition are expected to be weak factors in determining burning rate in the present work, because of the rather modest variation among the binder tested (none of them would burn unassisted in an inert atmosphere), and because of the tendency for rate to be dominated by the AP self-deflagration (high pressure) and the gas phase O/F flame (low pressure).

The effect of stoichiometric fuel ratio of the binder with AP is expected to be conspicuous, because the binders differed conspicuously in this respect. To argue this point, one must look at the effect of fuel value of the binder vapor on the conditions in the pre-mixing fan that feeds the KLLEF. If one assumes that the diffusion constants are not drastically different, the primary effect of a dilute fuel is in the rate of development of a composition profile that will support a KLLEF as the gases flow outward from the surface. Such a profile is determined primarily by the amount of heat that can be released (especially if a KLLEF is present) and hence be made available to support an equilibrium two dimensional heat balance necessary for a stable KLLEF. This is determined by the distance from the surface (time for mixing and rate of heat flow back to the surface), and by the

hotter, or if the O-F reaction kinetics are faster. At lower pressures, burning rate and its dependence on binder should be as described earlier until the pressure gets so low that marginal conditions for burning arise. These conditions were discussed in Ref. [54] without consideration of the effect of "fuel value" or endo-exothermicity of the binder. In that reference it was noted that a stable flame was possible only if KLLEFs could be established at or below the closure tip of the stoichiometric surfaces over the fuel lamina, a condition forced by thick binder laminar (all stoichiometric surfaces) or fast kinetics (small KLLEF stand-off), noted in Fig 5-7, the dilute fuel binder has a relatively short stoichiometric surface which would require relatively thick binder laminae to sustain burning. Low stoichiometric flame temperature would lead to the same trend because of increased flame stand-off. However this trend would be countered by exothermicity of the condensed phase decomposition which would reduce heat drain from the KLLEF and from the oxidizer. The net effect of these different binder contributions cannot yet be characterized for the three binders used here because of lack of quantitative kinetics and reaction energy data, and the deflagration limit data will only partially resolve the dominant mechanisms.

### 5.3.2 Expected Effect of Catalysts

In the present studies (and in heterogeneous solid propellants), burning rate catalysts are distributed in the binder matrix, and have little or no contact with oxidizer (the catocene catalyst is a liquid, and was observed to migrate into the pores of the dry pressed AP laminae). As a result, catalytic activity in the condensed phase is all, or mostly catalyst of binder decomposition. For the particulate catalysts, the opportunity for any catalyst in the condensed phase is limited by the low mobility of the binder molecules and the relatively small portion of molecules that contact the catalyst. In the gas phase, the opportunity for

catalysis by free-moving catalyst particles is limited because of short residence time and low collision probability. However the catalysts were observed to concentrate on the binder surface, providing a region of high collision probability, either in the binder surface melt or immediately above the binder surface. Thus it is reasonable to postulate that the burning rate enhancement results from catalytic action of the catalyst in this surface - near surface binder environment. The detailed effects could be:

1. Reduction of the heat required to vaporize the binder
2. Oxidation of some fuel with heat release
3. Break-down of large fuel vapor molecules to smaller (more easily oxidized) fuel species.

In the context of the previous discussion of fuel variables, case 1, is analogous to a binder that is more easily vaporized, case 2 is analogous to binder that is more exothermic, and case 3 is analogous to a binder with faster gas phase kinetics. The experimental results will be examined to determine their consistency with cases 1, 2, or 3 as controlling catalytic mechanisms.

## 5.4 Interpretation of Results

### 5.4.1 Comparison of BAMO-THF Binder Sandwich Results with PBAN

Compared to PBAN, BAMO-THF is an energetic binder that decomposes at lower temperatures than PBAN. At about 464 K the nitrogen contained in the azido groups of the BAMO molecules is released exothermally. Because of this, frozen bubbles were observed on the quenched binder surface of the BAMO-THF binder sandwiches (see fig. 4-48). The bubbling of BAMO-THF was also verified with laser pyrolysis tests of the binders. On the contrary PBAN sandwiches had always a smooth binder surface (see fig. 4-46). Because of the energetic, at relatively low temperature, decomposition of BAMO-THF, one will

expect much less lateral heat flow from the AP to the BAMO-THF than to the PBAN binder and consequently little or no retardation of the AP regression in the AP adjoining the oxidizer/binder interface (slight or no protrusion and possibly no smooth band are also expected). This is consistent with observations (fig 4-48). Under these conditions an increase of burning rate would be expected relative to the PBAN sandwiches. At the same time, since the stoichiometry of AP/BAMO-THF requires a lower O/F ratio than PBAN ( $O/F_{BAMO-THF} = 80:20$ ,  $O/F_{PBAN} = 88:12$ ) one should expect that the maximum of the burning rate curves has shifted towards thicker binders (note here that the stoichiometric adiabatic flame temperature for the two binders is almost the same:  $T_{PBAN} = 3090$  K,  $T_{BAMO-THF} = 3072$  K). In fact BAMO-THF sandwiches had a slightly higher maximum burning rate than PBAN and this maximum occurred at thicker binder lamina (see figure 4-3). It should be mentioned also that thick BAMO-THF sandwiches had an increased burning rate relatively to thick PBAN sandwiches, resulting from the significantly high adiabatic flame temperature for fuel rich mixtures of BAMO-THF; see figure 5-4 (at 1000 psi almost identical burning rate curves were observed; the AP self-deflagration rate governs the sandwich burning rate at high pressure).

The combination of dilute-fuel and slight exothermicity of BAMO-THF binder suggests that it might be a problem in igniting and burning thin binder lamina samples, especially at low pressures (below the AP self-deflagration limit) where chemical kinetics are more essential than at high pressures. Combustion photography proved that thin BAMO-THF sandwiches did not burn at pressures below the AP self-deflagration limit and the limiting thickness obtained from self-extinguished tapered sandwiches was measured much higher for BAMO-THF than for PBAN.

The low carbon percentage of BAMO-THF and the low O/F ratio suggest that BAMO-THF will have a less visible flame and less smoke than PBAN. Observation of the

sandwich burning movies proved that was a fact and BAMO-THF binder sandwiches developed a visible flame (which was not very luminous) only at very thick binder lamina cases.

Summarizing, although there is little quantitative knowledge on chemical kinetics and decomposition of BAMO-THF, the various details obtained from sandwich burning results reflect qualitative the properties decisively and verify the already known properties.

In an AP/BAMO-THF propellant, one might expect a burning rate higher than AP self-deflagration at pressures lower than about 1000 psi; especially at relatively low pressures. A high binder mass fraction will have an increased effect on the burning rate of a propellant.

#### 5.4.2 Comparison of NMMO Binder Sandwich Results with PBAN

Compared to PBAN, NMMO is an exothermic binder that decomposes at relatively low temperature. It is a relatively poor fuel for oxidation with AP. Because of low decomposition temperature one would expect an NMMO binder lamina to be relatively recessed during sandwich burning, which it is (Fig. 4-49). Because of the recessed surface and exothermic decomposition, one would expect (unlike PBAN) little or no lateral heat flow from the AP lamina to the binder, and consequently little or no retardation of the AP regression in the AP adjoining the contact plane (ie. no protrusion, possibly no smooth sublimation band). This also is consistent with the observations (Fig. 4-49). One might think that these conditions would lead to increased burning rate relative to sandwiches with PBAN binder, but this was not the case. In fact the NMMO sandwich burning rates were close to the AP self-deflagration rate (Fig. 4-5, the bump in the burning rate curve of NMMO is not a big enough effect to tell that the curve has reached a maximum), and the quenched sandwiches were nearly flat, indicating that the O-F flame contributed little to the

burning. This suggests that the O-F flame was either far from the surface or was a cool heat source or both. The calculated stoichiometric flame temperature for PBAN+AP is higher than the stoichiometric adiabatic flame temperature of AP+NMMO (see figures 5-3 and 5-5). However the lower flame temperature does not seem to be a sufficient cause for the very low contribution of the KLEEF to burning rate, and it seems reasonable to postulate that the gas phase kinetics are also slow. An appreciable effect of NMMO on the sandwich burning occurred only at pressures near or below the AP self-deflagration limit (where NMMO was responsible for the burning of sandwiches at low pressures). The fact that thin NMMO sandwiches (dilute fuel situation) burned at low pressures is attributed to the exothermicity of the binder (recall that thin sandwiches of the less energetic BAMO-TTFF binder did not burn under the same test conditions).

In summary, while basic data on NMMO thermochemistry and decomposition kinetics are only qualitatively known, the various details of the sandwich burning results reflect these properties decisively, and may in fact be viewed as independent evidence of low decomposition temperature, exothermic decomposition, and low flame temperature with AP (ie, as compared to PBAN binder). In an AP-NMMO propellant, this translates into burning rate characteristics similar to AP itself, except at low pressures (300 psi and below). In practical applications NMMO would be more effective in a propellant with HMX oxidizer which has a much higher self-deflagration rate than AP. An NMMO binder probably would have even smaller effect on burning in that system unless a high binder mass fraction were used.

#### 5.4.3 Results of Catalyzed Sandwiches

Various iron oxide catalysts have been used in AP composite propellants and in earlier sandwich burning studies, with consistent enhancement of burning rate. The three

catalysis employed in this study ( $\text{Fe}_2\text{O}_3$ ,  $\text{Fe}_3\text{O}_4$ , carocene) significantly augmented the sandwich burning rate. In a previous section (pg. 10) three mechanisms were proposed for the action of catalysts. Here the experimental results will be investigated to determine the controlling mechanisms behind catalysis.

The first mechanism proposed (reduction of the heat required to vaporize the binder) will be reflected in the combustion zone as either lowering the ingredient decomposition temperature or decreasing the heat of phase change of the catalyzed binders. If this is happening less lateral heat flow is expected to the binder, therefore a recessed binder lamina is anticipated and less or no AP protrusion of the AP adjoining the binder. At the same time thick catalyzed binder laminar would not require as much lateral heat flow from the AP and the flame as required by pure binders and hence they would protrude less than thick uncatalyzed laminar.

The existence of a catalytic concentration along the binder surface did not permit a clear observation on whether or not the binder was more recessed for thin laminar than the pure binder sandwich cases. Thick catalyzed binder laminar did protrude slightly less the respective uncatalyzed cases and almost no AP protrusion was observed next to the AP/Binder interface. While this evidence supports the idea that the catalyst facilitates binder vaporization, the effects do not seem to contribute strongly to the heat balance at the leading edge of the regression front in the AP.

It is notable that the rate enhancing effect of all of the iron-containing catalysts was comparable, and also notable that the catalyst concentrations were all  $\text{Fe}_3\text{O}_4$  when analyzed after the tests (as judged from color and magnetic properties). This result suggests that  $\text{Fe}_2\text{O}_3$  may act as a weak oxidizer, but this does not appear to be the dominant factor in the increase in burning rate since  $\text{Fe}_3\text{O}_4$  has a comparable rate-enhancing effect (the case of  $\text{Fe}_3\text{O}_4$  at high pressures is excluded). Therefore the second catalytic mechanism

suggesting oxidation of some fuel with heat release cannot be considered as controlling the overall catalysis process.

An hypothesis for the mechanism of burning rate enhancement that appears to be consistent with all the observations is that in passage of primary vapor decomposition products of the binder through the catalyst bed, these heavy fuel molecules are broken down to more easily oxidized species (postulated as case 3 in pg. 10). This in turn permits the KLLEF to stand closer to the burning surface, with correspondingly increased heating of the surface, including the leading edge of the AP burning front, that governs burning rate. The observations that conform to this interpretation start with the observation of a catalyst bed, the prior knowledge that such a bed would break down heavy fuel molecules and that this would lead to enhanced gas phase reaction rates in the O-F mixing fans and a correspondingly reduced flame stand-off distance (it is important to mention that either slight or no increase in the burning rate was measured when the concentration of catalyst on the binder was limited or did not occur - such cases were encountered with thick binder laminates or with  $\text{Fe}_3\text{O}_4$  in PBAN at high pressures). In addition to the higher burning rate that results, a corresponding contraction of the leading edge region of the profile indicates a smaller KLLEF standing closer to the surface and a corresponding reduction of the retarded AP region adjoining the binder. The profile of the AP near the AP-binder contact plane becomes almost flat, indicating effective heating by KLLEF, but the surface does not slope towards the binder in that region as would be expected if exothermic binder reaction were dominant. Further, the trend of burning rate with binder thickness retains the trends observed with uncatalyzed sandwiches and hence is rationalized on the basis of burning rate controlled by KLLEF - assisted AP self-deflagration and lateral heat flow into an endothermic binder. The burning rate maximum in the burning rate - binder lamina

thickness curves occurs at lower thickness with catalyst, an effect that is consistent with rate control with a smaller KLLEF standing closer to the surface.

On the basis of these arguments it appears that the dominant effect of the catalyst is catalytic breakdown of heavy fuel molecules which is conducive to lower KLLEF stand-off distance. This argument seems particularly compelling in the case of NMMO binder, which showed negligible effect of a KLLEF without catalyst, but then exhibited the usual trend of rate vs. binder thickness with catalyst (presumably because more favorable gas phase kinetics brought the KLLEF contribution to heat balance back in as a contributor).

### 5.5 Secondary Effects

1. **Observable Flames:** Flames seen in combustion photography of AP propellants are very rarely real flames. Instead, they are veils of hot carbon flowing out of the fuel-rich regions and trailing away from the flame. If interpreted in that way, information about amount, location, shape, and motion of these flames can be useful. The real flames, where most of the heat release occurs are not particularly luminous, and are usually so small that they are not readily resolved except by special optical diagnostic methods. Further, they may be locally intermittent. In that case, even if they are spatially resolved, the observations may be time-averaged over an extreme range of variations.

Conditions conducive to carbon formation result when the binder is thick enough so that unreacted fuel flows between the two KLLEFs and has time for fuel pyrolysis and carbon nucleation before reaching the diffusion flame sheets. This is consistent with observation of luminous veils from flames when the binder lamina is thick. It is also consistent with the lower luminosity of the BAMO-THF and NMMO binders, which have lower carbon content. It is likely that the observed trends are also linked to the details of the binder decomposition, which profoundly affect the fate of carbon atoms in the

combustion. However the decomposition reactions are not yet well known, so their contribution cannot be determined.

2. Tapered Sandwiches: Sandwiches with catalyzed tapered binder laminae were burned at low pressures where spontaneous quench occurred. It was found that for catalyzed BAMO-THF, quench occurred at lower binder lamina thicknesses (a result indicative of closer proximity of the KLEFs to the surface; this was also verified by the fact that thin catalyzed BAMO-THF binder sandwiches burned to completion at low pressures - recall that pure binder sandwiches could not sustain combustion under these conditions). For catalyzed PBAN sandwiches quench occurred at thicker binder laminae than without catalyst. The binder thickness at quench occurred was almost identical for both catalyzed binders (see fig. 4-62) suggesting that probably the heavy catalytic concentration is responsible for the self quench. In this regard, the concentration of catalyst while the binder lamina is getting progressively thinner may lead to obstruction of vapor outflow and heat inflow to a degree not present in normal sandwiches. Thus it is not clear how to interpret the quench limit results.

3. Stronger Catalysis of BAMO-THF Binder Sandwiches than of PBAN: The burning rate catalysts improved the chemical kinetics of BAMO-THF much more than the kinetics of PBAN. The effect of burning rate catalysts on chemical kinetics was verified by the fact that catalysis increased as the test pressure decreased. At low pressures the mixing process is fast and the time required to reach the final state is determined by chemical kinetics (which are improved by the catalysts). As the pressure increases the mixing process becomes slow compared to reaction rates and the time required to reach the final state is determined by diffusion rates.

## CHAPTER VI

### CONCLUSIONS AND RECOMMENDATIONS

The main objective of the sandwich burning studies is to understand and investigate the controlling mechanisms of composite solid propellant burning. The results indicate that a great deal can be learned about the combustion zone structure from the simplified sandwich system.

It is important to investigate the physical mechanisms governing the combustion process in a laminate system. Basic information on kinetics and thermochemistry of the binders is needed in order to explain the establishment and structure of the flame complex. The understanding of the controlling mechanisms and the knowledge of ingredient properties will help in suggesting new propellant formulations.

In the present study the qualitative theory of flame complex described in [54], was applied and extended for the case of new energetic binders. Some new postulates were developed and proposed for the action of the iron based catalysts introduced in the binder lamina.

This new expanded flame theory was able to qualitatively predict burning rate trends, surface profiles and flame structure based on ingredient properties related to combustion, thermochemistry of the Oxidizer/Binder system, pressure changes and binder lamina thickness variations.

kinetically limited flame close to the burning surface. The burning rate is increased because under these circumstances more heat reaches the burning surface.

Although concentration of catalyst was not proved to be a necessary and sufficient condition for rate enhancement there is no doubt that occurrence of concentration was encountered with all the burning rate catalysts employed in the present study (whenever burning rate increase occurred; when  $\text{Fe}_2\text{O}_3$  was added to PBAN at high pressure tests no burning rate enhancement was measured and no concentration was observed on the binder surface).

Most of the burning trends observed were determined either by the AP self-deflagration (high pressure) or by the efficiency of the KLLEF as a source of heat flow to the surface. Even though the KLLEF could not be observed directly, all conditions that were conducive to high heat flow from the KLLEF to the surface were conducive to high burning rate. These conditions included

1. High stoichiometric flame temperature
2. Binder thickness conducive to most effective heat flow to the surface (and the expected dependence of that thickness on binder fuel content)
3. Catalytic "cracking" of the fuel to give fast gas phase reaction.

In general, the results taken one at a time are only suggestive of mechanisms. The validity of the mechanistic interpretation rests on the overall consistency of many kinds of observations with the overall description of the combustion process, a description that has evolved from many past and present experimental studies and from qualitative consideration of combustion theory. The present studies have extended the observations and theoretical argument to encompass the effect of O-F flame temperature, stoichiometry of the binder, and catalysis, all of which had major effect on burning rate. Decomposition temperature and exothermicity of the binder were found to have some effect on details of

Some of the predictions made, which were consistent with the experimental results, are presented in the following paragraphs.

Compared to the non-energetic PBAN binder, BAMO-THF and NMMO are energetic binders that decompose at lower temperatures than PBAN. BAMO-THF releases nitrogen exothermally, while NMMO decomposes by energy release. Because of this exothermic activity of both binders it is expected that little or no lateral heat will flow from the AP lamina to the binder and therefore little or no retardation of the AP regression in the AP next to the oxidizer/binder interface. This was consistent with the experimental results of this work.

Under these conditions an increased burning rate is anticipated relative to sandwiches with PBAN binder. In fact in the case of BAMO-THF a slightly higher burning rate was measured for intermediate or thick binder lamina thicknesses. That was in agreement with the stoichiometric AP/BAMO-THF mixture composition which requires a higher fuel fraction than the AP/PBAN mixture.

On the contrary sandwich burning rate with NMMO binder was much lower than the sandwich burning rate of PBAN sandwiches. The lower flame temperature of NMMO with AP and the fact that its stoichiometric ratio with AP requires a high fuel content were perhaps partially responsible for the low burning rate, but the results suggest that the kinetics of the AP-NMMO vapor reaction were also too slow for the KLLEF to contribute significantly to burning rate without catalyst.

Enhancement of sandwich burning rate was measured when iron containing catalysts were employed in the binder lamina. Stronger catalysis of burning rate was accompanied by catalytic accumulation on the binder surface. The existence of this sintered formation provided an additional surface for the heavy fuel molecules to crack down to small fragments. These fragments are easily oxidized in a location near the surface, bringing the

the burning surface; effect on burning rate appears to have been small (none if the binder was strongly exothermic).

There were a number of results that deserve further investigation, some of which could not be unambiguously explained because they depended on the balance between competing mechanisms that are only known qualitatively. Such results include:

1. Results of tapered sandwich quench limit tests
2. Stronger catalytic effects with BAMO-TTFF binder than with PBAN, especially with Fe<sub>3</sub>O<sub>4</sub>
3. Details of catalyst bed formation, nature of the bed, difference with different catalysts.

In the future one might hope for a more decisive set of investigations that go more directly at the fundamental contributing mechanisms involved in the present scenario, and at construction of a qualitatively theory encompassing these mechanisms. This goal has become increasingly attainable because the problems are increasingly well defined, and the requisite experimental and analytical - computational methods are becoming attainable. Some of the detailed studies that are needed are:

1. Determination of ingredient pyrolysis mechanisms in high heating rate experiments that yield temperatures comparable to burning surface temperatures. Determination of resulting vapor species
2. Study of the KLEEF region of laminar diffusion flames (both experimental and theoretical)
3. Further study of catalyst bed formation, and effect of catalyst in the binder melt and on vapors identified in 1.

4. Development of a first generation 2-dimensional analytical model of sandwich burning, to permit more decisive resolution of importance of competing mechanisms and extrapolation of current results

5. Extension of present results to more energetic binders, and to modern oxidizers of interest (e.g., HMX). Further exploit the method in a search for best catalysts

6. Conduct of systematic studies of propellant combustion designed to establish the methodology for application of "sandwich results" to propellant combustion.

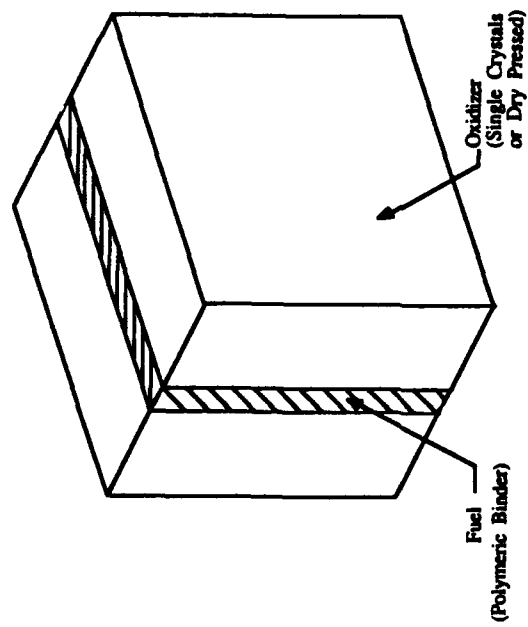


Figure 1-1. Oxidizer-Binder Sandwich

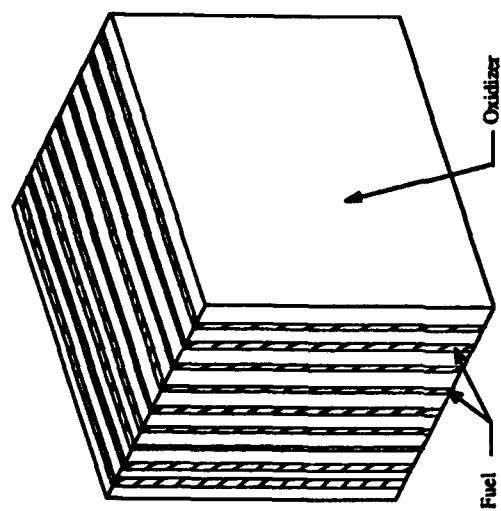


Figure 1-2. Multilayer Oxidizer-Binder Sandwich

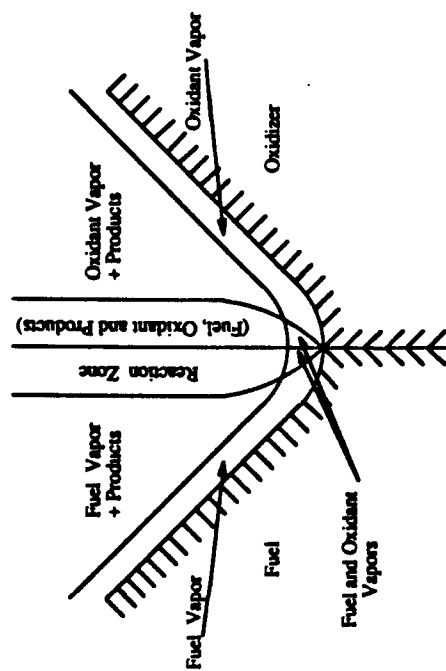


Figure 1-3. Phalanx Flame at Steady State

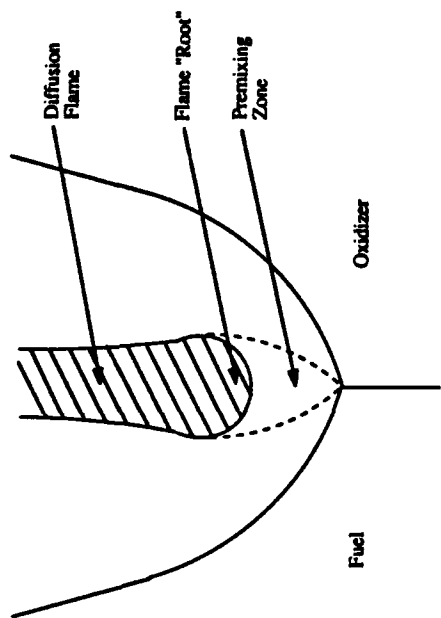
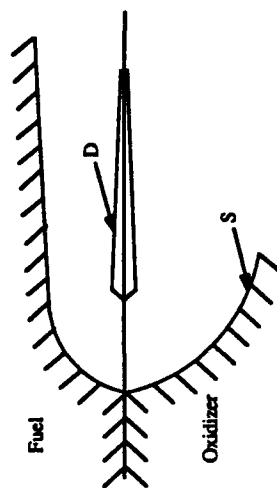
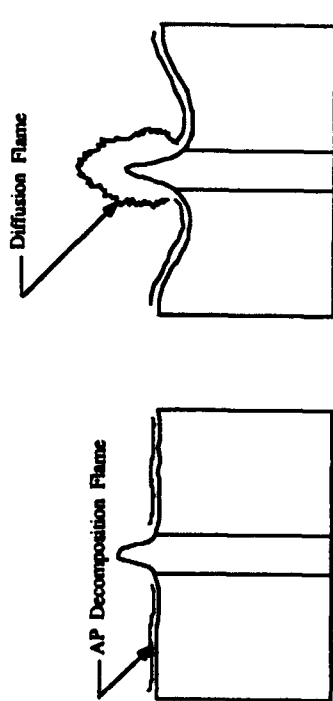
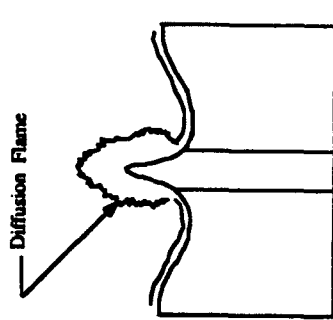


Figure 1-4. Sketch of Individual Flame

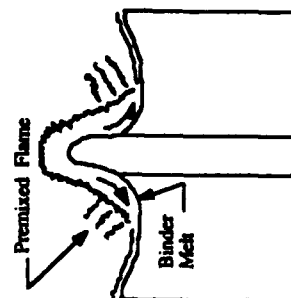
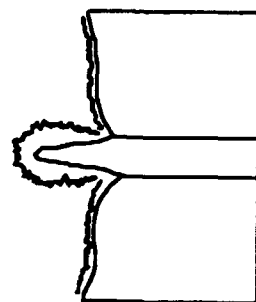
Figure 1-5. A Sketch of the "Cavity"  
S: Gasification Surface  
D: Diffusion Flame



a) Monopropellant Characteristics



b) Gas Phase Diffusion Flame Zone

c) Partially Premixed Flame  
resulting from Binder Melt Flow

d) Dominant Interfacial Reactions

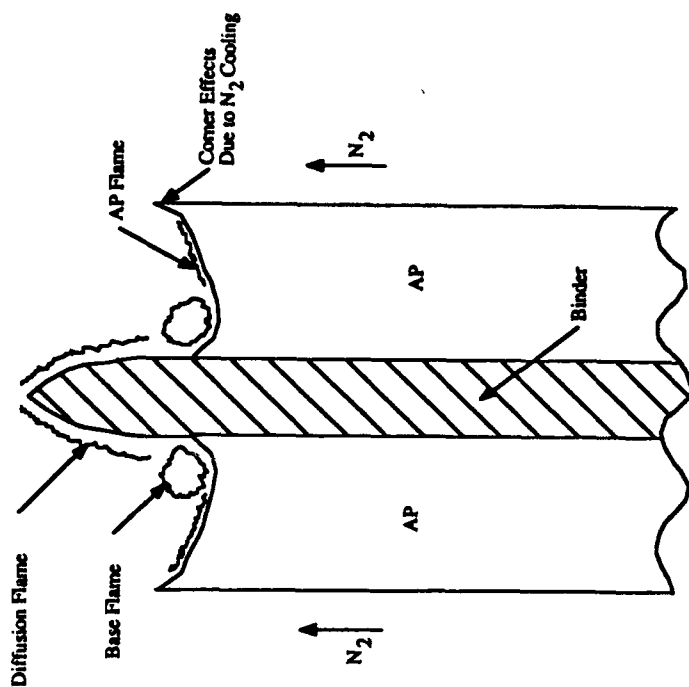
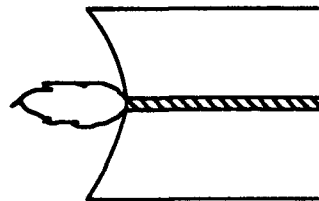
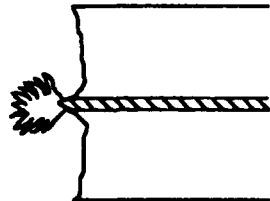


Figure 1-7. Analytical Sandwich Combustion Model

Figure 1-6. Mechanisms Influencing Sandwich Regression



Candle Diffusion  
Flame ( $p < 300$  psi)



Turbulent Diffusion  
Flame

Figure 1-8. Flame Structure

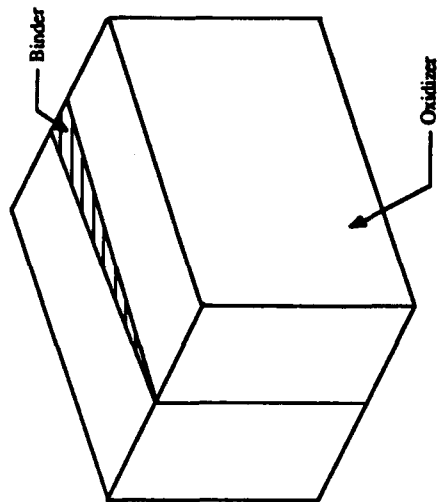


Figure 1-9. Tapered Oxidizer-Binder Sandwich

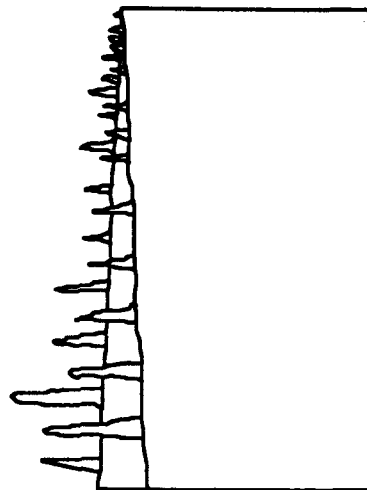


Figure 1-10. Sketch of Diffusion Flamelets from an  
AP-Binder Tapered Sandwich

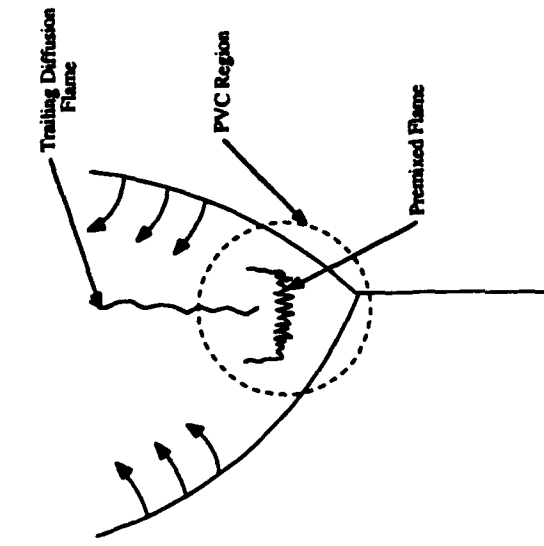


Figure 1-12. Model of Burning Down the Interface between an Oxidizer and a Fuel Slab with the Propagation Velocity Controlling Region

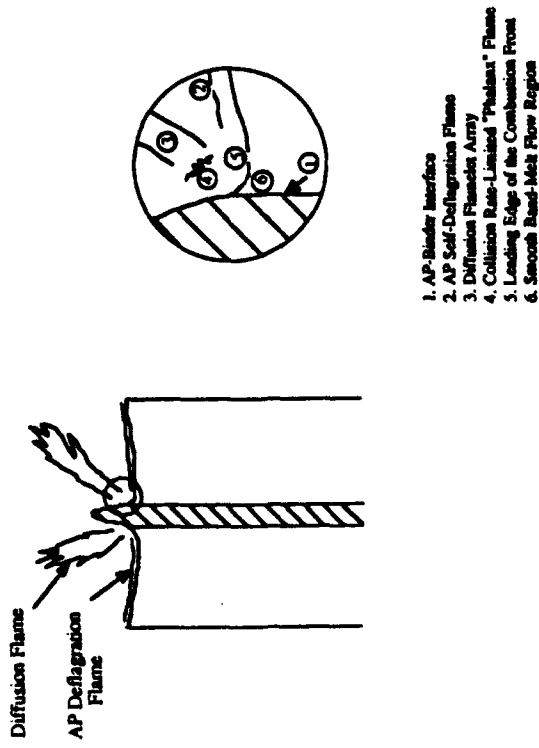


Figure 1-11. Structure of the Sandwich Combustion Zone

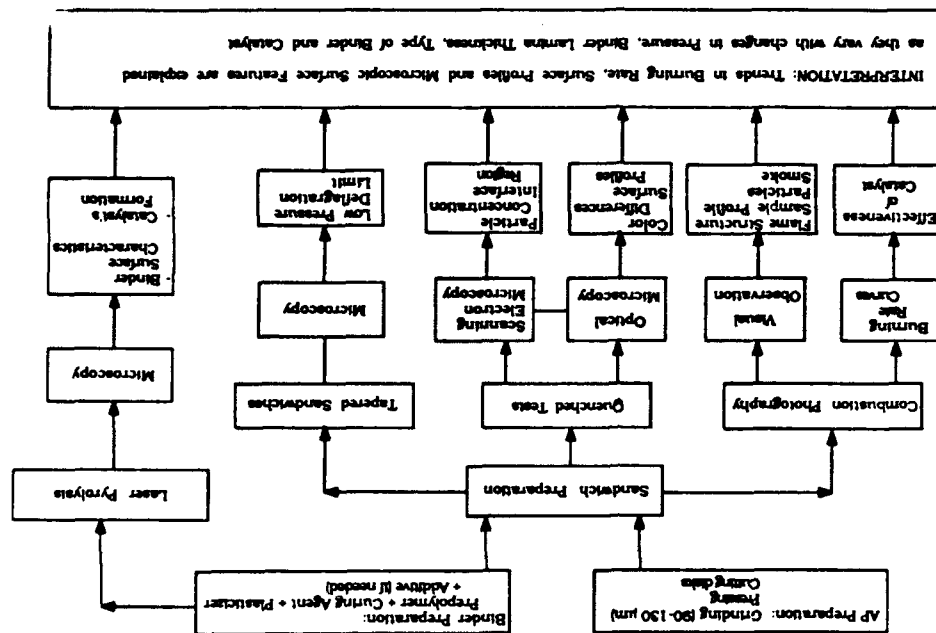


Figure 2-1. Experimental Procedure

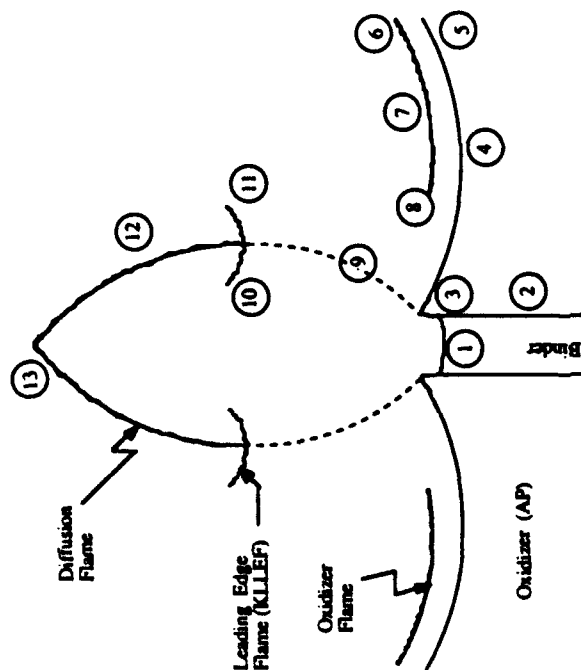


Figure 1-13. Principal features of the combustion zone microstructure and processes as suggested by accumulated results: 1) binder lamina, 2) interface plane between binder and oxidizer; 3) oxidizer surface adjoining binder-smooth band; 4) leading edge of the oxidizing burning front; 5) oxidizer region that regresses at the normal AP self-deflagration rate; 6) AP flame; 7) leading edge region of AP flame; 8) oxidizer flame, modified by the animalous decomposition in the smooth band; 9) oxidizer-fuel diffusion region, with stoichiometric surface indicated by broken line; 10-11) kinetically limited leading edge flame (KLLEF) (fuel-rich and oxidizer-rich sides); 12) diffusion flame; 13) tip of diffusion flame

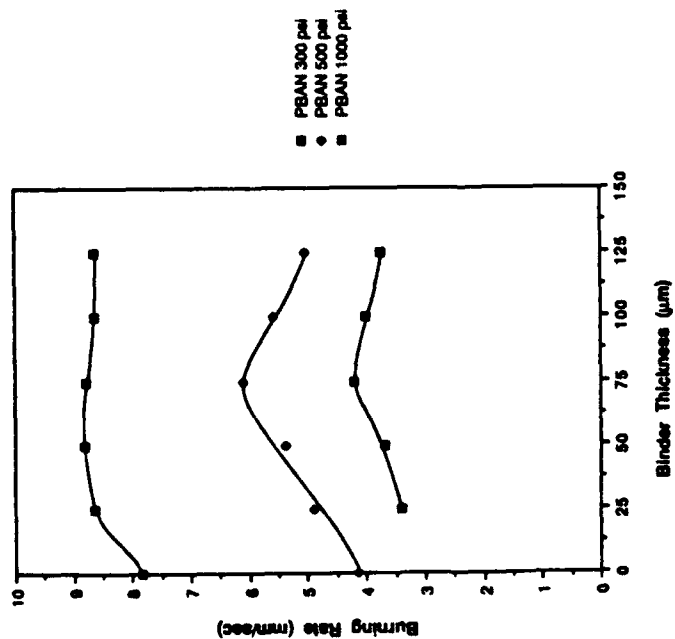


Figure 4-1: Burning Rate of PBAN Sandwiches

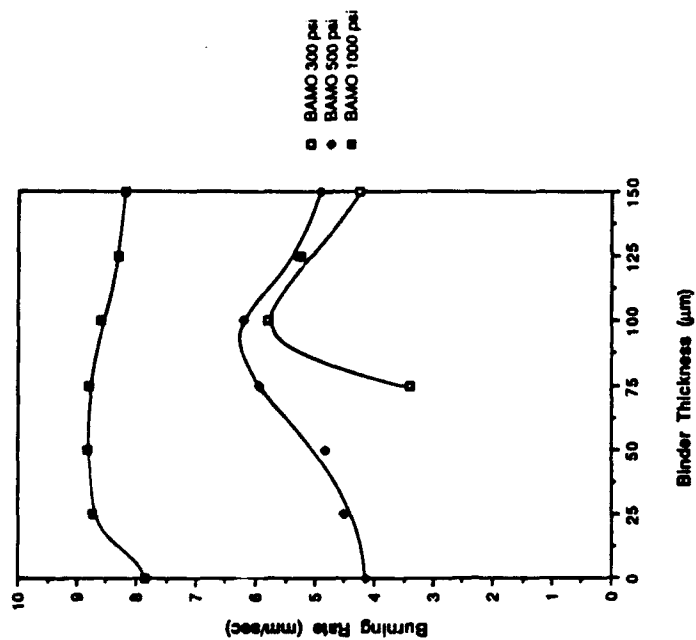


Figure 4-2: Burning Rate of BAMO-THF Sandwiches

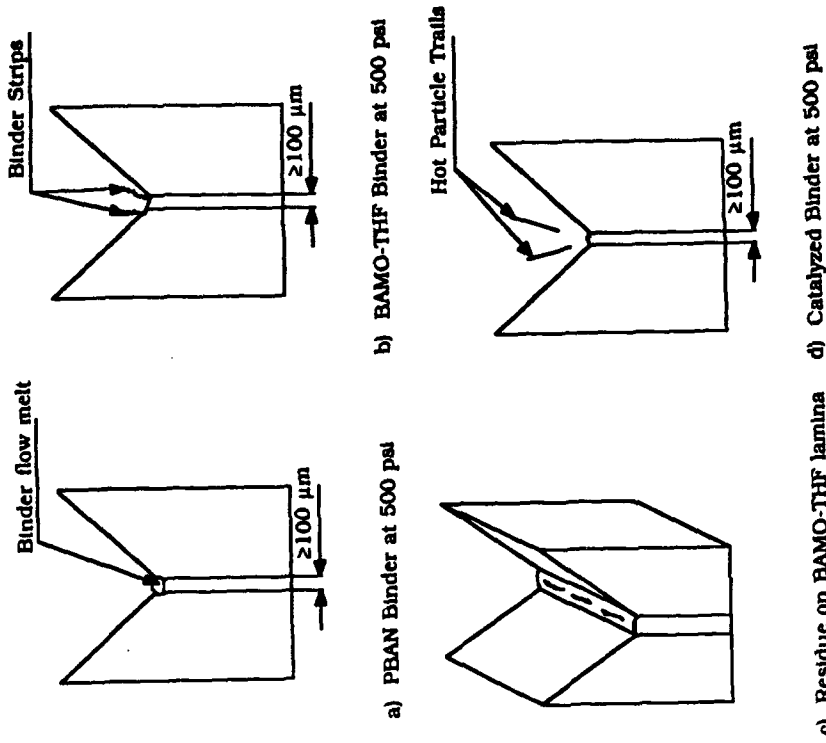


Figure 4-4: Some Details observed during Sandwich Burning

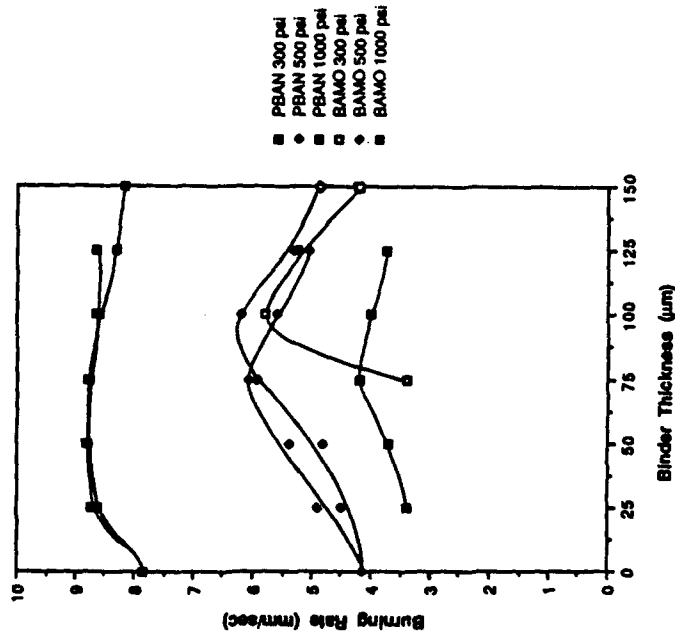


Figure 4-3: PBAN and BAMO-THF; Burning Rate Comparison

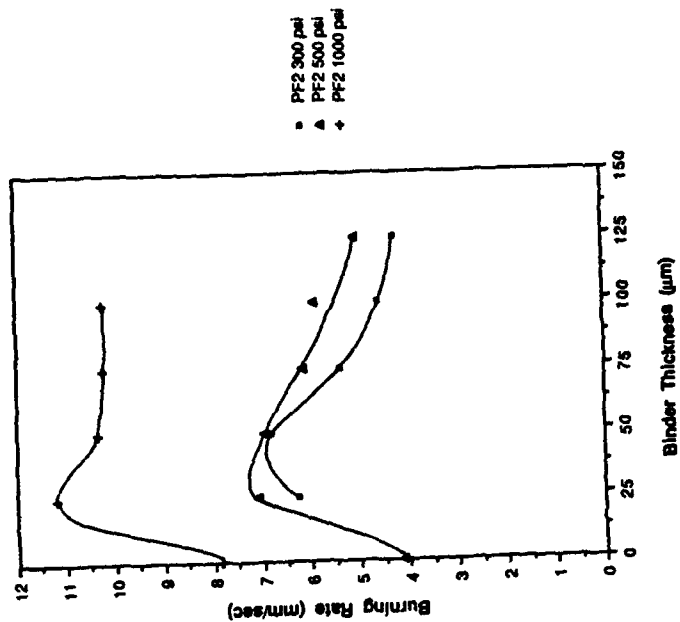


Figure 4-6: Burning Rate of PBAN + 10% Fe<sub>2</sub>O<sub>3</sub> Sandwiches

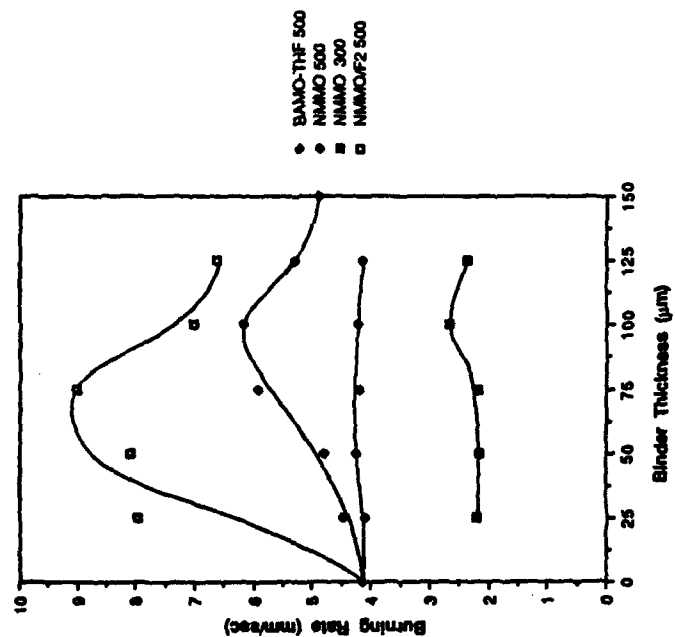


Figure 4-5: Burning Rate of NMMO Sandwiches (with NMMO+10%Fe<sub>2</sub>O<sub>3</sub>, BAMO-THF at 500 psi)

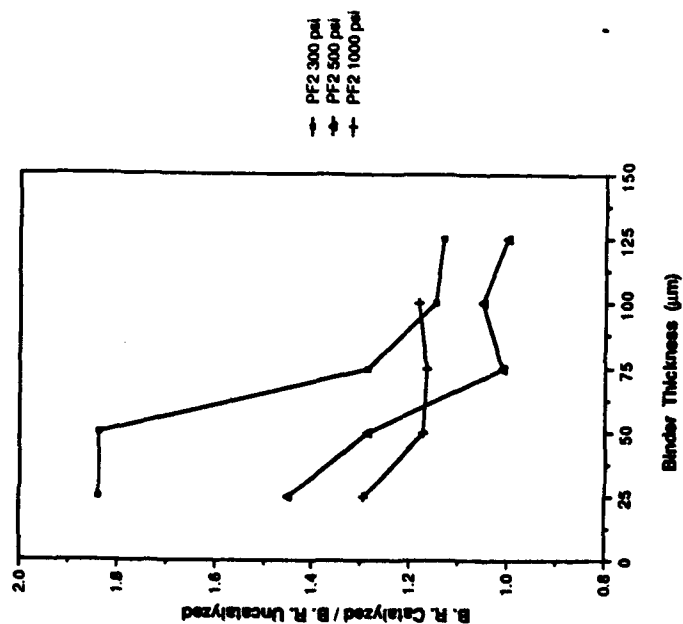
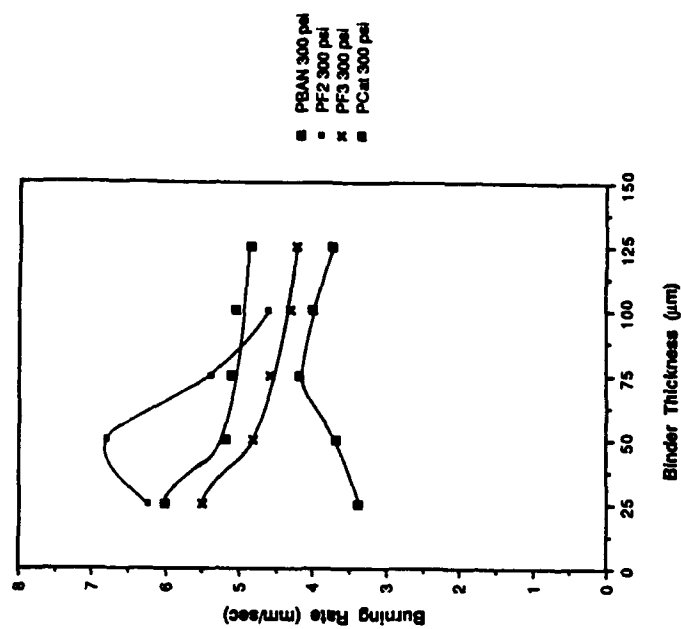
Figure 4-7: PBAN; Burning Rate Ratios (Fe<sub>2</sub>O<sub>3</sub> case)

Figure 4-8: Burning Rate of Catalyzed and Uncatalyzed PBAN at 300 psi

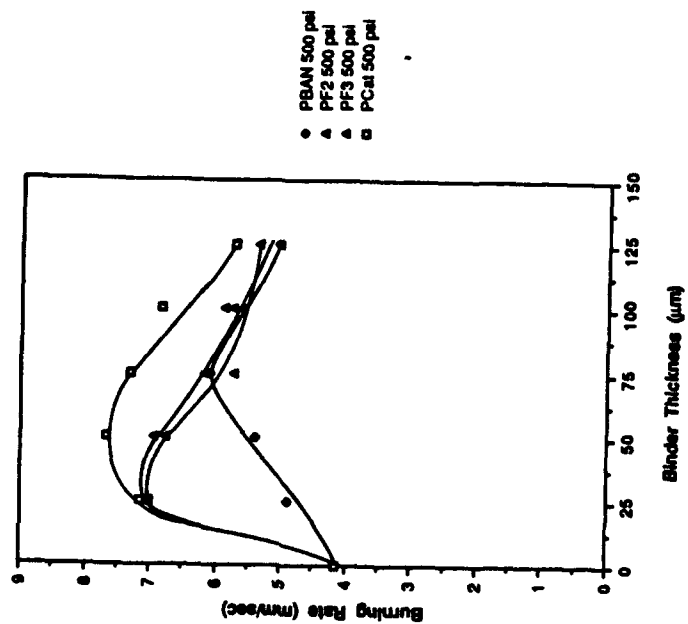


Figure 4-9: Burning Rate of Catalyzed and Uncatalyzed PBAN at 500 psi

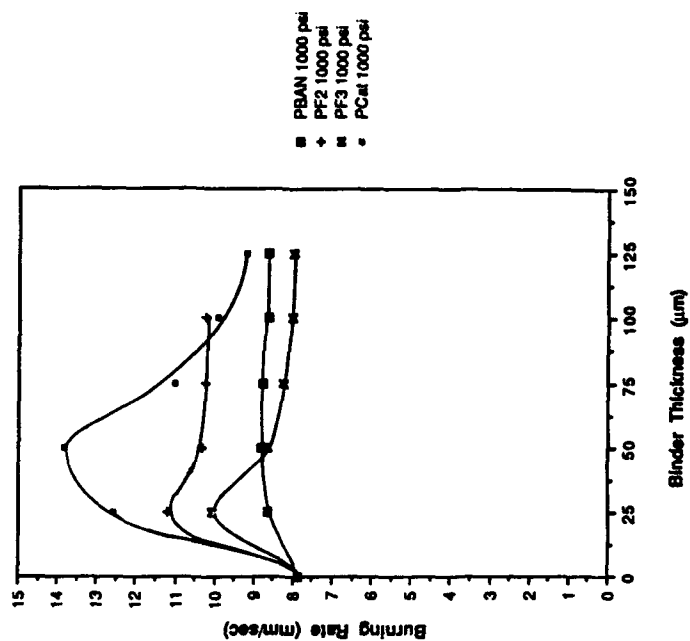
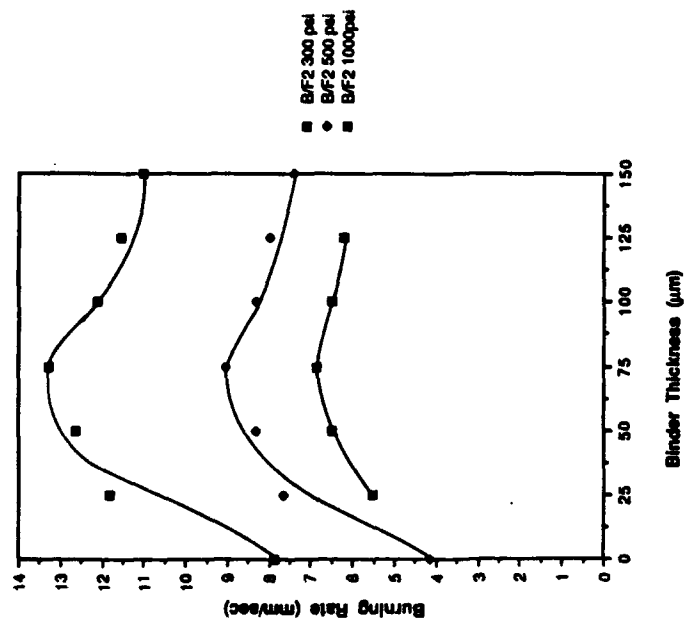
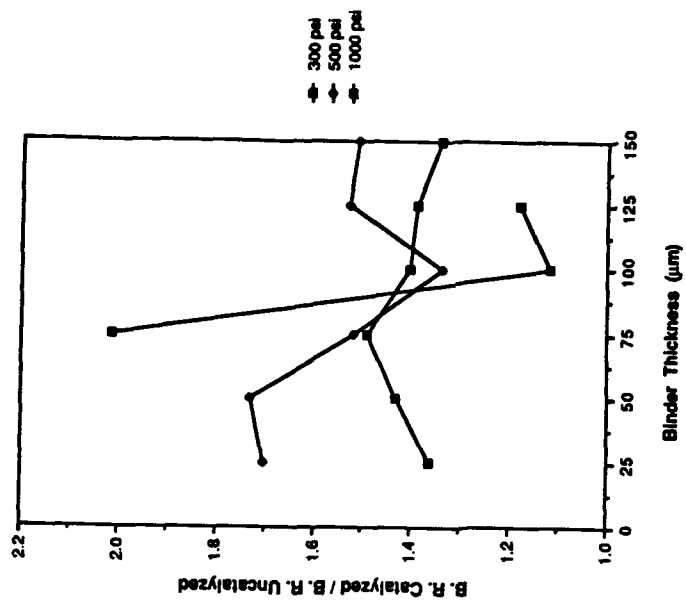


Figure 4-10: Burning Rate of Catalyzed and Uncatalyzed PBAN at 1000 psi

Figure 4-11: Burning Rate of BAMO-THF + 10%  $\text{Fe}_2\text{O}_3$  SandwichesFigure 4-12: BAMO-THF; Burning Rate Ratios ( $\text{Fe}_2\text{O}_3$  case)

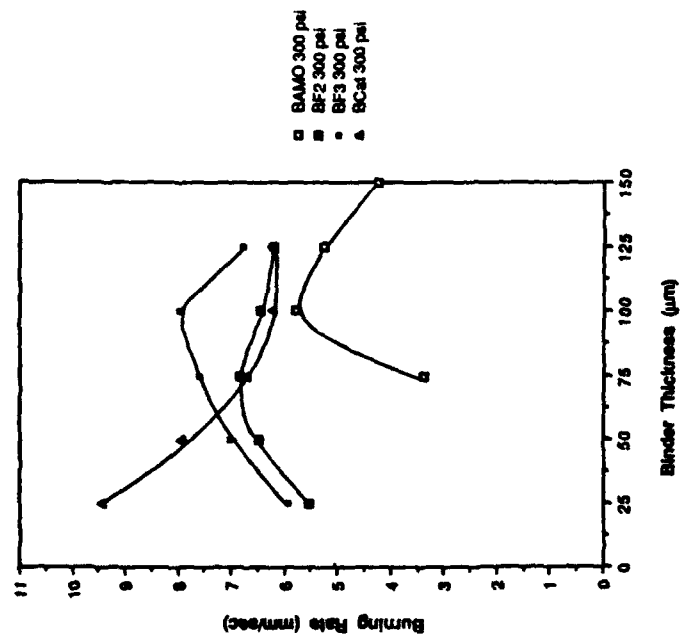


Figure 4-13: Burning Rate of Catalyzed and Uncatalyzed BAMO-THF at 300 psi

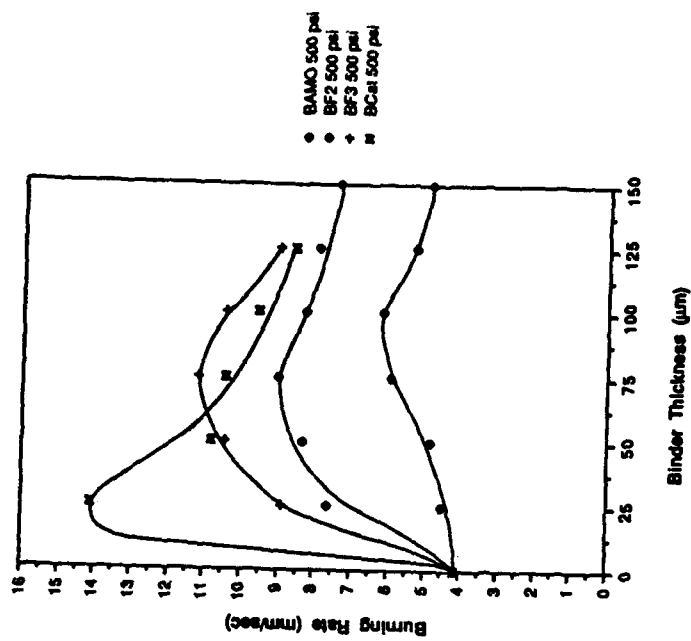


Figure 4-14: Burning Rate of Catalyzed and Uncatalyzed BAMO-THF at 500 psi

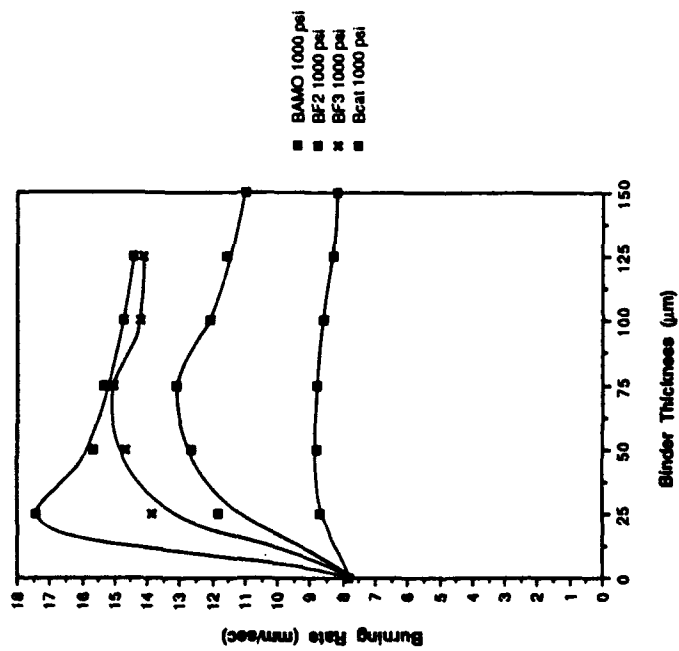
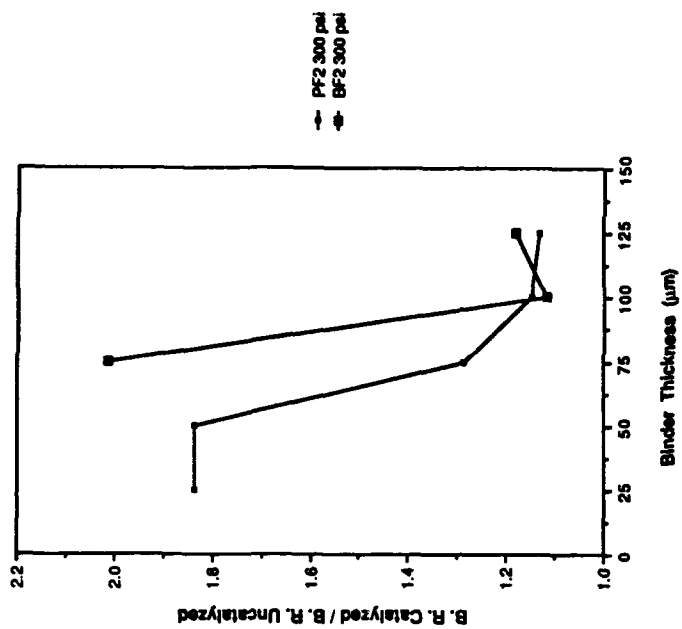
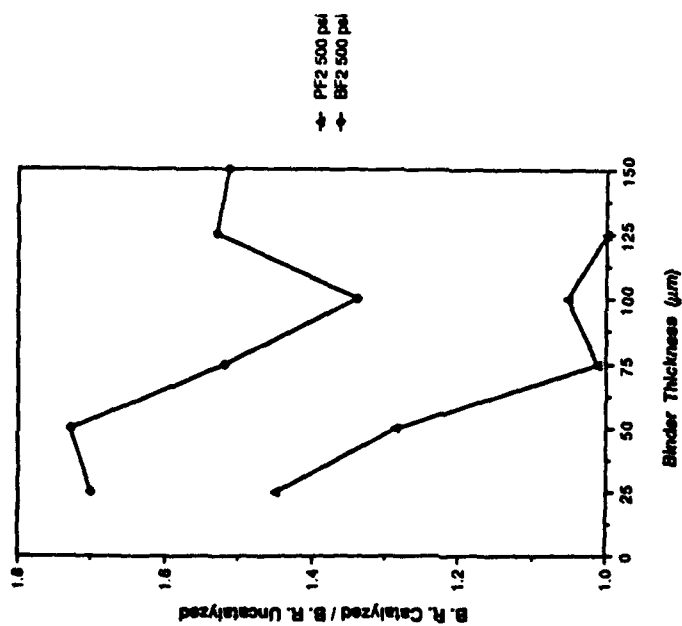
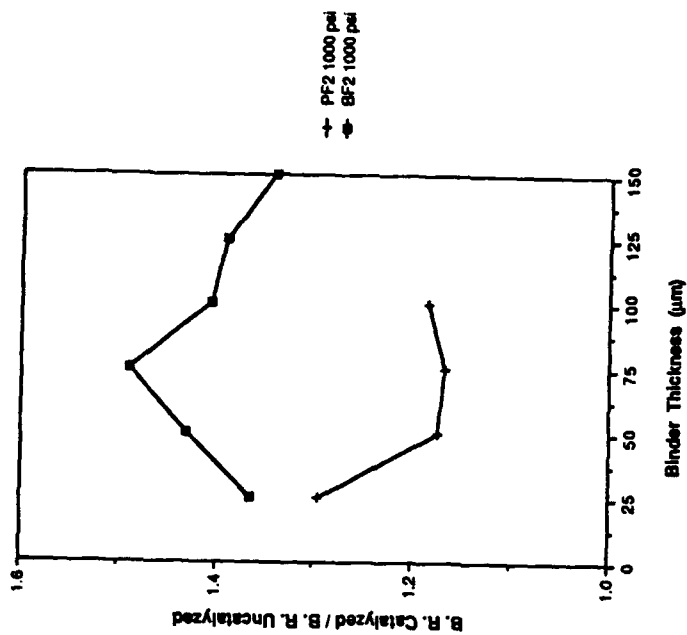


Figure 4-15: Burning Rate of Catalyzed and Uncatalyzed BAMO-THF at 1000 psi

Figure 4-16: Effect of Fe<sub>2</sub>O<sub>3</sub> on both binders at 300 psi

Figure 4-17: Effect of Fe<sub>2</sub>O<sub>3</sub> on both binders at 500 psiFigure 4-18: Effect of Fe<sub>2</sub>O<sub>3</sub> on both binders at 1000 psi

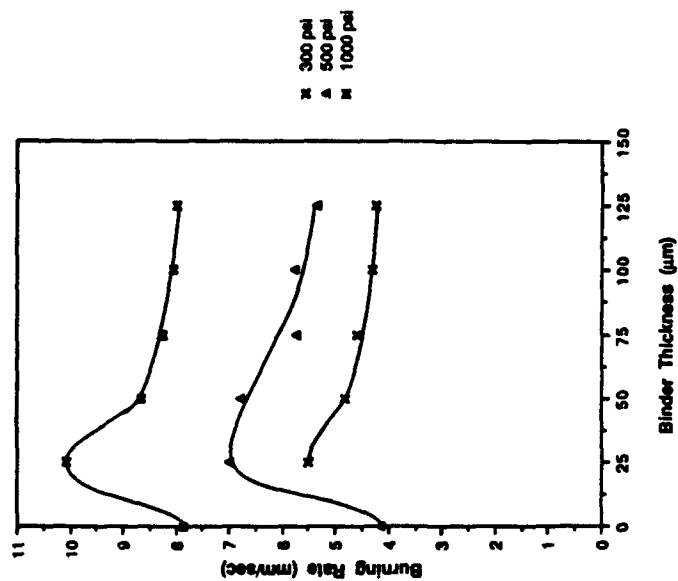


Figure 4-19: Burning Rate of PBAN + Fe<sub>3</sub>O<sub>4</sub> Sandwiches

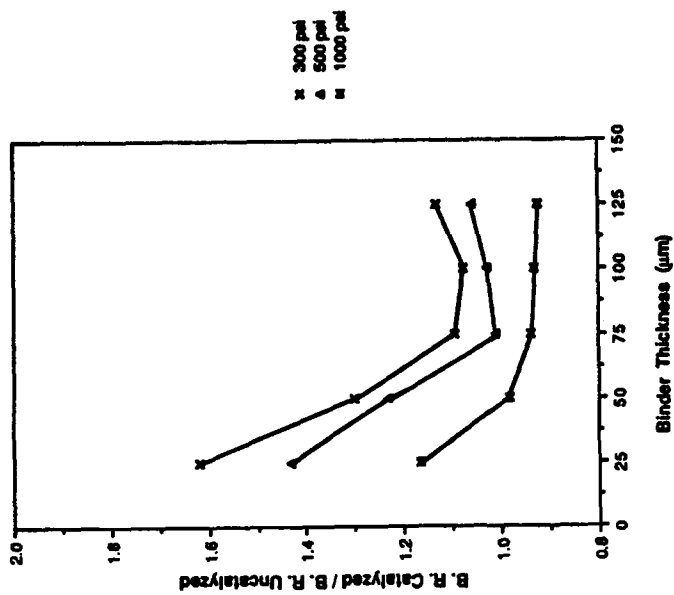


Figure 4-20: PBAN; Burning Rate Ratios (Fe<sub>3</sub>O<sub>4</sub> case)

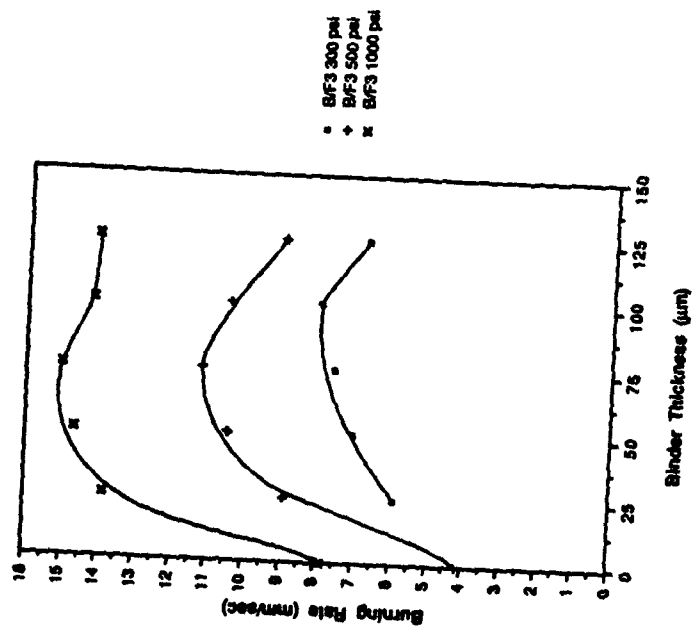


Figure 4-21: Burning Rate of BAMO-THF + 10% Fe<sub>3</sub>O<sub>4</sub> Sandwiches

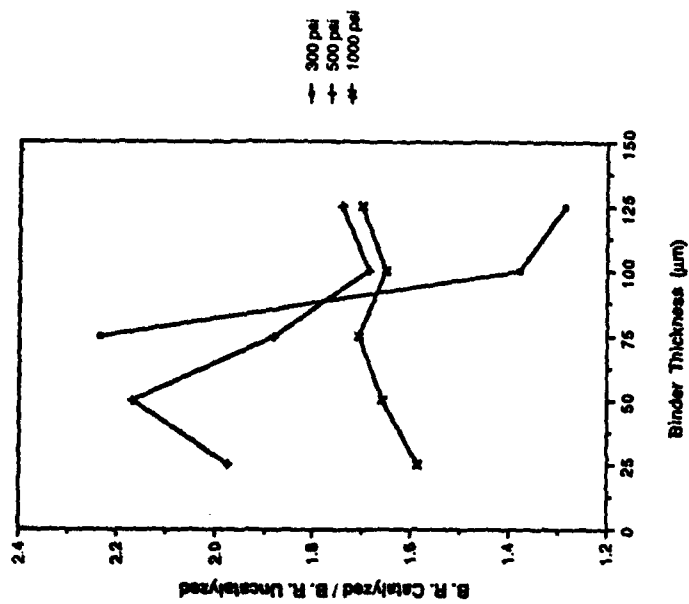
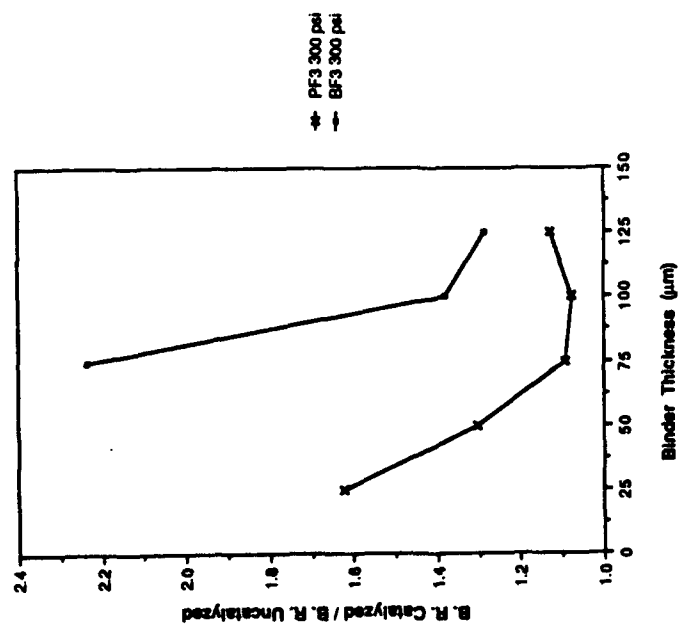
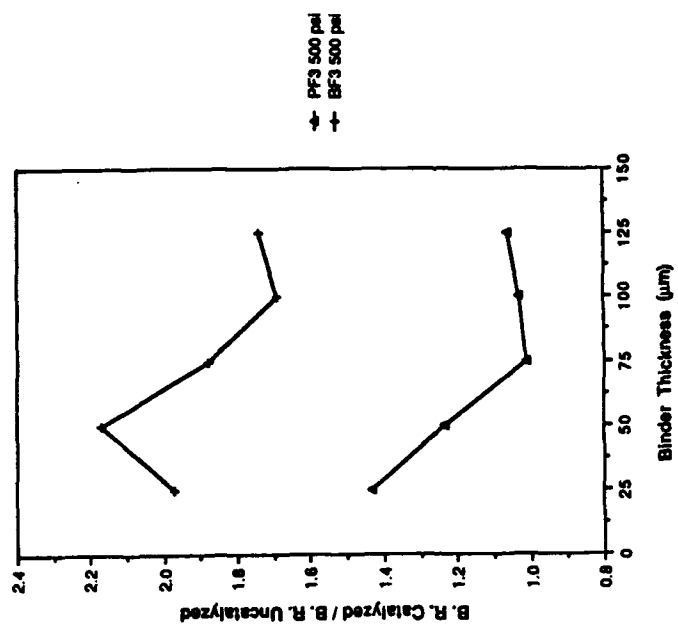


Figure 4-22: BAMO-THF; Burning Rate Ratios (Fe<sub>3</sub>O<sub>4</sub> case)

Figure 4-23: Effect of Fe<sub>3</sub>O<sub>4</sub> on both binders at 300 psiFigure 4-24: Effect of Fe<sub>3</sub>O<sub>4</sub> on both binders at 500 psi

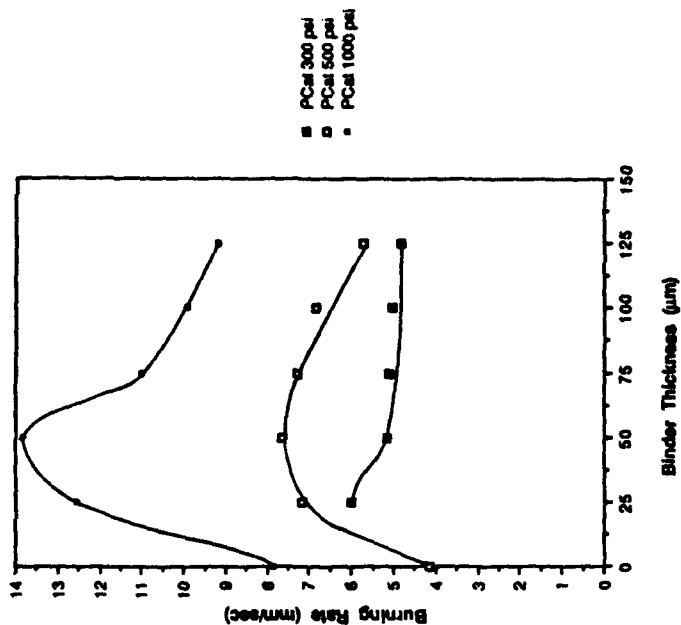


Figure 4-26: Burning Rate of PBAN + 20% Catocene Sandwiches

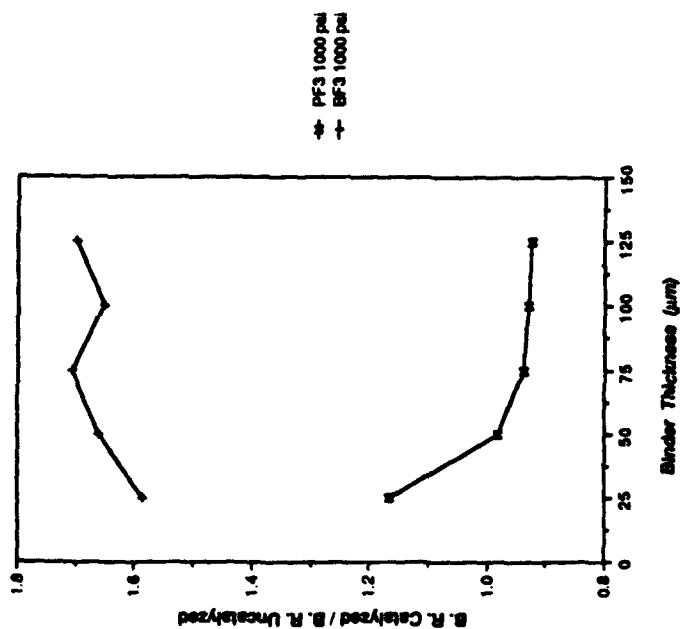


Figure 4-25: Effect of Fe<sub>3</sub>O<sub>4</sub> on both binders at 1000 psi

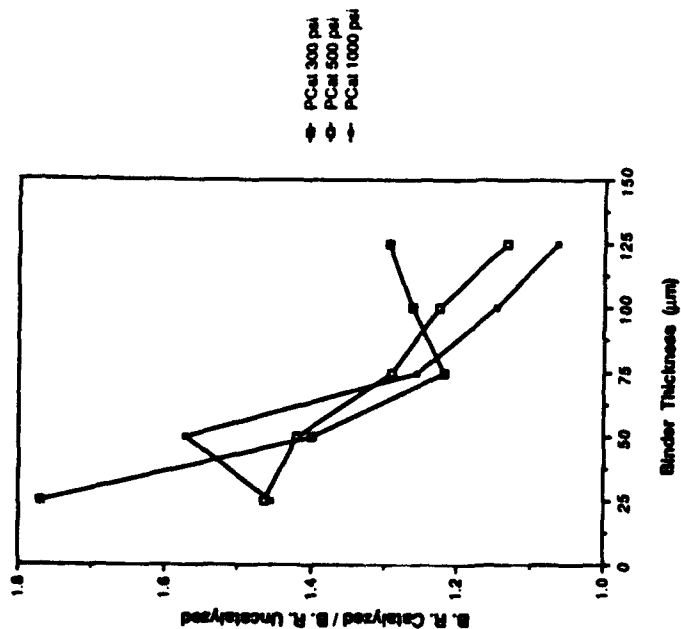


Figure 4-27: PBAN; Burning Rate Ratios (Calocene case)

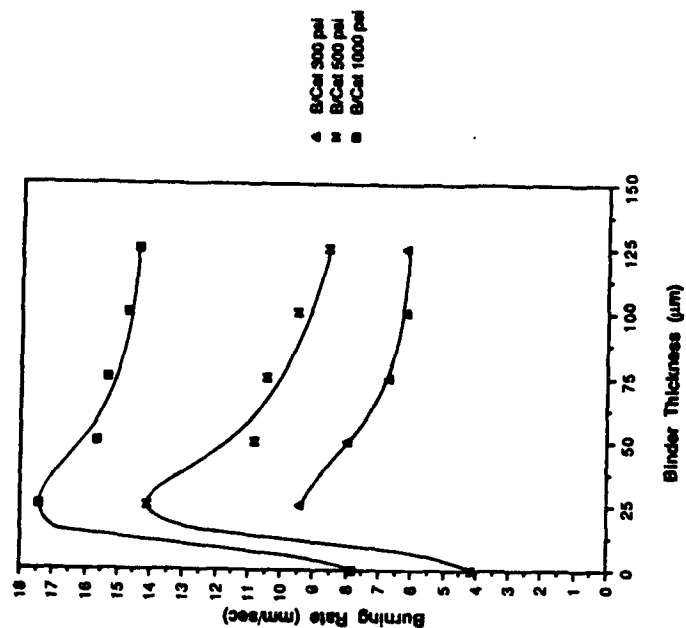


Figure 4-28: Burning Rate of BAMO-THF + 20% Calocene Sandwiches

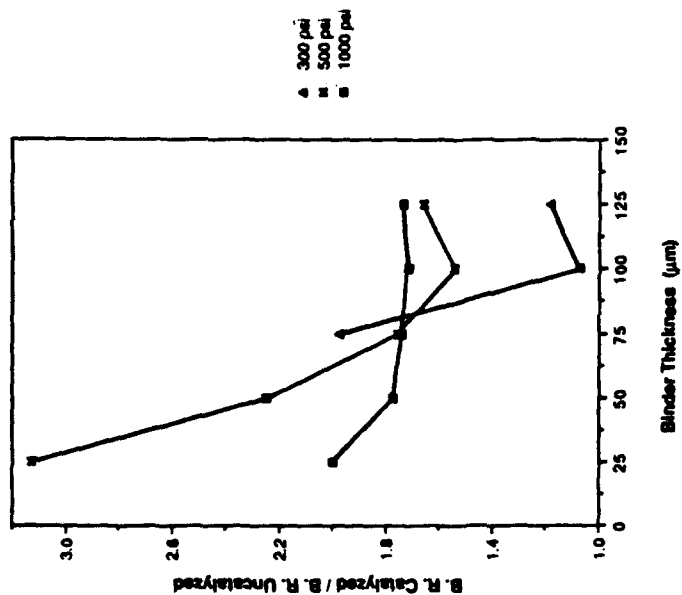


Figure 4-29: BAMO-THF; Burning Rate Ratios (Carotene case)

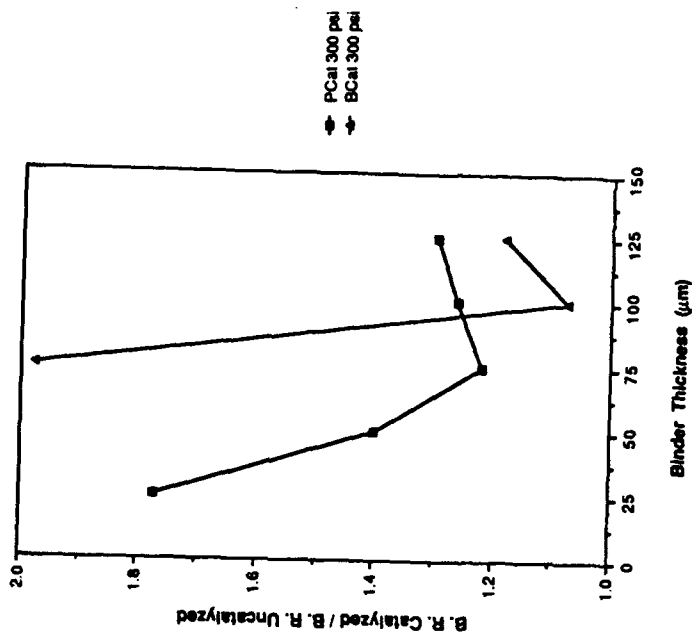


Figure 4-30: Effect of Carotene on both binders at 300 psi

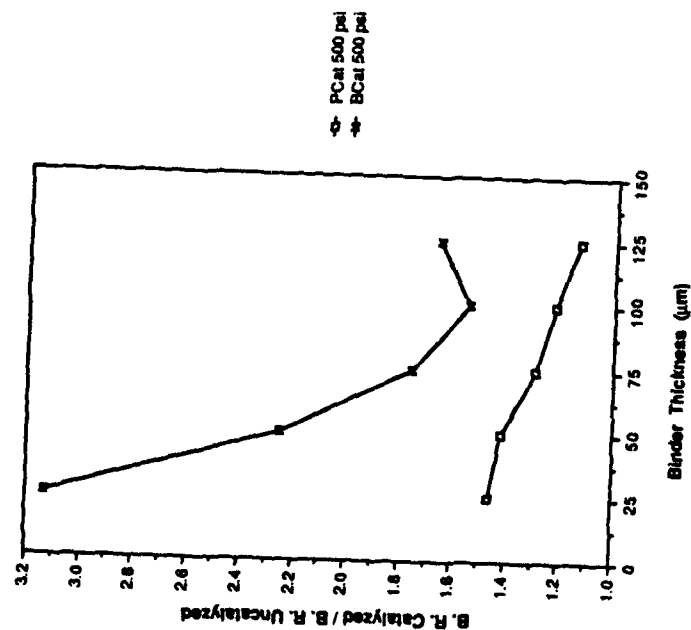


Figure 4-31: Effect of Catocene on both binders at 500 psi

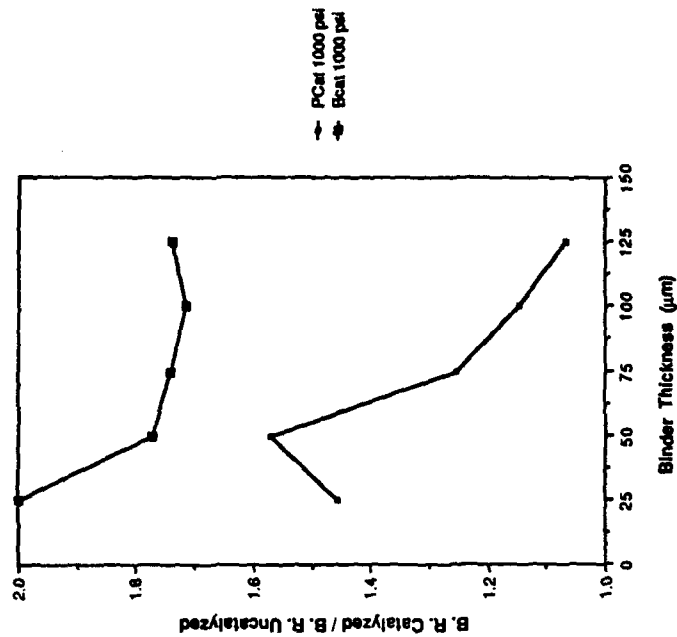


Figure 4-32: Effect of Catocene on both binders at 1000 psi

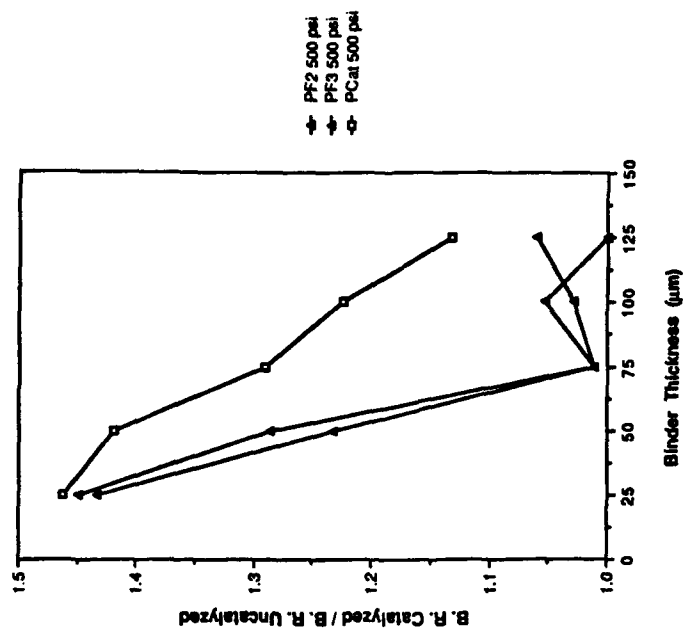


Figure 4-34: PBAN; Effect of Catalysts at 500 psi

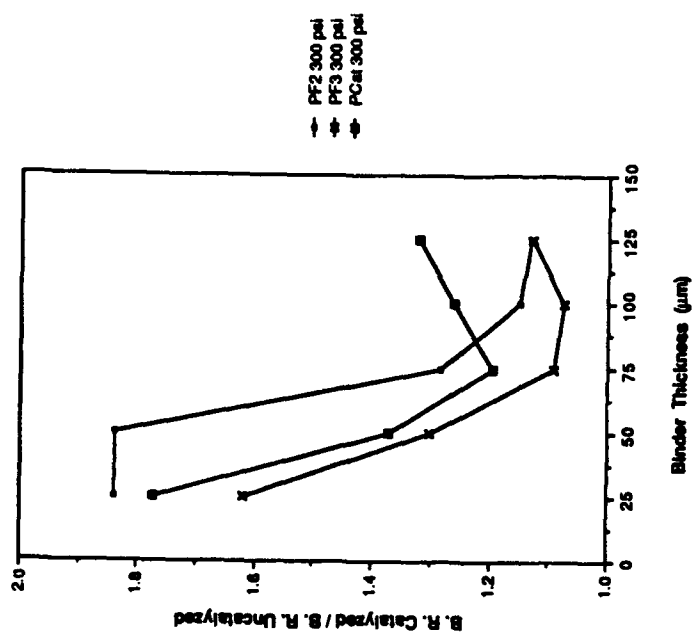


Figure 4-33: PBAN; Effect of Catalysts at 300 psi

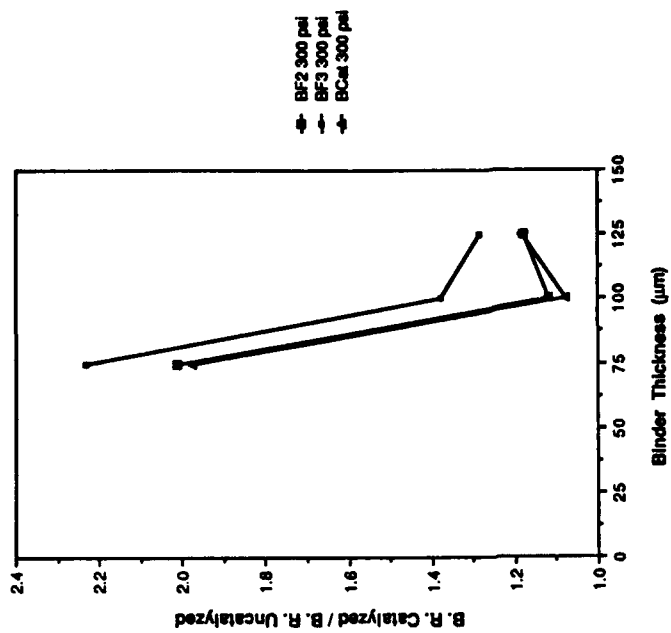


Figure 4-36: BAMO-THF; Effects of Catalysts at 300 psi

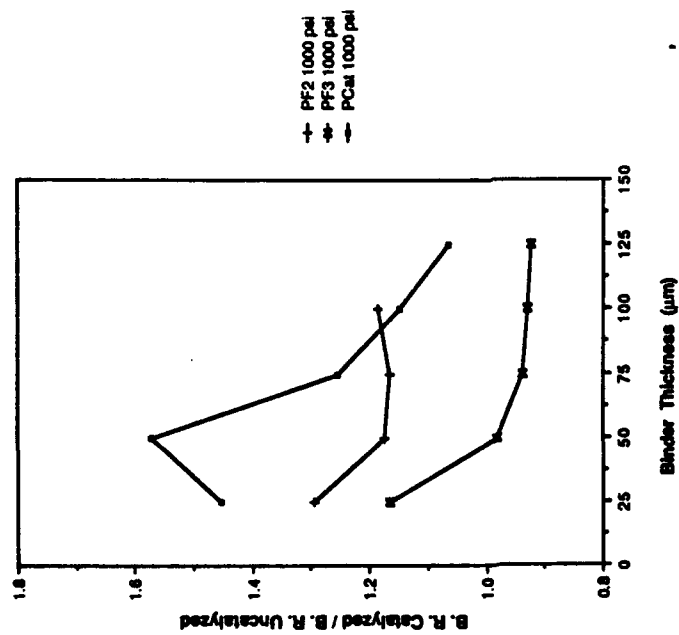


Figure 4-35: PBAN; Effect of Catalysts at 1000 psi

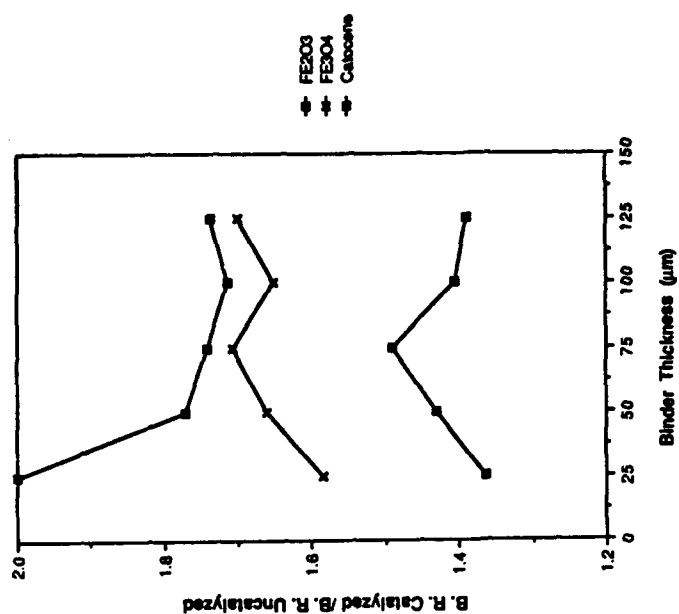


Figure 4-38: BAMO-THF; Effects of Catalysts at 1000 psi

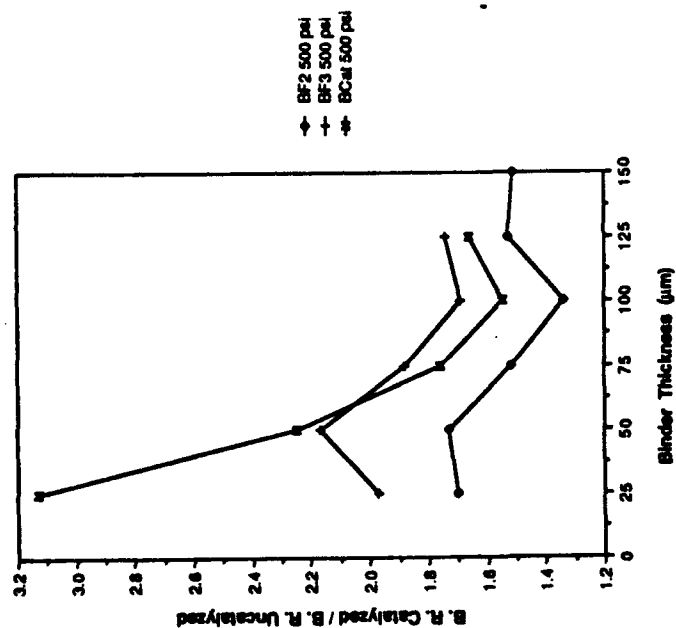


Figure 4-37: BAMO-THF; Effects of Catalysts at 500 psi

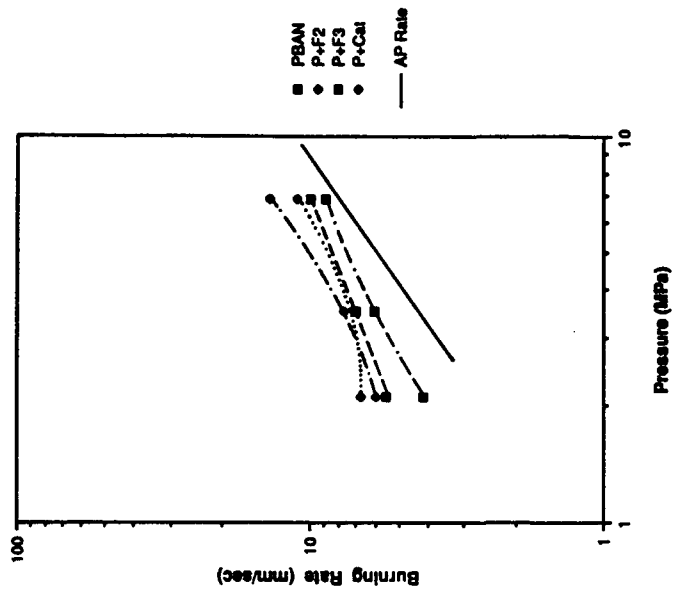


Figure 4-40 Maximum Burning Rate vs. Pressure: PBAN Sandwiches

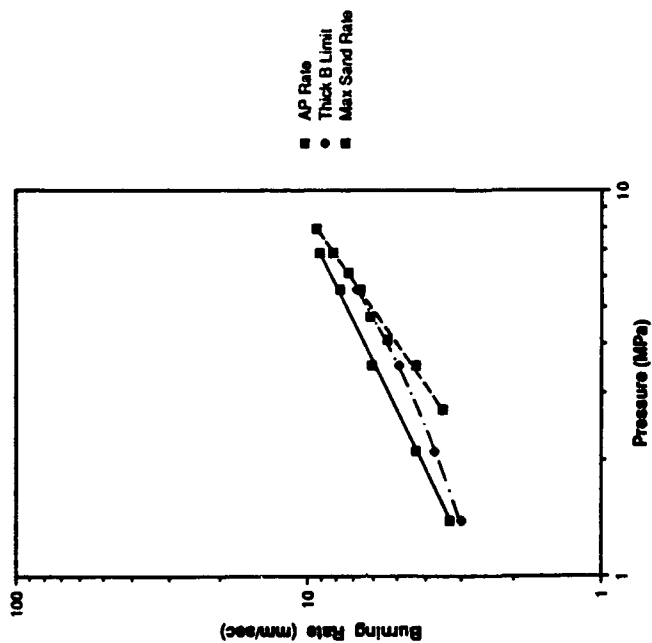


Figure 4-39: Burning Rate vs. Pressure

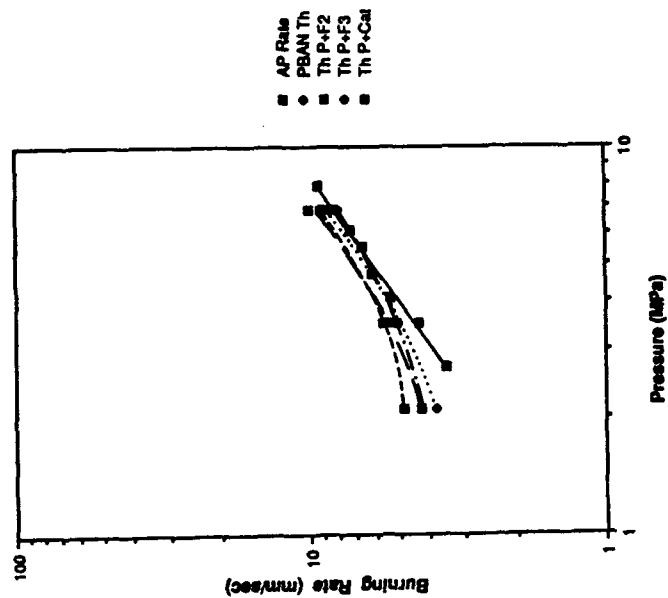


Figure 4-42: Burning Rate vs. Pressure: Thick PBAN case

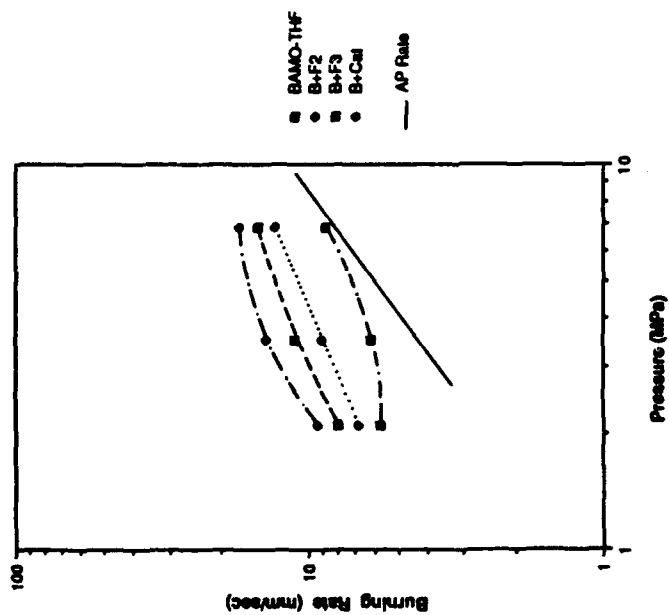


Figure 4-41: Maximum Burning Rate vs. Pressure: BAMO-THF Sandwiches



4-44 Quenched Surface Details of: a) A Composite Solid Propellant

b) An AP/Binder+AP filled Sandwich.

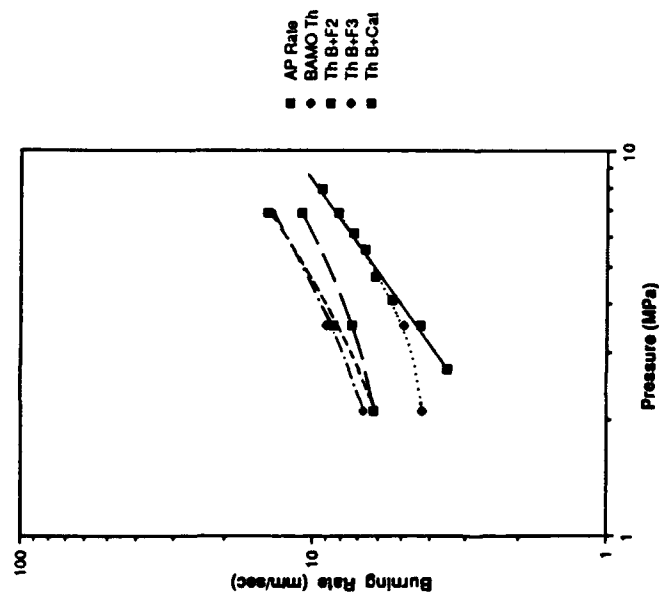
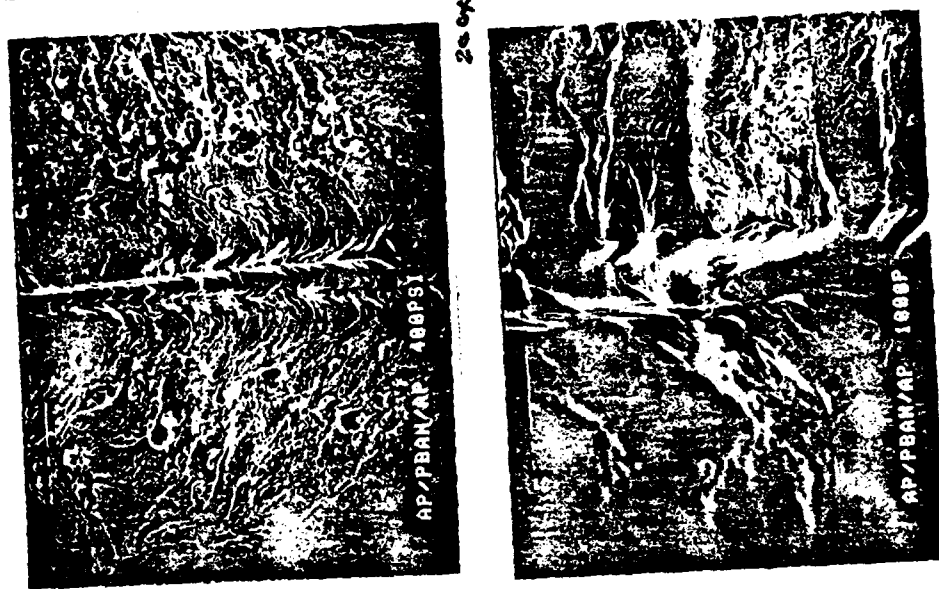


Figure 4-43: Burning Rate vs. Pressure: Thick BAMO-THF case



4-46 Quenched Surface of a PBAN Binder Sandwich

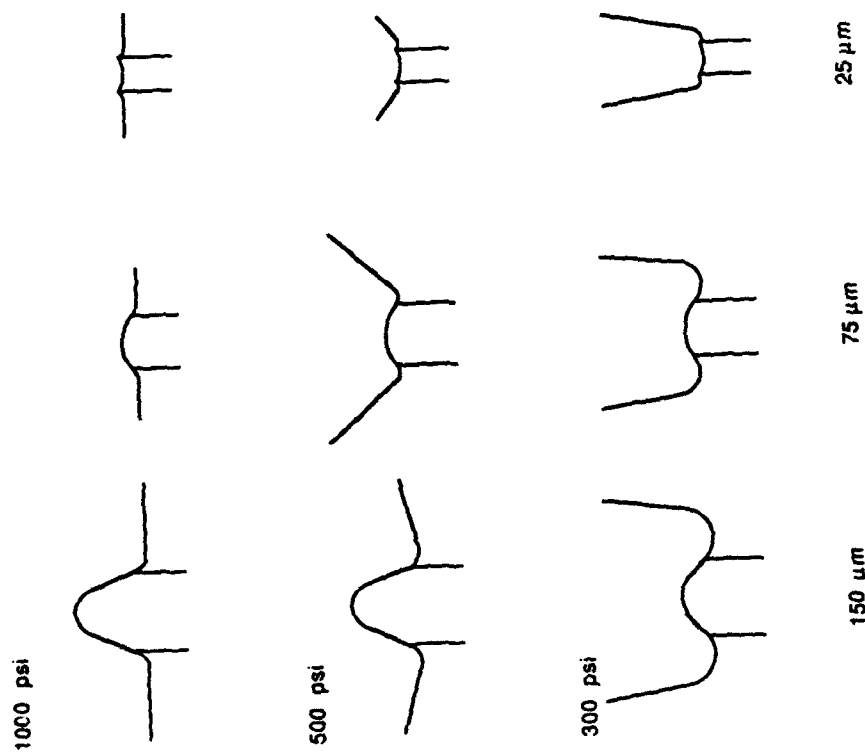
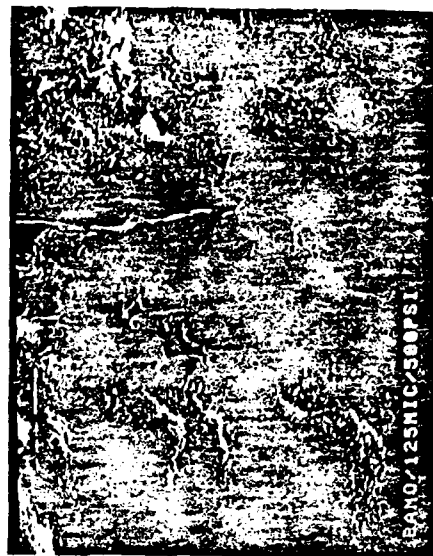


Figure 4-45. Dependence of the Surface Profile of PBAN Binder Sandwiches on Pressure for various Binder Lamina Thicknesses.



4-48 Quenched Surface of a BAMO-TIIF Binder Sandwich

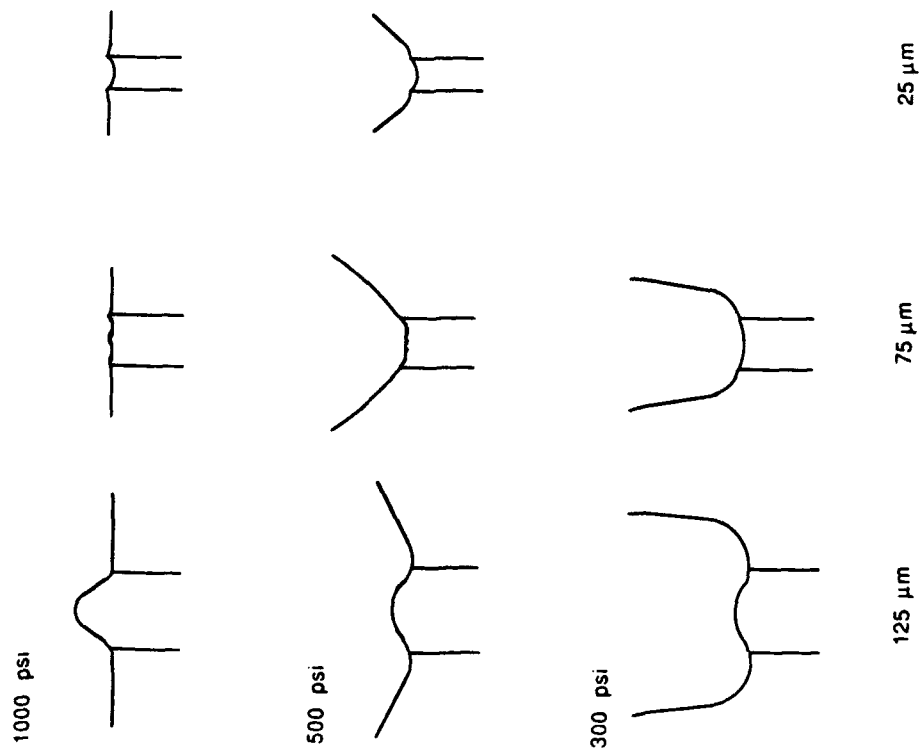


Figure 4-47. Dependence of the Surface Profile of BAMO-TIIF Sandwiches on Pressure for Various Binder Lamina Thicknesses.

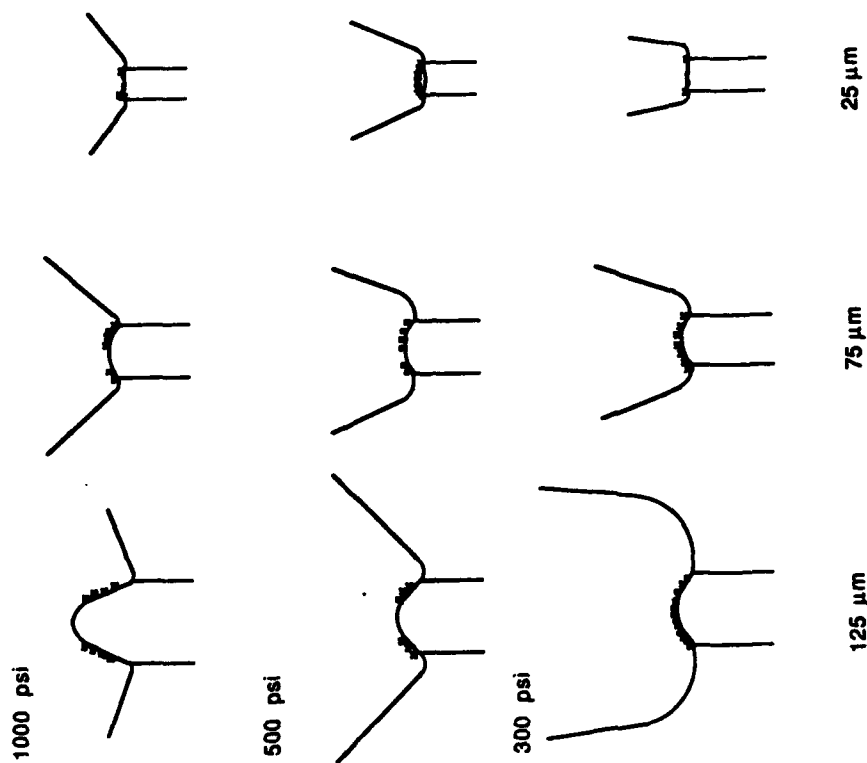
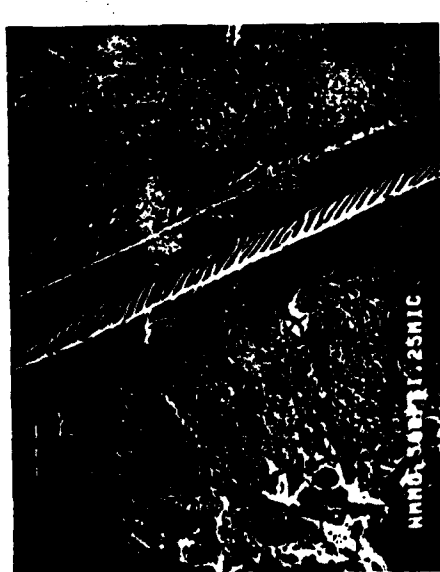
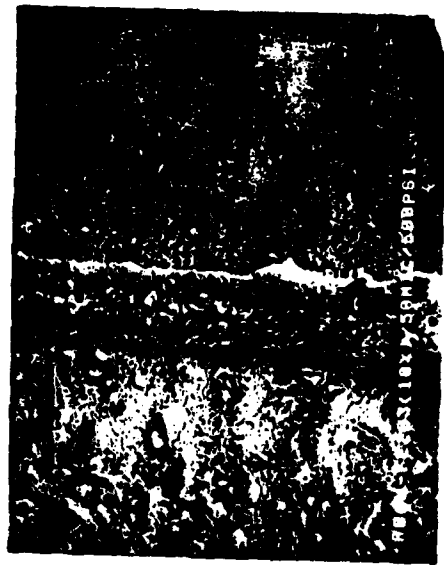


Figure 4-50. Dependence of the Surface Profile of PBAN + 10%Fe<sub>2</sub>O<sub>3</sub> Sandwiches on Pressure for Various Binder Lamina Thicknesses.



X50

4-49 Quenched Surface of a NMMO Binder Sandwich



4-51 Quenched Surface of a PBAN + 10% Fe<sub>2</sub>O<sub>3</sub> Binder Sandwich

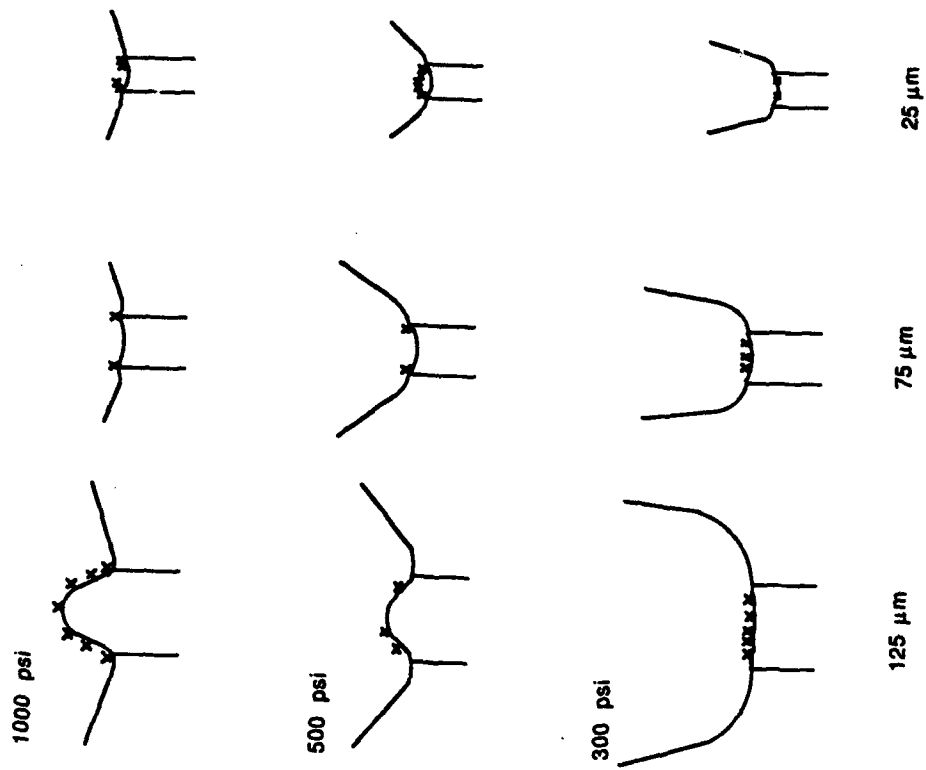
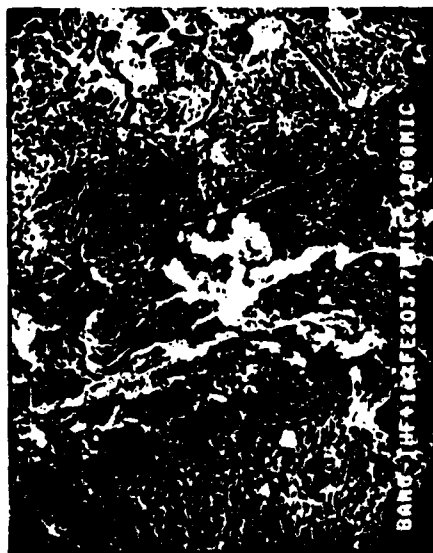


Figure 4-52. Dependence of the Surface Profile of BAMO-THIF + 10%Fe<sub>2</sub>O<sub>3</sub> Sandwiches on Pressure for Various Binder Lamina Thicknesses.



x500

4-53 Quenched Surface of a BAMO-THF + 10% Fe<sub>2</sub>O<sub>3</sub> Binder Sandwich

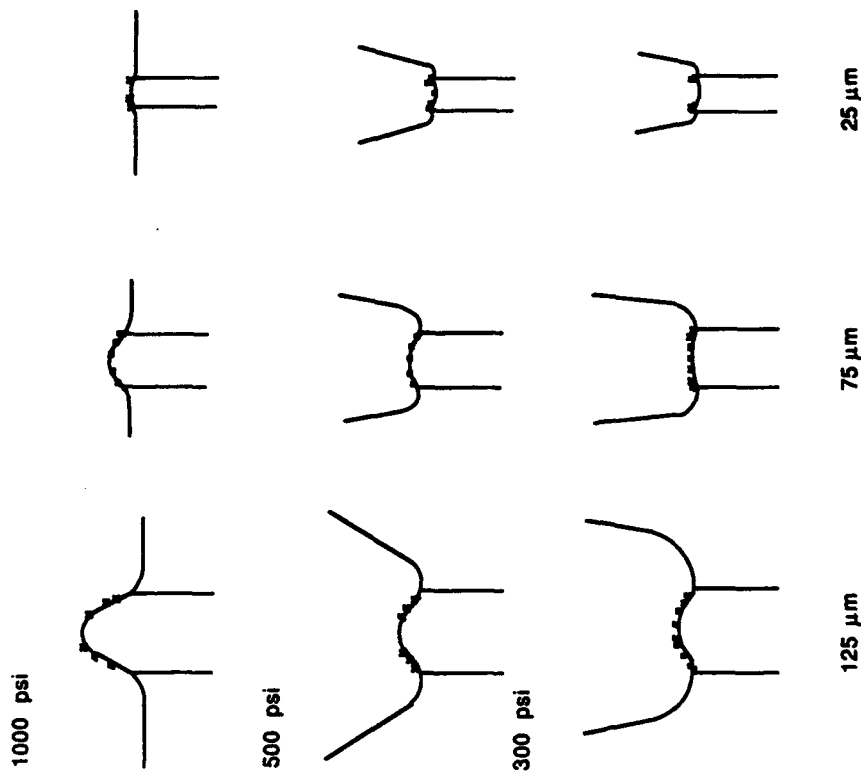
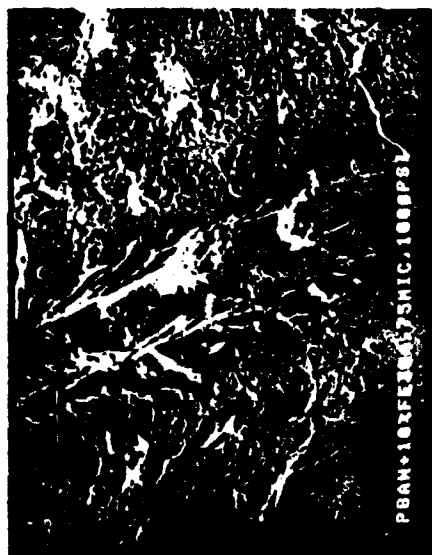
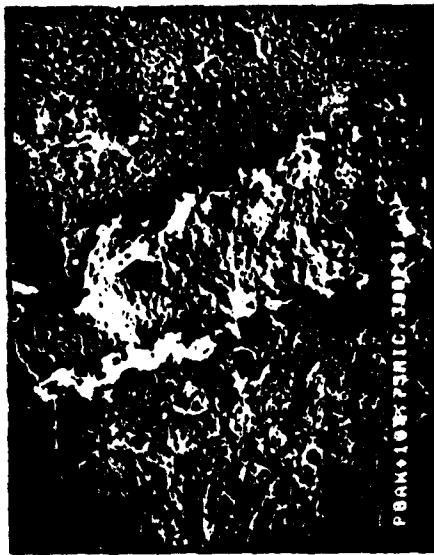


Figure 4-54. Dependence of the Surface Profile of PBAN + 10% Fe<sub>3</sub>O<sub>4</sub> Sandwiches on Pressure for Various Binder Lamina Thicknesses.



x 500

4-55 Quenched Surface of a PBAN + 10% Fe<sub>3</sub>O<sub>4</sub> Binder Sandwich

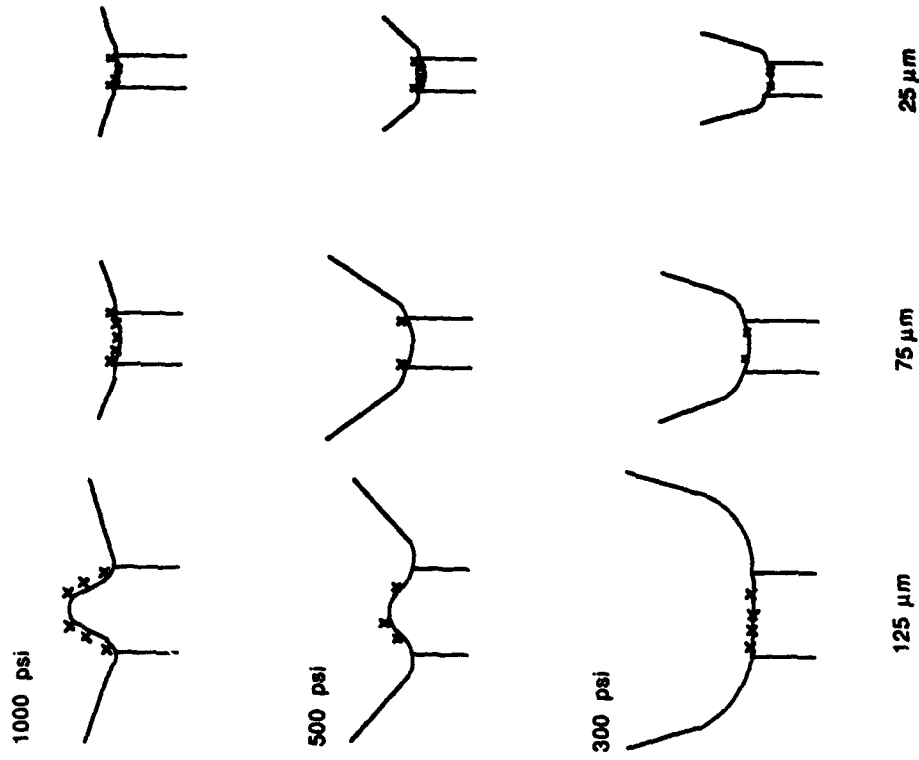


Figure 4-56. Dependence of the Surface Profile of BAMO-THF + 10% Fe<sub>3</sub>O<sub>4</sub> Sandwiches on Pressure for Various Binder Lamina Thicknesses.

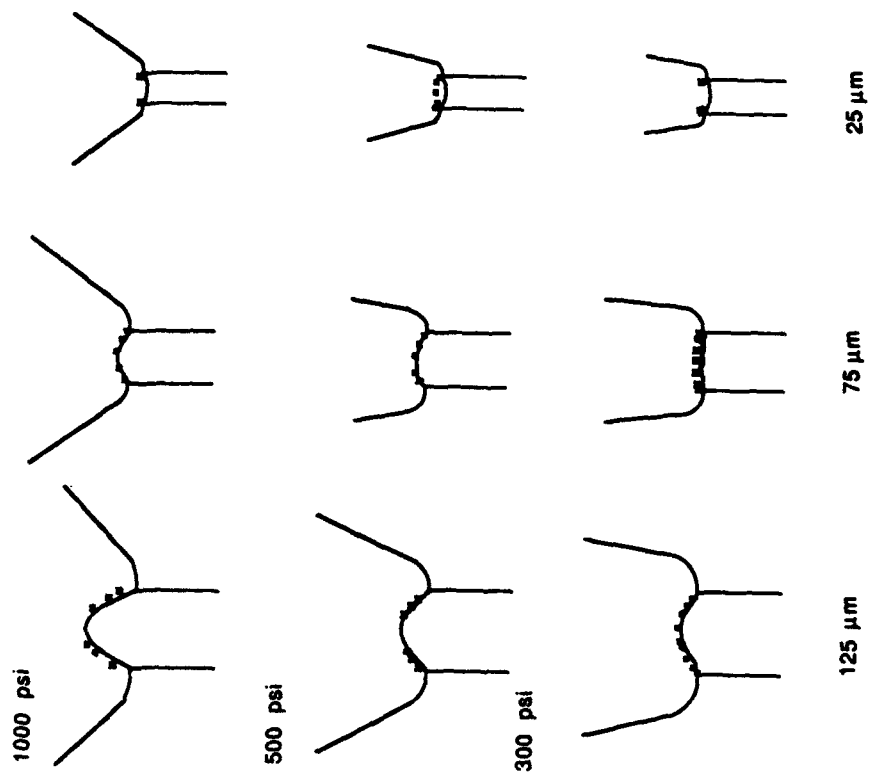
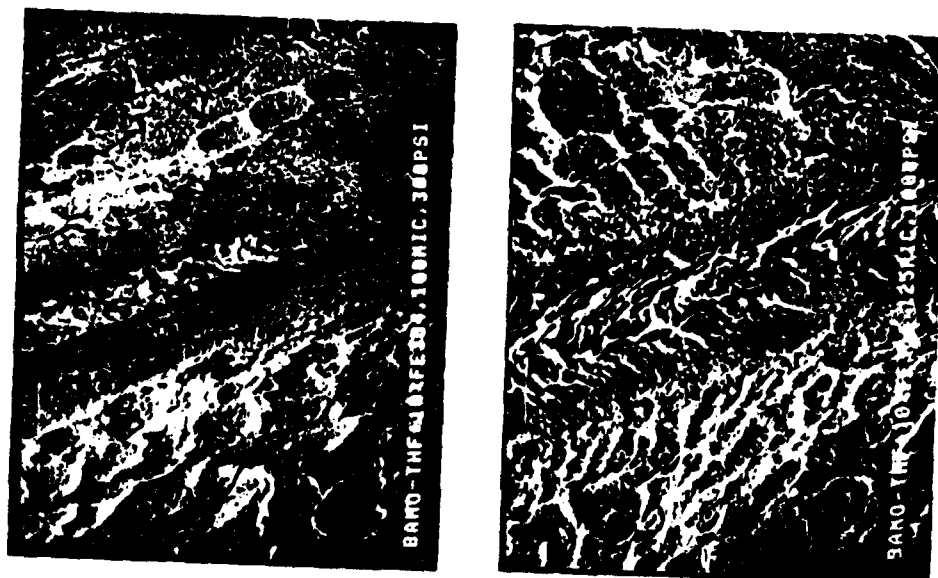
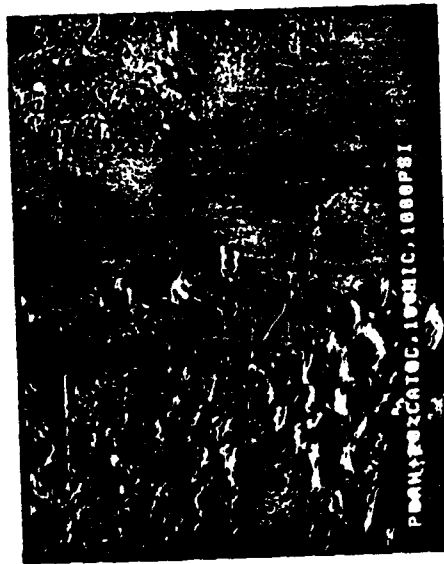
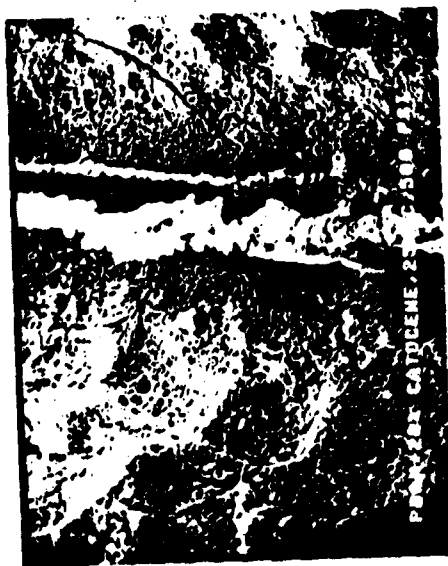


Figure 4-58. Dependence of the Surface Profile of PBAN + 20% Calocene Sandwiches on Pressure for Various Binder Lamina Thicknesses.



4-57 Quenched Surface of a BAMO-THF + 10%  $\text{Fe}_3\text{O}_4$  Binder Sandwich



4-59

4-59 Quenched Surface of a PBAN + 20% Catocene Binder Sandwich

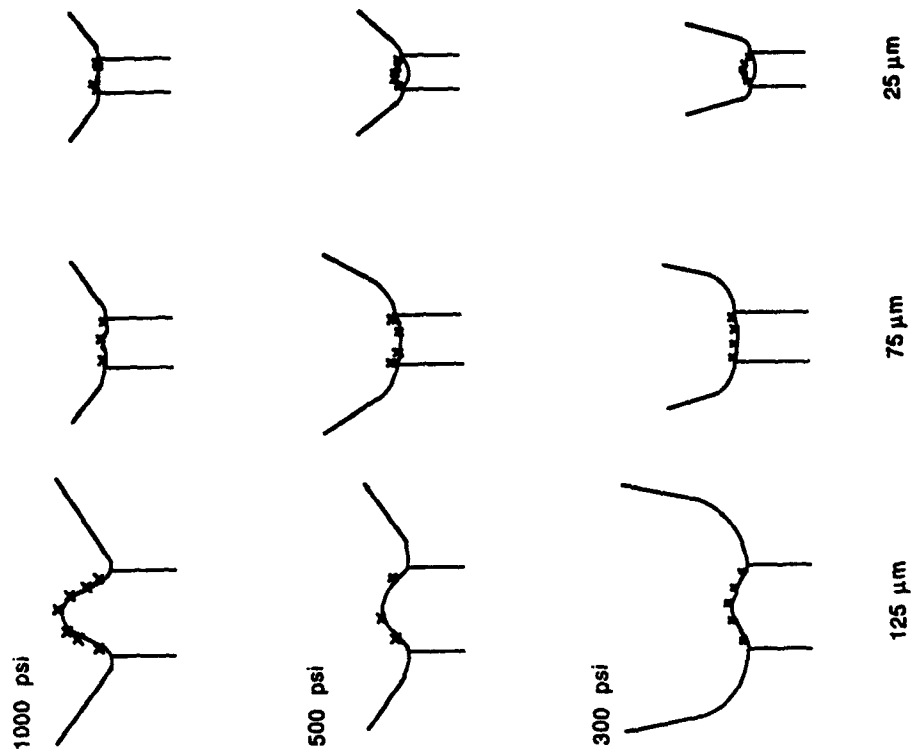


Figure 4-60. Dependence of the Surface Profile of BAMO-THF-20% Catocene Sandwiches on Pressure for Various Binder Lamina Thicknesses



4-61 Quenched Surface of a BAMO-THF + 20% Catocene Binder Sandwich

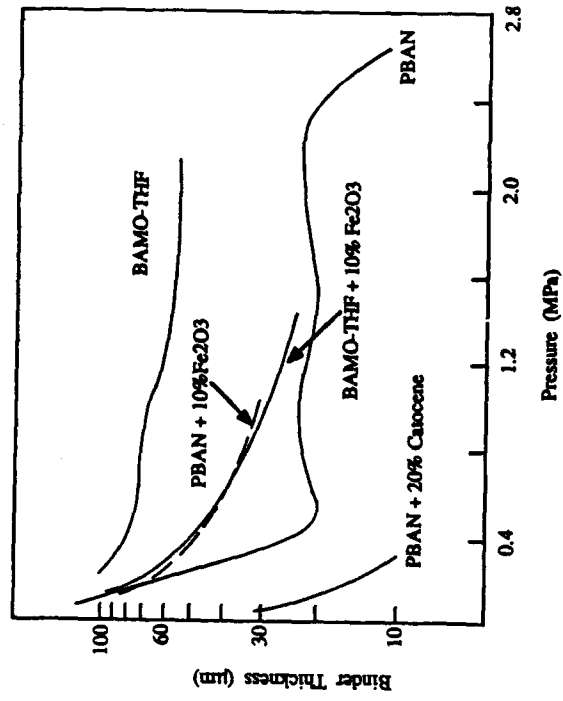
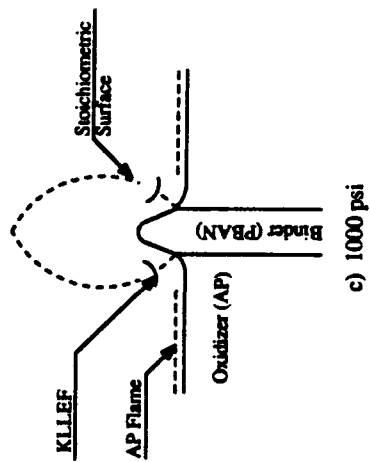
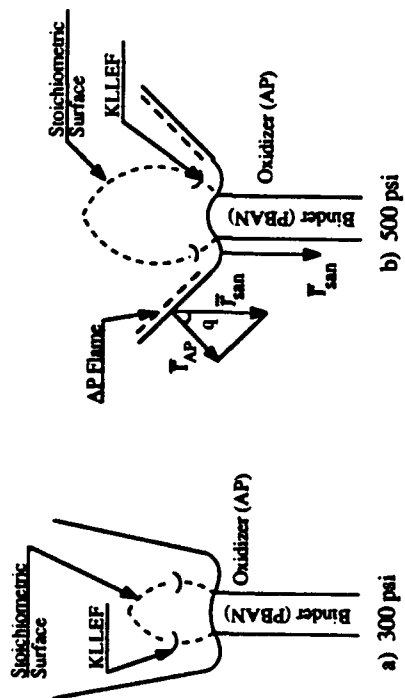


Figure 4-62 Spontaneous Quench Limits for Tapered Sandwiches Burning at Constant Pressure



a) Thick Binder Lamina

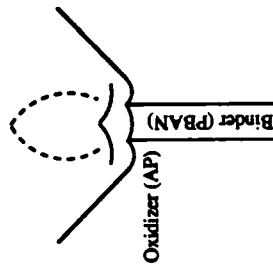
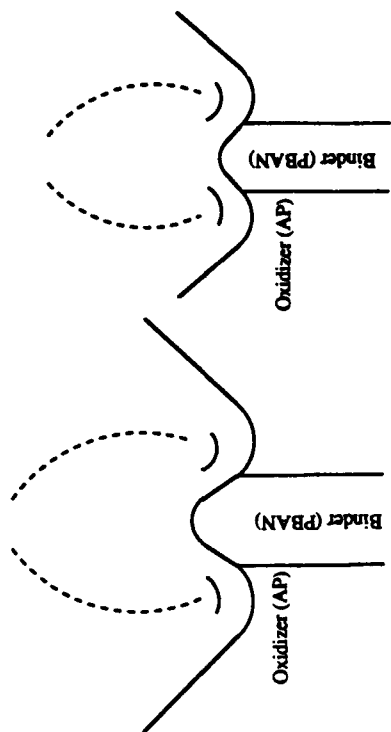
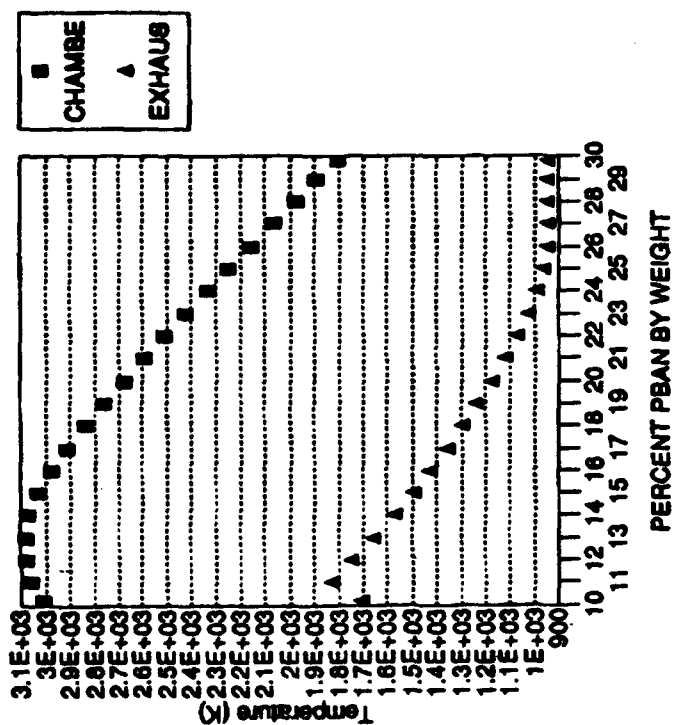
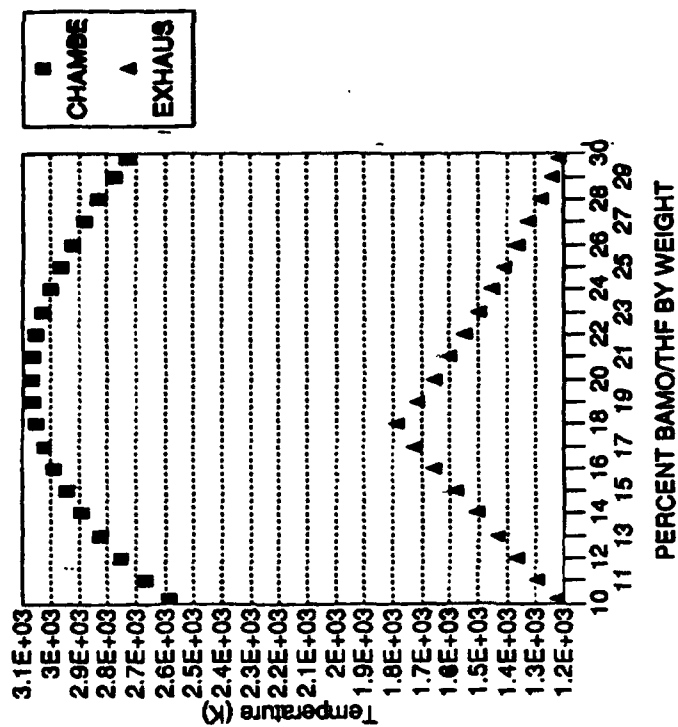


Figure 5-1. Details of the Surface Profile and the Flame Structure at Different Pressures (Binder Lamina Thickness is assumed Moderate; 50 - 75  $\mu\text{m}$ ).

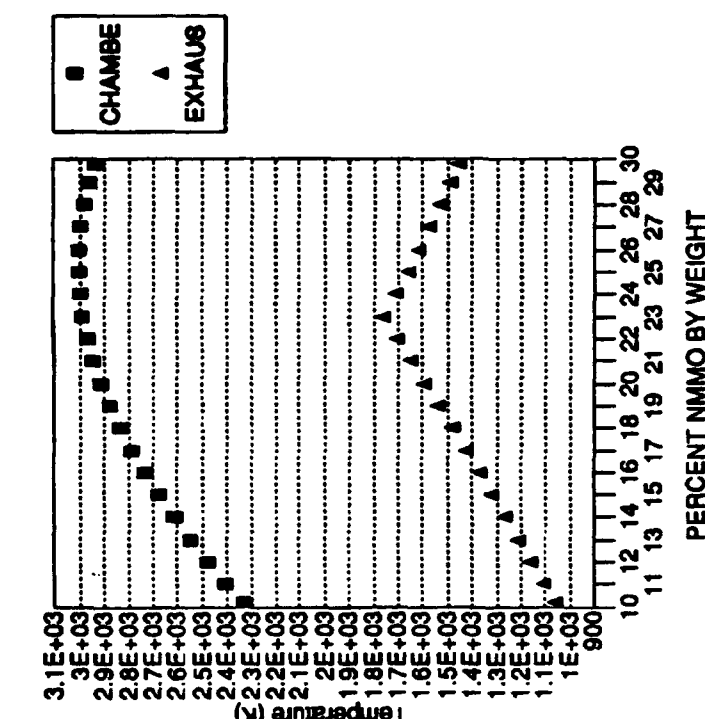
Figure 5-2 Flame Structure at Different Binder Lamina Thickness



5-3 Adiabatic Flame Temperature of an AP/PBAN Mixture



5-4 Adiabatic Flame Temperature of an AP/BAMO-THF Mixture



5.5 Adiabatic Flame Temperature of an AP/NMMO Mixture

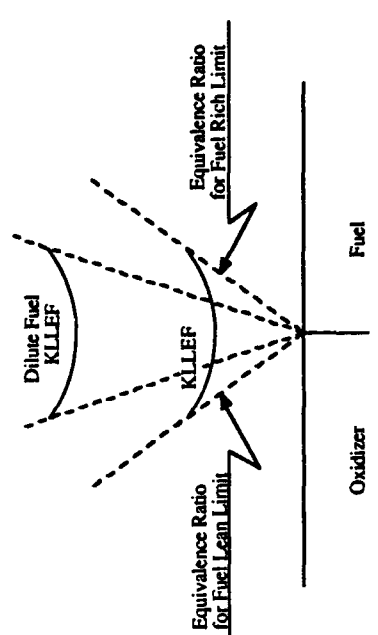


Figure 5-6 Comparison of mixing fields for a concentrated and a dilute fuel. The KLLF extends between two constant equivalence ratio lines that are similar to fuel lean and fuel rich flammability limits, and locates itself at a height that satisfies energy balance between flame heat release and heat flow away from the flame (especially to the surface). When the fuel is more dilute, the same equivalence ratio contours are closer together, and the equivalence ratio profile corresponding to the previous KLLF location occurs further from the surface. A KLLF located there would be similar to the rich fuel KLLF, and would have the same total heat release if the flame temperatures were the same. However the heat loss would be less because of remoteness from the surface, and the KLLF would move in and stabilize at some intermediate location. Other things being equal, this would lead to a lower sandwich burning rate for the dilute-fuel binder, and especially so if the dilute-fuel system also has a lower flame temperature.

## APPENDIX A

### PREPARATION OF BINDERS

#### Preparation of PBAN Binder

PBAN = Polybutadiene acrylic acid acrylonitrile

Ingredients	Weight %
Prepolymer PBAN	60.06
MNA Stabilizer	4.94
DOA Plasticizer	15.00
EPON 825 Epoxy Curative	20.00

#### Procedure:

Weigh out the prepolymer, the MNA and the DOA into a cup. EPON is a crystalline material. Sufficient quantity is heated in another cup (60 - 70 °C) till it forms a liquid and then added to the prepolymer mixture carefully. The mixture is stirred thoroughly before the curing agent recrystallizes. The stirred binder is placed under vacuum till all the entrapped air is removed.

The curing period for PBAN is seven days at about 70 °C.

Note: MNA (Methyl Nitro Analemt) is very viscous, so sometimes it is needed to be heated before adding it to the prepolymer.

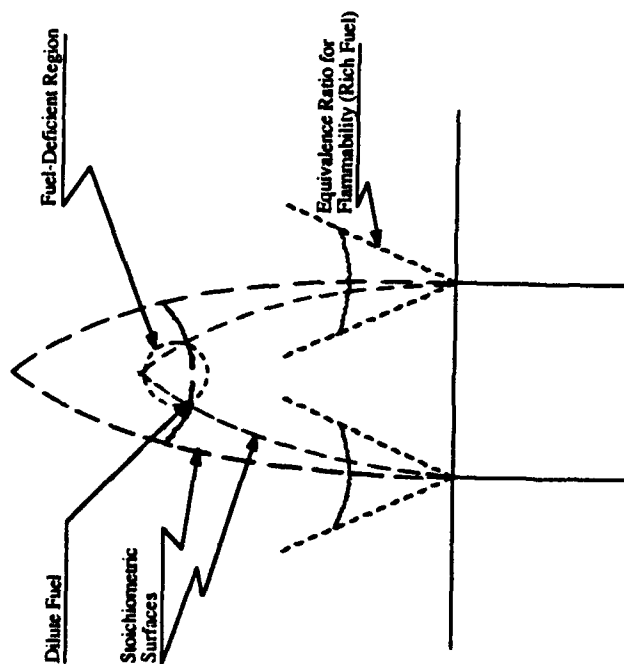


Figure 5-7 Fuel deficient condition with dilute-fuel (thin binder)  
(flammability limit equivalence ratio lines are shown only for rich fuel case)

Preparation of BAMO-THF

BAMO = 3,3-Bis (Azido Methyl) Oxetane

THF = Tetrahydrofuran

Ingredients	Weight %
BAMO-THF Prepolymer	89.33
N-100 Curing Agent	10.67

Procedure:

In a small beaker mix the BAMO-THF prepolymer and the curing agent in weight percentages shown above. The mixture should be stirred with a spatula until it is thoroughly mixed.

The curing period for BAMO-THF binder is about 24 hrs. at 50 °C.

Note: N-100 is a multifunctional isocyanate type curing agent.

Preparation of NMMO Binder

NMMO = 3-NitrazoMethyl-3-MethylOxetane

Ingredients	Weight %
NMMO Prepolymer	91.32
L-2291	2.61
HDI	6.07
T-12 Catalyst	3-4 drops in 10g of NMMO

Procedure:

Weigh out the prepolymer and the other ingredients in a small beaker. The mixture should be stirred until it is thoroughly mixed.

The curing period varies with the amount of catalyst used; if no catalyst is used it cures in 5 days at 50 °C.

## APPENDIX B

## EXPERIMENTAL DATA

TABLE 1. BURNING RATE DATA

## I. PBAN Binder Sandwiches

Pressure Binder Thickness	300 psi		500 psi		1000 psi	
	Exper.	Average	Exper.	Average	Exper.	Average
0 $\mu\text{m}$				4.15		7.85
25 $\mu\text{m}$	3.4	3.4	4.9	4.9	9.15	8.64
50 $\mu\text{m}$	3.7	3.7	5.5	5.4	9.25	8.94
75 $\mu\text{m}$	4.1	4.15	6.1	6.1	8.88	8.78
100 $\mu\text{m}$	4.09	4.0	5.4	5.6	8.6	8.65
125 $\mu\text{m}$	3.75	3.75	5.05	5.05	8.65	8.65

II. PBAN + 10% Fe<sub>2</sub>O<sub>3</sub> Binder Sandwiches

Pressure Binder Thickness	300 psi		500 psi		1000 psi	
	Exper.	Average	Exper.	Average	Exper.	Average
0 $\mu\text{m}$				4.15		7.85
25 $\mu\text{m}$		6.25		7.1		11.2
50 $\mu\text{m}$		6.8		6.95		10.35
75 $\mu\text{m}$		5.4	6.19	6.15		10.25
100 $\mu\text{m}$		4.6	5.6	5.97		10.25
125 $\mu\text{m}$		4.25	5.22	5.05		

TABLE 1. BURNING RATE DATA (continued)

III. PBAN + 10% Fe<sub>3</sub>O<sub>4</sub> Binder Sandwiches

Blinder Thickness	Pressure		300 psi		500 psi		1000 psi	
	Exper.	Average	Exper.	Average	Exper.	Average	Exper.	Average
0 $\mu$ m								
25 $\mu$ m	5.51	5.51	7.02	7.02	4.15	4.15	7.85	7.85
50 $\mu$ m	4.82	4.82	6.77	6.77	7.02	7.02	11.05	11.05
75 $\mu$ m	4.59	4.59	5.76	5.76	5.74	5.74	8.48	8.48
100 $\mu$ m	4.30	4.30	5.34	5.34	5.76	5.76	8.18	8.18
125 $\mu$ m	4.24	4.24	5.21	5.21	5.36	5.36	8.18	8.18

## IV. PBAN + 20% Catocene Binder Sandwiches

Blinder Thickness	Pressure		300 psi		500 psi		1000 psi	
	Exper.	Average	Exper.	Average	Exper.	Average	Exper.	Average
0 $\mu$ m								
25 $\mu$ m	6.02	6.02	7.38	7.38	4.15	4.15	7.85	7.85
50 $\mu$ m	5.2 5.1 5.24	5.18	7.4 7.94	7.67	7.17	7.17	12.46	12.46
75 $\mu$ m	5.12	5.12	7.32	7.32	7.32	7.32	13.14	13.14
100 $\mu$ m	5.05	5.05	6.86	6.86	6.86	6.86	11.20	11.20
125 $\mu$ m	4.86	4.86	5.72	5.72	5.72	5.72	9.93	9.93

TABLE 1. BURNING RATE DATA (continued)

## V. BAMO-THF Binder Sandwiches

Blinder Thickness	Pressure		300 psi		500 psi		1000 psi	
	Exper.	Average	Exper.	Average	Exper.	Average	Exper.	Average
0 $\mu$ m								
25 $\mu$ m	4.55 4.54 4.3 4.62	4.50	4.55 4.54 4.3 4.62	4.50	4.15	4.15	8.72 8.61 8.68	8.73
50 $\mu$ m	4.98 5.0 4.7 4.8	4.82	4.98 5.0 4.7 4.8	4.82	5.80	5.80	8.52 8.8 9.06 9.0	8.83
75 $\mu$ m	3.4	3.40	5.80	5.80	5.95	5.95	9.1 8.48 8.84	8.81
100 $\mu$ m	5.8	5.80	6.12 6.22	6.20	6.20	6.20	9.2 8.42 8.18	8.60
125 $\mu$ m	5.25	5.25	5.30	5.30	5.30	5.30	8.27 8.35	8.31
150 $\mu$ m	4.25	4.25	4.91	4.91	4.91	4.91	8.21	8.21

VI. BAMO-THF + 10% Fe<sub>2</sub>O<sub>3</sub> Binder Sandwiches

Blinder Thickness	Pressure		300 psi		500 psi		1000 psi	
	Exper.	Average	Exper.	Average	Exper.	Average	Exper.	Average
0 $\mu$ m								
25 $\mu$ m	5.54	5.54	8.3 7.54 7.3 7.58	7.66	4.15	4.15	11.91 11.73	11.82
50 $\mu$ m	6.94 6.04	6.49	8.6 8.4 7.99	8.33	8.33	8.33	12.64 12.64	12.64
75 $\mu$ m	6.84	6.84	9.03	9.03	9.03	9.03	13.27 13.00	13.13
100 $\mu$ m	6.48	6.48	8.31 8.3	8.31	8.31	8.31	12.41 11.77	12.09
125 $\mu$ m	6.22	6.22	7.82	7.82	7.82	7.82	11.58 11.54	11.55
150 $\mu$ m			7.43	7.43	7.43	7.43	11.01 11.03	11.02

TABLE 1. BURNING RATE DATA (continued)  
IX. NMMO Binder Sandwiches

Pressure Binder Thickness	300 psi		500 psi	
	Exper.	Average	Exper.	Average
0 $\mu$ m				4.15
25 $\mu$ m	2.23	2.23	4.08	4.08
50 $\mu$ m	2.17	2.17	4.25 4.27	4.26
75 $\mu$ m	2.20	2.20	4.08 4.20	4.13
100 $\mu$ m	2.68	2.68	4.23	4.23
125 $\mu$ m	2.36	2.36	4.12	4.12

X. NMMO + 10% Fe<sub>2</sub>O<sub>3</sub> Binder Sandwiches

Pressure Binder Thickness	500 psi	
	Exper.	Average
0 $\mu$ m		
25 $\mu$ m	7.97	7.97
50 $\mu$ m	8.09	8.09
75 $\mu$ m	9.02	9.02
100 $\mu$ m	7.04	7.04
125 $\mu$ m	6.62	6.62

TABLE 1. BURNING RATE DATA (continued)  
VII. BAMO-THF + 10% Fe<sub>3</sub>O<sub>4</sub> Binder Sandwiches

Pressure Binder Thickness	300 psi		500 psi		1000 psi	
	Exper.	Average	Exper.	Average	Exper.	Average
0 $\mu$ m				4.15		7.85
25 $\mu$ m	5.92	5.92	8.88	8.88	13.85	13.85
50 $\mu$ m	7.04	7.04	10.65 10.76	10.46	14.67	14.67
75 $\mu$ m	7.61 7.58	7.60	10.65 11.73	11.19	15.04	15.04
100 $\mu$ m	8.00	8.00	10.47	10.47	14.21	14.21
125 $\mu$ m	6.77	6.77	9.06	9.06	14.13	14.13

VIII. BAMO-THF + 20% Catocene Binder Sandwiches

Pressure Binder Thickness	300 psi		500 psi		1000 psi	
	Exper.	Average	Exper.	Average	Exper.	Average
0 $\mu$ m				4.15		7.85
25 $\mu$ m	8.88 10.04	9.46	14.10	14.10	17.45	17.45
50 $\mu$ m	7.97	7.97	10.83	10.83	15.64	15.64
75 $\mu$ m	6.72	6.72	10.47	10.47	15.34	15.34
100 $\mu$ m	6.25	6.25	9.57	9.57	14.74	14.74
125 $\mu$ m	6.23	6.23	8.63	8.63	14.44	14.44

TABLE 2. BURNING RATE RATIO DATA

I. PBAN + 10% Fe<sub>2</sub>O<sub>3</sub> Binder Sandwiches

Pressure Binder Thickness	300 psi	500 psi	1000 psi
25 $\mu$ m	1.838	1.449	1.296
50 $\mu$ m	1.838	1.287	1.175
75 $\mu$ m	1.286	1.012	1.167
100 $\mu$ m	1.150	1.054	1.185
125 $\mu$ m	1.133	1.016	

II. BAMO-THF + 10% Fe<sub>2</sub>O<sub>3</sub> Binder Sandwiches

Pressure Binder Thickness	300 psi	500 psi	1000 psi
25 $\mu$ m		1.702	1.364
50 $\mu$ m		1.728	1.431
75 $\mu$ m	2.012	1.518	1.490
100 $\mu$ m	1.117	1.340	1.406
125 $\mu$ m	1.180	1.530	1.390
150 $\mu$ m		1.513	1.342

TABLE 2. BURNING RATE RATIO DATA (continued)

III. PBAN + 10% Fe<sub>3</sub>O<sub>4</sub> Binder Sandwiches

Pressure Binder Thickness	300 psi	500 psi	1000 psi
25 $\mu$ m	1.624	1.433	1.166
50 $\mu$ m	1.303	1.234	0.982
75 $\mu$ m	1.093	1.012	0.939
100 $\mu$ m	1.075	1.029	0.931
125 $\mu$ m	1.131	1.061	0.925

IV. BAMO-THF + 10% Fe<sub>3</sub>O<sub>4</sub> Binder Sandwiches

Pressure Binder Thickness	300 psi	500 psi	1000 psi
25 $\mu$ m		1.973	1.586
50 $\mu$ m		2.170	1.661
75 $\mu$ m	2.235	1.881	1.707
100 $\mu$ m	1.379	1.689	1.652
125 $\mu$ m	1.285	1.742	1.700

# BIBLIOGRAPHY

1. Wimpers, R. N., "Internal Ballistics of Solid-Fuel Rockets," First Edition, McGraw-Hill, New York, 1950.
2. *Journal of Physics and Colloid Chemistry*, Vol. 54, No. 6, 1950.
3. Geckler, R. D., "The Mechanism of Combustion of Solid Propellants," *Selected Combustion Problems*, Butterworths, London, 1954.
4. Guzman, V. R., "Solid Propellant Burning Theory," *Aircraft Engineering*, Vol. 32, No. 379, 1960.
5. Rice, O. K., "The Theory of Burning of Rocket Powders," OSRD Report No. 5574, 1945.
6. Wilfong, R. E., Penner, S. S., and Daniels, F., "An Hypothesis for Propellant Burning," *Journal of Physical Chemistry*, Vol. 54, 1950.
7. Schultz, R. D. and Dekker, A. O., "Fundamental Studies of Aeroplex Propellant Rockets, Investigation of Solid Composite Propellant," Aerojet-General Corporation Report No. 576, Vol. 1, 1952.
8. Chaiken, R. F., "A Thermal Layer Mechanism of Combustion of Solid Composite Propellants: Application to Ammonium Nitrate Propellants," *Combustion And Flame*, Vol. 3, No. 3, 1959.
9. Anderson, W. H., Bills, K. W., Mischuck, B., Moe, G., and Schultz, R. D., "A Model Describing Combustion of Solid Composite Propellants Containing Ammonium Nitrate," *Combustion and Flame*, Vol. 3, 1959.
10. Chaiken, R. F. and Anderson, W. H., "The Role of Binder in Composite Propellant," *Solid Propellant Rocket Research, Progress in Astronautics and Rocketry Series*, Vol. 1, Academic Press, New York, 1960.
11. Sutherland, G. S., "The Mechanism of Combustion of an Ammonium Perchlorate-Polyester Resin Composite Solid Propellant," Ph.D. Thesis, Princeton University, 1956.
12. Summerfield, M., Sutherland, G. S., Webb, M. J., Taback, H. J., and Hall, K. P., "Burning Mechanism of Ammonium Perchlorate Propellants," *Solid Propellant Rocket Research, Progress in Astronautics and Rocketry Series*, Vol. 1, Academic Press, New York, 1960.
13. Blair, D. W., Bastress, E. K., Hermance, C. E., Hall, K. D., and Summerfield, M., "Some Research Problems in the Steady-State Burning of Composite Solid Propellants," *Solid Propellant Rocket Research, Progress in*

TABLE 2. BURNING RATE RATIO DATA (continued)

## V. PBAN + 20% Catocene Binder Sandwiches

Pressure Binder Thickness	300 psi	500 psi	1000 psi
25 $\mu$ m	1.771	1.463	1.454
50 $\mu$ m	1.400	1.420	1.572
75 $\mu$ m	1.219	1.291	1.255
100 $\mu$ m	1.263	1.225	1.148
125 $\mu$ m	1.296	1.133	1.065

## VI. BAMO-THF + 20% Catocene Binder Sandwiches

Pressure Binder Thickness	300 psi	500 psi	1000 psi
25 $\mu$ m		3.133	1.999
50 $\mu$ m		2.247	1.771
75 $\mu$ m	1.976	1.757	1.741
100 $\mu$ m	1.076	1.544	1.714
125 $\mu$ m	1.182	1.660	1.738

14. Seitz, J. A., Stang, P. L., and Summerfield, M., "The Burning Mechanism of Ammonium Perchlorate-Based Composite Propellants," Princeton University Aerospace and Mechanical Sciences Report No. 830, Princeton University, 1969.
15. Shannon, L. J., "Composite Solid Propellant Ignition by Radiant Energy," *AIAA Journal*, Vol. 8, 1970.
16. Boggs, T. L., Derr, D. L., and Beckstead, M. W., "Surface Structure of Ammonium Perchlorate Composite Propellants," *AIAA Journal*, Vol. 8, 1970.
17. Boggs, T. L., "The Deflagration of Pure Single Crystals of Ammonium Perchlorate," AIAA Paper No. 69-142, New York, 1969.
18. Varney, A. M., "An Experimental Investigation of the Burning Mechanisms of Ammonium Perchlorate Composite Solid Propellants," Ph.D. Thesis, Georgia Institute of Technology, 1970.
19. Hermance, C. E., "A Model of Composite Propellant Combustion Including Surface Heterogeneity and Heat Generation," *AIAA Journal*, Vol. 4, No. 9, 1966.
20. Fenn, J. B., "A Phalanx Model for the Combustion of Solid Propellants," *Combustion and Flame*, Vol. 12, No. 3, 1968.
21. Culick, F. E. C. and Deborah, G. L., "An Elementary Calculation for the Burning Rate of Composite Propellants," *Combustion Science and Technology*, Vol. 1, 1969.
22. Beckstead, M. W., Derr, R. L., and Price, C. F., "A Model of Composite Solid Propellant Combustion Based on Multiple Flames," *AIAA Journal*, Vol. 8, No. 12, 1970.
23. Glick, R. L., "Steady State Combustion of Nonmetalized Composite Solid Propellant," Report No. U-75-27, Thiokol Corporation, Huntsville, Alabama, 1975.
24. Renie, J. P., "Combustion Modeling of Composite Solid Propellants," Ph.D. Thesis, Purdue University, West Lafayette, Indiana, 1982.
25. Derr, J. M., and Glick, R. L., "Non-Steady Combustion in a Randomly Ordered Heterogeneous Propellant with Fraternal Heat Transfer," Paper No. AIAA-85-0233, AIAA 23rd Aerospace Sciences Meeting, Reno, Nevada, 1985.
26. Miller, R. R., "A Framework for a Totally Statistical Composite Propellant Combustion Model," CPIA Publication No. 366, Vol. 2, 1982.
27. Price, E. W., Strahle, W. C., Handley, J. C., and Sheshadri, T. S., "Combustion of Nonluminized Heterogeneous Ammonium Perchlorate Propellants," CPIA Publication No. 281, 1976.
28. Strahle, W. C., "Some Statistical Considerations in the Burning of Composite Solid Propellants," *AIAA Journal*, Vol. 16, No. 8, 1978.
29. Hightower, J. D. and Price, E. W., "Experimental Studies Relating to the Combustion Mechanism of Composite Propellants," *Astronautica Acta*, Vol. 14, No. 1, Pergamon Press, London, 1968.
30. Price, E. W., Derr, J. M., Markou, C., and Sigman, R. K., "Oscillatory Interaction of Solid Propellant Combustion and Combustor Flow," Annual Report to Morton Thiokol, Inc., 1987.
31. Lockheed Missile Systems Division, "A Sandwich Burner Model for the Composite Solid Propellant," by W. Nachbar and J. M. Parks, LMSD-2191, Palo Alto, 1957.
32. Nachbar, W., "A Theoretical Study of the Burning of a Solid Propellant Sandwich," *Solid Propellant Rocket Research*, Progress in Astronautics and Rocketry Series, Vol. 1, Academic Press, New York, 1960.
33. Bakhman, N. N. and Polikarpov, D. P., "Heterogeneous Combustion in a System Containing Condensed Components," Report FTD-TT-62-709, Foreign Technology Division, Air Force Systems Command, Wright-Patterson Air Force Base, Ohio, 1962.
34. Hightower, J. D., and Price, E. W., "Two-Dimensional Experimental Studies of the Combustion Zone of Composite Solid Propellants," Second ICRPG Combustion Conference, CPIA Publication No. 105, Vol. 1, 1966.
35. Powling, J., "Experiments Relating to the Combustion of Ammonium Perchlorate Based Propellants," *Eleventh Symposium (International) on Combustion*, The Combustion Institute, Pittsburgh, 1967.
36. Austin, T. D., "Flame Temperature Profile of Ammonium Perchlorate Fuel Binder Sandwiches," Fourth ICRPG Combustion Conference, CPIA Publication, No. 162, Vol. 1, 1967.
37. Nadaud, L., "Models Used at ONERA to Interpret Combustion Phenomena in Heterogeneous Solid Propellants," *Combustion and Flame*, Vol. 12, 1968.
38. Ermolaev, B. S., Korotkov, A. I., and Frolov, Yu. V., "Study of the Action of Catalysts Using Layered Systems," translated from *Fizika Gorenya i Vzryva*, Vol. 5, No. 2, 1969.
39. Ermolaev, B. S., Korotkov, A. I., and Frolov, Yu. V., "Laws of Combustion of a Solid-Propellant Sandwich," translated from *Fizika Gorenya i Vzryva*, Vol. 6, No. 3, 1970.
40. Bakhman, N. N. and Librovich, V. B., "Flame Propagation Along Solid Fuel-Solid Oxidizer Interface," *Combustion and Flame*, Vol. 15, No. 2, 1970.
41. Jones, H. E., "An Experimental Investigation Relating to the Combustion Mechanism of Ammonium Perchlorate Composite Perchlorate," Ph.D. Thesis, Georgia Institute of Technology, 1971.
42. Varney, A. M., and Strahle, W. C., "Experimental Combustion Studies of Two-

57. Boggs, T. L., and Kraeutle, K. J. "Role of the Scanning Electron Microscope in the Study of Solid Rocket Propellant Combustion. I. Ammonium Perchlorate Decomposition and Deflagration," *Combustion Science and Technology*, Vol. 1, 1969.
58. Boggs, T. L., "Deflagration Rate, Surface Structure, and Subsurface Profile of Self-Deflagrating Single Crystals of Ammonium Perchlorate," *AIAA Journal*, Vol. 8, No. 5, 1970.
59. Boggs, T. L., "The Deflagration of Pure and Doped Ammonium Perchlorate: A Basis for Discussion of Assumptions Commonly made in Modeling Composite Propellant Combustion," CPIA Publication No. 204, Vol. 1, 1971.
60. Manelis, G. B., Strutin, V. A., "The Mechanism of Ammonium Perchlorate Burning," *Combustion and Flame*, Vol. 17, 1971.
61. McHale, E. T., and von Elbe, G., "The Deflagration of Solid Propellants Oxidizers," *Combustion Science and Technology*, Vol. 2, 1970.
62. Boggs, T. L., and Zum, D. E., "The Temperature Sensitivity of the Deflagration Rates of Pure and Doped Ammonium Perchlorate," *Combustion Science and Technology*, Vol. 4, 1972.
63. Boggs, T. L., Price, E. W., and Zum, D. E., "The Deflagration of Pure and Isomorphously Doped Ammonium Perchlorate," *Thirteenth Symposium (International) on Combustion*, 1973.
64. Boggs, T. L., Zum, D. E., and Netzer, D. W., "Ammonium Perchlorate Combustion: Effects of Sample Preparation, Ingredient Type, and Pressure, Temperature and Acceleration Environments," *Combustion Science and Technology*, Vol. 7, 1973.
65. Boggs, T. L., Kraeutle, K. J., and Zum, D. E., "The Combustion of As-received and Preoxidized Aluminum in Sandwich and Propellant Configurations," CPIA Publication No. 231, 1972.
66. Boggs, T. L., Crump, J. E., Kraeutle, K. J., and Zum, D. E., "Cinephotomicrography and Scanning Electron Microscope as Used to Study Solid Propellant Combustion at the Naval Weapons Center," Naval Weapons Center, NWC-TP-5944, 1977.
67. Crump, J. E., Prentice, J. L., and Kraeutle, K. J., "Role of Scanning Electron Microscope in the Study of Solid Propellant Combustion: II. Behavior of Metal Additives," *Combustion Science and Technology*, Vol. 1, 1969.
68. Varney, A. M., and Strahle, W. C., "Thermal Decomposition Studies for Some Solid Propellant Binders," *Combustion and Flame*, Vol. 16, 1971.
69. Cohen, N. S., Fleming, R. W., and Derr, R. L., "Role of Binders in Solid Propellant Combustion," *AIAA Journal*, Vol. 12, No. 2, 1974.
70. Beck, W. H., "Pyrolysis Studies of Polymeric Materials Used as Binders in Composite Propellants: A Review," *Combustion and Flame*, Vol. 70, 1987.

- Dimensional Ammonium Perchlorate-Binder Sandwiches," *Combustion Science and Technology*, Vol. 4, 1972.
43. Boggs, T. L., and Zum, D. E., "The Deflagration of Ammonium Perchlorate-Polymeric Binder Sandwich Models," *Combustion Science and Technology*, Vol. 4, 1972.
44. Brown, W. E., Kennedy, J. R., and Netzer, D. W., "An Experimental Study of Ammonium Perchlorate-Binder Sandwich Combustion in Standard and High Acceleration Environments," *Combustion Science and Technology*, Vol. 6, 1972.
45. Murphy, J. L., and Netzer, D. W., "Ammonium Perchlorate and Ammonium Perchlorate-Binder Sandwich Combustion," *AIAA Journal*, Vol. 12, No. 1, 1974.
46. Abraham, M. III, and Netzer, D. W., "Nonmetallized Solid Propellant Combustion in Standard and High Acceleration Environments," *Combustion Science and Technology*, Vol. 11, 1975.
47. Price, E. W., Sigman, R. K., and Handley, J. C., "Microstructure of the Combustion Zone of Composite Solid Propellants," CPIA Publication No. 297, Vol. 2, 1979.
48. Handley, J. C., Price, E. W., and Ghosh, A., "Combustion of Non-Aluminized Binders in Tapered Sandwiches," CPIA Publication No. 308, Vol. 2, 1979.
49. Price, E. W., Panyam, R. R., and Sigman, R. K., "Microstructure of the Combustion Zone: Thin-Binder AP-Polymer Sandwiches," CPIA Publication No. 329, Vol. 1, 1980.
50. Price, E. W., Handley, J. C., Panyam, R. R., Sigman, R. K., and Ghosh, A., "Combustion of Ammonium Perchlorate-Polymer Sandwiches," *AIAA Journal*, Vol. 19, No. 3, 1981.
51. Price, E. W., Panyam, R. R., Sambamurthi, J. K., and Sigman, R. K., "Combustion of Ammonium Perchlorate-Polymer Sandwiches," CPIA Publication No. 366, Vol. 1, 1982.
52. Price, E. W., and Sambamurthi, J. K., "Dependence of Burning Rate of AP-Polymer Sandwiches on Thickness of the Binder Laminar," CPIA Publication No. 383, Vol. 1, 1983.
53. Price, E. W., Sambamurthi, J. K., Panyam, R. R., and Sigman, R. K., "Combustion of Ammonium Perchlorate-Polymer Sandwiches," Annual Contract Report to Office of Naval Research, Georgia Institute of Technology, 1984.
54. Price, E. W., Sambamurthi, J. K., Sigman, R. K., and Panyam, R. R., "Combustion of Ammonium Perchlorate-Polymer Sandwiches," *Combustion and Flame*, Vol. 63, 1986.
55. Hightower, J. D., and Price, E. W., "Combustion of Ammonium Perchlorate," *Eleventh Symposium (International) on Combustion*, 1967.
56. Beckstead, M. W., and Hightower, J. D., "Surface Temperature of Deflagrating Ammonium Perchlorate Crystals," *AIAA Journal*, Vol. 5, No. 10, 1967.

84. Kishore K., and Sunitha, M. R., "Effect of Transition Metal Oxides on Decomposition and Deflagration of Composite Solid Propellant Systems: A Survey," *AIAA Journal*, Vol. 17, No. 10, 1979.
85. Kishore K., Pul Venkatesh, V. R., and Sunitha, M. R., "Action of Transition Metal Oxides on Composite Solid Propellants," *AIAA Journal*, Vol. 18, No. 11, 1980.
86. Fouser, R. L., "The Effect of Additives on the Pressure Sensitivity of Composite Propellants," *CPIA Publication No. 347*, Vol. 1, 1981.
87. Price, E. W., and Sambamurthi, J. K., "Mechanism of Burning Rate Enhancement by Ferric Oxide," *CPIA Publication No. 412*, Vol. 1, 1984.
88. Price, E. W., Sambamurthi, J. K., and Sigman, R. K., "Further Results on the Combustion Behavior of AP/Polymer Sandwiches with Additives," *CPIA Publication No. 432*, Vol. 1, 1985.
89. Krishnan, S., and Periasamy, C., "Low-Pressure Burning of Catalyzed Composite Propellants," *AIAA Journal*, Vol. 24, No. 10, 1986.
90. Fong, C. W., and Hamshere, B. L., "The Mechanism of Burning Rate Catalysis in Composite HTPB-AP Propellant Combustion," *Combustion and Flame*, Vol. 65, 1986.
91. Fong, C. W., and Hamshere, B. L., "The Mechanism of Burning Rate Catalysis in Composite Propellants by Transition Metal Complexes," *Combustion and Flame*, Vol. 65, 1986.
92. Mellor, J. W., "A Comprehensive Treatise on Inorganic and Theoretical Chemistry," Longmans, Green and Co., New York, 1934.
93. Boggs, T. L., Zurn, D. E., Strahle, W. C., Handley, J. C., and Milkie, T. T., "Mechanisms of Combustion," Naval Weapons Center, NWC-TP-5514, 1973.
94. Price, E. W., Handley, J. C., Strahle, W. C., Sheshadri, T. S., Sigman, R. K., and Ghosh, A., "Combustion Mechanisms of Solid Propellants," Final Report to Office of Naval Research, Georgia Institute of Technology, 1980.
95. Powers, R. J., "Rapid Pyrolysis of Polymeric Solid Propellant Binders," Ph.D. Thesis, Georgia Institute of Technology, 1986.
96. Price, E. W., Sigman, R. K., Powers, R. J., Markou, C., and Sambamurthi, J. K., "Combustion Mechanisms of Solids," Final Report to Office of Naval Research, Georgia Institute of Technology, 1986.
97. Munson, W. O., McGee, L. R., and Walker, R. B., "Burning Rate Modifier Effects on a High Rate Tactical Propellant," *AIAA Paper 77-128*, 1977.
98. Deur, J. M., and Price, E. W., "Steady State One-Dimensional Pyrolysis of Oxidizer-Binder Laminates," *AIAA Paper 86-1446*, Huntsville, AL, 1986.
99. Panyam, R. R., "Combustion at the Interface of an Oxidizer-Fuel Slab System," Ph. D. Thesis, Georgia Institute of Technology, 1983.
71. Pittman, C. U., "Location of Action of Burning-Rate Catalysts in Composite Propellant Combustion," *AIAA Journal*, Vol. 7, No. 2, 1969.
72. Jones, H. E., and Strahle, W. C., "Effects of Copper Chromite and Iron Oxide Catalysts on AP/CTPB Sandwiches," *Fourteenth Symposium (International) on Combustion*, The Combustion Institute, Pittsburgh, 1972.
73. Inami, S. H., Rajapaseke, Y., Shaw, R., and Wise, H., "Solid Propellant Kinetics. I: The Ammonium Perchlorate-Copper Chromite-Fuel System," *Combustion and Flame*, Vol. 17, 1971.
74. Lobanov, I. N., Chuvayev, V. N., and Bakhtman, N. N., "Buildup of Catalyst on the Surface of a Charge During Combustion," translated from *Fizika Gorenya i Vryva*, Vol. 9, No. 3, 1973.
75. Strahle, W. C., Handley, J. C., and Milkie, T. T., "Catalytic Effects in the Combustion of AP-HTPB Sandwiches to 3200 PSIA," *Combustion Science and Technology*, Vol. 8, 1974.
76. Handley, J. C., and Strahle, W. C., "The Behavior of Several Catalysts in the Combustion of Solid Propellant Sandwiches," *AIAA Paper 74-122*, Washington, D. C., 1974.
77. Handley, J. C., and Strahle, W. C., "Behavior of Several Catalysts in the Combustion of Solid Propellant Sandwiches," *AIAA Journal*, Vol. 13, No. 1, 1975.
78. Strahle, W. C., Handley, J. C., and Kumar, N., "Catalytic Behavior in Solid Propellant Combustion," Annual Contract Report to Office of Naval Research, Georgia Institute of Technology, 1973.
79. Handley, J. C., "An Experimental Investigation of Catalysts in the Combustion of Composite Solid Propellants," Ph.D. Thesis, Georgia Institute of Technology, 1976.
80. Martynuk, V. F., Bakhtman, N. N., and Lobanov, I. N., "Catalysis and Inhibition in an Ammonium Perchlorate-Polyethylene Glycol-Laminated System," translated from *Fizika Gorenya i Vryva*, Vol. 13, No. 2, 1977.
81. Korobeinichev, O. P., Kovalenko, K. K., and Lesnikovich, A. I., "Investigation of Effect of Oxide and Organometallic Catalysts on Thermal Decomposition and Combustion of a Model Ammonium Perchlorate-Polymer System," translated from *Fizika Gorenya i Vryva*, Vol. 13, No. 4, 1976.
82. Kishore, K., and Sunitha, M. R., "Mechanism of Catalytic Activity of Transition Metal Oxides on Solid Propellant Burning Rate," *Combustion and Flame*, Vol. 33, 1978.
83. Foster, R. L., and Miller, R. R., "Experimental Studies of Fe<sub>2</sub>O<sub>3</sub> Catalysis in aluminized HTPB Propellants," Source unavailable.

100. Oyumi, Y., and Brill, T. B., "Thermal Decomposition of Energetic Materials 12. Infrared Spectral and Rapid Pyrolysis Studies of Azide-Containing Monomers and Polymers," *Combustion and Flame*, Vol. 65, 1986.
101. Oyumi, Y., and Brill, T. B., "Thermal Decomposition of Energetic Materials 22. The Contrasting Effects of Pressure on the High-Rate Thermolysis of 34 Energetic Compounds," *Combustion and Flame*, Vol. 68, 1987.
102. Sutton, G. P., "Rockets Propulsion Elements: An Introduction to the Engineering of Rockets," Fifth Edition, Wiley-Interscience, New York, 1986.
103. Williams, F. A., "Combustion Theory," Second Edition, The Benjamin/Cummings Publishing Company, Inc., Menlo Park, CA, 1985.
104. Kuo, K. K., and Summerfield, M., "Fundamentals of Solid-Propellant Combustion," Progress in Astronautics and Aeronautics, Vol. 90, AIAA, New York, 1984.